

STUDIES ON THE MECHANISM OF ASSEMBLY

OF

MYELIN

IN THE

CENTRAL NERVOUS SYSTEM

by

Pedro M. Pereyra

A thesis submitted to the Faculty of Graduate Studies and Research, McGill University, in partial fulfillment of the requirements for the degree of Doctor of Philosophy.

Department of Biochemistry

McGill University

Montreal, Canada

© April 1983

MECHANISMS OF MYELIN ASSEMBLY

## ABSTRACT

A novel myelination model that incorporates many morphological and morphometric observations of the developing nervous system is proposed. The model describes the formation of myelin spirals through the intracellular deposition of preformed and extended membrane elements (plates). This model predicts many common and unexplained features of the central nervous myelin under normal and pathological conditions. A mathematical description of protein translocation is also presented, as well as its application to time-staggered double isotope (TSDI) protocols. These ideas constitute a theoretical framework for the study of myelin assembly and its morphogenesis.

Experiments in this thesis focus on the developmental relationships among myelin related subfractions of 15 day old mouse brain. A specific subfractionation protocol was designed and subfractions characterized morphologically and biochemically. TSDI protocols were employed to study the kinetics of myelin protein deposition, and to distinguish between developmental or precursor-product relationships.

The results obtained indicate quantitative, qualitative and metabolic differences among myelin subfractions. Very short deposition times, less than 5 min, were found for the 14K, 17K and 18.5K dalton myelin basic proteins, and no more than 15 minutes for the proteolipid protein. Together these results suggest that, under specific conditions, myelin subfractions isolated from developing brain represent myelin "compartments" at different stages of development.

## RESUME

Un nouveau modèle de myélinisation incorporant plusieurs observations morphologiques et morphométriques est ici proposé. Dans celui-ci, on décrit la formation de la spirale myélinisée à travers le dépôt intracytoplasmique d'extensions de membranes préformées. Le modèle est capable de prédire des caractéristiques du système nerveux central. Une description mathématique du processus de translation des protéines ainsi que son application dans des expériences d'utilisation non-synchronisée de deux isotopes (TSDI) est aussi présentée. Les deux propositions constituent une base théorique pour l'étude de l'assemblage de la myéline et de sa morphogenèse.

Les expériences décrites dans cette thèse sont basées sur l'étude des relations d'ontogenèse entre les diverses sous-fractions de la myéline du cerveau de souris âgé de 15 jours. Un protocole de sous-fractionation spécifique a été élaboré, et les diverses sous-fractions ont été caractérisées par des moyens morphologiques et biochimiques. Des protocoles du genre TSDI ont été appliqués dans l'étude de la cinétique du dépôt des protéines dans la myéline et dans la distinction des relations d'ontogenèse ou de "précurseur-produit" entre les diverses sous-fractions.

Les résultats obtenus ont montré des différences quantitatives, qualitatives et métaboliques entre les diverses sous-fractions de myéline. Le temps nécessaire pour le dépôt des protéines basiques 14K, 17K et 18.5K dalton de la myéline a été de l'ordre de 5 minutes, tandis que le temps de dépôt de la protéine protéolipidique a été de l'ordre de 15 minutes.



L'ensemble des résultats suggère que, dans des circonstances spécifiques, les sous-fractions de la myéline isolée du cerveau en voie de maturité représentent des "compartiments" de myéline à différents états d'ontogenèse.

## RESUMEN

Haciendo uso de informes morfológicos sobre el sistema nervioso en desarrollo, se llegó a la elaboración de un nuevo modelo de mielinización. En éste se describe la formación de la espiral mielínica a través de la deposición intracitoplásmica de extensiones de membranas preformadas. El modelo es capaz de predecir características morfológicas típicas de la mielina en condiciones normales y patológicas del sistema nervioso central. Se presenta también una descripción matemática del proceso de translación de proteínas, así como su empleo en experimentos que hacen uso de la inyección asíncrona de dos isótopos (TSDI). Estos dos procedimientos constituyen el marco teórico para el estudio del ensamble y de la morfogénesis de la mielina.

Los experimentos expuestos en esta tesis están enfocados al estudio de las relaciones ontológicas entre las subfracciones de mielina del cerebro de ratón de 15 días de nacido. Para esto se diseñó un proceso de subfraccionamiento específico, cuyas subfracciones se caracterizaron por medios morfológicos y bioquímicos. Métodos del tipo TSDI fueron empleados para estudiar la cinética de deposición de proteínas mielínicas y para distinguir las relaciones ontológicas ó de "precursor-producto" entre subfracciones.

Los resultados obtenidos indican diferencias cuantitativas, cualitativas y metabólicas entre subfracciones de mielina. Se encontró que los tiempos de deposición de las proteínas básicas 14K, 17K y 18.5K de la mielina, son del orden de 5 minutos, mientras que la deposición de la proteína lipoafín toma alrededor

de 15 minutos. En conjunto, estos resultados sugieren que bajo circunstancias especiales, las subfracciones de mielina aisladas del cerebro en desarrollo, representan compartimientos de mielina en diferentes estados ontológicos.

a Nadja Linok,  
a mis padres.

## PREFACE

The work described in Chapters 4 and 5 of this thesis has been published :

Chapter 4. Pereyra, P.M. and Braun, P.E. with technical assistance of Elsa Horvath (1983)

J. Neurochem. in press

Chapter 5. Pereyra, P.M., Braun, P.E., Greenfield, S. and Hogan, E.L. (1983)

J. Neurochem. in press

In accordance with the regulations described in the general information booklet 1982 of the Faculty of Graduate Studies and Research and as approved by the Biochemistry Department, papers already published have been incorporated into the thesis.

The figures in Chapters 4 and 5 were prepared by Margo Oeltschner. Other drawings and figures are property of the author.

## TABLE OF CONTENTS

ABSTRACT	i
RESUME	ii
RESUMEN	v
DEDICATION	vii
PREFACE	viii
TABLE OF CONTENTS	ix
LIST OF ABBREVIATIONS	xiv
ACKNOWLEDGEMENTS	xvi

### PROLOGUE

#### References Prologue

### CHAPTER 1. BIOLOGY OF MYELIN

1.1. Introduction	6
1.2. Phylogenesis of Myelination	7
1.2.1 The Neuroglia in the Evolution of the Brain Architecture	8
1.2.2. The Glia-Neuron Interaction: An Organic Relationship	11
1.3. A General Outline of Myelination	13
1.3.1. Phase Zero : Proliferation, Differentiation and Axon Bundle Fasciculation.	21
1.3.2. Phase I : Axon Recognition and Induction of Myelin Formation.	23
1.3.3. Phase II : Active Deposition of Myelin Membranes.	30
1.3.4. Phase III : Terminal Phase.	37
1.4. Models of Myelin Lamellar Formation	41
1.5. References.	49

CHAPTER 2.	A NEW MODEL OF MYELIN MORPHOGENESIS	62
2.1.	Description of the Model	62
2.2.	Morphological Predictions of the Lamellation Model	70
2.3.	Abnormalities of Myelination and Their Simulation by the Model	74
2.4.	In Search for Molecular-Biological Evidence	80
2.5.	Final Considerations	84
2.6.	References	90
CHAPTER 3.	THE STUDY OF MYELIN MEMBRANE ASSEMBLY: DESCRIPTION OF A KINETIC APPROACH BASED ON THE THEORY OF MEMBRANE BIOGENESIS	93
3.1.	Concepts in Membrane Biogenesis and Turnover	94
3.2.	Kinetic Approaches to the Study of Membrane Biogenesis	103
3.2.1.	Isotopic Techniques in Studies of Membrane Flow and Turnover.	103
3.2.2.	Myelin Proteins : Topographic Localization in the Myelin Sheath and their Site of Synthesis.	110
3.2.3.	Myelin Protein Turnover	112
3.2.4.	Assembly of Myelin Proteins	113
3.3	A Mathematical Description of Protein Translocation and Its Application to Time-Staggered Double Isotope Experiments	115
3.3.1.	Definition of "Compartment Space".	117
3.3.2.	Definition of the General Transport Function $\alpha_i(\phi_n, t)$ and Degradation Function $\beta(\phi_n, t)$ .	120
3.3.3.	Definition of TSDI Parameters as a Function of $\alpha_i(\phi_n, t)$ and $\beta(\phi_n, t)$ .	125
3.3.4.	Interpretation of Q, $\Delta Q$ , and R Parameters Based on Temporal Inferences.	131

3.3.5.	Delay Times	135
3.3.6.	Closing Remarks	137
	Appendix	140
3.4	References	143

CHAPTER 4. STUDIES ON SUBCELLULAR FRACTIONS WHICH ARE INVOLVED IN MYELIN MEMBRANE ASSEMBLY : ISOLATION FROM DEVELOPING MOUSE BRAIN AND CHARACTERIZATION BY ENZYME MARKERS, ELECTRON MICROSCOPY AND ELECTROPHORESIS 151

4.1.	Introduction	151
4.2.	Experimental Procedures	153
4.2.1.	Materials	153
4.2.2.	Subcellular Fractionation	153
4.2.3.	Calculation of Sedimentation Coefficients.	156
4.2.4.	Determination of Protein	157
4.2.5.	Determination of RNA	157
4.2.6.	Electron Microscopy	158
4.2.7.	Gel Electrophoresis	158
4.2.8.	Immunochemical Identification of Myelin Proteins	159
4.2.9.	Enzyme Markers	159
4.3.	Results	161
4.3.1.	Subcellular Fractionation: Consideration of Sedimentation Parameters.	161
4.3.2.	Morphological Assessment by Electron Microscopy	165
4.3.3.	Recovery of Subfractions Determined by Protein Content.	167
4.3.4.	Enzyme Markers	169
4.3.5.	Distribution of RNA	174
4.3.6.	Myelin Markers	177



4.4. Discussion	182
4.5. References	190
CHAPTER 5. STUDIES ON SUBCELLULAR FRACTIONS WHICH ARE INVOLVED IN MYELIN MEMBRANE ASSEMBLY : LABELLING OF MYELIN PROTEINS BY A DOUBLE RADIOISOTOPE APPROACH INDICATES DEVELOPMENTAL RELATIONSHIPS	
5.1. Introduction	197
5.2. Experimental Procedures	199
5.2.1. Materials	199
5.2.2. Subfractionation Protocol	199
5.2.3. Isotope Administration	199
5.2.4. Determination of Radiolabel Purity	201
5.2.5. Separation of Proteins	202
5.2.6. Determination of Radioactivity	202
5.2.7. Data Handling and Standardization	204
5.3. Results and Discussion	204
5.3.1. Characteristics of the System and the TSDI Protocol	204
5.3.2. Application of the TSDI Protocol	207
5.3.3. Determination of Accumulative Product Compartments Through the Interpretation of Q values.	213
5.3.4. Determination of Degrading or Precursor Compartments Through the Interpretation of Q values.	220
5.3.5. Interpretation of P values	224
5.4. Concluding Remarks	225
5.5. References	232

CHAPTER 6. . . EPILOGUE	236
6.1. Commentary on Theoretical Contributions	236
6.2. Commentary on Experimental Results	237
6.3. References	239
CONTRIBUTIONS TO ORIGINAL KNOWLEDGE	241
FOOTNOTES	244

\*\*\*\*\*

## LIST OF ABBREVIATIONS

### Cytostructural and Histological terms :

CNS	Central Nervous System
EMP	Endomembrane plates
GA	Golgi Apparatus
LY	Lysosomes
MY	Myelin or Myelin Membranes
PM	Plasma Membrane
PNS	Peripheral Nervous System
RER	Rough Endoplasmic Reticulum
SER	Smooth Endoplasmic Reticulum
VS	Vesicles

### Myelin Constituents :

CNP	2', 3'-cyclic nucleotide 3'-phosphodiesterase
MAG	Myelin 'Associated' Glycoprotein
MBP	Myelin Basic Protein
Po	PNS Myelin Major Glycoprotein
P <sub>2</sub>	A myelin protein
PLP	Myelin Proteolipid Protein or Myelin Lipophilin

### Other Terms :

IDI	Isochronous Double Isotope experiments
K	Kilodalton
M	Molecular Weight

PAGE	Polyacrylamide Gel Electrophoresis
SDI	Synchronous Double Isotope experiments
TSD <sup>8</sup>	Time-Staggered Double Isotope experiments

## ACKNOWLEDGEMENTS

I wish to thank Dr. Peter E. Braun for the liberty he offered me to explore new avenues of research, for his help, his enthusiasm and his patience.

I am greatly indebted to the skillful technical assistance of Elsa Horvath, as well as to her friendship and accurate criticism.

I am grateful to all members of this laboratory for their cheerfulness and occasional technical assistance. Specially to Kim Kasperski for her collaboration in the morphological characterization of the subfractions and her participation in many discussions. To Benjamin Rovinski and Jeff Ulmer for their companionship, and to Dr. Hung Lee, for his friendship and help in proof-reading this thesis.

Brenda Macevicius, Isaac Sandler, Michelle Murin, Antoinette Gagne, Loraine Verner, Ellen Dempsey, René Cosgrove, Dr. Dolores Ramirez, Dr. Rafael Méndez, Dr. Pablo Aguilar, Dr. Sofia Leticia Morales, Dr. Sara Szuchet, Dr. Rosario Barroso-Moguel and Dr. Costero, deserve special mention for the part they all have played in shaping my personal and professional life.

I would like to thank to all members of the Department of Biochemistry, and specially to Eileen Relations, Dr. Walter Mushynski, Dr. Martin Zuckermann, Eduardo Pereira, Dr. Esau Hosein and Abraham Binder, for their help and encouragement.

I am grateful to Diana Iasenza, Michelle Murin and Samiun Khan for typing parts of this thesis. I am also grateful to Kathy Teng for photography and Kathy Wilmot for her help printing

this manuscript.

I acknowledge the Multiple Sclerosis Society for their uninterrupted financial help, for which I am greatly indebted.

I also thank the Faculty of Graduate Studies and Research for Fees Bursuaries and the Dean of the School of Medicine-Dr. Glorieux for a scholarship that allowed me to finish this thesis.

I thank all, for their hospitality.

## PROLOGUE

20 "During ontogeny and also during phylogeny (as judged by comparative anatomy) a number of characteristic changes occur in the cells and tissues of the brain. Chief among these are blood supply, cell form, and that intriguing phenomenon called myelination."; "The formation of myelin appears to be related not only to the taxonomic position of the animal, but also to the stage of embryological development and of the phylogenetic antiquity of the fiber in question." (Pinckey J. Harman, "Paleoneurologic, Neoneurologic, and Ontogenetic Aspects of the Brain Phylogeny", James Arthur Lecture on the Evolution of the Brain (1957); The American Museum of Natural History.)

In 1976 I received my BSc. degree at the Instituto Tecnológico y de Estudios Superiores de Monterrey. My area of concentration was Organic Synthesis and the isolation of natural products. In addition to chemistry I had long standing interests in membrane biology, as well as the ontogenesis of the brain. This interest became intensified after a year's training in the Mexican National Institute of Neurology. I was fortunate to be supervised by two excellent histoneuropathologists: Dr. Isaac Costero, a friend and a teacher, and Dr. Rosario Barroso-Moguel. Upon my arrival at McGill in 1977 I joined the research team supervised by Dr. P.E. Braun to pursue studies on the isolation and characterization of a putative myelin transport vesicle (Barbarese et al., 1978; Braun et al., 1980). The atmosphere of

the laboratory at that time played an important role in the development of many of my ideas. I soon realized that in order to understand the complex nature of many disastrous myelin neuropathies, the study of myelin needs to be approached within a much wider scope:

Recent work has shed further light on the role of myelogenesis<sup>1</sup> in the functional and behavioral maturation of the brain (Yakovlev and Lecour, 1967; Lecour, 1975). In addition, the excellent comparative studies of Flechsin (1920), Langworthy (1933) and Ariens Kappers et al., (1936), and a lengthy list of neurophysiological and ultrastructural studies, further attest to the specificity of myelination in both the PNS and the CNS (for a review see Waxman and Foster, 1980; Waxman, 1972). The study of these sources brings into focus a new perspective that I find necessary in order to fit the ultrastructural and molecular events underlying myelogenesis in the general context of brain development and the evolution of behavior. Hence, the reasons for myelin research should not be restricted to the problem of demyelinating neuropathies, or for that matter of any other narrow context, that will deprive the study of myelination, myelogenesis, and indeed demyelinating neuropathies from a multidisciplinary approach (Bunge, 1968; Johnston and Roots, 1972).

The first chapter presents a general description of the biology of myelin at the ultrastructural, biological and molecular levels. This approach is required to delineate the complexities encountered in the design of developmental experiments. It also has served as the guide to a complete reassessment of whole-brain subfractionation protocols used in myelin research (Chapter 4), with the potential to



create an empirical system of developmentally defined myelin subfractions. The search for intracellular carriers of myelin components led us to the use of a previously reported time-staggered double isotope (TSDI) kinetic approach (Benamins et al., 1976). However, the simplified interpretation of Benamins and Morell (1978) proved inadequate, and a more extensive conceptualization of the technique was developed. This gave rise to an interpretive model (Chapter 3) that has been applied to the analysis of our TSDI protocols (Chapter 5).

To keep in line with the holistic objectives of our experimental approach, the intuition of an intimate relationship between the molecular assembly of the myelin membrane and its morphogenesis led me to challenge the classical views of myelin morphogenesis (Geren Uzman, 1956) and to propose a novel intracellular mechanism of spiral formation (Chapter 2). A discussion of some of the particular biochemical consequences of this proposal are discussed in relationship to our experimental results (Chapter 5).

It would be next to impossible for anyone engaged in a narrow area of biochemical research to see and appreciate, at least some of the many directions and missing links of the field, would it not be for the explicit comments, proposals and discussions of so many excellent scientists whose work has triggered my interest during the last couple of years.

## REFERENCES PROLOGUE

- Ariens Kappers, C.U., Huber, G.C. and Crosby, E.C. (1936). 'The Comparative Anatomy of the Nervous System of Vertebrates, Including Man'. The Macmillan Co., N.Y.
- Barbarese, E., Carson, J.H. and Braun, P.E. (1979). Accumulation of the four myelin basic proteins in mouse brain during development. J. Neurochem., 31: 779
- Braun, P.E., Pereyra, P.M. and Greenfield, S. (1980). 'Mechanisms of Assembly of myelin in mice: A new approach to the problem'. In 'Neurological Mutations Affecting Myelination'. (Ed. Baumann, N.) Elsevier Biomedical Press. pp: 413
- Bunge, R.P. (1968). Glial cells and the central myelin sheath. Physiol. Rev., 48: 197
- Benjamins, J.A., Miller, S.L. and Morell, P. (1976). Metabolic relationships between myelin subfractions: entry of galactolipids and phospholipids. J. Neurochem., 27: 565
- Flechsig, P. (1920). 'Anatomie des menschlichen Gehirns und Rückenmarks auf myelogenetischer Grundlage'. Thieme, G. Leipzig. pp: 9
- Geren Uzman, B. (1954). The formation from the Schwann cell surface of myelin in the peripheral nerves of chick embryos. Exp. Cell Res., 7: 558
- Johnston, P.V. and Roots, B.I. (1972). 'Nerve Membranes: A study of the biological and chemical aspects of the neuron-glia relationships'. Pergamon Press. Toronto
- Lecours, A-R. (1975). 'Myelogenetic Correlates of the Development of Speech and Language'. In 'Foundations of Language Development: A multidisciplinary approach'. Vol 1. (Ed. Lenenberg). Academic Press. pp:122
- Langworthy, O. (1933). Development of behaviour patterns and myelination of the nervous system in the human fetus and infant. Contr. Embryol., 139: 1
- Waxman, S.G. (1972). Regional differentiation of the axon: A review with special reference to the concept of the Multiplex Neuron. Brain Res., 47: 269
- Waxman, S.G. and Foster, R.E. (1980). Ionic channel distribution and heterogeneity of the axon membrane in myelinated fibers. Brain Res. Rev., 2: 205

Yakovlev, P.I. and Lecours, A-R. (1967). 'Myelogenetic Cycles of Regional Maturation of the Brain'. In 'Regional Development of the brain in Early Life'. (Ed. Minkowski, A.). F.A. Davis Co. Pha. pp:3

## 1. BIOLOGY OF MYELIN

### 1.1. Introduction

Myelin can be considered a passive insulator that permits the conduction of impulses in a "saltatory" fashion. This interpretation applies, partially, to PNS fibers which require maximization of conduction, and which were the ones used as the experimental system to develop the theory of "saltatory" conduction (for a review see Rogart and Ritchie, 1977). However, other important aspects of myelin biology are beginning to be appreciated through studies of CNS myelinated axon conduction (Waxman, 1972) as well as the relationships between conduction velocity and the dimensions of the axon-myelin unit (Rushton, 1951; Waxman and Bennett, 1972). The emerging picture indicates that the mechanism of conduction is the same for the CNS and the PNS (Rogart and Ritchie, 1977) and that it requires a very intimate physiological cooperation between axon and myelin. The role of myelin in the biochemistry of conduction is undergoing revision in the light of new electrophysiological studies (Cohen et al., 1968; Adelman et al., 1977; Grisell, 1979), X-ray diffraction studies (Padron and Mateu, 1982), and biochemical characterizations (Ellisman et al., 1980; Huo Lin and Lees, (1982)). Moreover, changes in the dimensions of ensheathment (i.e. internodal length, axon and myelin diameters, etc.) may modulate axonal conduction velocities, a phenomenon commonly observed in various specialized regions of the CNS (Waxman and Foster, 1980). Ensheathing cells have also been implicated in the maintenance of the axoplasm under normal and

diseased conditions (Spencer and Thomas, 1974).

In the following sections I shall explore some of the biology of ensheathment from phylogenetic and ontological perspectives. On the one hand, this should allow for a broader appreciation of the role of myelin in the development and operation of the nervous system and on the other, it will lead to a reassessment of proposed mechanism of myelination as well as the exposition of a new model of myelin morphogenesis in the next chapter.

#### 1.2. Evolution and Ontophylogenesis of Myelination

Several important works have described the phylogenetic distribution of axonal ensheathment in vertebrates and invertebrates (Bunge, 1968; Johnston and Roots, 1972; Tréherne, 1981). However, the role of the neuroglia in the evolution and adaptations of the brain architecture has been overlooked or simply not approached. One reason for this can be found in the secondary role that has been assigned to these cells with respect to the maturation of neuronal networks.

Although well documented, many researchers have failed to recognize that nervous tissue has required the development of "glial" cells around axon bundles (e.g. some Coelenterates; the ring nerves of the *Hydromedusae*; Horridge, 1968) or neuronal cell bodies in order to organize themselves into ganglia (e.g. the primitive ganglia in annelida, arthropoda, mollusca, plathelminthes, and nemertinea; Bullock and Horridge, 1965; Bunge, 1968). Coincident with this new multicellular organization is the appearance of well differentiated synaptic transmission (Horridge, 1968). The relationship of

neuroglial differentiation to the maturation of brain functions and adaptive behaviours can thus not be further ignored (Lecours, 1975).

From the above observations I wish to advance the suggestion that the neuroglial cells must satisfy two complementary functions, first as a topographical delineator, and second as a metabolic coupler.

#### 1.2.1. The Neuroglia in the Evolution of the Brain Architecture

The study of the evolution of brain structures is restricted to the analysis of endocasts of fossil skulls (Jerison, 1973) with all the limitations that this method entails. Nevertheless, interesting relationships have been described among endocast volumes - which can be shown to be proportional to brain weight-body length, phylogenetic and paleontological distributions, and the Neuron-Glia index (Jerison, 1973; Friede and van Houten, 1962; Tower and Young, 1973a,b). The results of these investigations can be summarized as follows: Important transitions in the evolution of vertebrate brain can be traced as an increase in endocast volumes (and by inference, in brain weight). It can be shown that these changes occurred only at some discrete stages of the paleontological scale. Intermediary transitions involved either an increase in body weight and thus a proportional increase in brain weight to maintain the same brain-volume to body-length ratio, or new osteological adaptations that gave rise to new body shapes but without any considerable demand on brain structures. Hence, it can be observed that the transition from sea to land required minimal brain transformations. Some changes can be detected in the endocast volumes in the transformation of

amphibians to reptiles. However, the transition from reptiles to birds demanded one of the first considerable enlargements of the brain cavity and the development of complex cerebellar structures. An other small transition seemed to have occurred in the transformation of reptiles to mammals, which included some changes in the area of distance perception (olfactory and visual systems). Perhaps one of the most radical changes in brain architecture occurred during the Tertiary. During this period, a major flexure appeared at the level of what we know as the midbrain, greatly altering the shape of the tubular form of the brain in more ancient structures, and opening the way for the enlargement of the neocortex that characterizes the mammalian brain (Jerison, 1973; Romer 1969).

The role of the myelinating cells in the evolution of brain architecture and function can be perceived through the comparative study of specific brain structures. These studies, however, represent only a phylogenetic picture of events and thus the structures observed indicate primarily radial adaptations rather than evolutionary ones.

One of the most studied structures of the brain is the cerebellum (Llinas, 1969), an organ with important functions in body movement control (Crosby, 1969). The phylogenesis of myelinated fibers in this organ can be followed by analyzing the development of intrinsic fibers and the fiber paths constituting the peduncles. The intrinsic fibers of the cerebellum are of three types: Commissural fibers, association fibers and corticonuclear fibers (Crosby, 1969). The three cerebellar peduncles - the inferior, the middle, the superior - of higher forms carry fascicles interrelating the cerebellum on the one hand with brain stem centres and on the other with spinal cord levels. On the

basis of their components, the inferior and the superior peduncles have representation in essentially all vertebrates (Crosby, 1969).

In *Cyclostomes* the cerebellum appears as a rudimentary structure without a well defined Purkinje cell layer, and unmyelinated inferior peduncular fibers (Bertolini, 1964). In *Elasmobranchs* the cerebellar structure is more complex but still no white matter is present in the pontine fibers, although "myelinated" fibers are present in other regions of the CNS of the sharks (see Section 1.3) (Bakay and Lee, 1966). In *Actinopterygii* white matter can be detected in afferent and incoming fibers of the cerebellum. Their Purkinje and granular cell layers are, however, unevenly distributed and no clear corticonuclear path can be detected (Romer, 1969). *Teleostomi*, that represent a well established adaptive radiation of the *Actinopterygii*, contain some myelinated fibers between well defined Purkinje and granular layers (corticonuclear fibers) and myelinated peduncular fibers.

The line of the *Sarcopterygii* gave rise to the primitive amphibians, and counts among its contemporary representatives the *Dipnoi* and the *Coelacanth latimeria*. Cerebellar architecture and its hodography is very similar in these species to that of *Actinopterygii*. This situation extends up to the tailed amphibians. *Anurans*, *Urodeles* (both can be considered regressions of more primitive amphibians; Romer, 1969) and *Reptilia* begin to incorporate some new fiber paths and a more complex cerebellar architecture. Nevertheless, myelination of corticonuclear fibers does not appear until the birds and mammals. In these species myelination of the corticonuclear fibers is extensive, cerebellar lobulization is very complex and new myelinated and species specific peduncular paths have appeared (Crosby, 1969).



In mammals the situation is even more extreme with the appearance of direct corticocerebellar connections as a consequence of cephalization. Hodological studies of mammalian cerebellum (Voogd, 1969) indicate that each cerebellar lobule and sublobule display their own characteristic distribution of afferent fibers. This represents with respect to the afferent connections of the lobules and sublobules, regional specializations (radial adaptations) rather than mere expansions of the cerebellar structure (phylogenetic - evolutive - adaptations). Ontophylogenetic studies on the other hand, show a phylogenetic correlation of cerebellar myelogenesis (Harman, 1957; Crosby, 1969; Verbitskaya, 1969). Lastly, the human cerebellum is the only one to contain myelinated associative fibers which up to this species had become increasingly interconnected but no myelination had yet taken place.

#### 1.2.2. The Glia - Neuron Interaction: An organic relationship

Recent observation of the interrelationship between neurons and glia under normal and pathological conditions have brought to light a new way of thinking about the nervous system. Many of these ideas have been expressed in the work of Mugnaini (1978, ~~stet~~ Massa and Mugnaini, 1982), Johnston and Roots (1972), Waxman (1972, Waxman and Foster, 1980), among other physiologists and morphologists.

It is possible from the above discussion on the phylogenesis of myelination, from the close and complex membrane to membrane associations that have been characterized in recent years among all these cell types (see Table 1.2.1; taken from Mugnaini, 1978), and

# Microenvironment of myelin membrane

## CNS

- |                        |  |
|------------------------|--|
| 1) Exoplasmic aspect   | <ul style="list-style-type: none"> <li>general extracellular space</li> <li>intramyelinic extracellular space</li> <li>internodal periaxonal extracellular space</li> <li>paranodal periaxonal extracellular space</li> <li>central nodal substance (scarce)</li> </ul>  |
| 2) Protoplasmic aspect | <ul style="list-style-type: none"> <li>thick cytoplasmic mass</li> <li>thin cytoplasmic layer</li> <li>moiety of major dense line</li> </ul>   |
| 3) Next neighbor       | <div style="display: flex; align-items: center;"> <div style="writing-mode: vertical-rl; transform: rotate(180deg); margin-right: 5px;">outside the sheath</div> <div> <ul style="list-style-type: none"> <li>compact portion of outer myelin turn*</li> <li>myelinated fiber</li> <li>cytoplasmic portion of outer myelin turn**</li> <li>oligodendrocytic cell body or process**</li> <li>astrocytic cell body or process</li> <li>microglial cell body or process</li> <li>nerve cell body or dendrite or myelinated axon</li> </ul> </div> </div> <div style="display: flex; align-items: center; margin-top: 10px;"> <div style="writing-mode: vertical-rl; transform: rotate(180deg); margin-right: 5px;">within the sheath</div> <div> <ul style="list-style-type: none"> <li>compact portion of myelin lamella*</li> <li>cytoplasmic portion of myelin lamella**</li> <li>internodal axolemma</li> <li>paranodal axolemma</li> <li>nodal axolemma</li> </ul> </div> </div> |

## PNS

- |                        |   |
|------------------------|---|
| 1) Exoplasmic aspect   | <ul style="list-style-type: none"> <li>general extracellular space</li> <li>intramyelinic extracellular space</li> <li>internodal periaxonal extracellular space</li> <li>paranodal periaxonal extracellular space</li> <li>peripheral nodal substance</li> </ul>   |
| 2) Protoplasmic aspect | <ul style="list-style-type: none"> <li>thick cytoplasmic mass</li> <li>thin cytoplasmic layer</li> <li>moiety of major dense line</li> </ul>  |
| 3) Next neighbor       | <div style="display: flex; align-items: center;"> <div style="writing-mode: vertical-rl; transform: rotate(180deg); margin-right: 5px;">outside the sheath</div> <div> <ul style="list-style-type: none"> <li>basal lamina and collagen fibers</li> </ul> </div> </div> <div style="display: flex; align-items: center; margin-top: 10px;"> <div style="writing-mode: vertical-rl; transform: rotate(180deg); margin-right: 5px;">within the sheath</div> <div> <ul style="list-style-type: none"> <li>compact myelin lamella</li> <li>cytoplasmic myelin lamella</li> <li>internodal axolemma</li> <li>paranodal axolemma</li> <li>nodal axolemma</li> </ul> </div> </div> |

\*,\*\* Single and double asterisks mark membrane domains of presumably similar composition.

Table 1.2.1. Tentative list of the parameters which may correspond to differences in the microenvironment of the myelin membrane. [From Kugniari, 1978].

from the fragmentary evidence for the compartmentation of brain metabolism in specific cellular structures (Balazs and Cremer, 1971), to intuit that the relationship between neurons and glial cells represents a different level of biological organization. In the same manner as the organelles of a cell can be considered individual units that - only when coordinated by their mutual interactions - give rise to the cellular level of organization; so the cooperation of the neurons and glial cells through complex multipotential membrane to membrane interactions (see the concept of Multiplex neuron; Waxman, 1972), can give rise to a level of organization that is above the one encountered in other tissues.

The glial-neuron interaction becomes in this context a specialized working unit or ERGON, and a given area of the brain is then characterized by a specific set of ergonic units that are particular to the phylogenetic and adaptive state of the given brain region. Adaptive pressures will thus affect each brain area differently. This concept also implies, that to each set of ergons, the cooperative of glia-neuron cells will express specific metabolic adaptations that will allow the formation of a self contained metabolic compartment (i.e. specific neurotransmitters and their metabolism by surrounding neuroglia).

Moreover, implicit to the idea of ERGON is the concept of "Cooperating cell sets", as described by Boyse and Cantor (1978) in their hypothesis of "evolution by program duplication": ... in the context of ontogeny it is helpful to envisage the unit of differentiation not as a single cell but as a pair of cells that undergo complementary differentiative steps to prepare them for their

collaborative task".

The most obvious example of an ERGON is the ensheathment of axons by neuroglial cells. A closer ontological analysis of any subsystem of the nervous system will, however, disclose the clear ontological and architectonic cooperativity between the selective and controlled expression of specific intercellular associations and metabolic pathways. The optic system is especially accessible to research and is also one where the local variations in cellular architecture (retina, optic nerve, chiasma) originating from different clones, give rise to very specific ergonic relationships along the system (Bentley and Keshishian, 1982; Wiesel, 1982).

The intrinsic ontophylogenetic implications of the ERGON concept should give rise to a reinterpretation - when necessary - of the apparent disconnectiveness among the ultrastructural, metabolic and physiological adaptations of the neuroglia among invertebrates and between these and the vertebrates. (Bullock and Horridge, 1965; Bunge, 1968, 1969; Johnston and Roots, 1972; Lane, 1981). In the case of the myelin, the ERGON concept should be helpful to understand the physiological and metabolic interrelationship between axon and myelin-forming cells.

### 1.3. A General Outline of Myelination

Several lines of morphological and biochemical evidence (Rosenbluth, 1966; Smith, 1967; Banik and Davison, 1969) have indicated the presence of semi-discrete stages in the overall process of myelination. These observations led Johnston and Roots (1972) to a

conceptualization of a two stage myelin formation process. Their scheme centers strictly on the events of axonal ensheathment and their implication in specific demyelinating neuropathies: "The first stage may be seen as the formation of a myelin template in which the genetically determined protein component controls the lipid pattern with which it can associate. When the number of turns of the lamellae reaches a critical point, the myelin becomes an individual metabolic entity and a second stage of myelination commences. In the second stage the myelin may by itself synthesize and/or receive from the glia new protein and lipid constituents which engage in a self-assembly of lipoprotein units. Thus after the deposition of certain critical level of glial plasmalemma, the myelin would, in itself, 'grow outwards' from the axon."

With the experimental corroboration of the axon-mediated control of myelination (Aguayo et al., 1976, 1977, 1981; Weinberg and Spencer, 1975, 1976, 1979) and the extensive description of the high degree of specificity in the interaction between axons and myelin-forming cells (Waxman and Foster, 1980), myelogenesis in the PNS was conceptualized by Spencer and Weinberg (1978) into a scheme that includes myelination, remyelination and demyelination in the context of a selective expression of surface receptors on the axonal and Schwann cell's plasma membrane. In this hypothesis two sets of surface receptors would be involved in the regulation of axon bundle fasciculation and the identification of pro-myelin axons by the Schwann cells. A third set would regulate the initiation of ensheathment once a 1:1 relationship between pro-myelin axons and Schwann cells has been achieved (Martin and Webster, 1973; Webster et

al., 1973); Waxman and Foster, 1980).

In the PNS, axon bundle fasciculation is accomplished during the proliferative stage of Schwann cell differentiation into myelin-forming cells (Martin and Webster, 1973). In the CNS, on the other hand, fasciculation of axon bundles is region-specific and is performed by astrocytes during their proliferative stage. A second proliferation and differentiation of glioblasts is then required to give rise to CNS myelin-forming cells (oligodendrocytes) which will displace the initial astrocyte-axon association in those axons or neuronal perikarya that will become myelinated.

All these events require, in both the CNS and the PNS, very precise timing and a complex interdependence with the maturation of the vasculature of the nervous tissue (see Peters et al., 1976 for a review), with humoral factors (Walters and Morell, 1981) and with the nutritional levels of the animal during development (Martinez, 1982; Wiggins, 1982). If one accepts the regulation of axon ensheathment by 'local factors' other than just axonal surface signals, then many of the oligodendroglial morphological types described in the literature (Bunge et al., 1961; Mori and Leblond, 1970; Tennekoon et al., 1980), the regional variations in the chemical composition of CNS and PNS myelin (Zgorzalewicz et al., 1974; Banik and Smith, 1977; Sprinkle et al., 1978), and the formation of abnormally thin and short myelin sheaths during remyelination of CNS axons (Harrison and McDonald, 1977; Blakemore and Murray, 1981) can be accounted for by the adaptation of the neuroglia to specific ontological, trophic and humoral requirements (Remahl and Hildebrand, 1982).

The fundamental concepts behind these ideas are, that myelination is sequential and that the events involved in the regulation of its development are the same for both the PNS and the CNS systems. The phenotypic differences between the ensheathing cells of these two systems have not precluded the formation of the same spiral arrangement around an axon - a topology that can be traced far back in the phylogenetic tree of vertebrates (Section 1.2), and can be intuitively already in many of the "myelinated" giant axons of some invertebrates (Hama, 1959; Bullock and Horridge, 1965; Heuser and Doggenweiler, 1966; Johnston and Roots, 1972). Hence, it can be expected that the same spiralling mechanism is operative under all circumstances as proposed in the "Spiral-Wrapping" hypothesis for the PNS (Geren Uzman, 1956; Robertson, 1959) and its application to CNS myelination (Bunge *et al.*, 1961; Hirano and Dembitzer, 1967; Morell, 1977).

Nevertheless, a closer examination of the morphology of ensheathment seems to indicate more than one approach to the same functional-morphological relationship between axons and myelin-forming cells; for example: 1) the myelination of neuronal perikarya of some ganglia (Rosenbluth, 1962b; Dixon, 1963; Cantino and Mugnaini, 1975; King, 1976 a,b; Romand *et al.*, 1980); 2) of neuronal perikarya and dendrites in the olfactory bulb of several species (Willey, 1973; Braak, *et al.*, 1977; Diaz-Flores *et al.*, 1977; Burd, 1980; Tigges and Tigges, 1980); 3) of neurons in the dorsal horn of the mouse and monkey's spinal cords (Blinzinger *et al.*, 1972; Beal and Cooper, 1976); 4) of granular cells in the cerebellum of many higher vertebrates (Suyeoka, 1968; Cooper and Beal, 1977); 5) and the ensheathment of axons in lower vertebrates (Rosenbluth, 1966; Celio,

1979; Cullen and Webster, 1979). It seems, therefore, more appropriate to depart from the view that the molecular differences between the myelin of the CNS and that of the PNS, imply alternative adaptations of the mechanisms (biogenic and morphogenic) responsible for the formation of myelin.

In any case two fundamental elements are conserved between the CNS and the PNS systems. The first is the formation of a spiral, and the second is that the codes implicated in the regulation of ensheathment must produce a similar "Bauplan" (outline), albeit their integration and decoding by the different myelin-forming cells might be mediated through similar or different receptor/signal systems (Raine, 1976; Jung *et al.*, 1978; Benfey and Aguayo, 1982).

Evidence for the similarities between the general myelination Bauplan of the CNS and the PNS will be discussed below in the context of the biochemistry and morphogenesis of myelin development. The results further corroborate the existence of stages in the process of myelination. However, the literature seems to indicate that these stages represent discrete phases of a complex genetically programmed event. Furthermore, each phase, permits the myelin-forming cell and the axon to choose between specific phenotypic alternatives that will permit - within certain boundaries - the expression of the observed specificities of the axon-myelin interaction (Waxman and Foster, 1980; Blakemore, 1981). Table 1.3.1 summarizes the four phase outline of myelination in the PNS and the CNS.



TABLE 1.3.1.

# MYELINATION OUTLINE

CNS

PNS

## PHASE Zero :

- |   |  |
|---|--|
| 1) Astroblast proliferation and differentiation                             | 1) Schwann cell proliferation and differentiation                        |
| 2) Fasciculation of axon bundles  |  |
| 3) Activation of oligodendroblast differentiation                           | 3) Schwann cell proliferation and differentiation into promyelelin cells |
| 4) Initiation of nodal demarcation  |  |
| 5) Oligodendrocyte proliferation and differentiation into promyelelin cells | 5) 1:1 Relationship with axons   |

\*\*\*\*\*

## PHASE I :

- 1) Activation of ensheathment commitment
- 2) Second stage of nodal demarcation
- 3) Expression of lipid precursors and related gene products
- 4) Initial bidirectional and multivesicular ensheathment ( 1 to 10 lamellae )
- 5) Activation of cell specific myelin gene products

\*\*\*\*\*

## PHASE II :

- 1) Active phase of myelination
- 2) Elongation of internodes and enlargement of axonal diameter
- 3) Third stage of nodal demarcation (paranode formation)
- 4) Second proliferative phase to maintain a critical myelin to axon surface relationship

\*\*\*\*\*

## PHASE III :

- 1) Terminal phase
- 2) Fourth stage of nodal demarcation ( nodal-paranodal remodelling)
- 3) Physiological maturation of myelinated fibers (modulation of the g ratio through the removal of excess myelin or further deposition)
- 4) maintenance of Myelin

\*\*\*\*\*

The description of this outline will assume knowledge of some of the fundamental constituents of PNS and CNS myelin. For a review the following sources are recommended: Morell and Norton (1980), and Morell (1983). Briefly, myelin membranes in both the CNS and the PNS are composed of 30% protein and 70% lipid, with approximately equal parts of cholesterol, glycolipids and phospholipids. Differences between the two systems occur primarily among their protein classes.

A major integral membrane glycoprotein (Po) constitutes up to 80% of the PNS myelin protein. The rest is made up of many myelin specific proteins that are also shared by the CNS. The most controversial of these is the P2 protein; originally described as a specific PNS protein. Recent investigations, however, have revealed the presence of this protein in some specific regions of the spinal cord in various species (Trapp et al., 1983) and in only some myelinated segments of PNS fibers (Trapp et al., 1979). The implications of these findings indicate that this protein is a major component of some very particular myelin-forming cells.

The CNS contains two types of major protein components, the lipophilic protein (PLP) - an integral acylated membrane protein - and the family of myelin basic proteins (MBPs), that are associated with the cytoplasmic face of the myelin membrane. Together these two protein types comprise about 70% of all CNS myelin proteins. The other 30% is made up of a series of proteins that have been poorly described. Of them, the most important are the myelin associated glycoprotein (MAG - or as correctly suggested, the myelin glycoprotein MGP (Braun, 1983), and the 2',3' cyclic phospho-nucleotide 3' phosphohydrolase (CNP).

Myelin is also characterized by its abundance of specific lipid classes (cerebroside and sulfatide), long chain fatty acids which are more than 18 carbons long, and the lack of significant amounts of complex gangliosides.

In the context of this analysis, myelination phases are understood outside a specific temporal framework. They are intended to emphasize the phenomenological similarities between myelinating cells of the PNS and the CNS, as well as their phenotypic differences and the consequences of these in the biogenic mechanisms of myelin assembly.

#### 1.3.1. Phase ZERO: Proliferation, Differentiation and Axon Bundle Fasciculation

This phase is characterized by the proliferative activities of the neuroglia population after neuronal proliferation, migration, and major axonal commitment (Sidman and Rakic, 1973; Peters et al., 1976). This happens within a phylogenetic sequence of events which may have different time scales in all vertebrates.

PNS glial cells (Schwann cells) initiate the fasciculation of axon bundles by enclosing a given set of axons under a common basal lamina and "family" of Schwann cells (Martin and Webster, 1973; Webster et al., 1973). Specific associations with large axons and the selection of promyelinated axons begins by displacing axons to the periphery of the bundle and establishing a 1:1 relationship with them, within a unique basal lamina (Webster, 1973). Biochemically, no traces of Po have been found during this period (Wood and Engel,

1976), although more research on this aspect needs to be done.

The situation in the CNS is similar, but not identical. Here the complex architecture of the brain and the interaction of the glial population with early and late neuronal migrations (Sidman and Rakic, 1974), requires a more versatile and at the same time sophisticated approach to axon-bundle fasciculation.

Fasciculation of CNS axons has not been given full consideration, though this event has been clearly demonstrated in the optic nerve (Grossman, 1967; Sturrock, 1975; Skoff et al., 1976 a,b) and in some cervical regions of the spinal cord (Gilmore, 1971; Matthews and Duncan, 1971; Nagashima, 1979). In these cases initial axonal ensheathment is carried out by the astrocyte which at this stage, like its PNS counterpart, is engaged in an active state of proliferation and differentiation. This activity gives rise, on the one hand, to the formation of specific axon fascicles, while on the other, to the third element of the central nervous tissue, the oligodendrocyte (Cajal, 1925-26; del Rio Hortega, 1928) which will be responsible for the myelination of the axons.

It is necessary to draw attention at this point to the presence of centrioles and cilia in many of the (undifferentiated) astrocytes that fit the requirements for phase ZERO (Cajal, 1925-26; Bunge et al., 1961; Skoff et al., 1976a). Their function is still speculative. Schwann cells during this preparative phase have been described with an "axial process that originates at the level of the centrioles of the spindle pole, arches over and runs beyond the midnuclear level ... It contain(s) microtubules and 100nm vesicles." (Martin and Webster, 1973, page 423). If the astrocytic element is similar to that of the

Schwann cell, its function as a guidance to reestablish a specific symmetry or direction after mitosis, appears for the moment the most adequate explanation.

Recent reports have indicated the appearance of a group of proteins, in the molecular weight range of 30 to 40 kilodaltons, from cerebral and cerebellar aggregate systems that crossreact with specific MBP antibodies (Barbarese and Pfeiffer, 1981). These results have been interpreted in the context of gene modulation; the observed proteins being the translation product of unspliced genes that have been inappropriately activated by the experimental culture system. This would be in agreement with the inability to translate these proteins with mRNA isolated from intact systems (Coleman et al., 1982), although further research is required to come to any conclusion.

#### 1.3.2 Phase I: Spiral Template Formation

Oligodendrocyte proliferation indicates the transition from phase zero to phase I in the CNS (Matthews and Duncan, 1971; Skoff et al., 1976 a,b). In the PNS this transition occurs with the last proliferative burst that permits the exclusion of all pro-myelin axons within single basal laminae and in a 1:1 relationship with Schwann cells (Webster et al., 1973).

The connection between axon and myelin-forming cell becomes at this moment very apparent. Observations indicate that critical axonal dimensions are necessary for the ensheathing cells to engulf the axon. Initially, morphological measurements indicated a correlation between

Figures 1.3.1 a-g. The schematic reconstruction and scaled tracings of the electron micrographs (in Figures 16-21; Knobler et al. 1974). The length of the schematic reconstruction represents 5.0  $\mu$ m of tissue sectioned. Scaled tracings,  $\times 17\ 000$ .

Figure a. A reconstruction of 50 serial sections through a portion of a developing internode in the rat CNS. The outside portion of the counterclockwise-directed layer and the entire clockwise-directed layer are cut away to allow an unobstructed view of the inside leaflet of the counterclockwise-directed layer, and the vermicular process extending from it. The arrow on the right of the figure points to the last portion of the outside leaflet of the bifurcated counterclockwise-directed layer.

Figure b. A reconstruction identical to Figure a, with the outside portion of the counterclockwise-directed layer and the entire clockwise-directed layer intact... The axon (A) is ensheathed by uncompacted oligodendroglial cytoplasm (O). The clockwise-directed layer is inside (IL), and the counterclockwise-directed layer is outside (OL). The dotted line on the right of the figure represents the inside portion of the counterclockwise-directed layer.

Figure c. A reduced-scale tracing of an electron micrograph five sections removed from the first. There is a small round profile (VP) between the axon and the inside layer of ensheathment, in a position corresponding to the tip of the outside layer of ensheathment (OL).

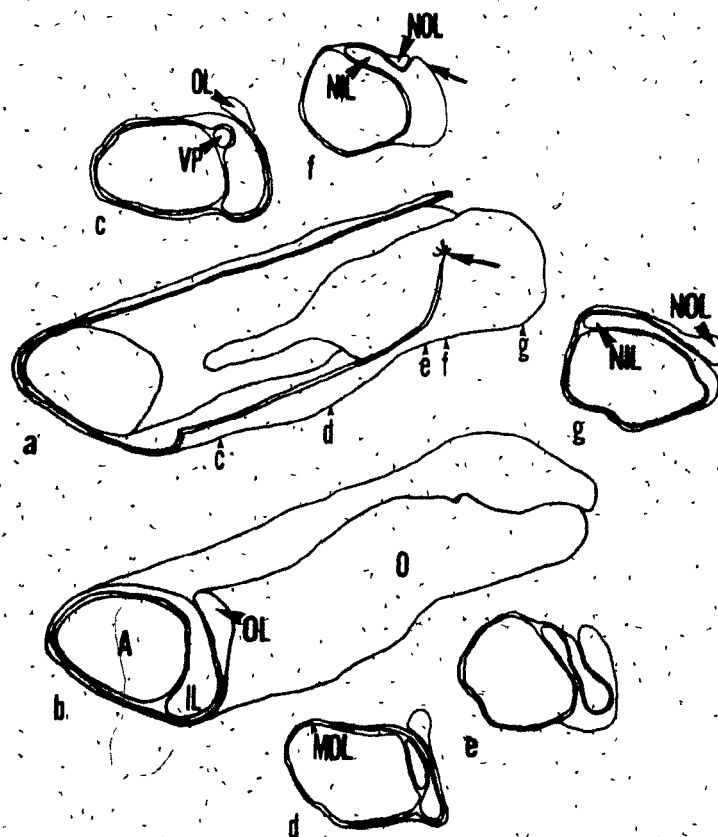
Figure d. A reduced-scale tracing of an electron micrograph 17 sections away. The profile is widening into a plate, and about half a layer of ensheathment is compacted in the form of a major dense line (MDL).

Figure e. A reduced-scale tracing of an electron micrograph 15 sections away. The original clockwise-directed inside layer is interdigitated between the two leaves of the counterclockwise-directed layer.

Figure f. A reduced-scale tracing of an electron micrograph four sections away. The ensheathment remains partially compacted. The clockwise-directed layer now forms the new outside layer (NOL) and the remaining portion of the counterclockwise-directed layer on the inside forms the new inside layer (NIL). The mound of cytoplasm (arrow) is the last portion of the outside leaflet of the bifurcated counterclockwise-directed layer, it is indicated by the squiggly lines in Figure a (arrow).

Figure g. A reduced-scale tracing of the electron micrograph nine sections away. The axon is once again surrounded by uncompacted cytoplasm. The new inside layer (NIL) and the new outside layer (NOL), are clearly visible.

C



ensheathment and a critical axonal diameter (Matthews, 1968; Friede, 1972). This idea, although unsatisfactory, persisted until the outcome of the Rosenbluth-Ellisman controversy indicated that during this preparative phase the axolemma undergoes important changes that will permit the demarcation of the nodal region (Ellisman, 1979; Rosenbluth, 1979; Wiley-Livingston and Ellisman, 1980; Waxman et al., 1982). Recent publications by Friede and Bischhausen, 1982), and the interpretations of Blakemore (1981) of CNS myelination control, further support the idea that the internodal axolemma contains the necessary information for initiating ensheathment as well as the extent of activation.

Morphological observations show that in the CNS, differentiated oligodendrocytes have to displace the astrocytes already in contact with the axons or that some other complex interactions between these two cell types is active during this phase (Nagashima, 1979; Noble, 1982). The initial axon ensheathment by myelin-forming cells has been described only for some regions of the nervous system; the optic nerve (Dermietzel and Krocze, 1980a), the spinal cord (Knobler et al., 1974, 1976) and the sciatic nerve (Webster, 1971). Irrespective of the localization, three dimensional reconstructions indicate that the initial ensheathment occurs by an irregular, bidirectional mechanism (see Figures 1.3.1 and 1.3.2 taken from Knobler et al., 1976; Webster, 1971).

The irregularities of this ensheathment are, however, more obvious in the CNS where complex vermicular processes (Knobler et al., 1976) have been implicated in the bidirectionality of ensheathment. Single field observations in the optic nerve (see Figures 1.3.3 and



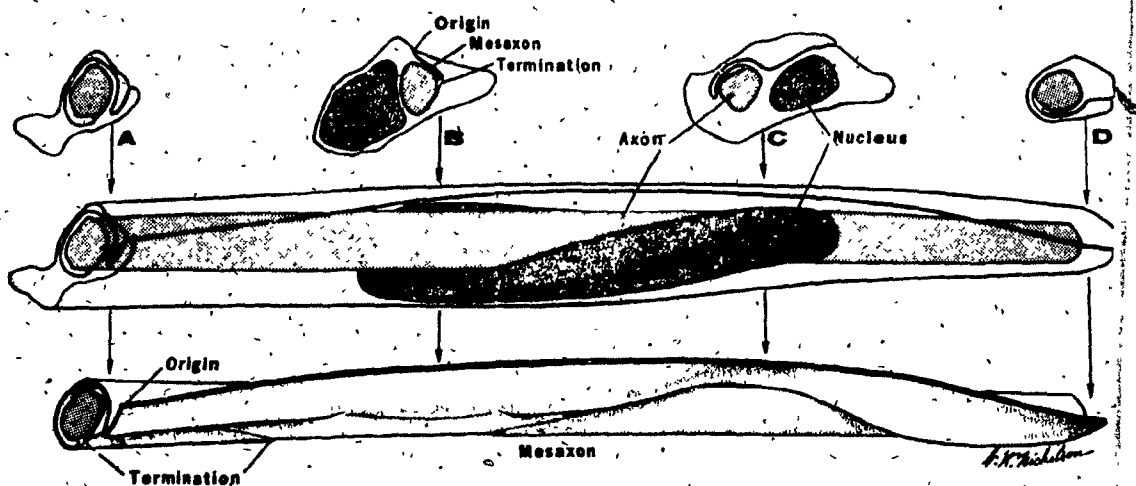


Figure 1.3.2. Three-dimensional representations of the Schwann cell with the position of four transverse levels indicated by arrows. The helical nucleus and relatively constant position of the mesaxon's surface origin are included in the upper figure. The lower one shows the mesaxon as a membrane sheet; its contour and transverse length vary. [From Webster, 1971].

1.3.4 from Dermietzel and KroczeK, 1980) show the formation of the initial wrap around the axon. The ensheathment begins with the first contact of the lips of the glial process, forming the first tight junction between the joining tips of the oligodendrocytic cup.

Morphometry of ensheathment indicates that at least in the CNS the position of the two engulfing tongues are randomly situated with respect to each other during this early stages of ensheathment (Peters, 1964).

Meaningful studies on the biochemistry of CNS myelin during this early stage of development are restricted to the possibility to access specific brain areas in the animals use for experimentation. Reports using whole brain preparations are the most abundant, but these are inappropriate for developmental studies and also limited in scope. Characteristic myelin components have not been found at this early stage. However, the active proliferation of oligodendroblasts must activate specific enzyme complexes in order to commit the oligodendrocytes to axonal ensheathment (Tennekoon et al., 1980). Scattered reports in the literature indicate active fatty acid synthesis from acetoacetate (Yeh et al., 1983), accumulation of C-14 fatty acids (Bourre et al., 1973), active synthesis of dolichol (James and Kandutsch, 1980), and the rapid incorporation of cerebroside into non-microsomal membranes (Yahara et al., 1980) prior to the appearance of distinctive myelin membranes in agreement with the differentiation of oligodendroblasts during phase I.

Biochemical reports for the PNS are very few. Cytochemical studies have indicated the localization of acyltransferase activity in vesicular structures in the periaxonal processes of the Schwann cells

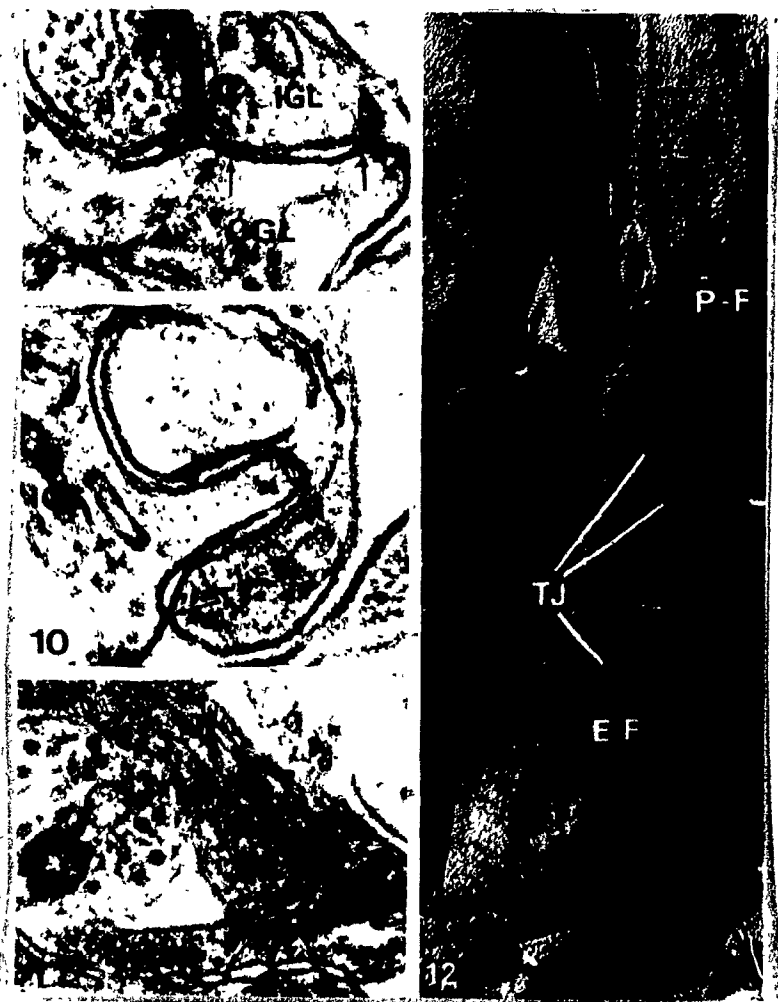


Figure 1.3.3. Illustrates the sequences of tight junction assembly during the onset of the spiralling process (Figure numbers correspond to the originals). [From Deraetzel and Kroczeck, 1980].

Fig 9 Elongation of the mesaxon with the initial formation of the outer (OGL) and the inner glial loop (IGL). Two points of fusion can be clearly discriminated (arrows). x153,000

Fig 10 Insinuation of the inner glial loop (IGL), and the development of the second glial turn; TJ tight junctions. x 153,000

Fig 11 The same phase of myelin development as shown in Figure 10. The tight junctions (TJ) appear as typical membrane thickenings in the potassium permanganate-stained material. x104,000

Fig 12 Tangential fracture of the early spiralization process exposing both E-face (E-F) and P-face (P-F) aspects. The typical configuration of the tight junction (TJ) at this stage of development consists of grooves bearing rows of globules on the E-face and corresponding membrane crests, the top of which is decorated by small furrows on P-face (arrows). Fragments of rows (double arrows) and isolated particles are present on both fracture faces. x46,000.

and the Golgi apparatus (Benes et al., 1973); and the localization of the Po protein in the Golgi apparatus (Trapp et al., 1981) during this early phases of myelin development.

Immunocytochemistry of the Corpus callosum during this early phase reveals the presence of MBPs in the soma of the oligodendrocytes and along their process. No reaction can be detected along the axons (Sternberger et al., 1978; Russel and Nussbaum, 1981). Antibodies against the W1 region (Mr 40 to 50 kdaltons) of the molecular weight spectrum of CNS myelin proteins (which contains among other things CNP and probably other cytoskeletal proteins of the oligodendrocyte), can be detected since the beginning of phase I (oligodendrocyte proliferation). At the moment of the initial ensheathment the activity is localized more intensely in the space below the plasma membrane and in the ensheathing processes, indicating a developmental pattern which is different from that for MBP (Rousell and Nussbaum, 1981).

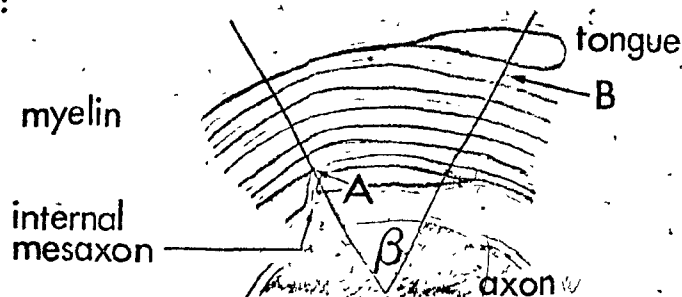
#### 1.3.3. Phase II: Active Deposition of Myelin Membranes

After the deposition of 1 to 6 lamellae, bidirectionality and other irregularities of the ensheathment disappear in PNS fibers (Webster, 1971) and Po protein can now be localized in the periaxonal membranes of the Schwann cell. Production of these and other PNS myelin related proteins and lipids is now accelerated (Wood and Engel, 1976). Compaction of lamellae begins leaving an uncompacted quadrant where cytoplasm and organelles can be found until late in this phase of myelin deposition (Webster, 1971). The number of lamellae increase

logarithmically at a rate that is dependent on fiber tract and initial internodal length (Friede, 1968; Webster, 1971; Williams and Wendell-Smith, 1971; Friede and Bischhausen, 1982; Smith et al., 1982). After the initial burst in axonal diameter during phase I, axons enlarge at a steady rate in phase II (Webster, 1971). Internodal elongation also takes place during this phase and relates in a non linear fashion to the increase in fiber diameter (Fried et al., 1982). The "g" ratio (diameter of the axon/diameter of the fiber) begins to drop rapidly from its unit value at the onset of myelination to its normal (.65) or below normal values by the end of this phase (Fried et al., 1982). Clear cut values are not found in these events and similar dispersions in axon-myelin dimensions are found in both mature and developing fibers. Hence, making use of the recent estimates of total internodal axonal surface area and myelin surface area (or myelin volume) (Friede and Bischhausen 1982; Smith et al., 1982) in developmental studies, it should be possible to predict that the relationships between axon and myelin dimensions during this active phase of myelin deposition maintain, after an initial critical moment (phase I), a linear correlation. Furthermore, the rate of internodal elongation which is directly related to body growth (see for example Friede et al., 1982), if assumed proportional to the extent of myelin production, (Blakemore, 1981), will be expected to control the extension of the active phase of myelination and the rate at which the activity will level off. The result will be the precise arrival at a "g" ratio which is the most appropriate for the internodal and diametral dimensions of the fiber (Friede and Bischhausen, 1982).

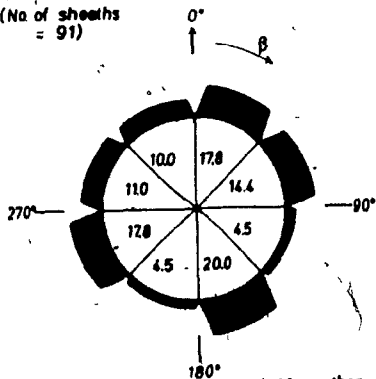
Figure 1.3.4. Diagrams to show the relative positions of internal mesaxons and external tongues of cytoplasm in transverse section of sheaths from the optic nerves in sheaths from 7-, 14-, and 20-day postnatal rats, on the basis of the number of complete lamellae within the sheath.

The relative position of the external tongue process and internal mesaxon of each sheath was determined by measuring the angle  $\beta$  subtended at the centre of the sheath, between the fixed points A and B:

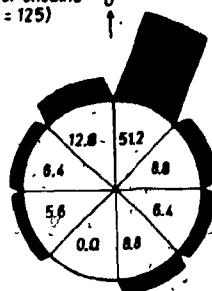


In measuring the angle  $\beta$ , the position of the fixed point related to the internal mesaxon was taken to be 0 and the angle between this point and that related to the external tongue process was measured in the direction taken by the spiral of the lamellae of the sheath. The frequency with which the angle  $\beta$  fell into each octant of a circle is given as a percentage in the middle of each diagram, and this frequency is also indicated by the size of the blackened area at the periphery of each octant. The number of sheaths measured during the construction of each diagram is given. The figures given within the sections of the sheaths are in per cent. [From Peters, 1964].

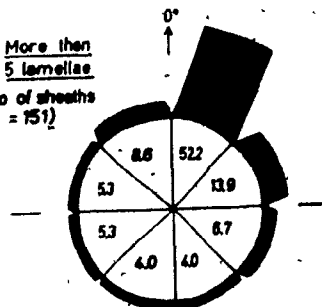
(a) 12 and 3 lamellae  
(No. of sheaths = 91)



(b) 4 and 5 lamellae  
(No. of sheaths = 125)



(c) More than 5 lamellae  
(No. of sheaths = 151)



Deposition of Po mimics the logarithmic increase in myelin content with development (Wood and Engel, 1976). Other biochemical information is not available for the PNS.

For the CNS, myelination data of this active period is restricted only to a few but very important morphometric determinations and to a more extensive body of biochemical characterizations. Peters (1964) reported the change in the localization of the inner and outer oligodendroglial tongues with respect to each other during myelination. His findings indicate that after the initial 1 to 5 lamellae, the localization of the two tongues is restricted to the same quadrant (see Figure 1.3.4 from Peters, 1964). Lamellar compaction in the CNS occurs immediately after the first or second turn. A complex series of junctions and radical-particle arrangements distinguish these membranes from their PNS counterparts (Peters, 1964; Tetzlaff, 1978; Mugnaini, 1978; Dermietzel and Kroczeck, 1980; Dermietzel et al., 1980). During development these arrangements (radial components, interlamellar tight junctions and the zonula occludentes) are continuously established as each new lamella appears (Dermietzel and Kroczeck, 1980, Tetzlaff, 1978). Recent work by Remahl and Hildebrand (1982) offers a clearer picture of the dynamics of CNS axon ensheathment. Their results indicate a dynamism similar to that in the PNS. The distinction between phases I and II are very clear in these data (see Figure 1.3.5A from Remahl and Hildebrand, 1982), as indicated by the transition from ensheathed to myelinated % of fibers. Similar data from PNS sciatic nerve is given in Figure 1.3.5B (from Friede, 1968) for comparison.

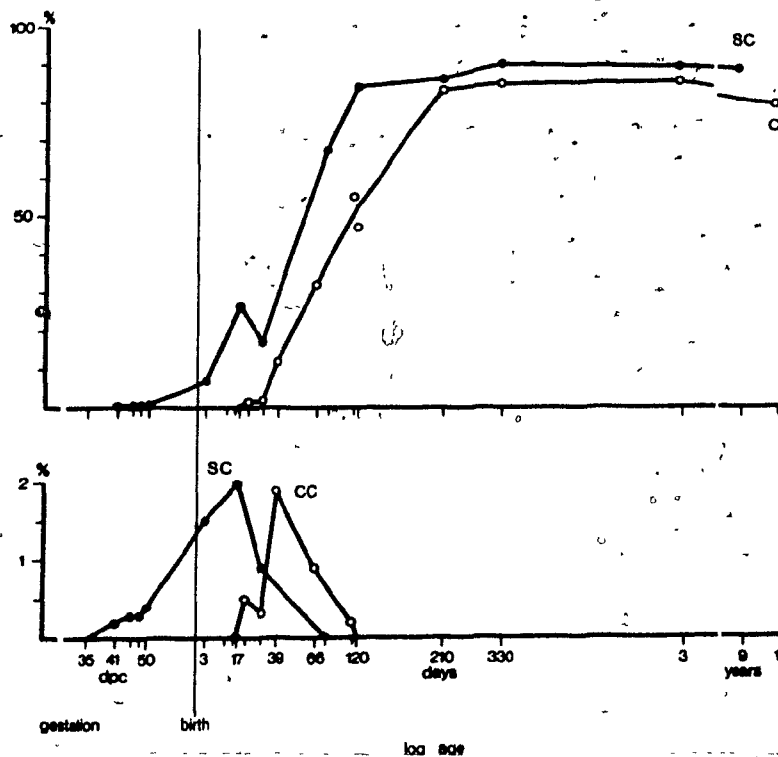


Figure 1.3.5. A) Graphs showing the developmental change in proportion of myelinated (top) and ensheathed (bottom) axons in the spinal and callosal areas. Along the x-axis (logarithmic scale) some ages only have been written out (long bars). Abbreviations: SC = spinal cord. CC = corpus callosum. [From Remahl and Mildebrand, 1982].



Biochemically, the oligodendroglia have initiated the synthesis of other important myelin proteins and lipids. PLP can be detected along the oligodendrocyte processes and rapidly deposited together with MBP and CNP in the myelin sheath (Barbarese *et al.*, 1978; Sprinkle *et al.*, 1978; Hartman *et al.*, 1982). Lipid deposition is also accelerated and important enzyme pathways become activated in this phase. The accumulation of C-14 fatty acids in the previous phase is followed by their elongation to C-18 to C-24 fatty acids (Bourre *et al.*, 1973). Cholesterol synthesis and cerebroside sulfate formation are also rapidly activated (Mandel *et al.*, 1971; James and Kandutsch, 1980). Myelin components accumulate in a coordinate fashion with the increase in lamellae although the enzyme systems responsible for their synthesis promptly respond to regulatory signals that turn the initial frantic activity off (see Figure 1.3.6, as exemplified for sulfotransferase activity; from Bourre, 1980). The curve of activity can be interpreted as the time differential of the rate of lamellation with a maximum at the turning point, that initiates the last phase of myelin formation. The temporal extension of phase II will determine the overall extent of the myelination cycle for each fiber (Yakovlev and Lecours, 1967).

One last point to consider is the important structure that has been in the making during this phase: the node - paranode compartment. This compartment is very different in both systems especially with respect to its paranodal architecture and junctional arrangements (Schnapp and Mugnaini 1975; Mugnaini, 1978). Nevertheless, these differences are valid if one compares the average CNS fibers - which in many instances don't reach more than 20 lamellae

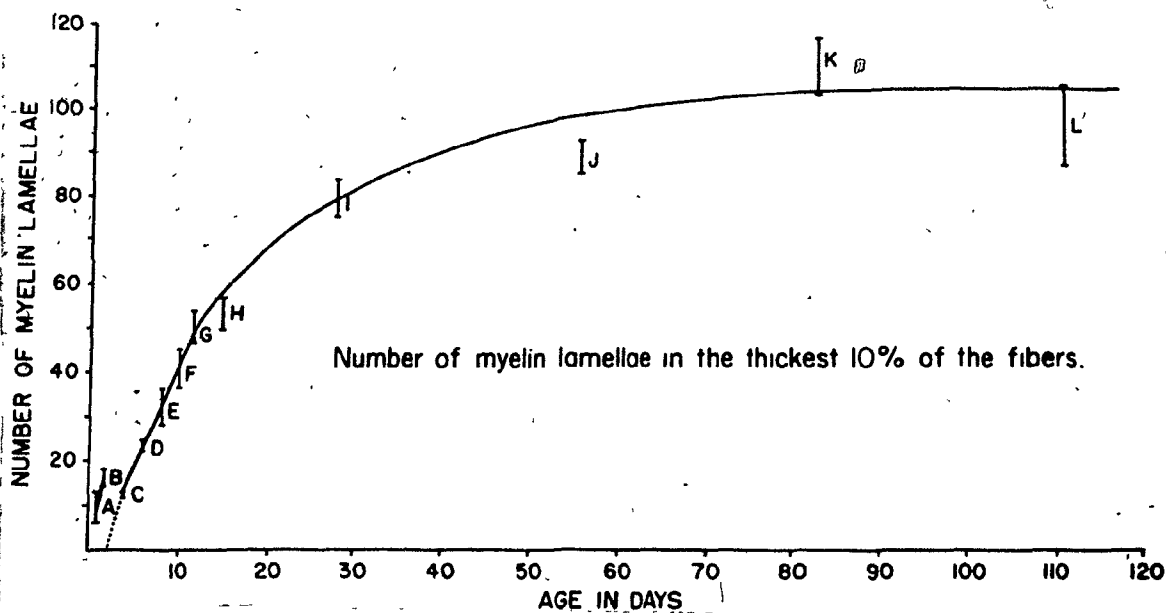


Figure 1.3.5. B) Similar graph showing the developmental change in the number of myelin lamellae in the thickest 10% of sciatic nerve fibers. [From Friede, 1968].

(e.g. in the corpus callosum, Sturrock, 1975). In many areas of the spinal cord, however, the average fibers can have up to 160 lamellae or more (Hildebrand 1971).

To reach these dimensions of ensheathment the oligodendrocyte has to approach a 1:1 relationship with the large axons it is going to myelinate and hence, become "schwannoid" in nature (its distinctive radial components and lack of Schmidt-Lantermann incisures indicating its oligodendroglial origin). Normally one oligodendroglial cell ensheaths approximately sixty axons with ten or less lamellae. As the number of lamellae increases the number of associations decreases in a "mitotic" relationship (Matthews and Duncan, 1971). Whether mitosis occurs prior to, or after ensheathment commitment is still a matter of controversy. However, in spinal cord where the largest fibers are localized, committed oligodendrocytes have been detected in mitotic state (Sturrock and McRae, 1980). Analysis of the paranodes of these large CNS fibers indicates many similarities to the topographical arrangements observed in equivalent PNS fibers (Hildebrand 1971a,b,c, and Berthold, 1978).

#### 1.3.4 Phase II: Termination and Myelin Maintenance

Modulation of the myelination activity takes place in a relatively short period of time. At this moment the axon-myelin unit begins to undergo a new series of metabolic and physiological changes that can be visualized as the maturation of the fiber into myelinated axon. As discussed above important metabolic pathways are depressed. Nevertheless, the activity, especially in large myelinated fibers, is

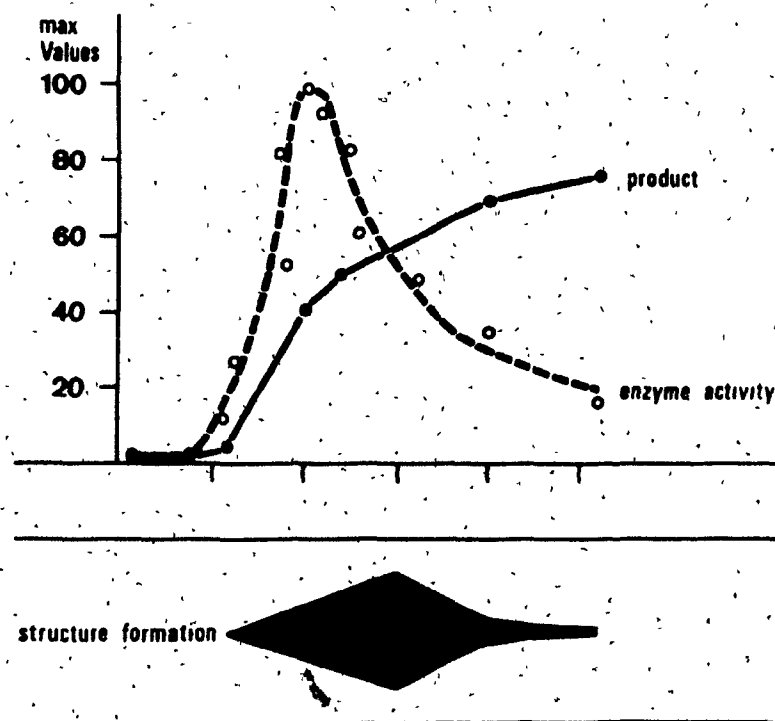


Figure 1.3.6. Relation of myelination to the deposition of myelin constituents and the enzymatic activities responsible for their formation. [From Bourre, 1980].

- product formation (cerebroside, sulfatide)
- enzyme activity (ceramide galactosyl transferase, cerebroside sulfo-transferase)

now localized in the formation of the paranodal apparatus (in PNS; Berthold, 1978) and in paranodal remodelling or "nodalization" (Berthold and Skoglund, 1968 a,b; Hildebrand, 1971 b,c). During this stage "superfluous" myelinated internodes (Myelin monsters, Berthold and Skoglund, 1968) and sections of normal myelinated internodes are being removed by still unknown mechanisms that seem to involve the potential enrichment of cholesterol esters in these sections of "redundant" myelin (Hildebrand and Skoglund, 1971). The function of cholesterol esters in myelination remains undefined, however, these lipids are well characterized in many important myelin neuropathies (Norton, 1977). During development myelin acquires a small but steady amount of cholesterol ester hydrolases that can be distinguished from other esterases of the endoplasmic reticulum (Eto and Suzuki, 1973; Igarashi and Suzuki, 1977). The potential enrichment of cholesterol esters in the myelinoid bodies or redundant paranodal myelin of large PNS and CNS fibers can indicate the momentary imbalance in an otherwise normal molecular mechanism of myelin assembly (see Section 6. ).

Characterization of myelinated fibers in both systems at this and older stages is abundant but extremely confusing, given that most studies consider an animal from this phase on, an "adult" specimen. However, developmental determinations of biochemical parameters indicate that true adult values have not been reached. During this phase, slow but continuous changes occur until the myelinated fiber path has terminated its physiological maturation (Conway et al., 1969; Lecours, 1975; Humphrey, 1960).

Figure 1.4.1. Developing Schwann cell Sheaths.

Although some of the axons (Ax) are still in bundles [phase zero], others have become individually separated [early phase I]. The majority of these separated axons (Ax1) have just been enclosed by Schwann cell processes whose lips come together to form a simple mesaxon (mes) [phase I]. Two axons (Ax2 and Ax3) enclosed by Schwann cells (SC) have sheaths at a later stage of development [late phase I and early phase II], in which the mesaxon has elongated into a loose spiral, and in the spiral around Ax3 the plasma membrane of the mesaxon has become partially apposed to form the beginning of the intraperiod line. Another axon (Ax4) has a more mature sheath in which the cytoplasm has disappeared from between the turns of the mesaxon so that compact myelin has formed [phase II].

Newborn rat sciatic nerve x 21,000. [From Peters et al., 1976].



#### 1.4. Models of Myelin Lamellar Formation

The events of phase I to III involve the formation of the characteristic myeloarchitecture that is observed in mature fibers in both the CNS and the PNS. Figures 1.4.1 and 1.4.2 (taken from Peters et al., 1976) show PNS and CNS fibers during the initial stages of ensheathment (late phase I and early phase II). On the basis of similar observations Geren Uzman (1953, 1954, 1956) proposed the "Spiral-Wrapping" hypothesis of PNS myelination (Figure 1.4.3).

Two main alternatives were proposed at that time. One by DeRobertis (1958), who studying CNS myelination proposed the intracellular deposition of modified endomembranes around the cytoplasmic embracement of the oligodendroglia around the axons. The events described involved the deposition of the first 8 to 10 layers of "myelin" as concentric layers of electron dense material. Alignment followed by internal fusion and the formation of the spiral. Contrary to the "Spiral-Wrapping" hypothesis, this model implies the active involvement of the cytoplasm in the formation of a multispiral arrangement.

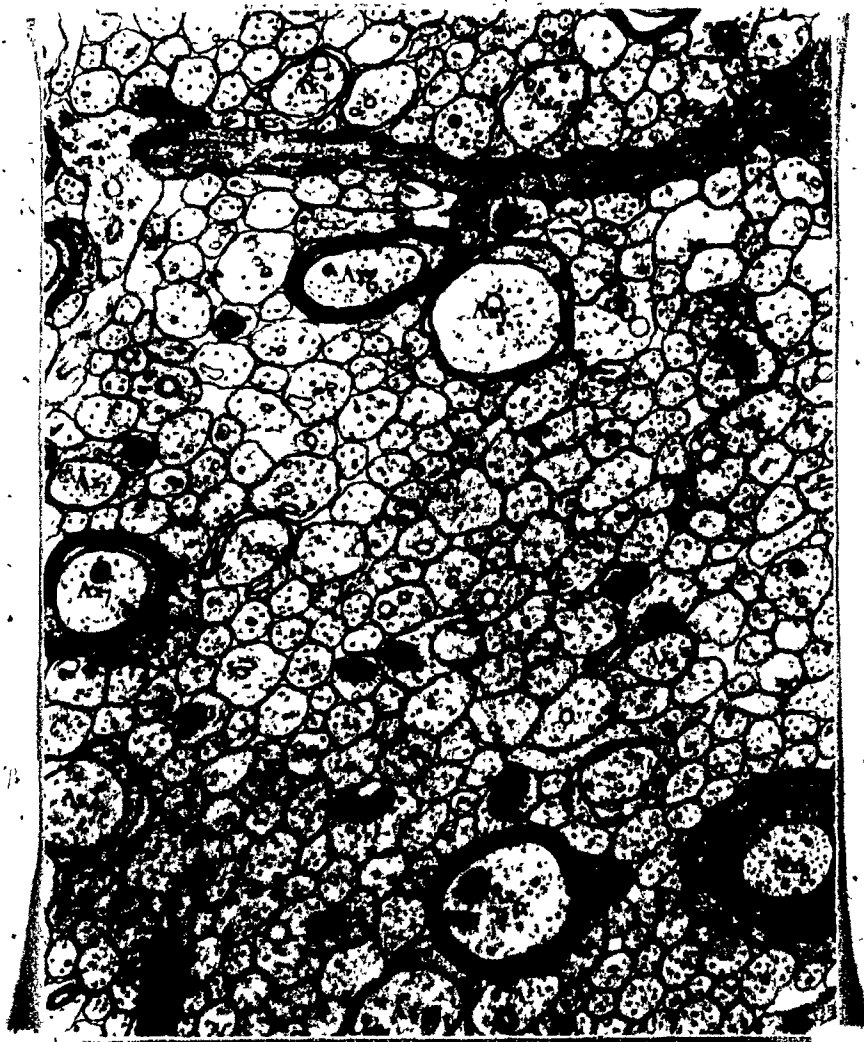
The second alternative was proposed by Luse (1956, 1958). The work of this author pointed out the complex and multiple cellular processes that engulfed and ensheathed axons during the initial events that lead to the appearance of myelin. Myelination was thus proposed to occur by a complex multiprocess ensheathment mechanism rather than a single process ensheathment as proposed in Geren's hypothesis.

Figure 1.4.2. Developing Myelin Sheaths, Central Nervous System.

Most of the transverse section axons (Ax) in this field are still unmyelinated but some of them are becoming myelinated [phase zero]. Some of the axons (Ax1) are being enveloped by a single process [early phase I]. In some cases (Ax2) cytoplasm is lost from the middle portion of the process so that it has a dumbbelled profile. Something of the sequence in the extension of this process into a spiral is shown around the axons labelled Ax3 to Ax5 [phase I to II]. Stages in the thickening of the compact myelin sheath are also shown (Ax6 and Ax7) [phase II], and in these cytoplasm is retained only at the inner (Ci) and outer (Co) ends of the spiral, the latter being equivalent to the external tongue process of the mature sheath. The sheath of the axon labelled Ax8 may be a stage in the myelination of an internode, but it could equally well be a section through a developing paranode.

At the upper right is part of the dense perikaryon of an active oligodendrocyte, from which a process (Op) extends across the field.

Developing white matter beneath the cerebral cortex of 15-day postnatal rat. x 40,000. [From Peters et al., 1976].



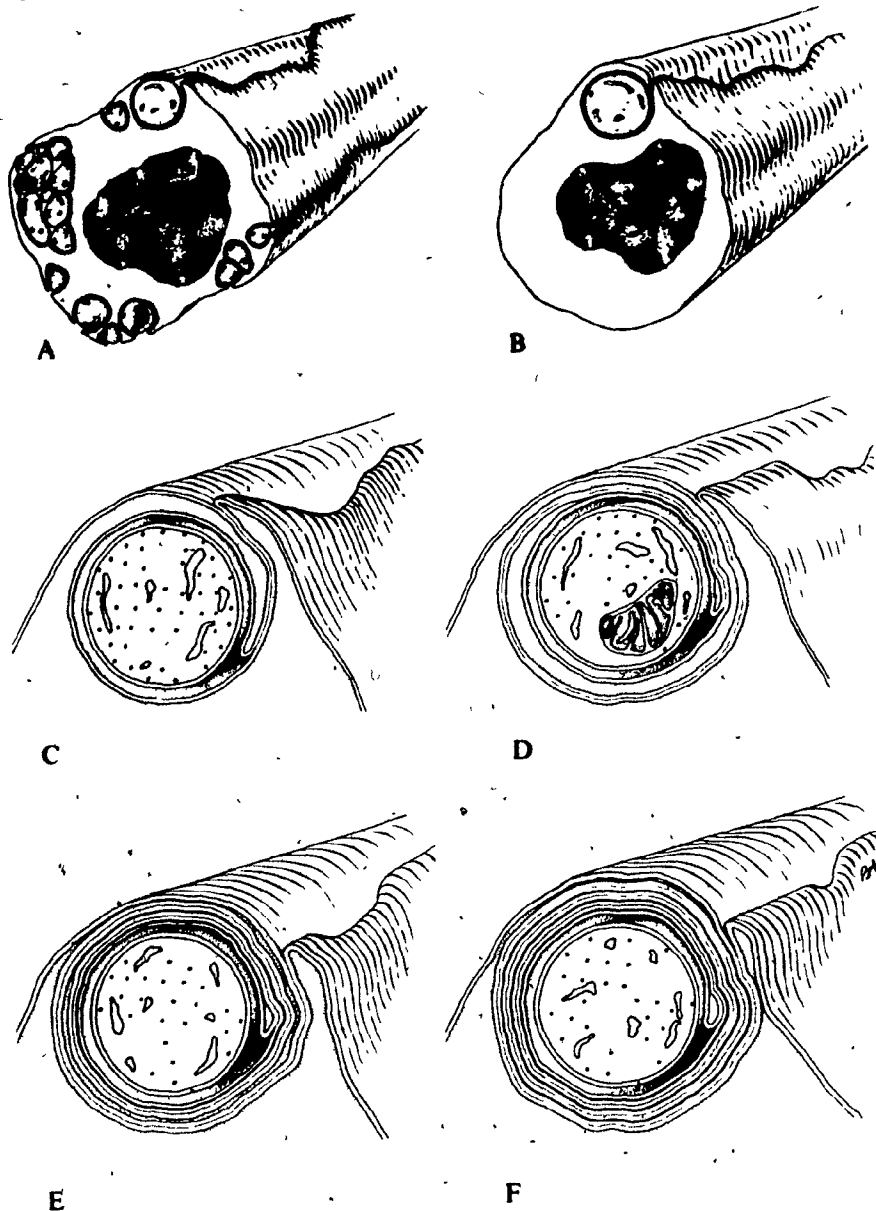


The lack of further corroboration of these observations and the attractive simplicity of the "Spiral-Wrapping" hypothesis, promoted the wide spread application of this latter model. Robertson's (1955) corroboration of a spiral arrangement of reptilian myelin was taken rapidly as a demonstration of Geren's argument. Bunge et al., (1961) assumed that a similar mechanism could be applied without much problems to the myelination of the CNS. The multiple irregularities that were reported for CNS myelin during and after development were "successfully" disproved by the work of Hirano and Dembitzer (1967), who interpreted the irregularities as discontinuities in an otherwise continuous shovel-shaped myelin sheath surrounded by a thickened rim of cytoplasm (see Figure 1.4.4). The demonstration of a "Spiral-Wrapping" mechanism in the formation of myelin has, nevertheless, not been formulated. All these studies demonstrate only that at any given time (at least in "adult" vertebrates) myelin is a continuous spiralled membrane.

Moreover, the "Spiral-Wrapping" hypothesis was based on single field observations of ensheathed axons that could be identified, given the limitations of the time, only by visual criteria. The introduction of serial section techniques in electron microscopy immediately indicated a complex sequence of events involved in the initial stages of ensheathment (phase I; Webster, 1971; Knobler et al., 1974, 1976). The bidirectional and multivermicular ensheathment observed by these authors further corroborated the incomplete observations by Luse (1958) and Lehrer (Ross et al., 1962).

Figure 1.4.3. Diagrammatic Representation of the Formation of Peripheral Myelin Sheaths.  
 "Spiral-Wrapping Hypothesis"

Early in development (A) a Schwann cell contains both bundles of small axons and individual axons. Through an increase in the number of Schwann cells by mitosis, each Schwann cell becomes concerned with only one axon (B), which is enclosed in a trough indenting the surface of the Schwann cell. At this time the lips of the enveloping process come together to form a mesaxon (C). The lips of the enveloping process then extend so that the mesaxon begins to elongate and the more extensive apposition of the external faces of the enveloping and spiralling process leads to the beginning of the intraperiod line (D). Next cytoplasm begins to be lost from the spiralling process and the major dense line results (E). As the sheath becomes more mature, the number of turns of the spiralling process increases and the lamellae of the sheath become more compact (F). (From Peters *et al.*, 1976).



The same clearness and distinction of events is lacking in our understanding of the events that take place during the active phase (phase II) of myelination, and that lead to the formation of PNS incisures of Schmidt - Lanterman (Hall and Williams, 1970; Berthold, 1978), CNS radial components (Peters, 1964; Tabira et al., 1978) and the zonula occludens (Schnapp and Mugnaini, 1975) among others. (For a review of CNS myelin structures see Mugnaini, 1978; for PNS structures see Kruger et al., 1979).

Reconsiderations about the validity of the "Spiral-Wrapping" hypothesis can be found in the work of Peters (1964), Robertson and Vogel, 1962; Peters and Vaughn (1970) and many others confronted with the inevitable complexities observed in an electron microscopic analysis of myelination (see for example Peters and Vaughn (1970 figures 1-9, 1-10, 1-20, 1-22 and 1-24).

The study of myelin can be characterized by an uninterrupted exchange of morphological and biochemical information. It is, nevertheless, surprising to find so little mutual critical assessment by members of both disciplines. The complexities that ultimately lead to the formation of myelinated axons imply a careful reconsideration of the fundamental axioms upon which biochemists and molecular biologists are going to base their interpretations. Expositions of myelination hypothesis from the molecular point of view have until recently made use of hypotheses derived from studies on secretion only (membrane biogenesis and membrane flow hypothesis - see Chapter 3). They have assumed a continuity of assembly between the plasma membrane of the myelin-forming cell and recently deposited myelin lamellae (Danks and Matthieu, 1979; Waehneltd and Linington, 1980; Braun et

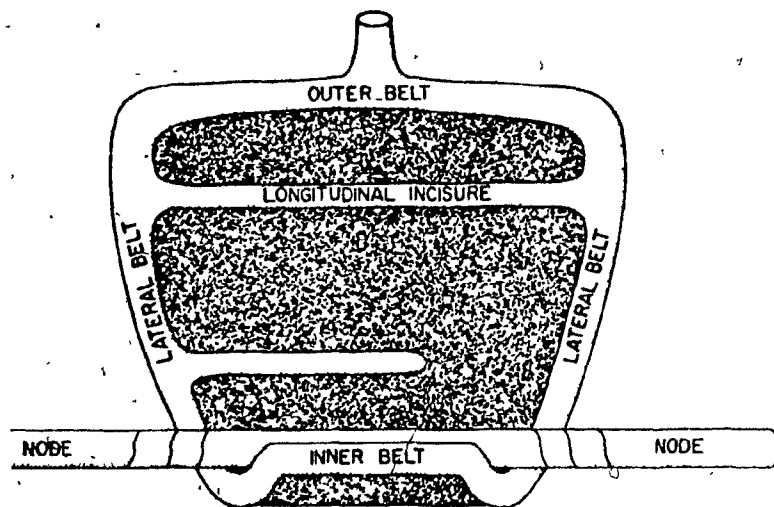


Figure 1.4.4. Unrolled CNS myelin sheath showing lateral, inner and outer cytoplasmic belts. The lateral belts when rolled will form the helically arranged paranodal apparatus. Note also the shovel like form of the unrolled myelin sheath in mature myelin. (From Hirano and Dembitzer, 1967).

al., 1980). Table 1.4.1 summarizes the combined implications of the "Spiral-Wrapping" hypothesis (Peters et al., 1976) and the most commonly accepted biogenic hypotheses by myelin researchers. This table can be compared with Table 2.5.1, where the biogenic implications of the new myelination model have been summarized.

TABLE 1.4.1

BIOGENIC IMPLICATIONS OF THE "SPIRAL-WRAPPING" HYPOTHESIS

1) Events in the Perinuclear Cytoplasmic Space:

- a) Synthesis of membrane components in the rough endoplasmic reticulum and free ribosomes of the perinuclear cytoplasm.
- b) Transport of integral myelin membrane components via a 'classical' endomembrane pathway: RER - SER - GA.
- c) Insertion of post - Golgi vesicles at the feet of the processes of oligodendrocytes or in the immediate perinuclear plasma membrane in the case of Schwann cells.
- d) Vectorial elongation of the plasma membrane in the direction of the growing myelin sheath.

2) Events at the Site of Myelination:

- a) Elongation of the external or internal mesaxon around the axon.
- b) Extrusion of interlamellar cytoplasm.
- c) Compaction of lamellae to form the major interperiod line.
- d) Intrinsic metabolic transformations (myelin maturation).

## REFERENCES CHAPTER 1

- Adelman, W.J., Moses, J. and Rice, R.V. (1977). An anatomical basis for the resistance and capacitance in series with the excitable membrane of the squid giant axon. J. Neurocytol., 6: 621
- Aguayo, A.J., Charron, L. and Bray, G.M. (1976). Potential of Schwann cells from unmyelinated nerves to produce myelin: a quantitative and autoradiographic study. J. Neurocytol., 5: 565
- Aguayo, A.J., Attiwell, M., Tracarten, J., Perkins, S. and Bray, G.M. (1977). Abnormal myelination in transplanted Trembler mouse Schwann cells. Nature, 265: 7
- Aguayo, A.J., David, S. and Bray, G.M. (1981). Influences of the glial environment on the elongation of axons after injury: Transplantation studies in adult rodents. J. Exp. Biol., 95: 231
- Ariens Kappers, C.U., Huber, G.C. and Crosby, E.C. (1936). 'The Comparative Anatomy of the Nervous System of Vertebrates, Including Man'. Vol 2. McMillan Co. N.Y. pp: 1660
- Bakay, L. and Lee, J.C. (1966). Ultrastructural changes in the Endematous CNS III. Edema in shark brain. Arch. Neurol., 14: 644
- Balazs, R. and Cremer, J.E. (1971). 'Metabolic Compartmentation in the Brain'. John Wiley & Sons. N.Y.
- Banik, N.L. and Davison, A.N. (1969). Enzyme activity and Composition of myelin and subcellular fractions in the developing rat brain. Biochem. J., 115: 1051
- Banik, N.L. and Smith, M.E. (1977). Protein determinants of myelination in different regions of developing rat central nervous system. Biochem. J., 162: 247
- Barbarese, E., Carson, J.H. and Braun, P.E. (1979). Accumulation of the four myelin basic proteins in mouse brain during development. J. Neurochem., 31: 779
- Barbarese, E. and Pfeiffer, S.E. (1981). Developmental regulation of myelin basic protein in dispersed cultures. Proc. Natl. Acad. Sci.(USA), 78: 1953
- Beal, J.A. and Cooper, M.H. (1976). Myelinated nerve cell bodies in the dorsal horn of the monkey. Amer. J. Anat., 147: 33

- Benfey, M. and Aguayo, A.J. (1982). Extensive elongation of axons from rat brain into peripheral nerve grafts. Nature, 296: 150
- Benes, F., Higgins, J.A. and Barnett, R.J. (1973). Ultrastructural localization of phospholipid synthesis in the rat trigeminal nerve during myelination. J. Cell Biol., 57: 613
- Bentley, D. and Keshishian, H. (1982). Path finding by peripheral pioneer neurons in grasshoppers. Science, 218: 1082
- Berthold, C-H. and Skoglund, S. (1968a). Postnatal development of feline paranodal myelin-sheath segments: I light microscopy. Acta Soc. Med. Upsal., 73: 123
- Berthold, C-H. and Skoglund, S. (1968b). Postnatal development of feline paranodal myelin-sheath segments: II Electron microscopy. Acta Soc. Med. Upsal., 73: 127
- Berthold, C-H. (1978). 'Morphology of Normal Peripheral Axons'. In 'Physiology and Pathobiology of Axons'. (Ed. Waxman, S.G.). Raven press N.Y. pp: 3
- Bertolini, B. (1964). Ultrastructure of the spinal cord of the Lamprey. J. ultrastruc. Res., 11: 1
- Blakemore, W.F. (1981). Observations on myelination and remyelination in the central nervous system. Adv. Cell. Neurobiol., 2: 289
- Blakemore, W.F. and Murray, J.A. (1981). Quantitative examination of internodal length of remyelinated nerve fibers in the central nervous system. J. Neurol. Sci., 49: 273
- Blinzinger, K., Anzil, A.P. and miller, W. (1972). Myelinated nerve cell perikarya in mouse spinal cord. Z.Zellforsch., 128: 135
- Bourre, J-M. (1980). 'Origin of aliphatic chains in the brain'. In 'Neurological Mutations Affecting Myelination'. (Ed. Baumann, N.). INSERM Symp. 14. Elsevier/North-Holland, Amsterdam. pp: 185
- Bourre, J-M., Pollet, S.A., Daudu, O.L. and Baumann, N.A. (1973). Evolution, in mouse brain microsomes, of lipids and their constituents during myelination. Brain Res., 51: 225
- Boyse, E.A. and Cantor, H. (1978). 'Immunogenetic Aspects of Biologic Communication: A hypothesis of evolution by Programm Duplication'. In 'Birth Defects: Originl Article Series'. Vol XIV(2). Liss. N.Y. pp:249



- Braak, E., Braak, H. and Strange, H. (1977). The fine structure of myelinated nerve cell bodies in the Bulbus olfactorius of man. Cell Tiss. Res., 182: 221
- Braun, P.E. (1983). 'Molecular Organization of Myelin'. In 'Myelin'. Morrel, P. (Ed.), 2nd ed. Plenum Press, N.Y.
- Braum, P.E., Pereyra, P.M. and Greenfield, S. (1980). 'Mechanisms of assembly of myelin: a new approach to the problem'. In 'Neurological Mutations Affecting Myelination'. (Ed. Baumann, N.) Elsevier/North-Holland Biomedical Press. pp 413.
- Bunge, M.B., Bunge, R.P. and Ris, H. (1961). Ultrastructural study of remyelination in an experimental lesion in adult cat spinal cord. J. Biophys. Biochem. Cytol., 10:67
- Bunge, R.P. (1968). Glial cells and the central nervous sheath. Ann. Rev. Biochem., 48: 197
- Bunge, R.P. (1969). 'Structure and Function of the Neuroglia: Some recent observations'. In 'The Neurosciences 2nd Study Program'. (Ed. Schmitt, F.O.) Rockefeller University Press pp: 782
- Bullock, T.H. and Horridge, G.A. (1965). 'Structure and Function in the Nervous Systems of Invertebrates'. Vols I and II, W.H. Freeman and Co. San Francisco
- Burd, G.D. (1980). Myelinated dendrites and neuronal perikarya in the olfactory bulb of the mouse. Brain Res., 181: 450
- Cajal, S.R. (1925-26). Beitrag zur Kenntnis der Neuroglia des Gross- und Kleinhirns bei der progressiven Paralyse mit einigen technischen Bemerkungen zur Silberimpraegnation des pathologischen Nervengewebes. Ztschr. f. d. ges. Neurol. Psychiat., Berl.: 738
- Cantino, D. and Mugnaini, E. (1975). The structural basis for electrotonic coupling in the avian ciliary ganglion. A study with thin sectioning and freeze-fracture. J. Neurocytol., 4: 505
- Celio, M.R. (1979). 'Tubular and undulated profiles' in the myelin sheath of axons in the goldfish spinal cord. Experientia, separatum, 35: 262
- Cohen, L.B., Keyenes, R.D. and Hille, B. (1968). Light scattering and birefringence changes during nerve activity. Nature, 218: 438

Colman, D.R., Kreibich, G., Frey, A.B. and Sabatini, D.D. (1982). Synthesis and incorporation of myelin polypeptides into CNS myelin. J. Cell Biol., 95: 598

Conway, Ch.J., Wright, F.S. and Bradley, W.E. (1969). Electrophysiological maturation of the pyramidal tract in the post-natal rabbit. Electroenceph. Clin. Neurophysiol., 26: 565

Cooper, M.H. and Beal, J.A. (1977). Myelinated granule cell bodies in the cerebellum of the monkey. Anat. Rec., 187: 249

Crosby, E.C. (1969). 'Comparative Aspects of Cerebellar Morphology'. In 'Neurobiology of Cerebellar Evolution and Development'. (Ed. Llinas, R.). American Medical Association. Chicago pp: 19

Cullen, M.J. and Webster, H. deF. (1979). Remodelling of optic nerve myelin sheath and axons during metamorphosis in *Xenopus laevis*. J. Comp. Neur., 184: 353

Danks, D.M. and Matthieu, J.M. (1979). Hypothesis regarding myelination derived from comparisons of myelin subfractions. Life Sci., 24(16):1425

De Robertis, E., Gerschenfeld, H.M. and Wald, F. (1958). Cellular mechanism of myelination in the central nervous system. J. Biophys. and Biochem. Cytol., 4: 651

del Rio Hortega, P. (1928). Tercera aportación al conocimiento morfológico e interpretación funcional de la oligodendroglia. Mem. Real Soc. Esp. Hist. Nat., 14: 5

Dermietzel, R. and Kroczeck, H. (1980). Interlamellar tight junctions of central myelin I. Developmental mechanisms during myelination. Cell Tiss. Res., 213: 81

Dermietzel, R., Leibstein, A.G. and Schunke, D. (1980). Interlamellar tight junctions of central myelin II.. Cell Tiss. Res., 213: 95

Díaz-Flores, L., Gayoso, J.M. and Garrido, M. (1977). Origin of the Myelin Sheath in myelinated nerve cell bodies of the olfactory bulb. Morfol. normal. si pat., 1: 339

Dixon, A.D. (1963). The ultrastructure of nerve fibers in the trigeminal ganglion of the rat. J. ultrastruc. Res., 8: 107

Ellisman, M.H. (1979). Molecular specializations of the axon membrane at nodes of Ranvier are not dependent upon myelination. J. Neurocytol., 8: 719

- Ellisman, M.H., Friedman, P.L. and Hamilton, W.J. (1980). The localization of sodium and calcium to Schwann cell paranodal loops at nodes of Ranvier and of calcium to compact myelin. J. Neurocytol., 9: 185
- Eto, Y. and Suzuki, K. (1973). Developmental changes of cholesterol ester hydrolases localized in myelin and microsomes of rat brain. J. Neurochem., 20: 1475
- Fried, K., Hildebrand, C. and Erdélyi, G. (1982). Myelin sheath thickness and internodal length of nerve fibers in the developing feline inferior alveolar nerve. J. Neurol. Sci., 54: 47
- Friede, R.L. (1963). The relationship of body size, nerve cell size, axon length and glial density in the cerebellum. Proc. Natl. Acad. Sci. (USA), 49: 187
- Friede, R.L. (1972). Control of myelin formation by axon caliber (with a model of control mechanism). J. Comp. Neurol., 144: 233
- Friede, R.L. and van Houten, W.H. (1962). Neuronal extension and glial supply: functional significance of glia.. Proc. Natl. Acad. Sci. (USA), 48: 817
- Friede, R.L. and Samorajski, T. (1968). Myelin formation in the sciatic nerve of the rat. J. Neuropathol. Exp. Neurol., 27: 546
- Friede, R.L. and Bischhausen, R. (1982). How are sheath dimensions affected by axon caliber and internode length?. Brain Res., 235: 335
- Friedrich, V.L., Massa, P. and Mugnaini, E. (1980). 'Fine structure of oligodendrocytes and Central Myelin Sheaths'. In Proc. I Inter. Symp. of the search for the cause of a M.S. (Ed. A. Boese). Ver. Chemie Weinheim. pp: 27
- Geren, B.B. and Raskind, J. (1953). Proc. Natl. Acad. Sci. (USA), 39: 880
- Geren Uzman, B. (1954). The formation from the Schwann cell surface of myelin in the peripheral nerves of chick embryos. Exp. Cell Res., 7: 558
- Geren Uzman, B. (1956). The formation of myelin in the peripheral nerves of vertebrates. J. Biophys. and Biochem. Cytol., 2: 219
- Grisell, R.D.S. (1979). Toward a multi-membrane model for potassium conduction in squid giant axon. J. theor. Biol., 76: 233

- Grossman, S.P. (1967). 'A Textbook of Physiological Psychology'. John Wiley & Sons, Inc., N.Y.
- Hall, S.M. and Williams, P.L. (1970). Studies on the 'incisures' of Schmidt and Lanterman. J. Cell Sci., 6: 767
- Hama, K. (1959). Some observations on the fine structure of the giant nerve fibers of the earthworm, *Eisenia foetida*. J. Biophys. and Biochem. Cytol., 6: 61
- Harman, P.J. (1957). 'Paleoneurologic, Neoneurologic, and Ontogenetic Aspects of the Brain Phylogeny'. James Arthur Lecture on the Evolution of the Brain. The American Museum of Natural History
- Harrison, B.M. and McDonald, W.I. (1977). Remyelination after transient experimental compression of the spinal cord. Ann. Neurol., 1: 542
- Hartman, B.K., Agrawal, H.C., Agrawal, D. and Kalmbach, S. (1982). Development and maturation of central nervous system myelin. Proc. Nat. Acad. Sci., 79: 4217
- Heuser, J.E. and Doggenweiler, C.F. (1966). The fine structural organization of nerve fibers, sheaths, and glial cells in the prawn, *Palaemonetes vulgaris*. J. Cell Biol., 30: 381
- Hildebrand, C. (1971a). Ultrastructural and light-microscopic studies of the nodal region in large myelinated fibers of the adult feline spinal cord. Acta Physiol. Scand., 364: 43
- Hildebrand, C. (1971b). Ultrastructural and light-microscopic studies of developing feline white matter I. The nodes of Ranvier. Acta Physiol. Scand. Supp., 364: 81
- Hildebrand, C. (1971c). Ultrastructural and light-microscopic studies of the developing feline spinal cord white matter. II. Cell death and myelin sheath desintegration in early postnatal period. Acta Physiol. Scand. Supp., 364: 109
- Hildebrand, C. and Skoglund, S. (1971). Histochemical studies of adult and developing feline spinal cord white matter. Acta Physiol. Scand. Supp., 364: 145
- Hirano, A. and Dembitzer, H.M. (1967). A structural analysis of the myelin sheath in the central nervous system. J. Cell Biol., 34: 555
- Horridge, G.A. (1968). 'The Origins of the Nervous System'. In 'The Structure and Function of Nervous Tissue', Vol I. Structure I. (Ed. Bourne G.H.). Academic Press. N.Y.

- Humphrey, T. (1960). The development of the pyramidal tracts in human fetuses, correlated with cortical differentiation. In 'Structure and Function of the Cerebral Cortex'. (Tower, D.B. and Schade, J.P. Eds) Elsevier, Amsterdam. p:93
- Huo Lin, L-F. and Lees, M.B. (1982). Interactions of dicyclohexylcarbodiimide with myelin proteolipid. Proc. Natl. Acad. Sci.(USA), 79: 941
- Igarashi, M. and Suzuki, K. (1977). Solubilization and characterization of the rat brain cholesterol ester hydrolase localized in the myelin sheath. J. Neurochem., 28: 729
- James, M.J. and Kandutsch, A.A. (1980). Evidence for independent regulation of dolichol and cholesterol synthesis in developing mouse brain. Biochim. Biophys. Acta, 619: 432
- Jerison, H.J. (1973). 'Evolution of the Brain and Intelligence'. Academic Press. N.Y.
- Johnston, P.V. and Roots, B.I. (1972). 'Nerve Membranes: A study of the biological and chemical aspects of the neuro-glia relationships'. Pergamon Press. Toronto.
- Jung, H.J., Raine, C.S. and Suzuki, K. (1978). Schwann cells and peripheral nervous system myelin in the rat retina. Acta Neuropathol., 44: 245
- King, D.G. (1976a). Organization of crustacean neuropil. I. Patterns of synaptic connection in lobster stomatogastric ganglion. J. Neurocytol., 5: 207
- King, D.G. (1976b). Organization of crustacean neuropil. II. Distribution of synaptic contacts on identified motor neurons in lobster stomatogastric ganglion. J. Neurocytol., 5: 239
- Knobler, R.L., Stempak, J.G. and Laurencin, M. (1974). Oligodendroglial ensheathment of axons during myelination in the developing rat central nervous system. A serial section electron microscopical study. J. Ultrastruc. Res., 49: 34
- Knobler, R.L., Stempak, J.G. and Laurencin, M. (1976). Nonuniformity of the oligodendroglial ensheathment of axons during myelination in the developing rat central nervous system. J. Ultrastruc. Res., 55: 417
- Kruger, L., Stolmski, C., Martin, B.G.H. and Gross, M.B. (1979). Membrane specializations and cytoplasmic channels of Schwann cells in mammalian peripheral nerve as seen in freeze-fracture replicas. J. Comp. Neurol., 186: 571

- Lane, N.J. (1981). Invertebrate neuroglia-junctional structure and development. J. Exp. Biol., 95: 7
- Lecours, A-R. (1975). 'Myelogenetic correlates of the development of speech and language'. In 'Foundations of Language Development: A multidisciplinary approach'. Vol 1, (Eds. Lenenberg). Academic Press. pp: 122
- Llinas, 1969 (1969). 'Neurobiology of Cerebellar Evolution and Development'. American Medical Association. Chicago.
- Luse, S.A. (1956). Developmental and functional alterations of fine structure of Schwann cells. J. Biophys. and Biochem. Cytol., 2: 777
- Luse, S.A. (1958). Formation of myelin in the central nervous system of mice and rats as studied with electron microscopy. Anat.Rec., 130: 333
- Martin, J.R. and Webster, H. deF. (1973). Mitotic Schwann cells in developing nerve: their change in shape, fine structure, and axon relationships. Devel. Biol., 32: 417
- Martinez, M. (1982). Myelin lipids in the developing cerebrum, cerebellum, and brain stem of normal and undernourished children. J. Neurochem., 39: 1684
- Mandel, P., Nussbaum, J.L., Neskovic, N.M., Sarlieve, L.L. and Kurihara, T. (1971). Regulation of myelinogenesis. Adv. Enzyme Regulation, 10: 101
- Massa, P.T. and Mugnaini, E. (1982). Cell junctions and intramembrane particles of astrocytes and oligodendrocytes: a freeze-fracture study. Neuroscience, 7: 523
- Matthews, M.A. (1968). An electron microscopic study of the relationship between axon diameter and the initiation of myelin production in the peripheral nervous system. Anat. Rec., 161: 337
- Matthews, M.A. and Duncan, D. (1971). A quantitative study of morphological changes accompanying the initiation and progress of myelin production in the dorsal funiculus of the rat spinal cord. J. comp. Neurol., 142(1):1
- Morell, P. (1977). 'Myelin'. Plenum Press, N.Y.
- Morell, P. (1983). 'Myelin'. 2nd ed. Plenum Press, N.Y.
- Morell, P. and Norton, W.T. (1980). Myelin. Scientific American, 242: 88

- Mori, S. and Leblond, C.P. (1970). Electron microscopic identification of three classes of oligodendrocytes and a preliminary study of their proliferative activity in the Corpus Callosum of young rats. J. Comp. Neurol., 139: 1
- Mugnaini, E. (1978). Fine structure of myelin sheaths. Proceedings of the European Society for Neurochemistry (Ed. V. Neuhöf), 1: 3
- Nagashima, K. (1979). Ultrastructural study of myelinating cells and sub-pial astrocytes in developing rat spinal cord. J. Neurol. Sci., 44:1
- Nobel, M.D. (1982). The astrocyte: unsung star of the central nervous system. Abstracts, Society for Neuroscience, 8 Part1: 241
- Norton, W.T. (1977). 'Chemical Pathology of Diseases Involving Myelin'. In 'Myelin'. (Ed. Morell, P.) Plenum Press. N.Y. pp: 383
- Padron, R. and Mateu, L. (1982). Repetitive propagation of action potentials destabilizes the structure of the myelin sheath. A dynamic X-ray diffraction study. Biophys. J., 39: 183
- Peters, A. (1964). Further observations on the structure of myelin sheaths in central nervous system. J. Cell Biol., 20: 28
- Peters, A. and Vaughn, J.E. (1970). 'Morphology and Development of the Myelin Sheath'. In 'Myelination' by Davison, A.N. and Peters, A. Charles C Thomas Publ. Illinois pp: 3
- Peters, A., Palay, S.L. and Webster, H. deF. (1976). 'The Structure of the Nervous System: The neurons and supporting cells'. W.B. Saunders Co. Pha.
- Raine, C.S. (1976). On the occurrence of Schwann cells within the normal central nervous system, J. Neurocytol., 5: 371
- Remahl, S. and Hildebrand, C. (1982). Changing relation between onset of myelination and axon diameter range in developing feline white matter. J. Neurol. Sci., 54: 33
- Robertson, J.D. (1955). The ultrastructure of adult vertebrate peripheral myelinated nerve fibers in relation to myelinogenesis. J. Biophys. and Biochem. Cytol., 1: 271
- Robertson, J.D. (1959). The ultrastructure of cell membranes and their derivatives. Biochem. Soc. Symposia, 16: 3

- Robertson, D. and Vogel, F. (1962). Concentric lamination of glial processes in oligodendrogliomas. J. Cell Biol., 15: 313
- Rogart, R.B. and Ritchie, J.M. (1977). 'Physiological Basis of Conduction in Myelinated Nerve Fibers'. In 'Myelin'. (Ed. Morell, P.). Plenum Press. N.Y. PP 117
- Romand, R., Romand, M.R., Mülle, Ch. and Marty, R. (1980). Early stages of myelination in the spiral ganglion cells of the kitten during development. Acta Otolaryngol., 90: 391
- Romer, A.S. (1969). 'Vertebrate history with special reference to factors related to cerebellar evolution. In 'Neurobiology of Cerebellar Evolution and Development'. (Ed. Llinas, R.). American Medical Association. Chicago
- Rosenbluth, J. (1962a). The visceral ganglion of *Aplysia californica*. Z. Zellforsch., 60: 213
- Rosenbluth, J. (1962b). The fine structure of acoustic ganglia in the rat. J. Cell Biol., 12: 329
- Rosenbluth, J. (1966). Redundant myelin sheaths and other structural features of the toad cerebellum. J. Cell Biol., 28: 73
- Rosenbluth, J. (1979). Aberrant axon-Schwann cell junctions in dystrophic mouse nerves. J. Neurocytol., 8: 655
- Ross, L.L., Bornstein, M.B. and Lehrer, G.M. (1962). Electron microscopic observations of rat and mouse cerebellum in tissue culture. J. Cell Biol., 14: 1962
- Rushton, W.A.H. (1951). A theory of the effects of fiber size in medullated nerve. J. Physiol., 115: 101
- Roussel, G. and Nussbaum, J.L. (1981). Comparative localization of Wolfgram W1 and myelin basic protein in the rat brain during ontogenesis. Histochem. J., 13: 1029
- Schnapp, B. and Mugnaini, E. (1975). 'The Myelin Sheath: Electron Microscopic Studies with Thin Sections and Freeze-Fracture'. In Golgi Centennial Symp. Proc. (Ed. M. Santini). Raven Press. N.Y. PP: 209
- Sidman, R.L. and Rakic, P. (1973). Neuronal Migration, with special reference to developing human brain: a review. Brain Res., 62: 1
- Skoff, R.P., Price, D.L. and Stocks, A. (1976a). Electron microscopic autoradiographic studies of gliogenesis in rat optic nerve I. Cell proliferation. J. Comp. Neurol., 169: 291



- Skoff, R.P., Price, D.L. and Stocks, A. (1976b). Electron microscopic autoradiographic studies of gliogenesis in rat optic nerve II. Time of origin. J. Comp. Neurol., 169: 31
- Smith, M.E. (1967). Metabolism of myelin lipids. Adv. Lipid Res., 5: 241
- Smith, K.J., Blakemore, W.F., Murray, J.A. and Patterson, R.C. (1982). Internodal myelin volume and axon surface area. A relationship determining myelin Thickness?. J. Neurol. Sci., 55: 231
- Spencer, P.S. and Thomas, P.K. (1974). Ultrastructural studies of the dying-back process II. The sequestration and removal by Schwann cells and oligodendrocytes of organelles from normal and diseased axons. J. Neurocytol., 3: 763
- Spencer, P.S. and Weinberg, H.J. (1978). 'Axon Specification of Schwann Cell Expression and Myelination'. In 'Physiology and Pathology of Axons'. (Ed. Waxman, S.G.). Raven Press. N.Y. pp: 389
- Sprinkle, T.J., Zaruba, M.E. and McKhann, G.M. (1978). Activity of 2'3'-cyclic-nucleotide 3'-phosphodiesterase in regions of rat brain during development. J. Neurochem., 30: 309
- Sternberger, N.H., Itoyama, Y., Kies, M.W. and Webster, H.deF. (1978). Immunocytochemical method to identify basic protein in myelin-forming oligodendrocytes of newborn rat C.N.S.. J. Neurocytol., 7: 251
- Sturrock, R.R. (1975). A light and electron microscopic study of proliferation and maturation of fibrous astrocytes in the optic nerve of the human embryo. J. Anat., 119: 223
- Sturrock, R.R. and McRae, D.A. (1980). Mitotic division of oligodendrocytes which have begun myelination. J. Anat., 131: 577
- Suyeoka, O. (1968). Small myelinated perikarya in the cerebellar granular layer of mammals including man. Experientia, 24: 472
- Tabira, T., Cullen, M.J., Reier, P.J. and Webster, H. deF. (1978). An experimental analysis of interlamellar tight junctions in amphibian and mammalian C.N.S. myelin. J. Neurocytol., 7: 489
- Tennekoon, G.I., Kishimoto, Y., Singh, I., Nonaka, G.I. and Bourre, J-M. (1980). The differentiation of oligodendrocytes in the rat optic nerve. Develop. Biol., 79: 149

- Tetzlaff, W. (1978). The development of a zonula occludens in peripheral myelin of the chick embryo. Cell Tiss. Res., 189: 187
- Tigges, M. and Tigges, J. (1980). Distribution and morphology of myelinated perikarion and dendrites in the olfactory bulb of primates. J. Neurocytol., 9: 825
- Tower, D.B. and Young, O.M. (1973a). Interspecies correlation of cerebral cortical oxygen consumption, acetylcholinesterase activity and chloride content. J. Neurochem., 20: 253
- Tower, D.B. and Young, O.M. (1973b). J. Neurochem., 20: 269
- Trapp, B.D., McIntyre, L.J., Quarles, R.H., Sternberger, N.H. and Webster, H.deF. (1979). Immunocytochemical localization of rat peripheral nervous system myelin proteins: P2 protein is not a component of all peripheral nervous system myelin sheaths. Proc. Natl. Acad. Sci. (USA), 76(7):3552
- Trapp, B.D., Itoyama, Y., Sternberger, N.H., Quarles, R.H. and Webster, H.deF. (1981). Immunocytochemical localization of P<sub>0</sub> protein in Golgi complex membranes and myelin of developing rat Schwann cells. J. Cell Biol., 90: 1
- Trapp, B.D., Itoyama, Y., MacIntosh, T.D. and Quarles, R.H. (1983). P2 protein in oligodendrocytes and myelin of the rabbit central nervous system. J. Neurochem., 40(1):47
- Treherne, J.E. (1981). Glial-Neuron Interactions. J. Exper. Biol., 95: 1
- Verbitskaya, L.B. (1969). 'Some aspects of the ontophylogenesis of the cerebellum'. In 'Neurobiology of Cerebellar Evolution and Development'. (Ed. Llinas, R.). American Medical Association. Chicago
- Voogd, J. (1969). 'The Importance of Fiber Connections in the Comparative Anatomy of the Mammalian Cerebellum'. In 'Neurobiology of Cerebellar Evolution and Development'. (Ed. Llinas, R.). American Medical Association. Chicago
- Weahneltd, T.V. and Livingston, C. (1980). 'Organization and assembly of the myelin membrane'. In 'Neurological Mutations Affecting Myelination'. (Ed. Baumann, N.). Elsevier/North-Holland Biomedical Press. pp: 389.
- Walters, S.N. and Morell, P. (1981). Effects of altered thyroid states on myelinogenesis. J. Neurochem., 36: 1792
- Waxman, S.G. (1972). Regional differentiation of the axon: a review with spetial reference to the concept of the multiplex neuron. Brain Res., 47: 269

- Waxman, S.G. and Bennett, M.V.L. (1972). Relative conduction velocities of small myelinated and non-myelinated fibers in the central nervous system. Nature New Biol., 238:217
- Waxman, S.G. and Foster, R.E. (1980). Ionic channel distribution and heterogeneity of the axon membrane in myelinated fibers. Brain Res. Rev., 2: 205
- Waxman, S.G., Black, J.A. and Foster, R.E. (1982). Freeze-fracture heterogeneity of the axolemma of premyelinated fibers in the CNS. Neurology, 32: 418
- Webster, H. deF. (1971). The geometry of peripheral myelin sheaths during their formation and growth in rat sciatic nerves. J. Cell Biol., 48: 348
- Webster, H. deF., Martin, J.R. and O'Connell, M.F. (1973). The relationship between interphase Schwann cells and axons before myelination: a quantitative electron microscopic study. Devel. Biol., 32: 401
- Weinberg, E.L. and Spencer, P.S. (1975). Studies on the control of myelinogenesis 1. Myelination of regenerating axons after entry into foreign unmyelinated nerve. J. Neurocytol., 4: 395
- Weinberg, E.L. and Spencer, P.S. (1976). Studies on the control of myelinogenesis 2. Evidence for the neuronal regulation of myelination. Brain Res., 113: 363
- Weinberg, R.L. and Spencer, P.S. (1979). Studies on the control of myelinogenesis 3. Signalling of oligodendrocyte myelination by regenerating peripheral axons. Brain Res., 162: 273
- Wiesel, T.N. (1982). Postnatal development of the visual cortex and the influence of the environment. Nature, 299: 583
- Wiggins, R.C. (1982). Myelin development and nutritional insufficiency. Brain Res. Rev., 4: 151
- Wiley, C.A. and Ellisman, M.H. (1980). Rows of dimeric-particles within the axolemma and juxtaposed particles within glia, incorporated into a new model for the paranodal glial-axon junction at the node of ranvier. J. Cell Biol., 84: 261
- Wiley-Livingston, C.A. and Ellisman, M.H. (1980). Development of axonal membrane specializations defines nodes of Ranvier and precedes Schwann cell myelin elaboration. Devel. Biol., 79: 334

Willey, T.J. (1973). The ultrastructure of the cat olfactory bulb. J. Comp. Neurol., 152: 211

Williams, P.L. and Wendell-Smith, C.P. (1971). Some additional parametric variations between peripheral nerve fiber populations. J. Anat., 109: 505.

Wood, J.G. and Engel, E.L. (1976). Peripheral nerve glycoproteins and myelin fine structure during development of rat sciatic nerve. J. Neurocytol., 5: 605

Yahara, S., Singh, I. and Kishimoto, Y. (1980). Cerebroside and cerebroside III-sulfate in brain cytosol evidence for their involvement in myelin assembly. Biochim. Biophys. Acta, 619: 177

Yakovlev, P.I. and Lecours, A-R. (1967). 'Myelinogenetic Cycles of Regional Maturation of the Brain'. In 'Regional Development of the Brain in Early Life'. (Ed. Minkowski, A.) F.A. Davis Co. Pha. pp:3

Yeh, Y-Y., Ginsburg, J.R. and Tso, T.B. (1983). Changes in lipogenic capacity and activities of ketolytic and lipogenic enzymes in brain regions of developing rats. J. Neurochem., 40: 99

Zgorzalewicz, B., Neuhoof, V. and Waehneltd, T.V. (1974). Rat myelin proteins. Compositional changes in various regions of the nervous system during ontogenetic development. Neurobiology, 4: 265

## 2. A New Model of Myelin Morphogenesis





From the preceding chapter it was possible to grasp some of the intricacies of the myelination event. It was also stated that many researchers have described numerous irregularities of ensheathment that are difficult to explain by the "Spiral-Wrapping" hypothesis (Peters et al. 1976). The model to be described in this chapter explains the mechanism of myelination by integrating biochemical and morphological descriptions. Care has been taken to distinguish, within a given organism, the association between myelination events and other neuro glial adaptations in other less developed organisms as well as with well characterized abnormalities as described for specific myelopathies or neurological mutations.

The primary intention of this model is to suggest imaginative experimentation conducive to the elucidation of biogenic principles which operate in the active phase of myelin deposition.

### 2.1. Description of the Model

It would be useful at the outset to recall the three dimensional image of a myelinated axon. Figure 2.1.1 illustrates longitudinal and perpendicular cuts through a CNS myelinated internode. The geometrical description of the model will be done on the perpendicular plane of the myelinated internode given that this is the most familiar image of myelinated fibers.

Table 2.1.1. Summary of Symbols in Figure 2.1.2.

Graphic Symbol	Code	Description
	MY	Unit myelin membrane of the spiral
	-	Unit membrane of intracellular or endomembrane plates ( EMP ).
	-	Complementary cytoskeletal elements for EMP anchoring.
	"2"	Interlamellar junction
	"1","3"	MY - EMP junction

Letters denote lamellar continuity; for example from C to C' and D to D' constitutes a whole turn of the lamella around the axon. Greek letters are reserved for the EMPs.

Nevertheless, the description extrapolates to a three dimensional space by extension of the construction principles to be described. The illustration in Figure 2.1.2. represents an amplified section of the quadrant containing the two ensheathing tongues separated by intervening lamellae. The explanation of symbols encountered in this and the two following figures are indexed in Table 2.1.1. ( it would be convenient to refer to this table and to become familiar with Figures 2.1.2 through 2.1.4, before continuing ).

In order to construct a spiral by the semiconcentric intra-cytoplasmic deposition of membrane, the following initial conditions have to be met :

i) A spiral template must exist prior to the active phase of myelination (phase I, Section 1.3.2).

ii) The deposition of endomembrane plates (EMP) has to occur at any of the ensheathing tongues and at the next immediate lamella.

iii) The EMPs have to be arranged with respect to a "line" of alignment which runs along the longitudinal plane of the two juxtaposed surfaces of the spiral.

iv) The 'plastic' properties of the EMPs and the membranes composing the spiral are such that fusion of membranes can only occur at locations defined by the chirality of the alignment.

v) The EMPs grow along the cytoplasmic side of the spiraled myelin membranes in two opposite directions until they meet.

The union of abstract and concrete biological requirements is inevitable in this case. Thus the term 'plastic' properties

Figure 2.1.1. This diagram illustrates both known and hypothetical aspects of the mature myelin sheath and its relationship to a glial cell. Taken from Bunge et al. 1961. Symbols represent: Unit plasma membrane (pm); Inner mesaxon (im) formed as a glial process completes the initial turn around an axon (a) and starts the second. Intramyelin trapped cytoplasm (cy). On the fully formed sheath exterior, a bit of glial cytoplasm is also retained. In transverse section, this cytoplasm is confined to the external and internal tongues or loops (ol and il). Along the internode this cytoplasm forms a ridge (r) which is continuous with a glial cell body (g) at c, and with the paranodal structure (pn). [From Bunge, 1968].





invokes specific, but yet undefined, physicochemical characteristics of biological membranes in relation to membrane fusion. The biological analogues for the 'line' of alignment and the mechanisms to maintain the chirality, can be found in the interlamellar tight junctions (Dermietzel et al. 1980), the zona pooludens (Mugnaini, 1978), and the versatile properties of the cytoskeleton - in particular the intermediate filaments as "mechanical integrators of cellular space" ( Lazarides, 1980).

The construction of these arguments is depicted in Figure 2.1.2. As stated in Table 2.1.1., the letters to the left are continuous with the ones to the right. The darkest lines denote the "old" myelin membrane and the fine triple lines denote the "new" endomembranes (note that the continuity of these membranes has been denoted with Greek letters to emphasize the difference in initial location and origin). Furthermore, the intracytoplasmic membranes have to be visualized in reality as double membrane plates (EMP) which extend along the cytoplasmic space of the external or outer tongue and that of the lamella immediately below. In order to comprehend the description that follows, it is necessary to recognize the continuity of the internal tongue with the first lamella, then from here to the next lamella above it, until we arrive at the outer tongue following the letters from E'F' to E F, to C'D', to C D, and so on. The rhomboids indicate two complementary proteins or protein aggregates with such chiral properties as to permit the alignment of the EMPs along the interlamellar junction "2". These putative structures may or may not be transmembrane

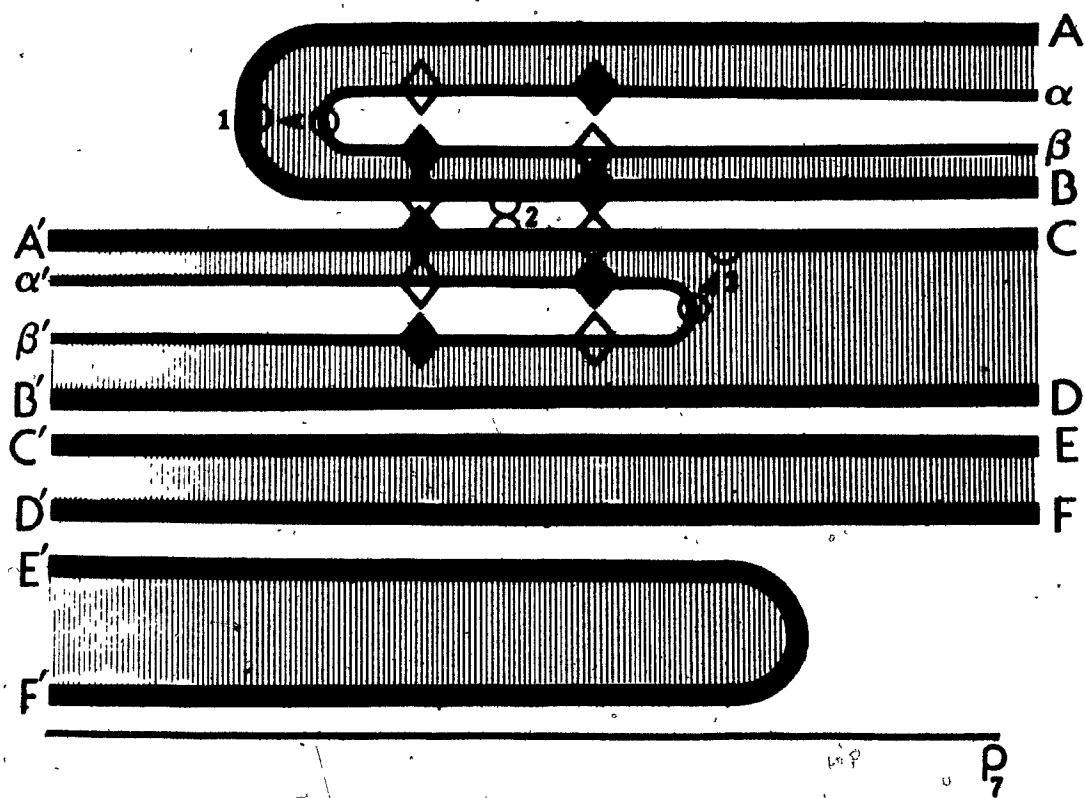


Figure 2.1.2. Myelination model; first step. Schematic representation of the zone of apposition of the internal and external tongues of early myelin forming a spiral template. In the cytoplasmic space of the outer tongue and the first outer lamellae two endomembrane plates (EMP's) are represented aligned to each other through a radial cytoskeletal structure. Numbers 1 through 3 indicate regions of membrane fusion. [For details see Table 2.1.1. and the text].

proteins, their postulated function being localized exclusively at the cytoplasmic side . The illustration, in this case, indicates transmembrane elements for the purpose of suggesting that the control of the 'propensity' of myelin for close membrane apposition occurs by the interaction of specific transmembrane proteins ( MAG ? ; Brady and Quarles, 1973 ) or by the regulation of particle distribution in the myelin membrane plane (Kirschner et al. 1979).

The model at this point requires the presence of at least two different physicochemical microenvironments on the two types of membrane surfaces. The first is the one between the two "old" MY membranes joined by "2". The second will be established by the formation of junctions at "1" and "3". EMPs and the joined MY membranes are ready to undergo a coordinated fusion as represented in Figure 2.1.3. The result of this operation, illustrated in Figure 2.1.4., is the establishment of new membrane continuities. Note the incorporation of "new" membrane between patches of "old" membranes, and also the incorporation of one more turn around the axon.

Although not shown (for sake of simplicity) the addition of this new lamella implies also the immediate compaction of the sheath and its enlargement as the EMPs grow in opposite directions (from a / b towards a'/b') until they meet. Biochemically this might imply the active incorporation of lipids directly at the site of myelination, together with 'envoys' of preformed membrane vesicles (see Section 2.4). Lamellation implies, then, a local "consumption" of cytoplasm rather than its

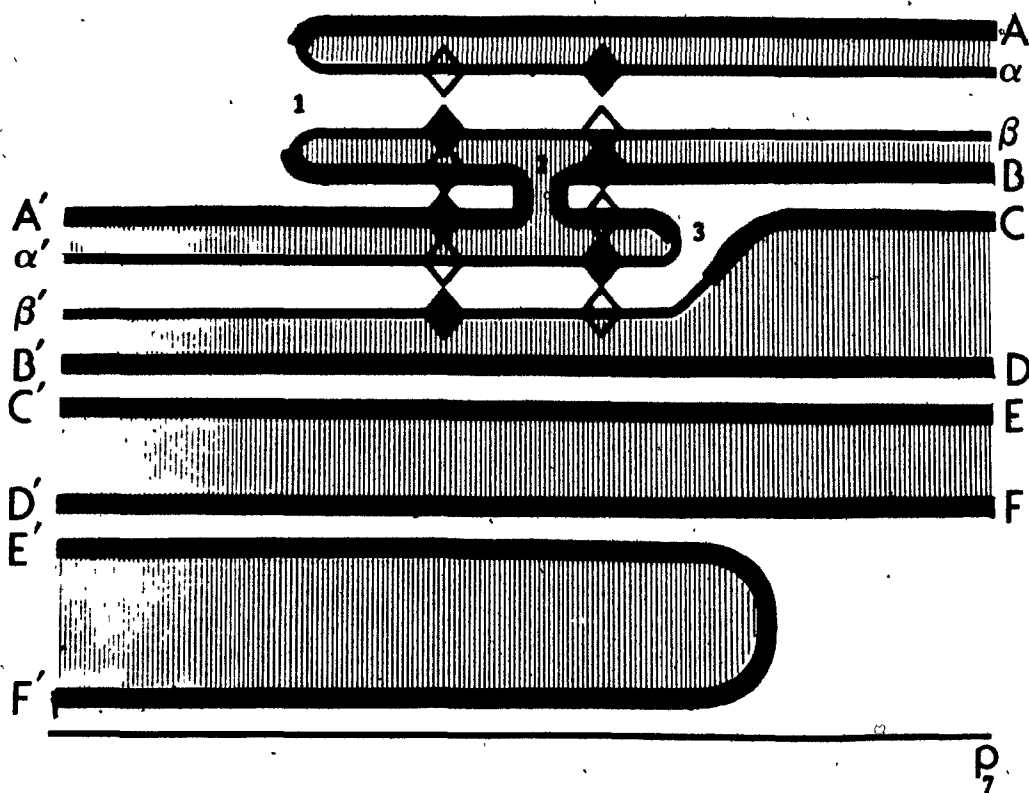


Figure 2.1.3. Myelination Model; second step. Representation of the three regional fusion of the EMP's and the two apposed outer myelin membranes. This transformation generates one more lamellae and ensures the radial alignment of the internal and external tongues [See Fig. 2.1.4 and text for further details].

extrusion, as suggested in the "Spiral-Wrapping" hypothesis (see in this context the ideas by Friede (1972) on spiral compaction).

## 2.2. Morphological Predictions of the Lamellation Model

The multifusion event can be initiated at any given locus in the internodal plane of the sheaths and can propagate as a 'perturbation' of the membrane until it reaches the paranodal regions, without altering the outcome of the spiral. In my hypothesis, however, the initiation of the fusion event occurs at the paranodal regions (and the 'incisures' of Schmidt-Lanterman in the case of PNS fibers), while the perturbation is expected to travel inwards along the internodal plane generating in its course a line of longitudinally organized particles (zona ocludens or interlamellar tight junctions Dermietzel et al. 1978; Mugnaini, 1978).

This mode of lamellar construction predicts that at any given time new membrane material is localized along the three outermost lamellae, and 'travels' from the outer paranodal regions towards the center of the sheath. Furthermore, it can be expected that the new material in this lamella will be diluted with "older" membrane in a predictable proportion as a function of sheath thickness and internodal length. It must be emphasized that this model does not presuppose that the initial axonal ensheathment (phase I; Section 1.3.2.) necessary to generate the spiral template, is comprised of membranes with the same composition as those that are being deposited during the active phase of myelination. Investigations of myelin membranes

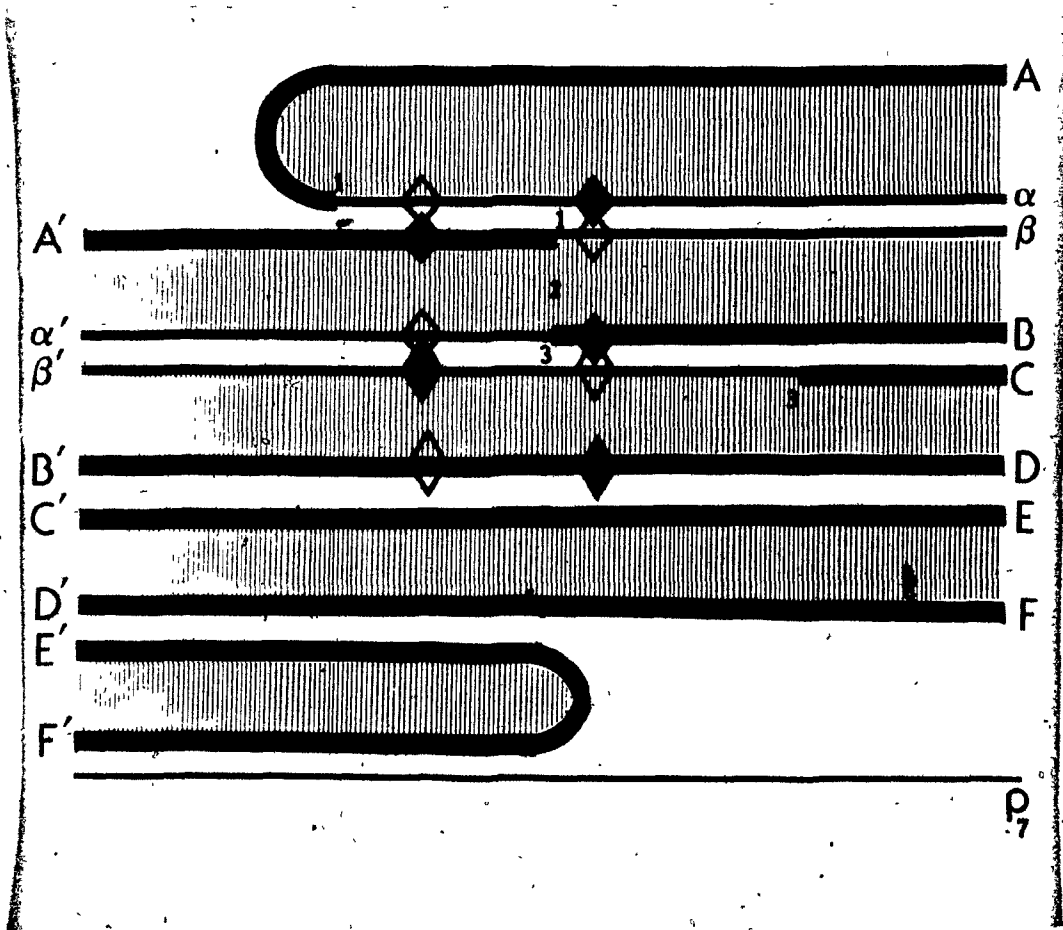


Figure 2.1.4. Myelination Model; third step. Reorganization of Fig. 2.1.3. to indicate completion of lamellar formation and total myelin enlargement in response to axonal growth. Note the distribution of "new" and "old" membranes among the two most outer lamellae and the outer tongue. [See text for details].

during development do indeed indicate a continuous "maturation" of myelin membranes rather than homogeneous myelin characteristics all through the myelination event (for a review see Benjamins and Morell, 1978). Morphological investigations also seem to indicate a marked difference between the periodicity of fibers myelinated with fewer than 10 lamellae and those myelinated with up to 50 lamellae (Hildebrand and Hahn, 1978). Moreover, in this context it is necessary to make clear that from the evidence discussed in the previous chapter ensheathment does not occur by a simple spiralling process; at least not in its initial stages, where irregularities are more the rule than the exception. The rapid multilamellation which occurs after this initial ensheathment is also unsatisfactorily explained by the "Spiral-Wrapping" hypothesis, a problem which is addressed in my model.

Inherent in this model is the formation of radial arrangements such as those commonly observed in CNS myelin (Peters, 1964; Tabira et al. 1978). Moreover, it should be noted that an alignment of the inner and outer tongues in this model is the expected norm. Any misalignment occurs with equal probability to the left or to the right of the reference quadrant, for any given fiber at any given location along the internode (see figure 1.3.4; taken from Peters, 1964).

The construction of the paranodal regions follows from that of the upper lamellae, which are, at any given moment during an active phase of myelination, the most active in their longitudinal enlargement. This ensures that the paranodal



Figure 2.3.1. Transverse section of a stage 65-66 tadpole optic nerve. Note the concentric and uncompact membranes around the axon to the right. The outer most membranes are only partially ensheathing the myelin-axon complex. Similarly in the upper curled myelinated axon to the left. (Picture is a courtesy of Dr. H. deF. Webster).



loops closest to the axon, are also the slowest in their enlargement, hence, generating the typical helical arrangement of the paranodal region.

### 2.3. Abnormalities of Myelination and Their Simulation by the Model

"An interesting study is that of Robertson and Vogel (1962) on the structure of the concentric laminations of the glial processes in some oligodendrogliomas. From their excellent illustrations there is no doubt that apart from the arrangement of the lamellae, the concentric laminations are similar in appearance to the loose myelin formed during the early stages of myelin formation in both central and peripheral sheaths. If the cells responsible for the formation of both these concentric laminations and central myelin sheaths are oligodendrocytes, then it is very interesting that the cells are capable, under different conditions, of forming both concentric and spiral lamellae." (Peters, 1964).

A very important consideration for any model of myelination is the possibility of predicting the appearance of specific abnormalities by manipulating its rules of formation. This model suggests immediately that the formation of spiral sheaths is dependent on a complex mechanism of membrane alignment and fusion. The absence of any of the proteins necessary for the process, will inevitably produce alterations in the outcome. Moreover, it is possible to recognize at least two types of



Figure 2.3.2. Portions of myelinated fibers of 70-day-old quaking mouse. Note the intramyelinic islands of oligodendroglial cytoplasm, the abundance of microtubules, and the abundant but disorganized radial components. [From Nagara and Suzuki, 1982].

abnormalities: first, those that produce strictly an alteration in the continuity of the spiral (like the example cited above); and second those that will alter the compaction and biochemical properties of the myelin sheaths. Hence, it should be possible to find some examples where one of the two possibilities is predominant.

Alterations of the alignment of EMPs and of the fusion events can produce :

1) Concentric lamellation : This scenario can be generated if fusion occurs only at "2"; examples of these abnormalities can be found in Robertson and Stephen (1962) and Cullen and Webster (1979) (see Figure 2.3.1).

2) Irregular arrangements of myelin with vermicular processes in the periphery of the myelin sheath, and interruption of lamellation : In this case the lack of fusion at "2" or misaligned deposition of EMPs will generate a series of disconnected lamellae, some of which can become completely separated from any cellular contact as if excluded to the extracellular space; examples can be found in the neurological mutants Quaking, Shiverer and perhaps in Jimpy (Nagara and Suzuki, 1982 and Rosenbluth, 1980; see Figures 2.3.2, 2.3.3. and 2.3.4).

On the other hand alterations of specific myelin membrane components other than those required for its assembly would be expected to produce uncompacted or unstable myelin membranes, or an arrest of myelination due to the lack of adequate myelin constituents. Several examples can be found in the literature,

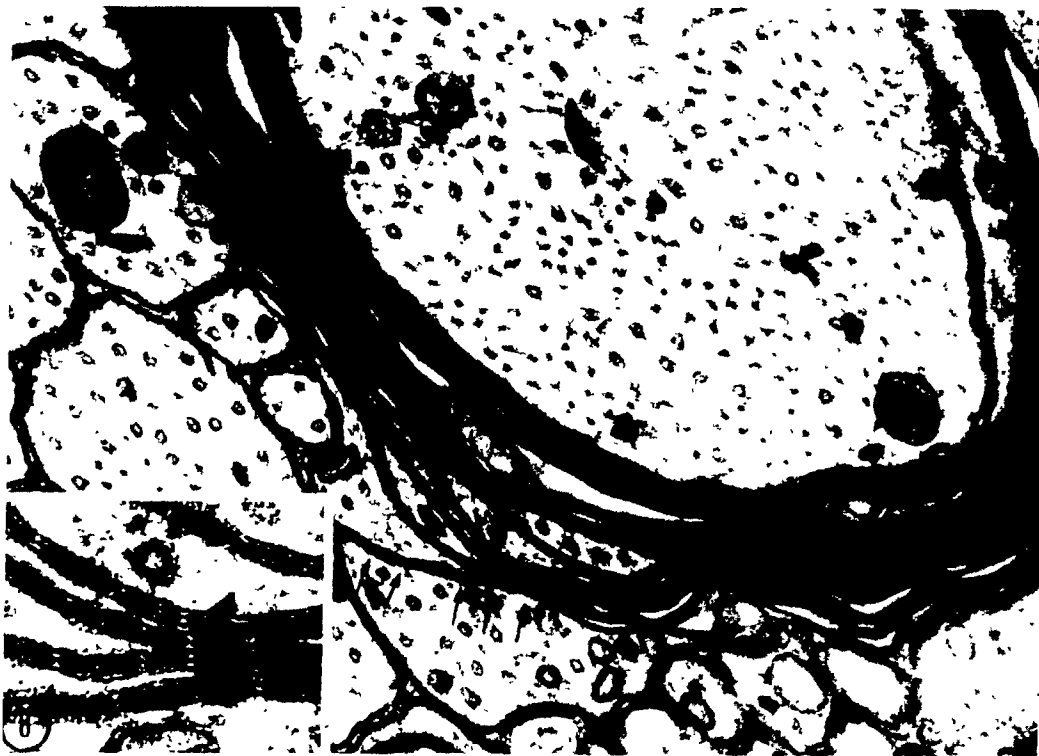
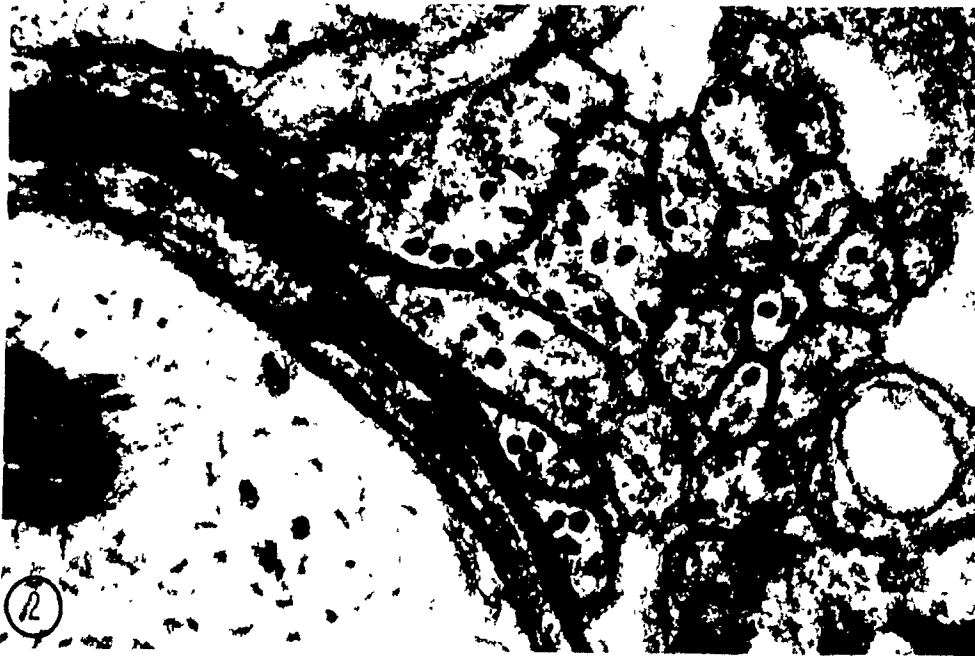


Figure 2.3.3. Rare jumpy myelinated axon showing intermyelinic islands of oligodendroglial cytoplasm and a major disorganization of both the intra and extra period lines. Focally increased (arrows) radial components are common at the sites of intermyelinic islands of cytoplasm. Note microtubules and endomembrane tubules (EMPs?) in these islands. [From Nagara and Suzuki, 1982].

such as the case of the Trembler and the Jimpy neurological mutants (see Figures 2.3.4), and the effect of certain gliotoxins during development (e.g. inhibitors of cholesterol synthesis, Rawlins and Geren Uzman (1970)).

Lastly, certain aberrant forms of myelination commonly observed under normal or pathological conditions may be considered in the context of this model, not because they can be simulated by specific alterations in the properties of the construction method used, but because of the ability of this model to generate spiral sheaths of compacted myelin under extraordinary circumstances. Examples of these circumstances have been described in Section 1.3. (myelination of neuronal perikarya and dendrites in the CNS of vertebrates). Other examples include the myelination around multiple axons in peripheral nerves under pathological conditions (see Figure 2.3.5, Dystrophic mouse - Brown and Radich, 1979; M. leprae inoculated rodents - Shetty and Antia, 1980) and the common encounter of redundant myelin forms in dystrophic and normal animals (see Figure 2.3.5, and 2.3.6 from Rosenbluth, 1966).

The point here is not to enumerate strange myelin configurations (of which there are many) but to indicate the adaptability of the ensheathing mechanism to topographies that in cases of 'need' can be successfully myelinated. This requires a myelination mechanism that can function independently of the outside topography, that is to say from within, but in obedience to some general principle of cellular ensheathment.



Figures 2.3.4. Portion of a shiverer myelin sheath showing several lamellae terminating in looplike structures that contain microtubules and amorphous background material. A cluster of about a dozen such oligodendrocyte processes closely apposed to each other is situated immediately adjacent to these loops. [From Rosenbluth, 1980].

#### 2.4. In Search of Molecular-Biological Evidence

This section will focus on some of the evidence available that supports an intracytoplasmic mechanism of active ensheathment by myelin-forming cells.

The presence of lamellated membranous and granulated bodies - called "gliosomes" (Scharrer, 1939; Pipa et al. 1962) - in neuroglia is well documented in invertebrates where they have been associated with lysosomal activities on the one hand, and with storage of specialized products on the other (Lane, 1981). In the oligochaete *Tubifex* gliosomes have been shown to increase in number during CNS differentiation and then to decrease after the completion of ganglionic development (Djaczenko and Cimmino, 1976).

The formation of gliosomes in vertebrates is common in specific experimental situations such as, astrocytes grown in organotypic cultures of the cerebellum and spinal cord (Raine and Bornstein, 1974) and cultured oligodendrocytes isolated during active myelination (see Figure 2.4.1. and 2.4.2; courtesy of Dr. Szuchet - Szuchet et al., 1980).

Oligodendroglisomes were described initially by Del Rio Hortega (1928) who drew attention to their presence at the time of active myelination. Immunocytochemistry at the light microscopic level seems to corroborate their presence (see figure 4. A-E in Hartman et al. 1979, 1982) during the active phase of myelination (note the general resemblance to Figure 2.4.2). In the context of CNS myelination these structures can be expected

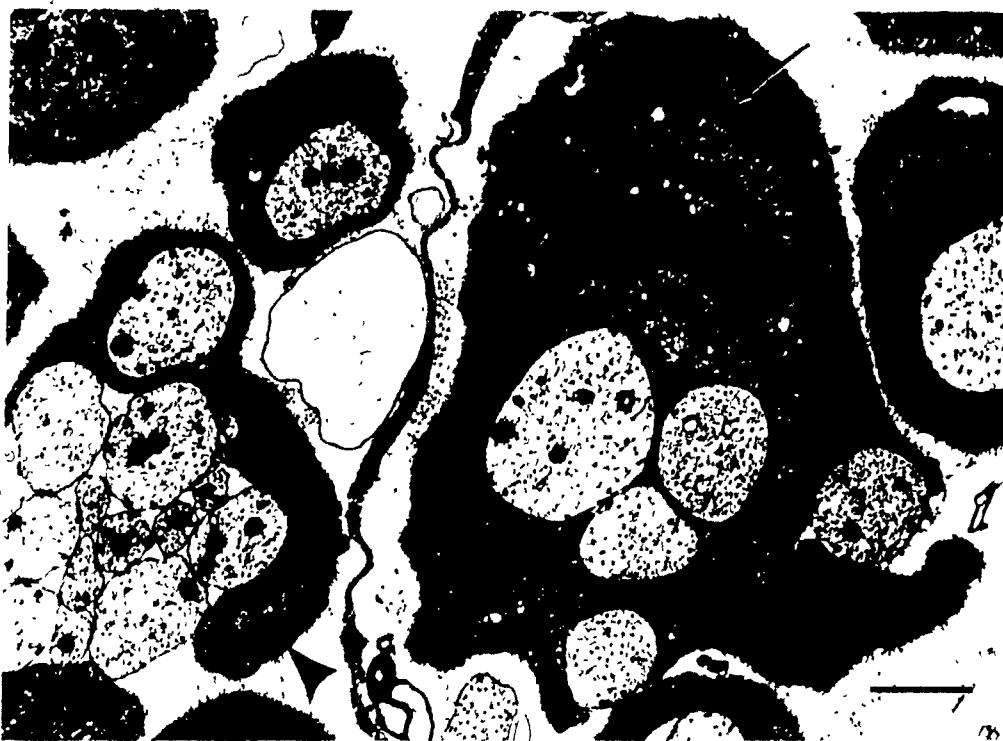


Figure 2.3.5. Proximal sciatic nerve of a three-day-old dystrophic mouse. One irregular myelin sheath encloses three axons and Schwann-cell cytoplasm. The redundant fold of myelin (arrow) resembles those associated with singly myelinated axons in developing normal and dystrophic (arrowhead) nerves. Bar= 1- $\mu$ m. [From Brown and Radich, 1979].



to represent 'envoys' of preformed membrane structures destined for the myelination compartment where they, in the light of this model, will generate the EMPs. The exact topology of these gliosomes can be expected to be of many forms as evidenced by the collection of observations of vesicular, tubular, crystalline and multilamellated and amorphous structures in the inner and outer cytoplasmic extensions of the myelin sheath during ontogenesis (see Figure 2.4.3. from Celio, 1979; see also Rawlins and Geren Uzman, 1970; Cullen and Webster, 1977 among others). The structure of each of them could represent different lipid-protein phases or a different metabolic stability of the membranes (lysosomal). Their presence in alterations of myelinating and demyelinating neuropathies has been amply documented and they are known as "myeloid bodies" (Peters, et al. 1976). Their relation to myelin development has, however, been considered only by a few authors (Cullen and Webster, 1977; Hildebrand, 1971). The accumulation of these structures in some neurological mutants and other circumstances that inhibit myelination can only suggest a role in myelin assembly.

Recent studies with undernourished developing rats has yielded some very interesting observations that strengthen the role of endomembrane arrangements ( gliosomes ?) in myelin formation (Sharma, 1983 personal communication). Dr. Sharma's interpretations resemble the early descriptions of DeRobertis (1958) (see Section 1.4) and suggest the complete 'endocytosis' of the axon into the oligodendroglial cytoplasm, followed by the



Figure 2.3.6. Granule cell almost completely enveloped by myelin. Terminal loops of glial cell cytoplasm occur at both ends of the sheath. No separation or light seam is visible within the sheath. From the unsheathed portion of the granule cell, a process emerges. [A, axon terminal. x 11,500 ]. (From Rosenbluth, 1966).

direct arrangement of pentalamellar structures of the endoplasmic reticulum around the engulfed axon. The described structures are very similar to the gliosomes of cultured oligodendrocytes isolated during active myelination ( see Figure 2.4.1).

The role of the endoplasmic reticulum in the relationship of glial cells to neurons is one striking feature of all invertebrate and lower vertebrate nervous systems (Holtzman et al. 1970; Lane, 1981). It is also involved in the functional adaptation of many other cell systems of which, the retinal fine structure in octopus (Yamamoto et al. 1965), the junctional subsurface organs in sympathetic ganglion cells of the frog (Watanabe and Burnstock, 1976) and the ergastoplasm of the parotid acinous cells (Parks, 1962) are only some examples.

## 2.5. Final Considerations

Reexamination of Figure 2.2.1. suggests that this model requires three fundamental cytological prerequisites :

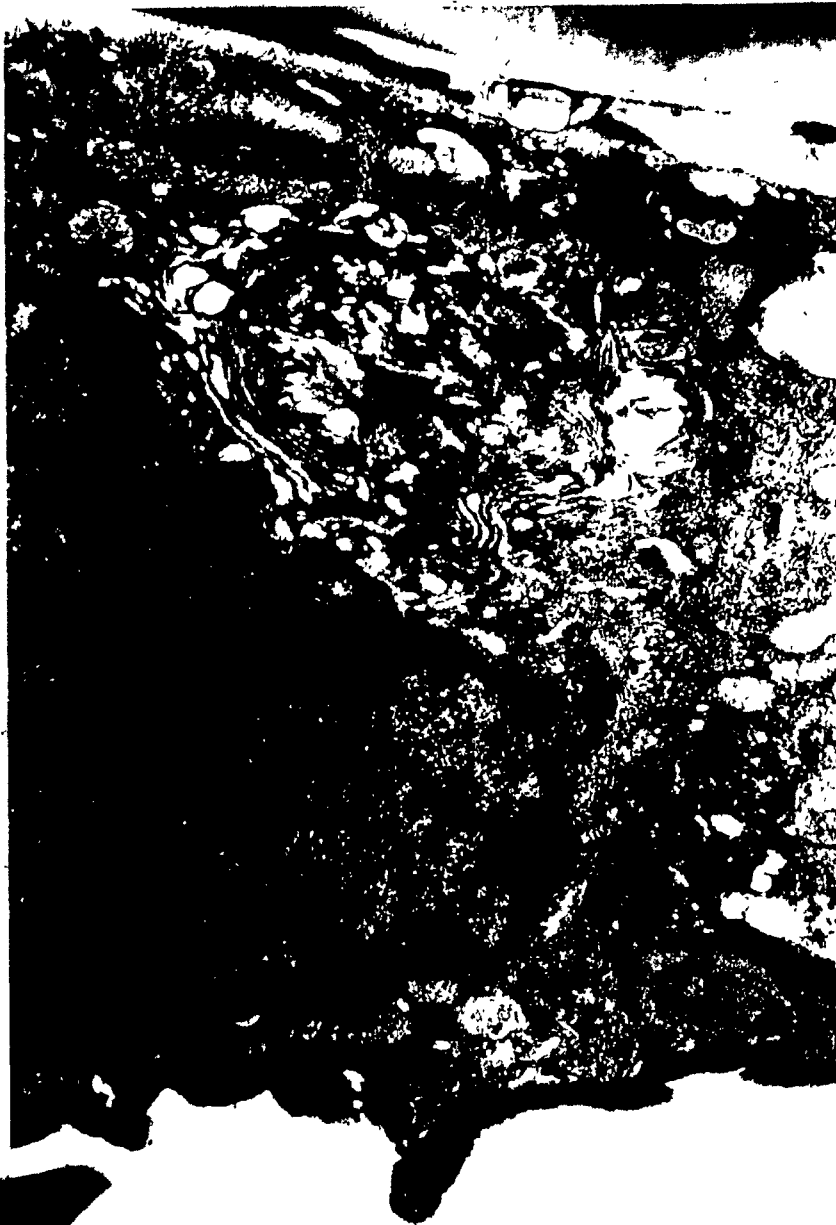
- 1 ) The metabolic compartmentation of the perimyelin space.
- 2 ) The formation of promyelin membranes that will constitute the EMPs.
- 3 ) The presence of a specialized alignment complex.

The first two considerations become immediately relevant in the context of CNS myelination, where oligodendrocytes connect to their myelin sheaths by tortuous and very fine processes ( dendrites; see Figure 2.5.1, from Roussel and Nussbaum, 1981).

This requires material from the cell's soma to be carried towards a well defined myelin compartment. In the PNS compartmentation of the perimyelium space is not so evident, although careful scrutiny of the morphological evidence seems to indicate the existence of a complex cytoplasmic compartmentation (Kruger et al. 1979). Furthermore, it is necessary to emphasize that the ideas which gave rise to this model are based on the assumption that there is no a priori indication that the mechanisms of myelin membrane assembly in the PNS and the CNS are the same. Nevertheless, the inclination to do so will always be there until clear evidence is presented of both, the true ensheathing mechanism of the myelin-forming cells in PNS and CNS, and of their assembly mechanisms.

Table 2.5.1 summarizes the most important biogenic inferences that can be gathered from this model. When compared to the biogenic inferences derived from the "Spiral-Wrapping" hypothesis as exposed in Table 1.4.1, the most important difference between the two models is, from the point of view of the kinetics of assembly, the continuity or discontinuity between the assembly of new membrane elements into myelin and the formation of new lamellae; that is, between membrane biogenesis and myelin morphogenesis. As will become evident in Chapter 5 this difference between the models is immediately relevant to the kinetic approach to be described in this thesis. The technology and theoretical approaches presented in Chapters 3 to 5, should permit the further investigation of this very important question.

Figure 2.4.1. Thin section through a cultured oligodendrocyte isolated from myelinating sheep brain showing encircled and juxtaposed arrangement of endomembranes. This feature has been described during the same period of extensive restructurization of processes by these cells and the appearance of glial bodies along the processes (see Fig. 2.4.2.) [the picture is a courtesy of Dr. S. Szuchet].



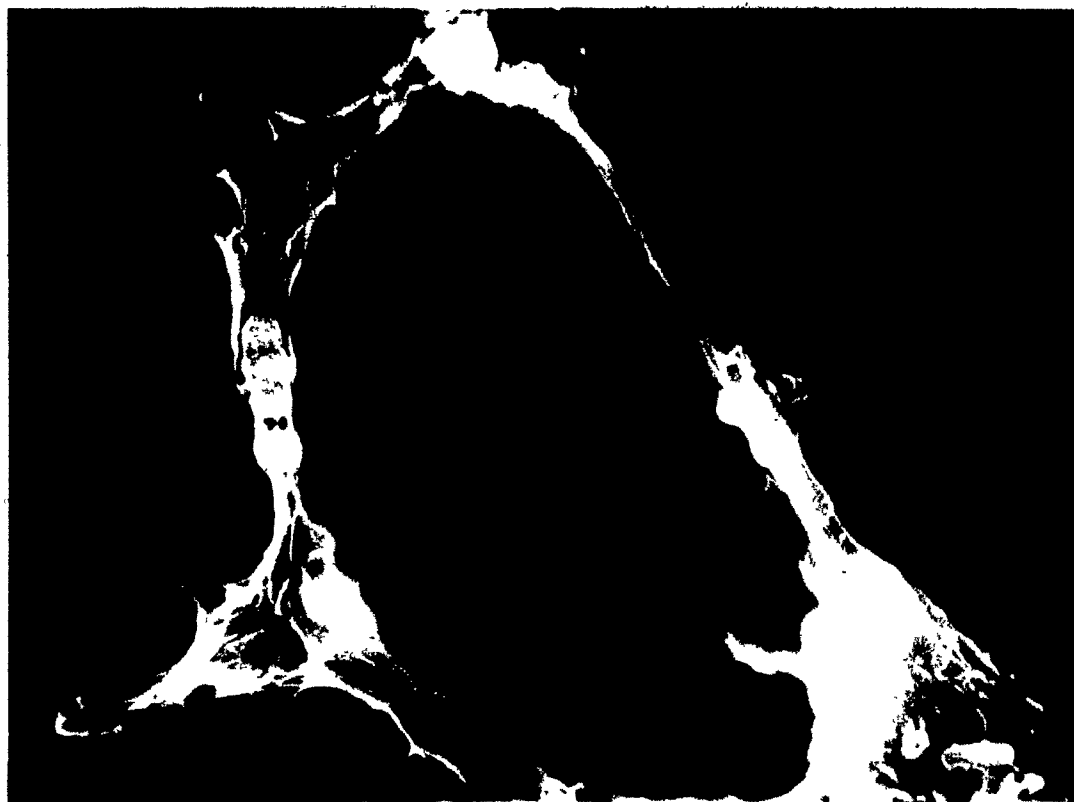


Figure 2.4.2. Scanning electron micrograph of a cultured oligodendrocyte isolated from myelinating sheep brain showing characteristic spherical bodies along newly made processes. [Picture is a courtesy of Dr. S. Szuchet]

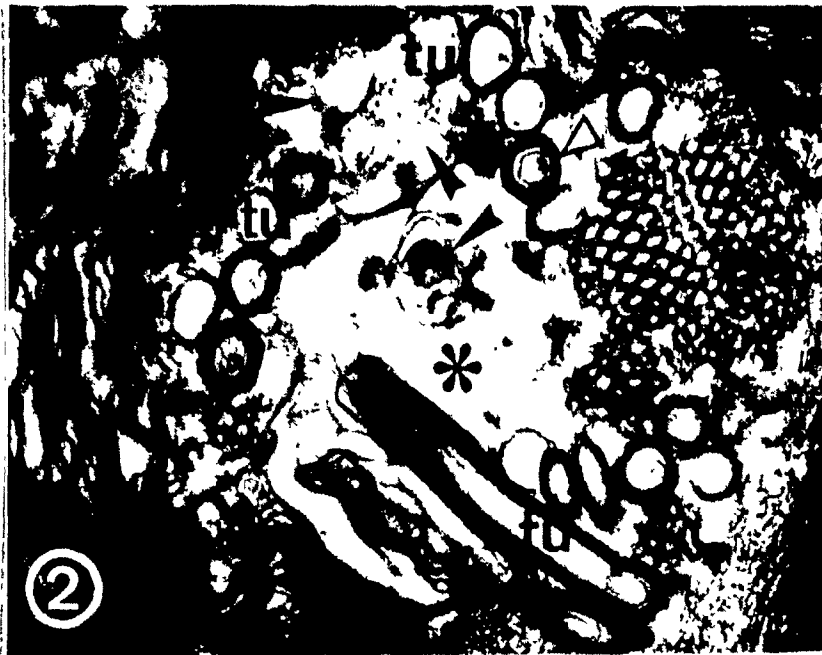


Figure 2.4.3. Transverse section through the myelin sheath of the Mauthner axon showing circular ordered structures in a widening of the myelin sheath composed of 'tubular' (tu) and 'undulated profiles' (pe). Structures with slightly rounded or oblong form (black arrowheads) and empty regions (asterisk) are also present. 'Tubular profiles' contain a structure similar to the inner tongue of usual myelin sheath (white arrowhead). x 28,000. [From Celio, 1979].

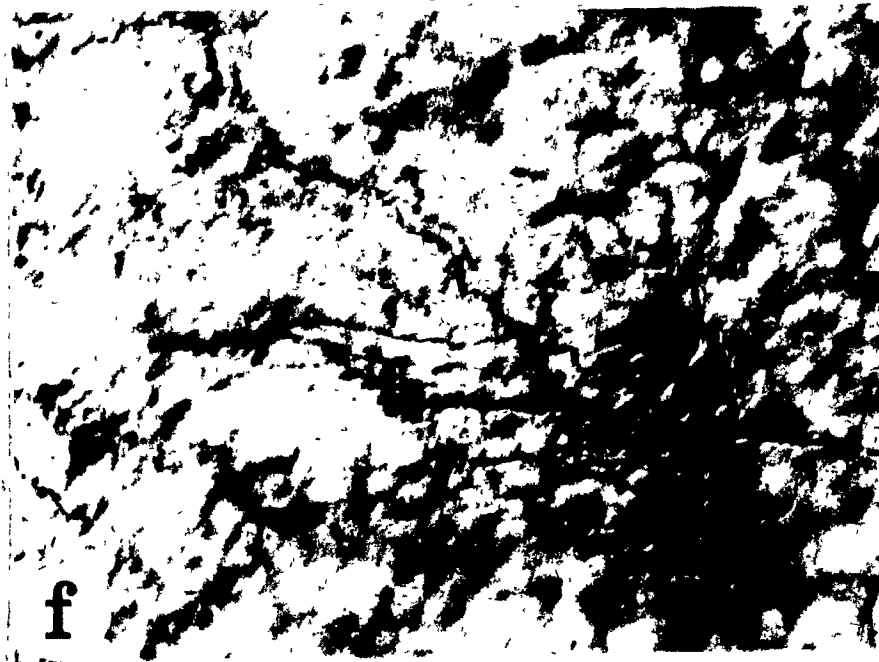


Figure 2.5.1. Cryostat section of 8-day-old rat corpus callosum immunostained with 1:100 antimyelin basic protein serum. All the cytoplasm of the oligodendroglial cell appears positive; numerous stained processes originating from this cell are visible. Interference contrast optics x 830. [From Roussel and Nussbaum, 1981].

TABLE 2.5.1.

Biogenic implications of the Model

---

1) Compartmentation of the Cytoplasm:

- a) Formation of a perinuclear metabolic space
- b) Formation of a periaxonal spiralled premyelin ensheathment space
- c) Transformation of the cytoskeletal apparatus
- d) Expression of myelin phenotypes in different compartments.

2) Events in the Perinuclear Compartment:

- a) Synthesis of integral membrane components in the RER
- b) Synthesis of lipids and cholesterol
- c) Processing of lipids and proteins through the GA to form glycolipids and glycoproteins
- \* d) Formation of pro-myelin membrane "granules" from membranes derived from the SER and GA
- \* e) Transportation of granules to the periaxonal space
- f) Direct insertion of Golgi derived vesicles in the perinuclear plasmalemma or their transport to the periaxonal compartment

3) Events at the Site of Myelination (Periaxonal space):

- a) Local synthesis of cytoplasmic enzymes, cytoskeletal elements and membrane adsorbed proteins
- b) Formation and arrangement of EMPs from the pro-myelin granules (CNS) or Golgi derived vesicles (PNS).
- c) Modulation of myelin membrane properties through biochemical modifications of lipids and proteins to achieve EMP fusion, myelin formation and lamellar compaction.
- d) Intrinsic metabolic transformation to stabilize the myelin sheaths

---

\* CNS only.



## REFERENCES CHAPTER 2

- Benjamins, J.A. and Morell, P. (1978). Proteins of myelin and their metabolism. Neurochem. Res., (3): 137
- Brady, R.O. and Quarles, R. (1973). The enzymology of myelination. Mol. Cell. Biochem., 2: 23
- Brown, M. and Radich, S. (1979). Polyaxonal myelination in developing dystrophic and normal mouse. Muscle & Nerve, May/June: 217
- Celio, M.R. (1979). 'Tubular and undulated profiles' in the myelin sheath of axons in the goldfish spinal cord. Experientia, separatum, 35: 262
- Cullen, M.J. and Webster, H. deF. (1977). The effects of low temperature on myelin formation in optic nerves of *Xenopus* tadpoles. Tissue & Cell, 9: 1
- Cullen, M.J. and Webster, H. deF. (1979). Remodelling of optic nerve myelin sheath and axons during metamorphosis in *Xenopus laevis*. J. comp. Neurol., 184: 353
- del Rio Hortega, P. (1928). Tercera aportación al conocimiento morfológico e interpretación funcional de la oligodendroglia. Mem. Real Soc. Esp. Hist. Nat., 14: 5
- Dermietzel, R., Schunke, D. and Leibstein, A. (1978). The oligodendrocyte junctional Complex. Cell Tiss. Res. 193:61
- Dermietzel, R., Leibstein, A.G. and Schunke, D. (1980). Interlamellar tight junctions of central myelin II.. Cell Tiss. Res., 213: 95
- Djaczenco, W. and Cimmino, C.C. (1976). 'Glia-neuron relationship during the post-embryonic development of the nervous system in *Tubifex*'. In Proc. 6th European Congress in Electron Microscopy. Vol 2. (Ed. Ben-Shaul, Y.) Jerusalem pp:602.
- Friede, R.L. (1972). Control of myelin formation by axon caliber (with a model of control mechanism). J. comp. Neurol., 144: 233
- Hartman, B.K., Agrawal, H.C., Kalmbach, S. and Shearer, W.T. (1979). A comparative study of the immunohistological localization of basic protein to myelin and oligodendrocytes in rat and chicken brain. J. Comp. Neurol., 188: 273
- Hartman, B.K., Agrawal, H.C., Agrawal, D. and Kalmbach, S. (1982). Development and maturation of central nervous system myelin. Proc. Natl. Acad. Sci.(USA), 79: 4217

Hildebrand, C. (1971). Ultrastructural and light-microscopic studies of the developing feline spinal cord white matter II. Cell death and myelin sheath desintegration in early postnatal period. Acta Physiol. Scand. Supp., 364: 109

Hildebrand, C. and Hahn, R. (1978). Relation between myelin sheath thickness and axon size spinal cord white matter of some vertebrate species. J. Neurol. Sci., 38: 421

Holtzman, E., Freeman, A.R. and Kashner, L.A. (1970). A cytochemical and electron microscope study of channels in the Schwann cells surrounding lobster giant axons. J. Cell Biol., 44: 438

Kirschner, D.A., Hollingshead, C.J., Thaxton, C., Caspar, D.L.D. and Goodenough, D.A. (1979). Structural states of myelin observed by X-ray diffraction and freeze-fracture electron microscopy. J. Cell Biol., 82: 140

Kruger, L., Stolmski, C., Martin, B.G.H. and Gross, M.B. (1979). Membrane specializations and cytoplasmatic channels of Schwann cells in mammalian peripheral nerve as seen in freeze-fracture replicas. J. comp. Neurol., 186: 571

Lane, N.J. (1981). Invertebrate neuroglia-junctional structure and development. J. Exp. Biol., 95: 7

Lazarides, E. (1980). Intermediate filaments as mechanical integrators of cellular space. Nature, 283: 249

Mugnaini, E. (1978). 'Fine structure of myelin sheaths'. In Proc. of the European Soc. for Neurochem. (Ed. Neuhoff, V.) Vol. 1 pp:3

Nagara, H. and Suzuki, K. (1982). Radial component of the central myelin in neurologic mutant mice. Lab. Invest., 47: 51

Parks, H.F. (1962). Unusual formations of ergastoplasm in parotid acinous cells of mice. J. Cell Biol., 14: 221

Peters, A. (1964). Further observations on the structure of myelin sheaths in central nervous system. J. Cell Biol., 20: 282

Peters, A., Palay, S.L. and Webster, H. deF. (1976). 'The Structure of the Nervous System: The neurons and supporting cells'. W.B. Saunders Co. Pha.

Pipa, R.L., Nishioka, R.S. and Bern, H.A. (1962). Studies on the hexapod nervous system. V. The ultrastructure of the cockroach gliosomes. J. Ultrastruc. Res., 6: 164

- Raine, C.S. and Bornstein, M.B. (1974). Unusual profiles in organotypic cultures of central nervous tissue. J. Neurocytol., 3: 313
- Rawlins, F.A. and Geren Uzman, B. (1970). Retardation of peripheral nerve myelination in mice treated with inhibitors of cholesterol biosynthesis. J. Cell Biol., 46: 505
- Robertson, D.M. and Stephen Vogel, F. (1962). Concentric lamination of glial processes in oligodendrogliomas. J. Cell Biol., 15: 313
- Rosenbluth, J. (1966). Redundant myelin sheaths and other structural features of the toad cerebellum. J. Cell Biol., 28: 73
- Rosenbluth, J. (1980). Central myelin in the mouse mutant Shiverer. J. comp. Neurol., 194: 639
- Roussel, G. and Nussbaum, J.L. (1981). Comparative localization of Wolfgram W1 and myelin basic proteins in the rat brain during ontogenesis. Histochem. J., 13: 1029
- Scharrer, B.C.J. (1939). The differentiation between neuroglia and the connective tissuesheath in the cockroach (*Periplaneta americana*). J. comp. Neurol., 70: 77
- Sharma, S.K. (1983). Dep. Neurology. All India Inst. Med. Sci. New Delhi, India.
- Shetty, V.P. and Antia, N.H. (1980). Myelination around multiple axons in the peripheral nerve. An unusual ultrastructural observation. Acta Neuropathol. (Berl), 50: 147
- Szuchet, S., Stefansson, K., Wollmann, R.L., Dawson, G. and Arnason, B.G.W. (1980). Maintenance of isolated oligodendrocytes in long-term culture. Brain Res., 200: 151
- Tabira, T., Cullen, M.J., Reier, P.J. and Webster, H.deF. (1978). An experimental analysis of interlamellar tight junctions in amphibian and mammalian C.N.S. myelin. J. Neurocytol., 7: 489
- Watanabe, H. and Burnstock, G. (1976). Junctional subsurface organs in frog sympathetic ganglion cells. J. Neurocytol., 5: 125
- Yamamoto, T., Tasaki, K., Sugawara, Y. and Tomasaki, A. (1965). Fine structure of Octopus retina. J. Cell Biol., 25: 345

### 3. THE STUDY OF MYELIN MEMBRANE ASSEMBLY:

#### DESCRIPTION OF A KINETIC APPROACH BASED ON

#### THE THEORY OF MEMBRANE BIOGENESIS

Myelin when compared to other cellular membranes stands out, not only because of its distinctive morphology, but also due to its particular molecular composition (Benjamins and Morell, 1978).

Furthermore, its function, morphology and evolution can be shown to be closely related to the biology of the axon (Bunge, 1968; Johnston and Roots, 1972).

Myelin can not be studied as though it were merely a specialized extension of the plasma membrane, but rather it must be seen as an adaptation that incorporates a new level of membrane to membrane, and cell to cell association. Myelin does not delimit the cell cytoplasm and it is not merely an intercellular association. Myelin and its related axonal segment can be seen as an extracellular "organelle" or elementary intercellular working unit. Hence, because of the unique nature of the myelin-axon association, it is important to appreciate that the study of myelin assembly requires concepts that embrace the molecular biology of plasma membrane biogenesis, and that of organelle biogenesis.

A brief review of current concepts in membrane biogenesis and the description of the ambiguities encountered will, I hope, illustrate this point more clearly.

Given that this thesis concentrates on the distinction between developmental and precursor-product relationships among myelin subfractions, making use of time-staggered double isotope (TSDI)

techniques, an understanding of this and other labelling techniques is essential. Furthermore, a review of the literature, reporting the use of these techniques to study myelin protein assembly and turnover, indicates that a reassessment of the conclusions and underlying concepts is necessary. The protein translocation model, presented in the third section of this chapter, is the product of theoretical and empirical research done in the last year and a half. It represents only the groundwork for a more detailed description currently underway. Nevertheless, the postulates derived from this model are sufficient to interpret isotopic ratios without further extenuating descriptions, and finds its application as a confirmation procedure in the analysis of developmental and biogenic relationships among subcellular fractions.

### 3.1. Concepts in Membrane Biogenesis and Turnover

The first concept to be discussed is "membrane biogenesis". This term implies the formation of new biological membranes from existing ones (Palade, 1965). Molecularly, this suggests that the biosynthetic machinery required to incorporate membrane components such as lipids and proteins, must be present in all or some of the cell membranes. Experimental evidence suggests that, in most cell types, the only endomembranes with these characteristics are the nuclear envelope (NE) and the rough endoplasmic reticulum (RER) (Morre et al., 1979). These membranes contain the most complete array of lipid, protein, and carbohydrate biosynthetic machinery. This contrasts with the plasma membranes (PM) which are potentially the least autonomous of the

cellular membranes with respect to their biogenesis. Other endomembrane systems, such as the Golgi apparatus (GA) and other smooth vesicular (VS) or trabecular endomembranes (SER), are intermediate to these two extremes and have a limited biogenic role (Morré, 1977).

Biochemical analysis of these discrete endomembrane structures attest further to their compositional and functional differences, as well as to their biogenic interrelationships. These complex properties have been expressed by Morré (1977) and Morré and Mollenhauer (1974) in their concept of "endomembrane system". In this thesis I will refer to this "endomembrane system" as "endomembrane network", for reasons that will become apparent in the context of the protein translocation model (Section 3.4).

The general picture which emerges from studies on membrane biogenesis is that integral lipid and protein components of the endomembrane network are synthesized and initially modified (enzymatically) in the RER/NE. Their translocation to the smooth (polysome free) endomembranes - SER, GA, VS - brings about further specific modifications to these components before they are translocated either to the plasma membrane<sup>2</sup>, lysosomes<sup>2</sup> and secretory vesicles<sup>2</sup>, or alternatively retained along the endomembrane pathways as intrinsic constituents.

Essential to this "flow of membrane" is the biochemical transformation of its constituents through specific and sequential enzymatic activities (peptidases, glycosyl transferases, phosphokinases, methyl transferases, etc...). In general terms, the nature of these modifications is specific to each component of the

endomembrane network and has been widely used to define these membranes (i.e. the concept of Enzyme Marker; De Duve et al., 1962).

The detailed picture, however, is much more complex. Contradictory observations made in the last decade have brought into question - not so much the validity as the generality - of the above picture. Research has concentrated on two major areas: the synthesis, translocation, degradation and compartmentalization of membrane components, and the biogenesis of the Golgi apparatus and the plasma membrane.

Protein synthesis has been shown to occur both in membrane bound (in the RER) and membrane free polyribosomes (see Shore and Tata, 1977 for a review). In general, intrinsic (deeply embedded) membrane proteins, and secretory proteins are synthesized by membrane-bound polyribosomes (Palade, 1975). However, certain integral membrane proteins as well as proteins that are translocated through membranes are known to be synthesized by membrane free polyribosomes (Parry, 1978; Morré et al., 1979).

Incorporation of proteins into membranes is currently envisioned in the context of two major hypotheses: the "Signal" hypothesis of Palade (1975) and the "Trigger" hypothesis of Wickner (1979, 1980) (For a critical assessment of these and other hypotheses see Waksman et al., 1980). The major difference between the two is the dependence, or independence, of protein insertion into the membrane on the binding of ribosomes to the membrane. In the "Signal" hypothesis protein insertion is dependent on the driving force produced by membrane-attached ribosomes during protein synthesis and the cleavage of an N-terminal "Signal" sequence. In the "Trigger" hypothesis,

insertion is a function of physiochemical factors inherent in the protein which allow the assembly of proteins synthesized by free polyribosomes into membranes.

The advantages of membrane bound polyribosomal protein synthesis can be easily appreciated in the case of secretion and the production of large amounts of membrane. On the other hand, free ribosomal protein synthesis and subsequent insertion into membranes can also be advantageous in retaining the functional versatility of endomembranes (See for example Golgi-associated free ribosomes, Morré, 1977). Hence the Trigger hypothesis can be viewed as a more generalized hypothesis, where membrane-bound polyribosomal protein synthesis can be considered as two composite events: protein synthesis and membrane insertion; making the "Signal" hypothesis the description of a specialized case.

We will now turn our attention to some of the current concepts on the translocation of membrane components along endomembranes. As mentioned above, there are strong indications for a vectorial transport of proteins and lipids from the RER/NE to other endomembranes. How this transport occurs is summarized in the "Membrane Flow" hypothesis (Franke et al., 1971; Palade, 1975) and the important modifications introduced later (Morré et al., 1979). The principal arguments in this model can be summarized as three distinct concepts:

- 1) "The biogenesis of certain membranes is accomplished by the physical transfer of membrane material from one cell component (e.g. RER) to another (e.g. PM) in the course of their formation or normal functioning" (Franke et al., 1971).



2) Membrane flow is selective, that is, some components are transferred while others are not, and membranes are not transferred in bulk. (Morré et al., 1979).

3) Membrane flow involves endomembrane differentiation (Membrane interconversion). (Morré et al., 1979). Hence, selective translocation of membrane lipids, enzymes and structural proteins can bring about the formation of specific endomembrane components with new physicochemical and biological properties.

Translocation of membranes from the RER/NE endomembrane components to the GA or PM is assumed to be mediated by membrane vesicles which pinch off from one component and coalesce to form the initial section of the next component. Net transfer of lipids and proteins is thus expected by this mechanism (discontinuous membrane flow). Alternatively, endomembrane continuity from one component to the next has also been described. In this case flow of components could occur vectorially along the membrane plane - reversal flow included (continuous membrane flow). (For a discussion on these two alternatives, see Morré et al., 1979.)

The Golgi apparatus is a complex component of the endomembrane network. Its role in endomembrane differentiation and membrane sorting is well recognized (Morré, 1977; Rothman et al., 1981). These important properties of the GA have been conceptualized in two different models, each emphasizing one or the other function in the context of three major roles assigned to the GA: 1) the formation and maintenance of the plasma membrane, 2) the organization of secretion, and 3) the compartmentalization of membrane degradation and endocytosis.

The most recent model is that proposed by Rothman (1980; Rothman et al., 1981). This model calls attention towards two biochemically different Golgi components which are proposed as two organelles in tandem (cis and trans Golgi). This model recognizes the problem of protein sorting and compartmentalization and discusses it in the context of a membrane fractionation mechanism (like fractional distillation) between the endoplasmic reticulum and the cis-Golgi. The trans-Golgi component organizes the differential transport of PM, lysosomes and secretory components through a complex three step shuttle process involving coated vesicles.

An alternative model was proposed by Morré and Outrecht (1977) based on cytochemical observations. This model also describes two Golgi compartments connected to the RER-SER by two different routes. The first compartment, composed of dilated sacules and trabeculae at the periphery of the GA, is called the "Boulevard Périphérique" and is assumed to be continuous with the RER (continuous flow). It is associated with glycosylation or other Golgi associated post-translational modifications of secretory proteins and major plasma membrane components. On the other hand, the core of the Golgi apparatus, the dictyosomes (or cisternae), are formed by the coalescence of smooth vesicles derived from the RER (discontinuous membrane flow), and are associated with the transformation of Golgi lipids. These results and descriptions imply the existence of two vectorial components: "vertical" (i.e. RER - GA - PM) and "horizontal" (i.e. from the core towards the "Boulevard Périphérique"). Furthermore, membrane translocation via both Golgi components were reported by these authors to probably be independent

(Morre et al., 1979). Both models have been derived from studies using different cell types and experimental conditions. For the moment it would be more appropriate to consider them complementary. They indicate the complex functions of the GA, and more importantly, they emphasize the adaptability of the endomembrane network to specific cell functions.

Coalescence of secretory vesicles or specific pre-plasma membrane vesicles with the plasma membrane produces a net increase in its surface area (Plasma membrane biogenesis). Furthermore, it has been recognized that secretory events and the production of plasma membrane, although mediated by the Golgi apparatus, are not necessarily the same events. (Mellman, 1982).

Plasma membrane compartmentalization is a poorly understood phenomenon. Several mechanisms have been postulated based on theories of membrane biogenesis and turnover (Evans, 1980). The role of the cytoskeleton in this event has become increasingly apparent since the observation of capping activity in antibody recognition and hormone internalization (Pastan and Willingham, 1981).

The "Membrane Flow" hypothesis does not make any specific predictions on the fate of the plasma membrane. It does however recognize the reinternalization of plasma membrane (endocytosis). PM can be either degraded in the lysosomal system (De Duve and Wattiaux, 1966; Morre et al., 1979) or recycled through some or all of the endomembrane components by a shuttle system (Rothman et al., 1981). (An alternative mechanism of plasma membrane elimination by shedding has been proposed, further supportive evidence is required Parry (1978)).

The synthesis and degradation of components of the cell as a whole, or of specific organelles is known as turnover<sup>3</sup> (Schimke, 1974). Analysis of cellular protein turnover has indicated the following general characteristics:

1) Turnover is extensive; that is, essentially all proteins of the cell take part in a continuous replacement process.

2) Turnover is largely intracellular and precludes cell replacement.

3) There is a marked heterogeneity in the rates of turnover of different proteins.

The precise mechanisms involved in the degradation of membrane components are not yet clear. Much of the work was carried out using two different methodologies which have yielded opposite results and interpretations of this phenomenon.

Schimke and collaborators (Taylor et al., 1973; Arias et al., 1969) have found that membrane (plasma and endomembranes) and cytoplasmic protein turnover occurs with varying half-lives (random, first order kinetics), and that a correlation exists between the half-life of a protein and its subunit molecular weight - with larger molecules being turned over faster. These observations have been interpreted to indicate the following: 1) individual protein components of the membrane can dissociate and associate freely with the membrane matrix; 2) while free in the cytoplasm, the proteins are subjected to degradation; 3) the surviving molecules in the cytoplasmic pool mix with the newly synthesized molecules, maintaining a constant pool size and can then be inserted into the membrane; and 4) dissociation from the membrane cannot be the rate-limiting step in

membrane protein degradation because both the "old" and newly synthesized membrane proteins must be degraded from the same pool to maintain first order kinetics (model of "heterogeneous" degradation).

An alternative mechanism for membrane protein turnover has been suggested by Tweto and Doyle (1976), Cohn (Hubbard and Cohn, 1975 (a,b) and Roberts and Yvan (1974, 1975). This model (model of "unit degradation") suggests that the proteins of the membrane must be inserted into (or removed from) the membrane in a coordinate fashion as predicted by the membrane flow hypothesis. The evidence supporting this interpretation indicates very similar half lives for various integral membrane proteins. (For an assessment of the implications of both models in the interpretation of kinetic analysis of membrane biogenesis, see section 3.3. and Tweto and Doyle (1977)).

No real alternative models exist to the "Membrane Flow" hypothesis, although important consideration has to be given to models that regard the three main endomembrane components, RER, GA and PM, as independent entities, sui generis; their membrane precursors received via special shuttle systems such as exchange proteins or membrane vesicles shuttling back and forth from a common cytoplasmic pool. These ideas have been developed from the isolation and identification of molecules or molecular aggregates with lipid exchanging properties. These molecules might play an important role in generating membrane lipid asymmetry (Parry, 1978).

One last factor to be considered is the compartmentalization of cytoplasm in zones of exclusion and zones of adhesion and the roles of these zones in differentiation, segregation and functional specialization of the endomembrane network (Mollenhauer and Morré,

1978). Zones of exclusion are characterized by the absence of ribosomes, glycogen and organelles such as mitochondria. They surround GA, GA equivalents, water expulsion vacuoles, microtubules, centrioles, flagellar bases, the cell surface, etc. Endoplasmic reticulum within zones of exclusion is devoid of ribosomes. These regions are characterized by fibrillar or coalesced material of varied composition (microfilaments, ribonucleo-protein complexes as well as other cytoskeletal protein types). Zones of adhesion on the other hand are characterized by organized, juxtaposed organelles or membrane elements (e.g. Golgi stacks, ER juxtapositions to PM or other endomembranes).

### 3.2. Kinetic Approaches to the Study of Membrane Biogenesis

#### 3.2.1. Isotopic Techniques in Studies of Membrane Flow and "Turnover"

Many of the concepts of membrane biogenesis discussed in Section 3.1 are based on the results of two basic experimental approaches. One is based on morphological and cytological observations while the other on subcellular isolation and characterization of endomembrane components. Moreover, endomembrane interconversion and differentiation have been studied mainly, by chemical, enzymatic and immunological approaches on broken (subcellular fractions) or whole cell systems (For a review on methods for the biochemical analysis of biological membranes see: Maddy, 1976. For a review on the evidence for membrane flow and interconversion among endomembranes see Morr   et al., 1979).

Typical approaches to the study of membrane flow and turnover have made use of isotope labelling procedures. In general, specific precursors to membrane constituents (amino acids, lipid precursors, carbohydrates, etc.) are administered to animals in vivo, or supplied to tissues or cells in vitro. Thereafter, at various time intervals, specific components of the endomembrane network or their specific constituents are analyzed for their radioactive content by biochemical or cytological methods. This approach offers both a corroboration of the membrane flow hypothesis and an insight into the dynamic events that can take place among components of the endomembrane network and among their constituents. The method of radio label administration, however, plays a very important role in determining the effectiveness and extent to which results may be interpreted. Turnover studies have in general used three labelling techniques: continuous labelling, pulse-labelling and double-labelling. On the other hand, membrane flow studies have made particular use of the pulse-labelling techniques. Each technique contains a number of obvious advantages as well as important limitations. These are dictated by the experimental system employed and the underlying assumptions applied to the interpretation of the results. Hence, a brief assessment of these techniques will enable a more critical evaluation of isotope studies on myelin protein synthesis and turnover, as well as on myelin membrane assembly.

a) Continuous Labelling. This method requires the continuous exposure of a cell or organism to labelled precursors. Under such conditions, the rate at which the specific radio-activity of the cell protein approaches its maximal value is proportional to the degradative rate.

(See Schmike, 1970 for an exposition of the method). With intact animals a constant level of intracellular specific activity of an amino acid is very difficult to maintain. Furthermore, in some cases an appreciable time lag of several hours is often required for some labelled precursors to reach their maximal intracellular specific radioactivity thereby limiting the usefulness of the method to components with a rapid "turnover". (Goldberg and Dice, 1974).

b) Pulse-Labeling. This is one of the most common isotopic techniques used in both turnover and membrane flow studies. In this approach the label is administered for a short period of time (pulse) and the radioactivity within a given protein is assayed as a function of time. Changes in the specific radioactivity of the protein or total amount of labelled protein are taken as a measure of the rate of protein degradation or turnover (flow). This is based on the assumption that new molecules of the same protein being synthesized are nonradioactive. Although the results obtained through this technique are very informative of the kinetics of macromolecular turnover in general, there are serious limitations that affect their interpretation. The most important limitation is label reutilization (Goldberg and Dice, 1974). This problem tends to produce over-estimations of degradative half-lives, especially in "stable" proteins (Koch, 1962; Poole, 1971). In studies of membrane biogenesis, label reutilization greatly affects the determination of label flow, specifically in those compartments closest to the site of synthesis. Several experimental approaches were used to minimize label reutilization (Goldberg and Dice, 1974). The most widely used method is the addition of large excess of nonradioactive amino acid,



after the initial pulse, to compete with the labelled residues for incorporation and to chase them out of the cell (pulse-chase labelling). This method, however, has some limitations when used in intact animals. The use of guanido-labelled arginine as a precursor with little reutilization has been used successfully in organs with large arginase activity (Swick and Handa, 1956; Glass and Doyle, 1972), although the degree of reutilization of this label varies with the nutritional state of the animal and the dietary intake of arginine. Other amino acids used in the same manner included C-1 labelled glutamate and aspartate, that after transamination and entrance into the Krebs cycle they are rapidly catabolyzed and the label diluted in the bicarbonate pool. This latter approach is to be taken into consideration when studying brain protein turnover or membrane protein assembly, given the very active metabolism of glutamate in this organ.

Lastly, the "sharpness" of the pulse plays a very important function in this labelling technique although very little attention has been paid to it. Pulse shape is dependent upon several factors, the most important of which are:

- 1) the extracellular and intracellular amino acid pool-shape and pool-size, and their relationship to protein synthesis (Robertson and Wheatley, 1979; Hod and Hershko, 1976; Mortimore et al., 1972; Fern and Garlick, 1974; Vidrich et al., 1977; O'Hara et al., 1981; Ames and Parks, 1976);

- 2) the kinetics of amino acid transport across membranes (Ames et al., 1976; Sershen and Lajtha, 1979; Guidotti et al., 1978);

3) the metabolism of the amino acid in question. (Patel and Balazs, 1970; Banker and Cotman, 1971; Smith, 1974) and

4) the blood flow or organ irrigation in experiments using intact animals or perfused organs, respectively (Sage et al., 1981; Bodsch and Hossmann, 1982).

c) Double-Label Techniques. Double pulse-labelling techniques are very powerful approaches used under many experimental conditions. These techniques are subjected to the same precautions that apply to single pulse labelling techniques. In addition, the validity of the interpretation of double-label results is dependent on the underlying assumptions and interpretative models used in the experiment. In this section we will discuss only two such approaches as they apply to research on myelin turnover and assembly.

1) Time-staggered double isotope techniques: Based on the interpretative models derived from non-isotopic determinations of enzyme turnover (Schimke, 1974), Arias et al., (1969) described the use of a time-staggered double isotope protocol for the determination of protein degradation. In this approach,  $^{14}\text{C}$ -leucine is first administered to the animal and then some days later  $^3\text{H}$ -leucine is given to the same animal which is sacrificed 4 hours later. Proteins with rapid turnover rates (rapid synthesis (high  $^3\text{H}$ ) and rapid degradation (low  $^{14}\text{C}$ ) will have high  $^3\text{H}/^{14}\text{C}$  ratios.

This approach is based on four inherent assumptions (Schimke, 1973);

1) the labelled precursors are not metabolized to other compounds which are also incorporated into proteins;

- 2) the rates of protein synthesis and breakdown are the same when the first and second injections of isotope are given;
- 3) the proteins under study follow exponential decay kinetics; and
- 4) at the time the animal is killed, the amounts of  $^3\text{H}$  and  $^{14}\text{C}$  in tissue proteins are decreasing at identical rates.

The first two assumptions are the easiest to satisfy if adequate notice is taken of the precautions noted for the case of pulse-labelling techniques.

Margiveanu and Ghetie (1981) in their paper on a selective model of plasma protein degradation argue that: "The assumption that plasma protein catabolism would be a first-order, randomly occurring process, is commonly accepted today. This rather large consensus does not arise from a true understanding of the mechanism of protein catabolism but is supported by the satisfactory fit of the experimental points describing the time decrease of a labelled plasma protein concentration by first-order kinetics." This argument can be extrapolated to the assumption of exponential decay kinetics for intracellular protein catabolism made in the above third clause. In cases of both plasma and intracellular proteins, experimental observations indicate catabolic specificity (Goldberg and St-John, 1976) and even ATP dependent degradation of proteins (Hershko *et al.*, 1979). This provides strong indications against the view of randomly occurring protein catabolism.

Glass and Doyle (1972) have shown the dependence of the fourth assumption of Schimke (1973) on the time interval used between isotope injections. Furthermore, the consequence of the random catabolism assumption as well as that of synchronicity between  $^3\text{H}$  and  $^{14}\text{C}$  decay

rates has been challenged by Tweto and Doyle (1976) on the basis of other experimental approaches.

Tsdi protocols have been applied to study myelin membrane assembly (Benjamins et al., 1976 a, b; Braun et al., 1980). The basic assumptions in these studies are: (1) isotope ratios are independent of amino acid and protein pool size and rates of synthesis of individual proteins; (2) ranking of isotope ratios for a given protein isolated from different membrane compartments indicates precursor-product relationships among such compartment under the assumption that the experiments take place during the period of linear uptake of radioactive precursor into the membranes. As will be discussed in Section 3.3 the assumption in (2) is misleading, and from the arguments presented for pulse-labelling techniques, none of the assumptions in (1) are tenable unless properly accounted for. Furthermore, none of these studies take into consideration the effect of pulse "sharpness", protein degradation, or label reutilization in the interpretation of isotope ratios.

ii) Isochronous double isotope experiments (IDI). These protocols have been widely used to study the effects of specific agents or differences between mutant strains, on protein turnover or the kinetics of membrane assembly. In all cases one label is administered to the control, while the other label is administered to the experimental system under identical conditions. Interpretation of the effects are, again, contingent on the assumptions and models used. The random degradation model for example, is widely used in turnover studies (Schimke, 1974; Kafatos and Gelinas, 1974). On the other hand, studies comparing alterations in the biogenesis of myelin

membranes between neurological mutants and their "normal" litter mates (Brostoff et al., 1977; Greenfield et al., 1977) assume that the pools of labelled amino acids for protein synthesis in the mutant and control animals are the same. Thus, a comparison of label per unit of protein isolated from a given compartment indicates the difference in relative change in the rates of incorporation. How tenable this assumption can be is open to discussion. (Further notes on IDI experiments are presented in Section 3.3.4 (see P ratios). A complete description of this protocol is not attempted.)

### 3.2.2. Myelin Proteins: Topographic Localization in the Myelin Sheath of Synthesis.

Characterization of myelin membranes by X-ray diffraction (Kirshner et al., 1983); histochemical and immunochemical techniques (Omlin et al., 1982); and through iodination reactions and chemical crosslinking reagents (Poduslo and Braun, 1975; Golds and Braun, 1976, 1978 a,b), supports the idea that MBP is located on the intracellular side of the myelin membrane (major period line). Accessibility of PLP for chemical modification using intact myelin membranes, and the large affinity of PLP to a lipid environment (Lees et al., 1979) support the idea that this protein constitutes an integral myelin membrane component. Similar procedures using lectin and antibody binding led to the conclusion that the MAG is localized at least partially, on the external side of the myelin membrane (extraperiod line) (Poduslo et al., 1976). Other myelin proteins, like CNP and constituents of the Wolfram region ( $M_r$  40 K to 70 K daltons), are not yet well

characterized and no conclusive data are yet available. (For a review see Boggs et al., 1982; Braun, 1983).

Hence, from the above, we can conclude, on the basis of the concepts of "Membrane Biogenesis", that the MBP should be synthesized by free polyribosomes while PLP and MAG should be incorporated into myelin via membrane bound ribosomal protein synthesis.

MBP mRNA has been shown to be translatable in vitro by isolated free polyribosomes (Campagnoni et al., 1980; Colman et al., 1982) although a fraction of membrane bound polyribosome has been reported in some studies to contain translatable message for MBP (Townsend and Benjamins, 1983). Recent characterization of myelin proteins with immuno-techniques has confirmed the existence of 2 MPBs ( $M_r$  21.5K and 18.5K daltons) in all vertebrates and 4 MPBs in some rodents ( $M_r$  21.5K, 18.5K, 17K and 14K daltons). That none of the higher molecular weight MPBs is a precursor to any of the lower ones has been confirmed by in vitro translation (Yu and Campagnoni, 1982; Colman, et al., 1982). Amino acid sequencing has confirmed that their differences lie in the presence or absence of two internal domains (Barbarese, 1978). Nevertheless higher molecular forms ( $M_r$  35K daltons) of proteins that crossreact with antibodies directed against MBP have been described prior to myelination (Barbarese and Pfeifer, 1981). Translation of the message for PLP on the other hand, occurs only through membrane bound polyribosomes (Colman et al., 1982), but no proteolytic processing of this protein has been reported (See section 5.4).

No in vitro translation data is yet available for MAG or the PNS Po protein, although a classical glycoprotein translocation process would be expected for both.

### 3.2.3. Myelin Protein Turnover

The general consensus is that MPB and the PLP, once in the myelin sheath, are degraded or removed from myelin at very slow rates (half-lives in the range of 100 days). Other high molecular weight myelin components ( $M_r$  larger than 30K daltons) on the other hand, have been described to have faster turnover rates (Half-lives in the order of weeks); (Benjamins and Morell, 1978).

Pulse-labelling techniques using intraperitoneal and intraventricular routes of label administration (Sabri et al., 1974; Singh and Jungawala, 1979), as well as a pellet implantation technique (Lajtha et al., 1977), have indicated the existence of a fast and a slow turnover component for the MBPs and PLP. Contamination of these proteins by fast turnover components has been implicated as a plausible artifactual cause for the observed bimodal turnover; however, the same results have been obtained using different purification methods. Nevertheless, myelin turnover studies have not taken into account other important factors that could affect these conclusions. Among them are label recycling, local (paranodal and axonal) amino acid pools, stable extramyelin pools (Benjamins and Morell, 1978), and paranodal protein synthesis of myelin components<sup>4</sup>. Moreover, the model of random first order degradation kinetics has been assumed to be valid for all proteins studied, and the data has been fitted to this model without any statistical analysis of validity.

Given the importance of the question addressed, it seems that more careful research is required before any final statements can be made with regard to the stability of the myelin compartment. It might be that myelin is a very "stable" compartment, but it also could be that myelin is a very "autonomous" compartment when referring to its own maintenance. The strategies as they have been applied to myelin turnover, only point to the existence of a complex picture.

#### 3.2.4. Assembly of Myelin Proteins

Given the heterogeneity of associations and postranslational modifications of myelin proteins, their translocation from their site of synthesis to their site of deposition will probably require more than one mechanism.

From the available information on glycoprotein processing and their translocation through the endomembrane network (Sabatini *et al.*, 1981), it can be concluded that the two main myelin glycoproteins, MAG and PNS Po protein, must be delivered to the myelin via the Golgi apparatus. Both proteins are postranslationally glycosylated. In other systems studied, fucosylation occurs primarily in the Golgi apparatus. Pulse labelling with <sup>3</sup>H fucose has been applied to study MAG and Po incorporation kinetics (Benjamins and Morell, 1978; Rapaport and Benjamins, 1981). These authors conclude that both proteins show a 30 to 60 minute time lag in their transit from the Golgi apparatus to the myelin sheath. Net inhibition of both the peptide and the carbohydrate moieties of Po can be demonstrated with monensin and tunicamycin (Rapaport *et al.*, 1982; Smith and Sternberger, 1982) which



indirectly supports the role of the Golgi apparatus in their processing.

In vitro translation studies on PLP indicate that this protein is made by membrane bound ribosomes (Colman et al., 1982). Kinetic analysis of the incorporation of this protein into myelin membranes has been done using single pulse and double pulse isotopic techniques (Benjamins et al., 1975, 1976b, 1978). These results seem to confirm a delayed incorporation of PLP, that is 15 to 30 minutes less than that for MAG or PNS Po. Although acylation of PLP has been confirmed (Jollés et al., 1977) analysis of this modification and its relationship to the kinetics of PLP assembly into myelin remains unresolved (Townsend et al., 1982).

Immediate incorporation of MBPs into myelin has been reported by Benjamins et al., (1975, 1978) using pulse labelling techniques, in agreement with its synthesis by free polyribosomes close to the site of insertion of MBPs. (Coleman, et al. 1982).

Many of the kinetic analyses done to elucidate the mechanisms of myelin protein assembly must be considered to be at an initial stage. The choice of brain slice systems (Benjamins and Iwata, 1979; Rapaport and Benjamins, 1980; Rapaport et al., 1982; Konat and Clausen, 1980; Smith, 1980; Smith and Stenberger, 1982) resolves some problems of amino acid pools and pulse "sharpness". Nevertheless, it introduces many more problems that have not been accounted for in these over-simplified incubation procedures (e.g. cell viability, accessibility of the medium to the core of the slice, etc.; Pavlik and Jakoubek, 1976; Lipton, and Heimbach, 1977). Intracranial label administration procedures (Benjamins et al., 1975, 1976a, b, 1978;

Braun et al., 1980; Shapira et al., 1981) on the other hand, have not been corrected for blood flow effects, differential metabolism of label (see section 3.3.6 and Chapter 5), and other variations due to animal age, state of nutrition etc. (Wiggins, 1982). The unaccounted limitations of all these studies have restricted the scope of the interpretations to qualitative descriptions, greatly reducing the quantitative potential of pulse labelling techniques to elucidate the dynamics of membrane assembly.

### 3.3 A Mathematical Description of Protein Translocation and Its Application to Time-Staggered Double Isotope Experiments.

As discussed in section 3.1, endomembranes can be differentiated into semi-discrete entities or ensembles with particular biochemical and morphological characteristics. According to the "Membrane Flow" hypothesis, and the recent observations on the molecular biology of secretion and plasma membrane biosynthesis, integral and luminal membrane proteins are vectorially translocated from their site of synthesis (rough endoplasmic reticulum) to their destination (i.e. plasma membrane) via intracellular membranes. Along this vectorial transit specific biochemical alterations are known to occur to the protein (postranslational modifications) and lipid components (lipid interconversions) of the membrane.

Throughout the intracellular milieu, membrane or cytoplasmic proteins will be subjected to various types of field effects (i.e. transmembrane voltage, proton gradients, intercellular ionic flow, etc.) and their response towards these local or intracellular

potential fields will be altered by the biochemical modifications that affect each protein within a given intracellular domain. In this context I wish to propose that the pathway that a given integral membrane component will take - from its site of synthesis to that of its deposition - is determined by the sequential modification of the physicochemical relationship of proteins towards other cytoplasmic or membrane elements through chemical alterations (postranslational modification).

On the basis of the above terms an endomembrane "compartment" is understood as a region of the intracellular endomembrane network where only a limited type of biochemical and physicochemical modifications are taking place. This region is isolated from other regions of the network in the sense that no chemical reactions occur across its boundary. However, there is always a directed transfer of metabolic products among compartments by either a shuttle-like mechanism or diffusion along the membrane plane.

Hence, the specific pathway that any given integral membrane protein will follow will be defined by the response of the protein to the combination of all field effects affecting a given region or domain of the cell.

The above arguments lead us to invoke the role of specialized cellular structures in the maintenance and regulation of the constraints imposed at each level of the translocation and transformation processes. Compartmentalized synthesis of specific membrane proteins in the cytoplasm (free ribosomal synthesis) and their incorporation together with other lipid constituents or precursors into membranes at specific sites along the pathway is one

obvious way of altering the physicochemical milieu of a given membrane "compartment". On the other hand, cytoskeletal anchoring of enzymes, RNA and lipid complexes at discrete locations, offers other regulatory possibilities (Fujita, 1981). Nevertheless, the important aspect discussed in here is that the intracytoplasmic organization of the endomembrane network, and for that matter, of the cytoskeleton is due to the direct response of these structures, and their components to the action of internally and externally generated physicochemical fields. This point of view is important, specially in the context of the ascribed role of the extracellular matrix in gene expression and differentiation (Bissell et al., 1982). This approach will force us to describe the various biochemical and biological alterations of the intracellular and extracellular environment in terms of more rigorous physical effects.

### 3.3.1. Definition of Compartment Space

Within the 3-d space of the cell, a given membrane "compartment" (n) can be represented as a volume domain  $V_n(\vec{r}_n)$  defined by an arbitrary position vector  $\vec{r}_n$ . In these terms the cellular space can be described as a lattice or "compartment space" made up of a finite number of volume elements or "compartments" (Fig 3.3.1.).

If we let  $g_n(\vec{r}_n)$  be the expenditure of chemical, kinetic and thermodynamic work by intracellular or extracellular potential fields at a point P in the volume element  $V_n(\vec{r}_n)$ , then the total energy associated with the displacement of the protein through the nth compartment is given by:

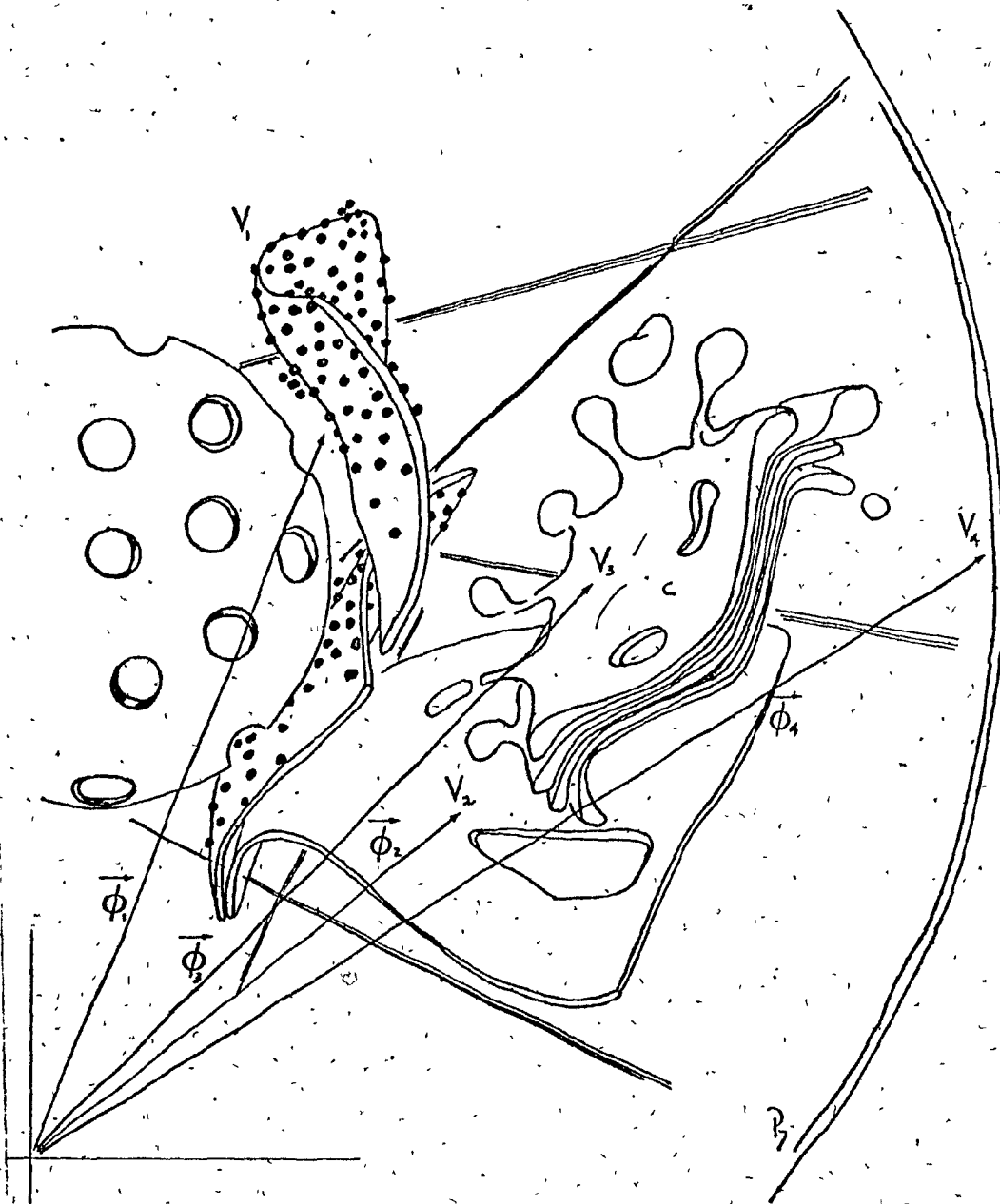


Figure 3.3.1. Diagrammatic 3-D representation of a cell where each endomembrane structure has been represented as a volume domain  $V_n(\phi_n)$  defined by an arbitrary position vector  $\phi_n$ .

$$G_n(\vec{r}_n) = \int_{V_n(\vec{r}_n)} g_n(\vec{r}_n) dV \quad 3.3.1.a$$

$$[ n = 1, 2, \dots, N ]$$

The net potential field in terms of the "compartment space" is then defined by:

$$H = - \text{grad} (G_n(\vec{r}_n)) \quad 3.3.1.b$$

Note, however, that the invariance of  $G_n(\vec{r}_n)$  with time can be assumed only if the system is in a steady state. Non steady state conditions, which may occur during cellular differentiation or during the modulation of protein synthesis and membrane biogenesis, could involve alterations of the acting potential fields and hence modifications of the intracellular cytoskeletal and endomembrane milieu.

At this point it is important to note that the specific sequence of events to which a given membrane component is subjected to, from its moment of synthesis until it reaches its final destination, will be given by the chemical history of the component and its specific response to the field  $H(\vec{r}_n)$  at any given location  $\vec{r}_n$ . The response  $r(\vec{r}_n)$ , is a measure of the effect that any given set of chemical transformations has on the susceptibility of the protein to specific field effects and also on its activation to overcome specific physical or thermodynamic barriers (boundaries) that impede its translocation. The response  $r(\vec{r}_n)$  can then be defined as:

$$r(\vec{\phi}_n) = g_n(\vec{\phi}_n) p_n(\vec{\phi}_n) = p_n(\vec{\phi}_n) \int_{V_n(\vec{\phi}_n)} g_n(\vec{\phi}_n) dv \quad 3.3.1.b$$

$$[n = 1, 2, \dots, N]$$

where  $p_n(\vec{\phi}_n)$  is a weight function characteristic for each compartment.

At each point of the lattice, a given protein will be subjected to new or altered field effects that, in turn, will define the extent of residence of the protein in the compartment and its destination. Thus the intracellular flow of the protein is not predetermined, but is determined at each point by the local effects taking place at each "compartment".

Under steady-state conditions it is possible to identify a pathway along which a given protein will be translocated from its site of synthesis to its destination. This pathway can be then viewed as a unidimensional path ( $\phi$ ) in the compartment space  $\vec{\phi}_n$ .

### 3.3.2 Definition of the General Transfer Function $\alpha(\phi, t)$ and the Degradation Function $\beta(\phi, t)$

The flow of proteins along a membrane can be investigated by applying the equation of change for a multicomponent system (Bird et al., 1960), and by including the effect of the response  $r(\vec{\phi}_n)$  as a forced diffusion term. Furthermore, if one assumes a system where proteins exist under constant mass density the concentration profile for the flow of the  $i$ th protein in the "fluid" environment of the cell sytoplasm or the endomembrane network will be given by:

$$Dc_i/Dt = D_{im} \nabla^2 c_i - (\nabla \cdot J_i) + R^* S \quad 3.3.2.a$$

where  $c_i$  is the molar concentration of the  $i$ th protein,  $D/Dt$  is the substantial time derivative, and  $R^* S$  is the molar rate of synthesis of protein " $i$ ". In fulfilment with the condition of continuity  $R^* S = \partial c_i / \partial t + (w \cdot \nabla c_i)$ .  $D_{im}$  is the effective diffusivity of the protein in the mixture and will be, as a first approximation, assumed to be constant along the pathway  $\phi$ .  $J_i$  is the forced flux of the protein at any given location  $\vec{\phi}_n$  in the "compartment space" and is written in terms of the response function  $r(\vec{\phi}_n)$  of the  $i$ th protein to the field  $H(\vec{\phi}_n)$  as follows:

$$J_i = R_{\phi n}^* c_i (\nabla \cdot r) \quad 3.3.2.b$$

where  $R_{\phi n}^*$  is a parameter dependent on the molar fraction of the  $i$ th protein in a given compartment (pool size).

Under the conditions of a pulse labelling protocol, the specific radioactivity which is a function of the path  $\phi$  and time  $t$ , is given by:

$$\alpha_i(\vec{\phi}_n, t) = kc_i(\vec{\phi}_n, t) \quad 3.3.3$$

If we assume that the labelling procedure does not perturb the system and that a steady state exists, then  $Dc_i/Dt = 0$ , and the equation for  $\alpha_i$  becomes, from equations 3.3.2.a and 3.3.3.;



$$\partial \alpha_i / \partial t = D_{im} \nabla^2 \alpha_i(\vec{\phi}_n, t) - (\nabla \cdot \mathbf{J}_i) + R_s \quad 3.3.4.$$

In addition  $\alpha_i$  will be separable in  $\vec{\phi}_n$  and  $t$ , i.e.

$$\alpha_i(\vec{\phi}_n, t) = F_n(\vec{\phi}_n) G(t) \quad 3.3.5.$$

Hence, the distribution of label along the pathway  $\phi$  can be described in terms of the "compartment space"  $\vec{\phi}_n$  by a time dependent distribution function  $G(t)$  and a function  $F_n(\vec{\phi}_n)$  characteristic for each compartment.

This discussion gives us, at least, two important temporal parameters. The first one is the time which a membrane component takes to go from its site of synthesis to a given location in the network. We call this the time of deposition,  $t_d$ . The second, is the extent to which a protein resides in a "compartment", or time of residence,  $t_R$ . The time of residence is, in itself, a reflection of the kinetics of the metabolic transformations that modulate the response  $r(\vec{\phi}_n)$  of the membrane component to any given potential field. For slow transformations,  $r(\vec{\phi}_n)$  will tend to zero and we define this region of the pathway as the destination "compartment". Hence, the different compartments of the network are defined by chemical and physical transformations, that in turn define the temporal characteristics of the system.

In this description, the profile of label deposition does not reflect a net transfer of mass through the cellular space, but rather the changes imposed on the labelled protein by the metabolic transformations which take place along the translocation pathway and

by the size of the protein pool at each compartment.

For the moment we shall focus our attention of the temporal characteristics of this description and their implication in the interpretation of time-staggered double isotope experiments as used in myelinating systems.

From the description of our system, we can assign the initial condition  $\alpha(\vec{\phi}_0, 0) = 0$  and  $\alpha(\vec{\phi}_0, t) = G(t)$ , where  $\vec{\phi}_n = \vec{\phi}_0$  at the site of the component's insertion into the membrane or at its site of synthesis.

Other boundary conditions, however, are difficult to assign due to the complexities of intracellular membrane interconversions. All cellular constituents are turned over or replaced in a finite amount of time. Under normal experimental time conditions, the components (i.e. proteins) under study may be degraded or retained in a compartment within that time span, while the other surrounding membrane, components constituting its immediate space can continue their flow, perhaps to the extent of complete recycling (Rothman et al., 1981). Under these conditions, the surrounding membrane elements could be considered unbound, while the component under study would become bound at the point of its removal from the flow of membrane (secretion, lysosomal degradation, accumulation in a specific organelle, etc.).

None of the events described up to now account for enzymatic degradation of proteins or lipids. We will describe the effect of degradation by a distribution function  $\rho$  such that:

$$\rho = \rho(\vec{\phi}_n, t) \leq 1$$

3.3.6-1

When degradation occurs along one or all of the compartments of the endomembrane path, the labelled compound will be locally removed (or irreversibly dissipated). This removal will be expected to follow enzymatic kinetics (first order or not). Although it will not affect the rate of label flow it will affect the absolute content of labelled proteins or lipids in the membrane ( $F(\vec{\phi}_n)$ ). On the other hand, lysosomal degradation can be considered as a specific and compartmentalized degradation for some membrane components. Kinetically, it can be visualized as a label sink towards which labelled components in a membrane section are vectorially directed. In this case the function  $s(\vec{\phi}_j, t)$  follows a form that describes the flow characteristics of membranes from the "main" endomembrane path (at the compartment  $\{j\}$ ) toward the lysosomal sink  $\{L\}$  rather than enzyme kinetics. The random distribution (exponential decay kinetics) described by many authors for the turnover of membrane proteins (Schimke, 1975), is also in agreement with this description.

Degradation prior to, in, or after the compartment of interest is independent of the form of the degradation distribution function  $s(\phi_n, t)$  and will determine the manner by which  $s(\phi_n, t)$  is affected. If degradation is occurring prior to a given compartment  $\{j\}$  then

$$s'(t) = \int_{\phi_0}^{\phi_n} s(\vec{\phi}_n, t) d\phi \quad 3.3.6-2$$

For degradation occurring after  $\{j\}$  then

$$s(\vec{\phi}_n, t) = 0 \quad 3.3.6-3$$

In the case of a multi-port compartment, where proteins are specifically diverted to a lysosomal compartment (L), or if degradation occurs only at that point, the degradation function is represented by

$$\rho'(t) = \rho(\vec{\phi}_j, t)$$

3.3.6-4

Hence, in general terms, the effect of  $\rho$  on  $\alpha(\vec{\phi}_n, t)$  can be described by the equation

$$\alpha'(\vec{\phi}_n, t) = \alpha(\vec{\phi}_n, t)[1 - \rho'(t)]$$

3.3.7

#### 3.4.3 Definition of TSDI Parameters as a Function of $\alpha(\phi, t)$ and $\rho(\phi, t)$

The function  $\alpha(\vec{\phi}, t)$  can be used in its general form (equation 3.3.4) to define the flow of an integral membrane protein through a series of intermediary endomembrane compartments. For a given compartment  $\{j\}$ , the flow of a given protein along the compartment will be given by the function  $G(t)$ , while  $F(\vec{\phi}_j)$  becomes an average fixed value function which characterizes that given compartment (protein pool size of the compartment).

For the specific case of membrane proteins that accumulate in a specific compartment (A) (terminal or accumulating compartment), the rate of accumulation of labelled proteins during a time interval  $\Delta t$ , is given by

$$a_{(A)}(\vec{p}_n, t) = \int_t^{t+\Delta t} a'(\vec{p}_n, t) dt = F(\vec{p}_{(A)}) \int_t^{t+\Delta t} G(t)[1 - \rho'(t)] dt \quad 3.3.8$$

In this situation the accumulation of label becomes independent of the net membrane flow, which may or may not proceed to other compartments.

Let us consider a time-staggered double isotope (TSDI) pulse incorporation (for technical details see Chapter 5) of a specific amino acid into proteins.

$\Delta t_1$  denotes the interval between the incorporation of the first isotope at  $t_0$  and the second isotope at  $t_1$ , and  $\Delta t_2$  is the interval between the incorporation of the second isotope at  $t_1$  and the termination of the experiment at  $t_2$ .  $\Delta t_1$  is greater than  $\Delta t_2$  under all circumstances.

Myelin can be considered a net terminal boundary for the translocation of myelin proteins, and will be denoted specifically as (M). Note that this compartment will have the properties defined for a terminal accumulative compartment ((A)). Furthermore, if we take the assumption that certain protein components once assembled in the myelin membrane are very stable (Benjamins and Morell, 1978; see also Section 3.2.3.), then it can be expected that the degradation function  $\rho(\vec{p}, t)$  for these myelin components will be approximately zero.

The isotope ratio (R) of the second isotope over the first isotope, for a given protein in any compartment ((j)), will be given by:

$$R_{(j)} = \frac{SR|_{t_1}^{t_2}}{SR|_{t_0}^{t_2}} \quad 3.3.9$$

If the compartment in question is an intermediate compartment then the SR is defined by  $\alpha'(\vec{x}, t)$  as in equation 3.3.6. By substitution,  $R_{(j)}$  becomes:

$$R_{(j)} = \frac{G(\Delta t_2)[1 - \rho'(\Delta t_2)]}{G(\Delta t_1 + \Delta t_2)[1 - \rho'(\Delta t_1 + \Delta t_2)]} \quad 3.3.10$$

On the other hand, if the compartment is (A) then equation 3.3.6 and 3.3.7 by substitution into 3.3.8 give

$$R_{(A)} = \frac{\int_{t_1}^{t_2} G(t)[1 - \rho'(t)]dt}{\int_{t_0}^{t_2} G(t)[1 - \rho'(t)]dt} ; \quad 3.3.11$$

which for the case of a myelin compartment (M) reduces to

$$R_{(M)} = \frac{\int_{t_1}^{t_2} G(t)dt}{\int_{t_0}^{t_2} G(t)dt} \quad 3.3.12$$

if no degradation occurs along the entire pathway or if degradation occurs after the compartment (M).

Note that the isotope ratio  $R$  is "unbound" since it reflects only a relationship of the flow rates of the protein's label contained in the membrane segment as a whole. It is also ambiguous with respect to the cause of the change in  $SR$ , because variations in  $SR$  can be due to a change in net flow as well as to degradation, unless this latter cause can be eliminated by other criteria. This ambiguity can be resolved partially by the auxiliary use of "bound" parameters and by the selection of at least two sets of experimental time intervals. A "bound" parameter is one that establishes boundary conditions by referring the  $SR$  of a particular protein in a given intermediate compartment  $\{j\}$  to the  $SR$  of the same protein in its terminal or accumulative compartment  $\{A\}$ . For our studies on myelin the reference compartment of choice has been one that fulfills the criteria for  $\{M\}$ . (Chapter 5). Under these premises we can then define the ratio  $Q$  for a given isotope "i" as:

$$Q_{\{j\}}^i = \frac{\text{SR protein in } \{j\}}{\text{SR protein in } \{M\}} = \frac{F(\dot{\phi}_j) G(\Delta t) [1 - \rho'(\Delta t)]}{F(\dot{\phi}_M) \int_{t_0}^{t_2} G(t) [1 - \rho'(t)] dt} \quad 3.3.13$$

With this parameter, the difference of  $Q$ -values between the first and the second label can be used to compare the degree of metabolic similarity between the compartments  $\{j\}$  and  $\{M\}$ :

$$\Delta Q = \frac{F(\dot{\phi}_j)}{F(\dot{\phi}_M)} \left[ \frac{G(\Delta t_1 + \Delta t_2) [1 - \rho'(\Delta t_1 + \Delta t_2)]}{\int_{t_0}^{t_2} G(t) [1 - \rho'(t)] dt} - \frac{G(\Delta t_2) [1 - \rho'(\Delta t_2)]}{\int_{t_1}^{t_2} G(t) [1 - \rho'(t)] dt} \right] \quad 3.3.14$$

The use of this parameter, together with R in the interpretation of TSDI protocols, will be the center of the discussion in the next section. It should be noted, for the moment, that the sign of the expressions within the brackets ( $\Delta Q < 0$ ,  $\Delta Q > 0$ ,  $\Delta Q = 0$ ) will depend on the relationship between the time of deposition ( $t_d$ ) and the time of residence ( $t_R$ ) of the labelled protein in the compartment (j). The compartment (M), by definition has a very large time of residence ( $t_R \gg (\Delta t_2 + \Delta t_1)$ ), and a time of deposition ( $t_{dM}$ ) that is always larger than that of any precursor compartment. Values of Q can be used to define differences in pool size between compartments that approximate the criteria of "M" compartments ( $(j) = (M)$ ). Under these circumstances

$$\Delta Q = 0 \text{ and } Q_{(j)} = \frac{F(\vec{p}_j)}{F(\vec{p}_M)} \quad 3.3.15$$

Lastly, a second type of "bound" parameter can be defined as:

$$P = \frac{\text{SR of protein x in (j)} \quad (\text{moles of protein bound amino acid in 14KMBP})}{\text{SR of 14KMBP in (j)} \quad (\text{moles of protein bound amino acid in x})}$$

This parameter should be sensitive to the variations in the labelled protein-bound amino acid pool of the compartment. This difference can indicate diversity of amino acid pools at the site of protein synthesis and variation in their site of insertion into the endomembrane pathway (see Chapter 5).



The choice of the 14KMBP as a reference in this system is not arbitrary. This protein is synthesized by free ribosomes and is incorporated rapidly onto the membrane (see Section 3.2). The difference between membrane dependent deposition and cytoplasmic deposition pathways will become more obvious using the 14KMBP as reference. Note also that in IDI experiments (Section 3.2.1) the isotope ratio is given by

$$P = \frac{F^*(\bar{\alpha}_j) G^*(\Delta t) [1 - \rho'(\Delta t)]^*}{F(\bar{\alpha}_j) G(\Delta t) [1 - \rho'(\Delta t)]}$$

From the relationship between treatment (\*) and control it can be appreciated that variations between treatments cannot be interpreted by simplified assumptions as the ones assumed by Schimke (1974) and Brostoff et al., (1977); Greenfield et al., (1977).

### 3.3.4 Interpretation of Q, ΔQ and R Parameters Based on Temporal Inferences.

We are now in a position to apply the definitions of Q, ΔQ and R parameters to the interpretation of brain subfractions. A subfraction can be equated with an endomembrane "compartment" based on biochemical and morphological criteria. The enrichment of a given protein in a subfraction is however, no indication of the position of a protein in the context of a biogenic pathway, without further biochemical or kinetic criteria.

In this section we shall outline these kinetic criteria and their interpretation from TSDI parameters.

To simplify our analysis the following equivalences will be used in this section

$$G = G_j (\Delta t_1 + \Delta t_2) \quad ; \quad g = G_j (\Delta t_2)$$

$$M = \int_{t_0}^{t_2} G(t) dt \quad ; \quad m = \int_{t_1}^{t_2} G(t) dt \quad 3.3.16$$

$$B = [1 - \rho'(\Delta t_1 + \Delta t_2)] \quad ; \quad b = [1 - \rho'(\Delta t_2)]$$

Capital letters denote the value of the function through the total experimental interval of the first isotope,  $(\Delta t_1 + \Delta t_2)$  and the small letters for the second isotope interval  $(\Delta t_2)$ .

Equations 3.3.9, 3.3.11, and 3.3.13 can then be rewritten respectively as:

$$R_{(j)} = \frac{g \phi b}{G \phi B}$$

$$R_{(j)} = \frac{m}{M} \quad 3.3.17$$

$$\Delta Q = \frac{F(\bar{\phi}_j)}{F(\bar{\phi}_M)} \quad \frac{G \phi B - g \phi b}{M - m}$$

In this analysis we will make use of another empirical parameter  $R_0$ . It will be defined as the isotope ratio, should the two isotopes have been mixed together at time zero. This ratio  $R_0$  represents the value that the isotope mixture would reach if the labelled protein accumulates in a compartment with no or minimal degradation, and if the isotope variations, due to metabolism of the amino acid used have

been accounted for:

$$\lim_{t \rightarrow T} R_j \rightarrow R_0 \quad \text{if: } \{M\}, \text{ and } \rho^*(t) = 0,$$

and T is any given finite time.

For a fixed second isotope interval  $\Delta t_2$ , the following relationships:  $R_M < R_0$  and  $R_M = R_0$ , will indicate that  $t_{\alpha M} > \Delta t_2$  and  $t_{\alpha M} < \Delta t_2$  respectively. That is to say, the function 'm' will have reached its maximum value ( $m = M$ ) only if the time of deposition  $t_{\alpha}$   $< \Delta t_2$ .

Hence, from the equations of 3.3.16 we can infer that the following statements hold at all times:

- s1) If  $\rho(t) = 0$  then  $B = b = 1$
- s2) If  $\rho(t) \neq 0$  then  $B < b \leq 1$
- s3) If  $M = m$  then  $t_{\alpha M} < \Delta t_2$  and  $R_M = R_0$
- s4) If  $M > m$  then  $t_{\alpha M} > \Delta t_2$  and  $R_M < R_0$

If we make  $\Delta t_2$  our temporal point of reference, then from statements s3 and s4 we can construct two main scenarios. The first will contain the reference compartment {M} within the experimental time frame ( $t_{\alpha M} \leq \Delta t_2$ ) and the other outside of it ( $t_{\alpha M} > \Delta t_2$ ). Furthermore, similar arguments can hold for the functions G and g, depending on whether  $t_{\alpha j}$  is larger or smaller than  $\Delta t_2$  and  $t_{\alpha M}$ . Then, incorporating into our considerations the time of residence  $t_R$ , the relationships of G and g to  $t_{\alpha M}$ ,  $\Delta t_2$  and  $R_0$  will suffice to define four types of kinetic compartments:

- 1) Precursor compartment {P} + ( $t_{\alpha j} < \Delta t_2$ ;  $t_R < \Delta t_1 + \Delta t_2$ ); and  $R_j > R_0$ ; and for {P} to be precursor to any given compartment {k},

the conditions  $t_{aj} \leq t_{uk}$  and  $t_R < (t_{aj} - t_{aR})$  have to be satisfied.

- 2) Accumulative compartment (A)  $\equiv \{t_{aj} < \Delta t_z; t_R > (\Delta t_1 + \Delta t_z)\}$ ;  
and  $R = R_0$ .
- 3) Myelin compartment (M)  $\equiv \{t_{aj} < \Delta t_z; t_R >> (\Delta t_1 + \Delta t_z)\}$ ;  
and  $R = R_0$ .
- 4) Postcursor compartment (\*)  $\equiv \{t_{aj} > \Delta t_z; t_R\}$ ; and  $R < R_0$ .

This compartment describes undefined kinetic relationships because of inappropriate experimental parameters  $\Delta t_1$  and  $\Delta t_z$ . Note that for certain temporal conditions developmentally related compartments (D) (e.g. maturation of myelin) will be always postcursor within the time frame of endomembrane transformations.

Interpretation of  $\Delta Q$  requires an analysis of the interrelationship among the functions  $G$ ,  $M$ ,  $B$  and  $g$ ,  $m$ ,  $b$  (see equations 3.3.17). It is possible to see that all cases of  $\Delta Q$  ( $\Delta Q = 0$ ;  $\Delta Q < 0$  and  $\Delta Q > 0$ ) can be reduced to a relationship between

TABLE 3.3.1

Summary of the Conditions for the Interpretation of TSDI Protocols for Proteins Having a Time of Deposition in the Reference Compartment Less Than the Interval for the Second Label ( $t_{AM} < \Delta t$ )

TSDI Parameters		Inferred Compartment	Conditions to be Met		
$\Delta Q$	$R_j$	$\{j\}$	Degradation $\rho_j(t)$	Deposition Time $t_{aj}$	Residence Time $t_R^{++}$
$= 0$	$= R_0$	$\{A\}$	$0$	$< \Delta t_2$	
$> 0$	$\leq R_0$	$\{*\theta\}$	$> 0$	$> \Delta t_2$	
$> 0$	$< R_0$	$\{*\}$	$0$	$> \Delta t_2$	
$< 0$	$> R_0$	$\{P\}$	$0$	$< \Delta t_2$	$< (\Delta t_1 + \Delta t_2)$
$< 0$	$> R_0$	$\{P\theta\}$	$> 0$	$< \Delta t_2$	$< (\Delta t_2 + \Delta t_2)$
$< 0$	$> R_0$	$\{A\theta\}$	$> 0$	$< \Delta t_2$	

$++ t_R > (\Delta t_1 + \Delta t_2)$  otherwise.

functions  $G$  and  $g$  (primitive relationships) if statements S1 to S4 are applied (see Appendix 1). Hence these primitives of  $G$  and  $g$  will determine the relationship of the compartment under study with respect to (M). Tables 3.3.1 and 3.3.2 summarize the plausible situations given nominal values of  $R_j$  and  $\Delta Q$  for both reference scenarios. Hence for a pair of experimentally determined  $R$  and  $\Delta Q$  values, only a certain set of possible kinetic relationships can satisfy that specific combination. However, unless other circumstances are known e.g. (biogenic), a simple TSDI experiment is inadequate to determine the true kinetic nature of a compartment with respect to all its proteins.

### 3.3.5 Delay Times

The time necessary for the first appearance of labelled protein in a given compartment is defined as the delay time. This temporal parameter represents only the minimal time required for deposition, while  $t_a$  indicates the average delay time of the labelled protein pulse.

By relating the isotope ratio  $R_j$  of a given protein in a given compartment (j) to the reference isotope ratio  $R_0$  (see Section 3.3.4), it is possible to determine the extent of label incorporation into the compartment (j). For this to be meaningful, (j) has to be an accumulative compartment and no degradation of label can occur along the assembly pathway ( $\rho'(t) = 0$ ). The time required for the label front to reach the given compartment can be calculated from the relationship of the proportion  $R_j/R_0$  to the time interval of the second isotope:

TABLE 3.3.2

Summary of the Conditions for the Interpretation of TSDI Protocols  
for Proteins Having a Time of Deposition in the Reference Compartment  
Larger Than the Interval for the Second Label ( $t_{\alpha M} > \Delta t$ )

TSDI Parameters		Inferred Compartment	Conditions to be Met		
$\Delta Q$	$R_j$	$(j)^+$	Degradation $\rho_j(t)$	Deposition time $t_{\alpha j}$	Residence time $t_R^{++}$
$> 0$	$< R_0$	$(*)$	0	$> \Delta t_2$	
$< 0$	$< R_0$	$(*)$	0	$> \Delta t_2$	
$< 0$	$= R_0$	$(A)$	0	$> \Delta t_2$	
$< 0$	$> R_0$	$(P)$	0	$> \Delta t_2$	$< (\Delta t_1 + \Delta t_2)$
$> 0$	$< R_0$	$(*\beta)$	$> 0$	$> \Delta t_2$	
$< 0$	$\leq R_0$	$(*\beta)$	$> 0$	$> \Delta t_2$	
$< 0$	$= R_0$	$(A\beta)$	$> 0$	$< \Delta t_2$	
$< 0$	$> R_0$	$(P\beta)$	$> 0$	$< \Delta t_2$	$< (\Delta t_1 + \Delta t_2)$

+ For  $(*)$  compartments:  $(R_j < R_m)$   $((A)$  or  $(D))$ ;  $(R_j = R_m)$   $((M))$ ;  
 $(R_j > R_m)$   $((*)$  or  $(D))$ .

$++ t_R > (\Delta t_1 + \Delta t_2)$  otherwise.

$$\text{delay time} = \Delta t_z - \Delta t_z \frac{R_1}{R_0} + \gamma$$

where  $\gamma$  is the minimal time for protein synthesis.

### 3.3.6 Closing Remarks.

Initial experiments using TSDI protocols to study myelin membrane biogenesis (Benjamins et al., 1976 a, b; Braun et al., 1980), have assumed that:

- 1) isotope ratios (R), are independent of amino acid and protein pool size and rates of synthesis of individual proteins; and
- 2) ranking of isotope ratios (R), for a given protein isolated from different membrane compartments, indicates precursor-product relationships among such compartments under the assumption that the experiments take place during the period of linear uptake of radioactive precursor into the membranes.

As pointed out in Section 3.2.1, none of these assumptions are tenable for reasons that fall within the context of the limitations of pulse labelling techniques or within the context of the model presented here:

- 1) There is evidence that oscillations in the rates of protein synthesis occur within intervals of an hour (circadian rhythms, Brodsky, 1975). Probably both the rates of synthesis and the amino acid pools, are affected by these oscillations. TSDI experiments, subjected to these variations tend to show large scatter of values for a given time point if several experiments are not performed within certain times of the day. Hence, unless properly controlled, the



injection of both labels can be non equivalent. Furthermore, given the different labelled sites in amino acids, it can be shown that in the case of  $^3\text{H}$  and  $^{14}\text{C}$  isotopes of say, leucine (see Section 5.2.1), the distribution in the free amino acid pool of both label species is non equivalent, even if the main metabolic fate of leucine is its incorporation into proteins (Gaitonde et al., 1979; Wiggins et al., 1979).

ii) In relationship to the model, isotope ratios  $R$  were defined in equation 3.3.9 by:

$$R_{(j)} = \frac{G(\Delta t_2)[1 - \rho'(\Delta t_2)]}{G(\Delta t_1 + \Delta t_2)[1 - \rho'(\Delta t_1 + \Delta t_2)]}$$

Note that this relationship assumes that  $F(r_j)$  for both labels is equivalent or that necessary corrections were taken into consideration.

If the incorporation of label is assumed to be linear for both isotopes, and each label corresponds to the same type of molecules, then both labels will be incorporated at the same rate into the compartment. The value of the isotope ratio will be linearly proportional to the time interval between injections and to the rates of deposition of the labelled molecules into the given compartment. Deviations from this linearity can be attributed only to degradation. Hence ratio differences for a given protein among compartments will indicate variations in the rates of deposition. From this it is clear that the only possible inference, for a sequence of ratios among myelin and myelin related subfractions, is that the differences in

ratios imply different metabolic needs (rates of deposition) among subfractions, and not precursor-product relationships.

In order to evaluate TSDI results with this approach (see Tables 3.3.2 and 3.3.3) it is necessary to ensure that certain conditions are met:

1) Precautions, as outlined for pulse labelling procedures (Section 3.2.1), must be accounted for. One has to keep in mind that the pulse shape will determine in TSDI protocols the resolution that will be possible given short intervals of label incorporation.

2) The reference ratio  $R_0$  has to be accurately determined for all experiments in order to allow for proper normalization of results.

3) A minimum of two experiments with time intervals ( $\Delta t_2$ ) must be performed for adequate interpretation.

4) The reference compartment must be chosen carefully in order to ensure that its  $t_R \gg (\Delta t_1 + \Delta t_2)$ . Whether or not degradation occurs along the pathway, or within the compartment, will play a secondary role since the inferences are only relative. Corrections to the interpretations can be introduced by solving for  $\Delta Q$  given the adequate initial conditions, as exemplified in Appendix 1.

## APPENDIX 1

### Interpretation of $\Delta Q$

A.1 Under each of the two scenarios  $t_{aM} < \Delta t_z$  and  $t_{aM} > \Delta t_z$ ,

$\Delta Q$  can be of three forms:  $\Delta Q = 0$ ,  $\Delta Q < 0$  and  $\Delta Q > 0$ .

In the scenario  $t_{aM} < \Delta t_z$ ,  $M = m$  and  $\Delta Q$  reduces to the form:

$$\Delta Q = \frac{F(\vec{\phi}_j)}{F(\vec{\phi}_M)} [GB/M - gb/M] \begin{matrix} > 0 \\ = 0 \\ < 0 \end{matrix} \quad \text{A.1.1}$$

while for the scenario  $t_{aM} > \Delta t_z$ ,  $M > m$  and  $\Delta Q$  keeps its original description:

$$\Delta Q = \frac{F(\vec{\phi}_j)}{F(\vec{\phi}_M)} [GB/M - gb/m] \begin{matrix} > 0 \\ = 0 \\ < 0 \end{matrix} \quad \text{A.1.2}$$

In both cases the sign of  $\Delta Q$  will be given by the expression within brackets, independent of the protein pools ( $F(\vec{\phi}_j)/F(\vec{\phi}_M)$ )

A.1.2 Scenario  $t_{aM} < \Delta t_z$ .

$$\Delta Q \propto [GB/M - gb/M] \propto [GB - gb] \begin{matrix} > 0 \\ = 0 \\ < 0 \end{matrix} \quad \text{A.1.3}$$

A.1.2.1 If  $\Delta Q = 0$  and  $\rho = 0$  then  $B = b = 1$  hence  $G = g$   
 $GB = gb$

If  $\Delta Q = 0$  and  $\rho \neq 0$  then  $B < b \leq 1$  hence  $G' > g$   
 $GB = gb$

A.1.2.2 If  $\Delta Q > 0$  and  $\rho = 0$  then  $B = b = 1$  hence  $G > g$   
 $GB > gb$

If  $\Delta Q > 0$  and  $\rho \neq 0$  then  $B < b \leq 1$  hence  $G >> g$   
 $GB > gb$

A.1.2.3 If  $\Delta Q < 0$  and  $\rho = 0$  then  $B = b = 1$  hence  $G < g$   
 $GB < gb$

If  $\Delta Q < 0$  and  $\rho \neq 0$  then  $B < b \leq 1$  hence  $G \leq g$   
 $GB < gb$

A.1.3 Scenario  $t_{\alpha M} > \Delta t_2$

$\Delta Q \propto [GB/M - gb/m]$   $\begin{matrix} < 0 \\ = 0 \\ > 0 \end{matrix}$  A.1.4

A.1.3.1 If  $\Delta Q = 0$  then  $GB/M = gb/m$   
 $GB/gb = M/m > 1$   
 $GB > gb$

If  $\rho = 0$  then  $B = b = 1$  hence  $G > g$   
 $GB > gb$

If  $\rho \neq 0$  then  $B < b \leq 1$  hence  $G >> g$   
 $GB > gb$

A.1.3.2 If  $\Delta Q > 0$  then  $GB/M > gb/m$   
 $GB/gb > M/m > 1$

If  $\rho = 0$  then  $B = b = 1$  and  $GB > gb$   
hence  $G > g$

If  $\rho \neq 0$  then  $B < b \leq 1$  and  $GB > gb$   
hence  $G >> g$

A.1.3.3 If  $\Delta Q < 0$  then  $GB/M < gb/m$   
 $GB/gb \leq M/m$ ;  $M/m > 1$   
 $GB > gb$  or  $GB \leq gb$

If  $\rho = 0$  then  $B = b = 1$  and  $GB > gb$   
hence  $G > g$   
 $GB \leq gb$  hence  $G \leq g$

If  $\rho \neq 0$  then  $B < b \leq 1$  and  $GB > gb$   
hence  $G > g$   
 $GB \leq gb$  hence  $G > g$   
or  
 $G \leq g$

In the case of postcursor compartments (\*) (see section 3.3.4), distinction among some of the other compartment types is possible if the isotope ratio of the compartment in question is compared with that

of the reference compartment. This comparison is only valid for those cases where no degradation ( $\rho = 0$ ) occurs.

If  $R_j < R_M$ , then  $t_{aj} > t_{aM}$ , hence the compartment is a pure postcursor compartment (\*), that is kinetically localized after the reference compartment due to slower deposition rates or longer metabolic distances.

If  $R_j = R_M$  then  $t_{aj} = t_{aM}$ , hence the compartment is kinetically equivalent to (M).

If  $R_j > R_M$  then  $t_{aj} < t_{aM}$ , hence the compartment has a deposition time that is shorter than the reference compartment, either because faster rates of deposition or shorter metabolic distances.

### REFERENCES    CHAPTER 3

- Agrawal, H.C., Randle, Ch.L. and Agrawal, D. (1982). In vivo acylation of rat brain myelin proteolipid protein. J. Biol. Chem., 257: 4588
- Ames III, A., Parks, J.M. and Neskettt, F.B. (1976). Transport of leucine and sodium in central nervous tissue. J. Neurochem., 27: 999
- Ames III, A. and Parks, J.M. (1976). Functional homogeneity of leucine pool in retina cells. J. Neurochem., 27: 1017
- Arias, I.M., Doyle, D. and Schimke, R.T. (1969). Studies on the synthesis and degradation of proteins of the endoplasmic reticulum of rat liver. J. Biol. Chem., 244: 3303
- Banker, G. and Cotman, C.W. (1971). Characteristics of different amino acids as protein precursors in mouse brain: Advantages of certain carboxy-labelled amino acids. Arch. Biochem. Biophys., 142: 565
- Barbarese, E. (1978). Ph. D. Thesis Disertation; McGill University.
- Barbarese, E. and Pfeiffer, S.E. (1981). Developmental regulation of myelin basic protein in dispersed cultures. Proc. Natl. Acad. Sci.(USA), 78: 1953
- Benjamins, J.A. and Morell, P. (1978). Proteins of myelin and their metabolism. Neurochem. Res., (3): 137
- Benjamins, J.A. and Iwata, R. (1979). Kinetics of entry of galactolipids and phospholipids into myelin. J. Neurochem., 32: 921
- Benjamins, J.A., Jones, M. and Morell, P. (1975). Appearance of newly synthesized protein in myelin of young rats. J. Neurochem., 24: 1117
- Benjamins, J.A., Miller, S.L. and Morell, P. (1976a). Metabolic relationships between myelin subfractions: Entry of galactolipids. J. Neurochem., 27: 565
- Benjamins, J.A., Gray, M. and Morell, P. (1976b). Metabolic relationships between myelin subfractions: Entry of proteins. J. Neurochem., 27: 571
- Benjamins, J.A., Iwata, R. and Hazlett, J. (1978). Kinetics of entry of proteins into the myelin membrane. J. Neurochem., 31: 1077

- Bissell, M.J., Hall, H.G. and Parry, G. (1982). How does the extracellular matrix direct gene expression? J. theor. Biol. 99:31
- Braun, P.E. (1983). 'Molecular organization of myelin'. In 'Myelin'. (Ed. Morell, P.) 2nd ed. Plenum Press. N.Y.
- Braun, P.E., Pereyra, P.M. and Greenfield, S. (1980). 'Mechanisms of assembly of myelin: a new approach to the problem. In 'Neurological Mutations Affecting Myelination'. (Ed. Baumann, N.). Elsevier/North-Holland Biomedical Press. pp: 413.
- Brodsky, W. Ya. (1975). Protein Synthesis Rhythm. J. theor. Biol., 55:167
- Brostoff, S.W., Greenfield, S. and Hogan, E.L. (1977). The differentiation of synthesis from incorporation of basic protein in quaking mutant mouse myelin. Brain Res., 120: 517
- Bodsch, W. and Hossmann, K-A. (1982). A quantitative regional analysis of amino acids involved in rat protein synthesis by high performance liquid chromatography. J. Neurochem., 40(2):371
- Boggs, J.M., Moscarello, M.A. and Papahadjopoulos, D. (1982). Structural organization of myelin- Role of Lipid-protein interaction determined in model systems. Lipid-Protein Interactions, 2: 1
- Bunge, R.P. (1968). Glial cells and the central myelin sheath. Ann. Rev. Biochem., 48: 197
- Campagnoni, A.T., Carey, G.D. and Yu, Y-T. (1980). In vitro synthesis of the myelin basic proteins: Subcellular site of synthesis. J. Neurochem., 34: 677
- Colman, D.R., Kreibich, G., Frey, A.B. and Sabatini, D.D. (1982). Synthesis and incorporation of myelin polypeptides into CNS myelin. J. Cell Biol., 95: 598
- de Duve, C. (1964). Principles of tissue fractionation. J. theoret. Biol., 6: 33
- de Duve, C. and Wattiaux, R. (1966). Function of lysosomes. Ann. Rev. Physiol., 28: 435
- Evans, W.H. (1980). A biochemical dissection of the functional polarity of the plasma membrane of the hepatocyte. Biochim. Biophys. Acta, 604: 27
- Fern, E.B. and Garlick, P.J. (1974). The specific radioactivity of the tissue free amino acid pool as a basis for measuring the rate of protein synthesis in the rat in vivo.. Biochem. J., 142: 413

- Franke, W.W., Morre, D.J., Deumling, B., Cheetham, R.D., Kartenbeck, J., Jarásh, E-D. and Zentgraf, H-W. (1971). Synthesis and turnover of proteins in rat liver. Z. Naturforsch., 26: 1031
- Fujita, M. (1982). Bioassembly Lines. J. theor. Biol., 99:9
- Gaitonde, M.K., Davies, L.T. and Evans, G. (1979). Is leucine the source of glutamic and aspartic acids in brain proteins. J. Neurochem., 32: 1135
- Glass, R.D. and Doyle, D. (1972). On the measurement of protein turnover in animal cells. J. Biol. Chem., 247: 5234
- Goldberg, A.L. and Dice, J.F. (1974). Intracellular Protein degradation in mammalian and bacterial cells. Ann. Rev. Biochem., 43: 835
- Goldberg, A.L. and St. John, A.C. (1976). Intracellular protein degradation in mammalian and bacterial cells: part 2.. Ann. Rev. Biochem., 45: 747
- Golds, E.E. and Braun, P.E. (1976). Organization of membrane proteins in the intact myelin sheath: Peridoxal phosphate and salicylaldehyde as probes of myelin structure. J. Biol. Chem., 251: 4729
- Golds, E.E. and Braun, P.E. (1978a). Cross-linking studies on the conformation and dimenrization of myelin basic protein in solution. J. Biol. Chem., 253: 8171
- Golds, E.E. and Braun, P.E. (1978b). Protein associations and basic protein conformation in the myelin membrane. J. Biol. Chem., 253: 8162
- Greenfield, S., Brostoff, S.W. and Hogan, E.L. (1977). Evidence for defective incorporation of proteins in myelin of the quaking mutant mouse. Brain Res., 120: 507
- Guidotti, G.G., Borghetti, A.F. and Gazzola, G.C. (1978). The regulation of amino acid transport in animal cells. Biochim. Biophys. Acta, 515: 329
- Hartman, B.K., Agrawal, H.C., Agrawal, D. and Kalmbach, S. (1982). Development and maturation of central nervous system myelin. Proc. Natl. Acad. Sci.(USA), 79: 4217
- Hershko, A., Ciechanover, A. and Rose, I. (1979). Resolution of the ATP dependent proteolytic system from reticulocytes. A component that interacts with ATP.. Proc. Natl. Acad. Sci. (USA), 76: 3107
- Hod, Y. and Hershko, A. (1976). Relationship of the pool of intracellular veline to protein synthesis and degradation in cultured cells. J. Biol. Chem., 251: 4458



- Hubbard, A.L and Cohn, Z.A. (1975a). Externally disposed plasma membrane proteins I. Enzymatic iodination of mouse L cells. J. Cell Biol., 64: 438
- Hubbard, A.L. and Cohn, Z.A. (1975b). Externally disposed plasma membrane protein II. Metabolic fate of iodinated polypeptides of mouse L cells. J. Cell Biol., 64: 461
- Johnston, P.V. and Roots, B.I. (1972). 'Nerve Membranes: A study of the biological and chemical aspects of the neuro-glia relationships'. Pergamon Press. Toronto.
- Jolles, J., Nussbaum, J-L., Schoentgen, F., Mandel, P. and Jolles, P. (1977). Structural data concerning the major rat brain myelin proteolipid P7 apoprotein. FEBS Letters, 74: 190
- Kafatos, F.C. and Gelinas, R. (1974). 'mRNA stability and the control of specific protein synthesis in highly differentiated cells'. In 'Biochemistry of Cell Differentiation' Biochemistry Series one Vol 9. (Ed. Paul, J.). Butterworths, London pp: 223
- Kirschner, D.A. and Caspar, D.L.D. (1977). 'Diffraction studies of molecular organization in myelin'. In 'Myelin'. (Ed. Morell, P.). Plenum Press, N.Y. pp: 51
- Koch, A.L. (1962). The evaluation of the rates of biological processes from tracer kinetic data. J. theor. Biol., 3: 283
- Konat, G. and Clausen, J. (1980). Suppressive effect of triethyllead on entry of proteins into the CNS myelin sheath in vitro. J. Neurochem., 35: 382
- Korey, S.R. (1959). 'The Biology Of Myelin'. Hober-Harper Book. N.Y. pp: xvii
- Lajtha, A., Toth, J., Fijimoto, K. and Agrawal, H.C. (1977). Turnover of myelin proteins in mouse brain in vivo. Biochem. J., 164: 323
- Lees, M.B., Sakura, D.J., Saperstein, V.S. and Curatolo, W. (1979). Structure and function of proteolipids in myelin and non-myelin membranes. Biochim. Biophys. Acta, 559: 209
- Lipton, P. and Heimbach, C.J. (1977). The effect of extracellular potassium concentration on protein synthesis in Guinea-pig hippocampal slices. J. Neurochem., 28: 1347
- Maddy, A.H. (1976). 'Biochemical Analysis of Membranes'. Chapman and Hall, London.

- Margineanu, I. and Ghetie, V. (1981). A selective model of plasma protein catabolism. J. theor. Biol., 90: 101
- Mellman, I. (1982). Multiple pathways of membrane transport. Nature, 299: 301
- Mollenhauer, H.H. and Morre, D.J. (1978). Structural compartmentation of the cytosol: zones of exclusion, zone of adhesion, cytoskeletal and intracisternal elements. Subcell. Biochem., 5: 327
- Morre, D.J. (1977). The Golgi apparatus and membrane biogenesis. Cell Surface Rev., 4: 1
- Morre, D.J. and Mollenhauer, H.H. (1974). 'The endomembrane concept: a functional integration of endoplasmic reticulum and Golgi apparatus'. In 'Dynamic Aspects of Plant Ultrastructure'
- Morre, D.J. and Mollenhauer, H.H. (1974). 'The endomembrane concept: a functional integration of the endoplasmic reticulum and the Golgi apparatus'. In 'Dynamic Aspects of Plant Ultrastructure'. (Ed. Robards, A.W.). McGraw-Hill, N.Y. pp: 84
- Morre, D.J. and Ovtracht, L. (1977). Int. Rev. Cytol. Suppl., 5: 61
- Morre, D.J., Kartenbeck, J. and Franke, W.W. (1979). Membrane flow and interconversion among enomembranes. Biochim. Biophys. Acta, 559: 71
- Mortimore, G.E., Woodside, K.H. and Henry, J.E. (1972). Compartmentation of free valine and its relationship to protein turnover in perfused rat liver. J. Biol. Chem., 247: 2776
- O'Hara, D.S., Curfman, G.D., Trumball, C.G. and Smith, T.W. (1981). A procedure for measuring the contributions of intracellular and extracellular tyrosine pools to the rate of myocardial protein synthesis. J. Molecular Cell. Cardiol., 13: 925
- Omilin, F.X., Webster, H. deF., Palkovits, Ch.G. and Cohen, S.R. (1982). Immunocytochemical localization of basic protein in mayor dense line regions of central and peripheral myelin. J. Cell Biol., 95:242
- Palade, G. (1965). Intracellular aspects of the process of protein synthesis. Science, 189: 347
- Parry, G. (1978). Membrane assembly and turnover. Subcell. Biochem., 5:261

- Pastan, I.H. and Willingham, M.C. (1981). Journey to the center of the cell: role of the receptosome. Science, 214: 504
- Patel, A.J. and Balazs, R. (1970). Manifestation of metabolic compartmentation during the maturation of the rat brain. J. Neurochem., 17: 955
- Patsalos, P.N., Bell, M.E. and Wiggins, R.C. (1980). Pattern of myelin breakdown during sciatic nerve Wallerian degeneration: reversal of the order of assembly. J. Cell Biol., 87: 1
- Pavlik, A. and Jakoubek, B. (1976). Distribution of protein-bound radioactivity in brain slices of the adult rat incubated with labelled leucine. Brain Res., 101: 113
- Peterson, R.G., Baughman, S. and Schneider, D.M. (1981). Incorporation of fucose and leucine into PNS myelin proteins in nerves undergoing early Wallerian degeneration. Neurochem. Res., 6: 213
- Poduslo, J.F. and Braun, P.E. (1975). Topographical arrangement of membrane proteins in the intact myelin sheath. J. Biol. Chem., 250: 109
- Poduslo, J.F., Quarles, R.H. and Brady, R.O. (1976). External labeling of galactose in surface membrane glycoproteins of the intact myelin sheath. J. Biol. Chem., 251(1):153
- Poole, B. (1971). The kinetics of disappearance of labelled leucine from the free leucine pool of rat liver and its effect on the apparent turnover of catalase and other hepatic proteins. J. Biol. Chem., 246: 6587
- Pressman, B.C. (1976). Biological application of ionophores. Ann. Rev. Biochem., 45: 501
- Rapaport, R.N. and Benjamins, J.A. (1981). Kinetics of entry of Po protein into peripheral nerve myelin. J. Neurochem., 37: 164
- Rapaport, R.N., Benjamins, J.A. and Skoff, R.P. (1982). Effects of monensin on assembly of Po protein into peripheral nerve myelin. J. Neurochem., 39: 1101
- Roberts, J.R. and Yuan, B.O. (1974). Chemical modification of the plasma membrane polypeptides of cultured mammalian cells as an aid to study protein turnover. Biochemistry, 13: 4846

- Roberts, J.R. and Yuan, B.O. (1975). Turnover of plasma membrane polypeptides in non proliferating cultures of Chinese hamster ovary cells and human skin fibroblasts. Arch. Biochem. Biophys., 171: 234
- Robertson, J.H. and Wheatley, D.N. (1979). Pools and protein synthesis in mammalian cells. Biochem., 178: 699
- Rothman, J.E., Fries, E., Dunphy, W.G. and Urbani, L.J. (1981). Golgi apparatus, coated vesicles, and the sorting problem. Cold Spring Harbor Symp. on Quan. Biol., 46: 797
- Rothman, J.E. (1981). The Golgi apparatus: two organelles in tandem. Science, 213: 1212
- Sabatini, D., Colman, D., Sabban, E., Sherman, J., Marimoto, T., Kreibich, G. and Adensnik, M. (1981). Mechanisms for the incorporation of proteins into plasma membrane. Cold Spring Harbor Symp. on Quan. Biol., 46: 807
- Sabri, M.I., Bone, A.H. and Davison, A.N. (1974). Turnover of myelin and other structural proteins in the developnig rat brain. Biochem. J., 142: 499
- Sage, J.I., van Vitert, R.L. and Duffy, T.E. (1981). Simultaneous measurement of cerebral blood flow and unidirectional movement of substances across the blood-brain barrier: Theory, method and application to leucine. J. Neurochem., 36: 1731
- Sershen, H. and Lajtha, A. (1979). Inhibition pattern by analogs indicates the presence of ten or more transport sysytems for amino acid in brain cells. J. Neurochem., 32: 719
- Schimke, R.T. (1970). In 'Mammalian Protein Metabolism'. Vol4 (Ed. Munro, H.N.). Academic Press, N.Y. pp: 177
- Schimke, R.T. (1973). Control of enzyme levels in mammalian tissues. Adv. Enzymol., 37 135: 135
- Schimke, R.T. (1974). 'Protein synthesis and degradation in animal tissue'. In 'Biochemistry of Cell Differentiation'. (Ed. Paul, J.). University Parks Press, Baltimore. pp: 183
- Shapira, R., Wilhelmi, M.R. and Kibler, R.F. (1981). Turnover of myelin proteins of rat brain, determined in fractions separated by sedimentation in a continuous sucrose gradient. J. Neurochem., 36: 1427
- Shore, G.C. and Tata, J.R. (1977). Functions of polyribosome-membrane interactions in protein synthesis. Biochim. Biophys. Acta, 472: 197

- Singh, M.I. and Jungalwala, F.B. (1979). The turnover of myelin proteins in adult rat brain. Inter. J. Neuroscience, 9: 123
- Smith, M.E. (1974). Labelling of lipids by radioactive amino acids in the central nervous system. J. Neurochem., 23: 435
- Smith, M.E. (1982). Biosynthesis of peripheral nervous system myelin proteins in vitro. J. Neurochem., 35: 1183
- Smith, M.E. and Sternberger, N.H. (1982). Glycoprotein biosynthesis in peripheral nervous system myelin: effect of tunicamycin. J. Neurochem., 38: 1044
- Swick, R. and Handa, D.T. (1956). The distribution of fixed carbon in amino acids. J. Biol. Chem., 218: 557
- Taylor, J.M., Dehlinger, P.J., Dice, J.F. and Schimke, R.T. (1973). The synthesis and degradation of membrane proteins. Drug Metab. Disposition, 1: 84
- Townsend, L.E., Agrawal, D., Benjamins, J.A. and Agrawal, H.C. (1982). In vitro acylation of rat brain myelin proteolipid protein. J. Biol. Chem., 257(16):9745.
- Townsend, L.E. and Benjamins, J.A. (1983). Effects of monensin on posttranslational processing of myelin proteins. J. Neurochem., 40(5):1333
- Tweto, J. and Doyle, D. (1976). Turnover of plasma membrane proteins of hepatoma tissue culture cells. J. Biol. Chem., 251: 872
- Tweto, J. and Doyel, D. (1977). Turnover of proteins of the eukaryotic cell surface. Cell Surface Reviews, 4(3): 137
- Tkacz, J.S. and Lampen, J.O. (1975). Tunicamycin inhibition of polyisoprenyl-N-acetyl glucosaminyl pyrophosphate formation in calf-liver microsomes. Biochem. Biophys. Res. Commun., 65: 248
- Vidrich, A., Airhart, J., Bruno, M.K. and Khairallah, E.A. (1977). Compartmentation of free amino acids for protein synthesis. Biochem. J., 162: 257
- Wahnefeldt, T.V. and Linington, C. (1980). 'Organization and assembly of the myelin membrane'. In 'Neurological Mutations Affecting Myelination'. (Ed. Baumann, N.). Elsevier/North-Holland Biomedical Press. pp: 389

- Waksman, A., Hubert, P., Cremel, G., Rendon, A. and Burgun, C. (1980). Translocation of proteins through biological membranes. A critical review. Biochim. Biophys. Acta, 604: 249
- Wickner, W. (1980). Assembly of proteins into membranes. Science, 210: 861
- Wickner, W. (1979). The assembly of proteins into biological membranes: the Membrane Trigger hypothesis. Ann. Rev. Biochem., 48: 23
- Wiggins, R.C., Fuller, G.N. and Bell, M.E. (1979). Incorporation of leucine metabolites into brain and sciatic nerve myelin. J. Neurochem., 32: 1579
- Wiggins, R.C. (1982). Myelin development and nutritional insufficiency. Brain Res. Rev., 4: 151
- Yu, Y-T. and Campagnoni, A.T. (1982). In vitro synthesis of the four mouse myelin basic proteins: evidence for the lack of a metabolic relationship. J. Neurochem., 39: 1559

4. STUDIES ON SUBCELLULAR FRACTIONS WHICH ARE INVOLVED  
IN MYELIN MEMBRANE ASSEMBLY: ISOLATION FROM DEVELOPING MOUSE  
BRAIN AND CHARACTERIZATION BY ENZYME MARKERS,  
ELECTRON MICROSCOPY AND ELECTROPHORESIS

4.1 Introduction

Myelinogenesis in the developing CNS is one experimental system which offers several major advantages for a study of eucaryotic cell membrane assembly. The oligodendroglial cell, like the PNS Schwann cell, produces vast quantities (up to 1 mm<sup>2</sup> per cell) of plasma membrane (Norton, 1976) which undergoes molecular modification to become the lamellar myelin sheath. In mice the synthesis of this membrane occurs at an exponential rate for approximately a two-week period, beginning about day 10. Moreover, the protein composition is relatively simple; the well-characterized myelin basic proteins (MBP) and the intrinsic protein lipophilin (proteolipid protein) each comprise about 30% of the total myelin protein (Braun and Brostoff, 1977). These and other favorable considerations suggested to us the possibility of 1) defining the intracellular events in the process of oligodendroglial membrane assembly; 2) testing the validity of several aspects of existing hypothetical assembly mechanisms (for reviews see Rothman and Lenard, 1977; Morré et al., 1979; Wickner, 1979; Waksman et al., 1980; Sabatini et al., 1982) as they pertain to myelination.

In an earlier report we described a microsomal fraction (obtained as a "light" fraction by rate sedimentation in a sucrose gradient) in which the oligodendroglial-specific MBP accumulated very differently from that of all other membrane fractions during development (Barbarese et al.,

1979). As a working hypothesis, it seemed reasonable that this fraction could contain precursor vesicles involved in the membrane assembly process, as has been described in preliminary reports (Braun and Pereyra, 1979; Braun et al., 1980; Greenfield et al., 1981). Subsequent equilibrium-density centrifugation of this still-heterogeneous fraction yielded several microsomal subfractions of which one appeared at a density lighter than myelin (1.04 g/cc), consisted mostly of smooth vesicles, and contained all the proteins and enzymes typical of myelin. In further studies designed to show the relationship of these vesicles to myelin assembly, and to obtain other intracellular membranes from brains of developing animals it became clear that the use of non-equilibrium sedimentation protocols resulted in myelin-containing fractions which contained many types of endomembranes, some of which could be associated with myelination. This fractionation is complicated by the fact that during development the CNS contains axons at various stages of myelination. For example, at 15 days of age, the mouse brain has structures which are just beginning to myelinate while other regions have myelin which varies from one to seven days of "age".

The homogenization and fractionation procedure which we have devised for our developmental studies provides reproducible fractions of myelinated axons and endomembranes during myelination. In view of the above considerations the morphological and biochemical characteristics, which we report here, lead us to suggest that the myelin-containing fractions are largely composed of myelinated axons and membranes, differing in both size and buoyant density which represent different stages of myelination that coexist in developing brain. Additional support of this interpretation is provided by the metabolic studies described in a companion paper (Pereyra et al., 1983).



## 4.2 Experimental Procedures

### 4.2.1 Materials

All radioisotopes and chemicals for scintillation counting were purchased from New England Nuclear Corp., Boston, Mass. All other biochemicals were products of Sigma Chemical Co., St. Louis. Rabbit anti-proteolipid protein (bovine) was a generous gift from Drs. W. Macklin and M. Lees, Boston. Rabbit anti-MAG was generously provided by Dr. N. Sternberger, Rochester, N.Y. Rabbit anti-basic protein, raised against purified bovine 18.5 K MBP, was prepared by a standard procedure (Barbarese et al., 1977). BEEM embedding capsules were purchased from J.B. EM Services Inc.

### 4.2.2 Subcellular Fractionation

Our fractionation scheme represents the extended development of our earlier procedure (Barbarese et al., 1979) and has been influenced by the detailed discussions of procedures for other tissues as given by DePierre and Dallner (1976); Adelman et al. (1974); and Whittaker (1969).

Typically, brains from 40 young mice of a specific age were rapidly (20 sec) removed to cold sucrose (0.25 M) and rinsed of adhering blood. A 30% w/w homogenate was prepared in fresh 0.25 M sucrose, using a glass homogenizer and Teflon pestle with a medium fit (clearance range 0.15 to 0.23 mm).

Ten up-and-down cycles at 800 rpm was a rigidly adhered to condition for all preparations; these and all other procedures were carried out in a coldroom at 4°C. The homogenate was diluted to 10% w/w with cold 0.25 M sucrose and centrifuged for  $1.7 \times 10^3$  g-min (5 min/2 Krpm/Ty 30) to remove broken cells and nuclear material. The supernatant ( $S_0$ ) was

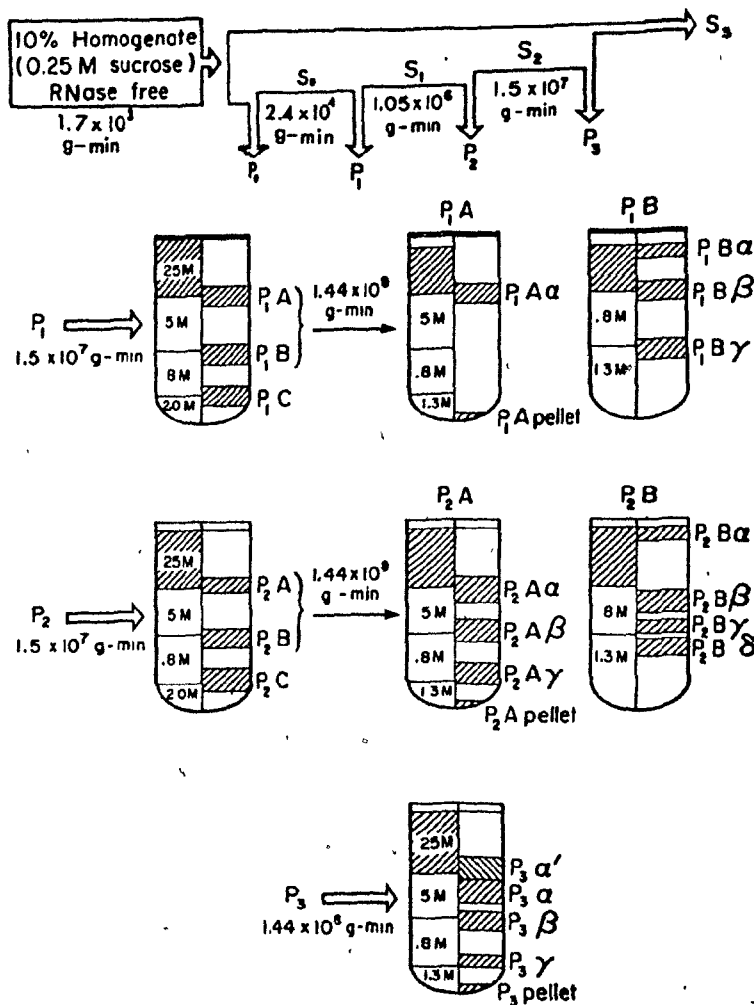


Figure 4.2.1. Subcellular fractionation procedure for developing mouse brain.

then fractionated by differential velocity centrifugation in a Type 30 rotor according to the scheme in Figure 1. Briefly, centrifugation for  $2.4 \times 10^4$  g-min (17 min/4 Krpm) produced the pellet P1. Further centrifugation of S1 for  $1.05 \times 10^6$  g-min (20 min/27 Krpm) yielded pellet P2, with S2 being centrifuged for another  $1.5 \times 10^7$  g-min (200 min/25 Krpm) to produce pellet P3 and supernate S3.

Pellets P1 and P2 were each further fractionated during the time that S2 was centrifuging. They were rehomogenized in 0.25 M sucrose (20% v/v homogenate) using 3 up-and-down cycles at 800 rpm, and applied as a 16 ml sample to a sucrose gradient consisting of 12 ml 0.8 M sucrose overlaid with 10 ml of 0.5 M sucrose. Rate zonal separations were achieved by centrifuging for  $1.5 \times 10^7$  g-min (180 min/25 Krpm/SW 27). Figure 4.2.1 illustrates the location of resultant fractions. The visualization of bands was aided by positioning a Tensor Mini-lamp directly above the gradient tube. Fractions were collected with a 10 ml syringe fitted with a 10 cm, blunted, 19 gauge needle. Sucrose concentrations were determined by the refractive index measurements of each fraction.

The pellet P3 was fractionated somewhat differently from P1 and P2. It was re-suspended in 1 ml of 0.25 M sucrose by gentle agitation with a syringe needle as described above, followed by 3 cycles of gentle aspiration ending in the transfer to a single tube. The pooled material was diluted to a 10% (v/v) homogenate immediately prior to the next step.

Density equilibrium separations of particles were obtained as illustrated in Figure 4.2.1. The resuspended material of fraction P3, and the bands recovered as P1A and P2A were applied as a 14 ml sample to

a gradient consisting of 4 ml 1.3 M sucrose overlaid with 10 ml 0.8 M sucrose, followed by 10 ml 0.5 M sucrose. Similarly 14 ml samples of P1B and P2B were applied to a tube containing 10 ml 1.3 M sucrose overlaid with 14 ml 0.8 M sucrose. All tubes were centrifuged for  $1.44 \times 10^8$  g-min (24 hr/23 Krpm/SW 27). Particle distribution was unchanged upon additional centrifugation and a linear gradient resulted from this operation.

Subfractions of P1C and P2C are complex and have not yet been completely characterized; they will be described in future communications. Preliminary studies show that they contain the bulk of the mitochondrial, synaptosomal, Golgi, and endoplasmic reticulum membranes.

All fractions were collected into pre-weighed vials and weighed. This weight and the density of the sucrose solution containing the membranous particles, as determined by refractive index measurement, permits a rapid and reproducible calculation of the volume this fraction occupies. This parameter is used to calculate total enzyme activities and protein recovery.

All subfractions were diluted 1:1 with cold water and were pelleted as follows: P2B and P3 subfractions required 60 min at 35000 rpm in the Beckman Ti 75 rotor for complete pelleting; all other subfractions were centrifuged under the same conditions for 35 min. This operation was done in order to separate membrane bound and trapped proteins from soluble proteins.

Pellets were resuspended such that the final protein concentration was 2 to 5 mg per ml.

#### 4.2.3 Calculation of Sedimentation Coefficients

Calculation of sedimentation coefficient ranges for particles

pelleted by velocity sedimentation, as a function of equivalent radius ( $r_{eq}$ ) and the fraction of material left in the supernatant ( $q$ ) were done by computer, using a program based on the equations of Rasmussen (1973).

For particles centrifuged in discontinuous sucrose gradients in swinging bucket rotors the minimum sedimentation coefficients at a given particle density ( $\rho_p$ ) which are required for a particle to traverse a given gradient step were calculated with a computer program based on the equations of McEwen (1967). These values were calculated as a function of the radius difference between the uppermost meniscus and the interface of each gradient, as well as a function of particle density. The sucrose concentrations was assumed to be constant throughout each gradient step, a valid assumption for centrifugation times less than 3 hours. Particles with densities equal to or less than the sucrose density were assumed to be immobile or to move centripetally.

#### 4.2.4 Determination of Protein

We used a slightly modified version of the dye-binding assay of Bradford (1976), with bovine gammaglobulin as standard, and the Biorad R protein assay reagent. Assays were performed with the standard procedure in the range of 10 to 140  $\mu$ g of protein, or by a semi-micro assay in the range of 1 to 14  $\mu$ g. In the latter assay, samples were contained in a volume of 0.1 ml to which was added 1.5 ml of Biorad R reagent.

Standard curves were computed by linear regression analysis.

#### 4.2.5 Determination of RNA

We employed the standard procedure of Fleck and Munro (1962) for the isolation of RNA and its spectrophotometric assay. We used the equation

$C_{RNA,P} (\mu g/ml) = 11.87 E_{260} - 10.4 E_{275}$  to calculate the amount of RNA recovered from each subfraction, assuming that the absorbances of RNA and of polypeptides were additive. Values of RNA represent relative content amongst subfractions and cannot be assumed to be absolute values.

#### 4.2.6 Electron Microscopy

Subcellular fractions were prepared for electron microscopy by suspending them in Karnovsky's glutaraldehyde fixative for 8 hr. The suspended material was then pelleted in BEEM capsules by centrifugation for 60 min at 23000 rpm in a SW 50.1 rotor fitted with special adapters. This produced a pellet 2 - 3 mm thick. The supernatant was removed and the pellet gently rinsed 3 times with fresh fixative. The pellet was carefully recovered by slicing away the capsule. It was then transferred intact to a 3 ml screwcap vial and the samples were post-fixed with  $OsO_4$ -potassium ferrocyanide, stained en bloc with uranyl acetate and dehydrated prior to embedding in Vestopal.

Representative sections were cut from all regions of the tissue blocks and examined in a Philips 300 electron microscope.

#### 4.2.7 Gel Electrophoresis

Proteins were separated by SDS-polyacrylamide gel electrophoresis in slab gels (1.5 mm X 10 cm X 15 cm) made with a linear gradient of 5 - 25% acrylamide, using the system of Laemmli (1970). Gels were aged overnight and pre-run at 70 Volts for 1 hr. Electrophoresis was carried out at 80 Volts for 16 hr, or until the cytochrome c marker just reached the bottom of the gel. Gels were stained overnight by Coomassie blue (0.1%) in 25% isopropanol-10% acetic acid, and destained first in 10% isopropanol-10% acetic acid, then 10% acetic acid. Gels were stored in the hydrated

state on a glass plate tightly wrapped in Saran<sup>R</sup> wrap.

Spectrophotometric scans were obtained by scanning strips of stained gels at 555 nm in the Gilford Gel Scanner.

#### 4.2.8 Immunochemical Identification of Myelin Proteins

An immunochemical assessment of the presence or absence of specific myelin proteins in subcellular fractions was made. Membrane proteins, separated by SDS-PAGE as described above, were transferred electrophoretically from the gels to nitrocellulose sheets (Towbin et al., 1979) and identified by the peroxidase-conjugated antibody technique (Barbarese and Pfeiffer, 1981). Typically, this procedure permitted an unequivocal identification on the gel of as little as 50 ng myelin basic proteins, 1 µg proteolipid protein (Macklin et al., 1981) and 50 ng myelin-associated glycoprotein (Braun et al., 1982).

#### 4.2.9 Enzyme Markers

##### a) Acetylthiocholinesterase

This activity was measured by the procedure of Klingman et al. (1968).

##### b) 2',3'-Cyclic Nucleotide 3'-Phosphohydrolase (CNP, EC 3.1.4.37)

Activity was assayed by measuring the conversion of 2',3'-cyclic NADP to 2'-NADP (Sogin, 1976), modified by the addition to the assay mixture of 2% Triton X-100 and sufficient NaCl to bring the final ionic strength to 0.75, as recommended by Sims et al. (1979).

##### c) NADH-Cytochrome C Reductase

Activity was measured both in the absence and in the presence of anti-mycin A as recommended by Mahler (1955); the procedure of Huang et al. (1979) was used.

d) Succinate Dehydrogenase

Activity was measured as described by Huang et al. (1979).

e) PAPS-Galactocerebroside Sulfotransferase

The assay was an amalgamation of procedures described by Farrell and McKhann (1971) and Siegrist et al. (1977).

<u>Stock Solution</u>	<u>Volume Used in Assay</u>
Tris HCl, pH 7.1, 250 mM	
ATP, 6.25 mM	0.2 ml
MgCl <sub>2</sub> , 50 mM	
NaCl, 385 mM	
PAP <sup>35</sup> S, 2.0 µCi per ml in 0.9% NaCl	0.1 ml
Galactocerebroside, 1 mg per ml in 2% Triton X-100 and 0.9% NaCl	0.1 ml
Enzyme (0.1 to 0.2 mg protein)	0.1 ml

All ingredients in screw-capped tubes, were brought to 37°C and the reaction was initiated by the addition of the PAP<sup>35</sup>S. The reaction was terminated by the addition of 5 ml CHCl<sub>3</sub>/CH<sub>3</sub>OH (2:1) with mixing. A two-phase mixture was obtained by the addition of 1.2 ml 0.74% KCl, with vortexing and centrifuging at room temperature. Phases were separated and the lower phase was washed twice with theoretical upper phase (Folch et al., 1957). Samples were transferred to vials and dried, then incubated at 50°C for 60 min with 0.4 ml Protosol solubilizer. Econo-fluor scintillation mix was added and <sup>35</sup>S-sulfatide was determined by scintillation counting.

f) N-Acetyl Glucosaminyltransferase Utilizing Endogenous Acceptors

Activity was measured by the procedure of Ko and Raghupathy (1972). Each assay tube contained 0.3 µCi <sup>3</sup>H-UDP-N-Acetyl glucosamine. ATP (2 mM) was also added to protect the substrate against endogenous pyrophosphatase, as suggested by Bretz et al. (1980). The P3 fraction (500



µg total protein per assay) served as the acceptor source. This material was resuspended in the assay buffer.

#### g) Galactosyltransferase Utilizing Endogenous Acceptors

Activity was measured by the procedure of Ko and Raghupathy (1971). Each assay tube contained 0.08 µCi  $^{14}\text{C}$ -UDP-galactose. ATP (2 mM) and the P3 endogenous acceptor source were also added as in (f).

### 4.3 Results

#### 4.3.1 Subcellular Fractionation: Consideration of Sedimentation

##### Parameters

Since our approach to the study of myelinogenesis is to examine early events it is imperative that intracellular membrane fractions which participate in this process be dissociated from myelin fragments, and that myelin elements be separated as extensively as possible into fractions which reflect structural and compositional differences. Thus, we developed a fractionation procedure (Fig. 4.2.1) for young myelinating animals based on both size and buoyant density characteristics of particles.

Although there are a number of methods entirely suitable for the isolation of mature myelin from adult animals they are inadequate for isolating myelin fractions representing various stages of development at a given moment during myelinogenesis. Thus, a detailed assessment of how particles separate under several centrifugational procedures seemed appropriate in view of the many different protocols which are being used in research on myelinogenesis and the misinterpretation of results from procedures which fail to separate membranes on the basis of defined sedimentation parameters, but rather produce fractions of mixed characteristics. This has been a serious problem which makes it impossible to

Minimum particle size pelleted after a given time (min)

Rotor Ti 75: 35 Krpm

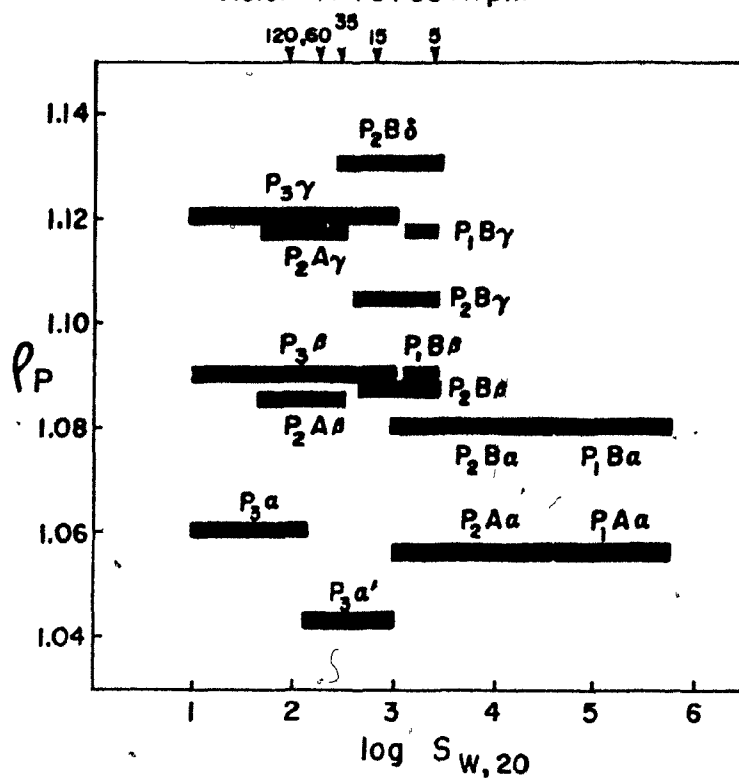


Figure 4.3.1. Two-dimensional sedimentation map of mouse brain (15 d) subfractions, illustrating both average particle density ( $\rho_p$ ) and size (sedimentation coefficient) characteristics.

obtain meaningful comparison of results amongst the various reports in the literature.

In preliminary experiments we determined the overlap of particle size which can be expected for a given set of velocity sedimentation conditions (data not shown), since the success of subsequent separations in discontinuous gradients under non-equilibrium conditions depends on the degree of size overlap of a given fraction. In our first gradient (Fig. 4.2.1) small particles originating from plasma membranes, endoplasmic reticulum, Golgi elements, etc., were retained in the upper two or three layers of the gradient even though their density is higher than that of sucrose. Water-shock followed by velocity centrifugational collection of particles is no improvement since small particles still remain intermixed with other membranes of interest. A specific example of the inadequacy of non-equilibrium sedimentation procedures to separate complex mixtures is the presence of large quantities of ribosomes and ribonucleoprotein particles which fill the perikarya of oligodendroglia during active myelination (Peters et al., 1976). We have observed that these small free ribosomal elements ( $S < 80$ ) are present in most fractions, especially those that contain myelin obtained by rate zonal centrifugation on discontinuous sucrose gradients. They can be removed by centrifuging these fractions to their equilibrium densities, or they can be maintained in an aggregated state with the aid of low-salt buffers containing 2 - 4 mM  $Mg^{++}$  as recommended for the isolation of endoplasmic reticulum and other intracellular membranes (Adelman et al., 1974).

In the case of very large myelin or myelinated axon fragments ( $S_{w,20} = 10^4$  to  $10^5$ ) the careful choice of a sedimentation rate can render isopycnic centrifugation unnecessary. For example, the small free

TABLE 4.3.1.

Characteristics of Mouse Brain (15 d) Subfractions: Density, {  
Range of Sedimentation Coefficients and Electron Microscopic Morphology

SUBFRACTION	Density* (g/ml)	log S <sub>w,20</sub> range	MORPHOLOGICAL DESCRIPTION
P1Aα	1.055	4.6 - 5.75	large, highly compacted, multi-lamellar myelinated axons with axoplasm
P1Bα	1.080	4.6 - 5.75	large, highly compacted, myelinated (few lamellae) axons
P1Bβ	1.090	3.1 - 3.4	some large membrane fragments and loosely ensheathed axons
P1Bγ	1.117	3.1 - 3.4	heterogenous population of vesicles with or without entrapped electron-dense material
P2Aα	1.055	3.0 - 4.6	small, highly compacted, multi-lamellar, myelinated axons
P2Aβ	1.085	1.7 - 2.5	heterogenous population of vesicles with or without entrapped electron-dense material
P2Aγ	1.118	1.7 - 2.0	same as in P2Aβ
P2Bα	1.080	3.0 - 4.6	small, uncompacted myelinated axons (cytoplasmic inclusion in the myelin)
P2Bβ	1.087	2.7 - 3.4	loosely wrapped myelin membranes around axons with cytoplasmic content
P2Bγ	1.105	2.6 - 3.4	Golgi bodies and some denser vesicles with electron-dense contents
P2Bδ	1.13	2.4 - 3.4	Golgi bodies and a larger proportion of vesicles with electron-dense content
P3α'	1.043	2.1 - 3.0	heterogenous population of smooth vesicles with electron-dense contents and some with enclosed multi-membrane structures
P3α	1.060	1.0 - 2.1	tentatively described as RNP complex aggregates and smooth vesicles
P3β	1.090	1.0 - 3.0	rough endoplasmic reticulum (RER) vesicles and polysomes
P3γ	1.120	1.0 - 3.0	RER vesicles, ribonucleoprotein (RNP) aggregates and polysomes

\* Densities represent averaged values as determined from refractive index measurements.

ribosomal contamination (5% on a RNA basis) of P1A can be eliminated by simple rate sedimentation under appropriate conditions. However, the isolation of smaller myelin and membrane elements ( $S_{w,20} = 10^2$  to  $10^4$ ) requires centrifugation to density equilibrium in order to achieve adequate separations, i.e. subfractionation.

Figure 4.3.1 is an attempt to obtain a summary perspective of these subfraction characteristics in terms of a two-dimensional representation of their particle-size range and particle density. This has broad biochemical implications in the context of size and density differences that occur amongst organelles or membranes of a given type in the developing brain. Myelin itself undergoes considerable change in morphology and in its relationship to the axon during development (see Discussion).

#### 4.3.2 Morphological Assessment by Electron Microscopy

Four distinct myelin and myelinated axon fractions, P1A $\alpha$ , P2A $\alpha$ , P1B $\alpha$ , P2B $\alpha$  (Table 1), were consistently obtained from 15-day old mice (Fig. 4.3.2). Most of the axonal fragments in the light subfractions (P1A $\alpha$ ; P2A $\alpha$ ) contain aggregated filaments, identifiable axolemma, and compact myelin. The axonal fragments in the denser subfractions (P1B $\alpha$ ; P2B $\alpha$ ) contain non-aggregated filaments and well-preserved mitochondria in the axoplasm, and the myelin has fewer lamellae.

The heterogenous subfractions, P1B $\beta$  and P2B $\beta$ , also contain myelinated axons with well-defined and non-aggregated axoplasmic filaments and in many cases, axoplasmic mitochondria. These axonal elements frequently have cytoplasm entrapped mesaxonally and in intramyelinic pockets. Many large vesicles and membrane fragments are also present, but few lamellar myelin fragments are observed.

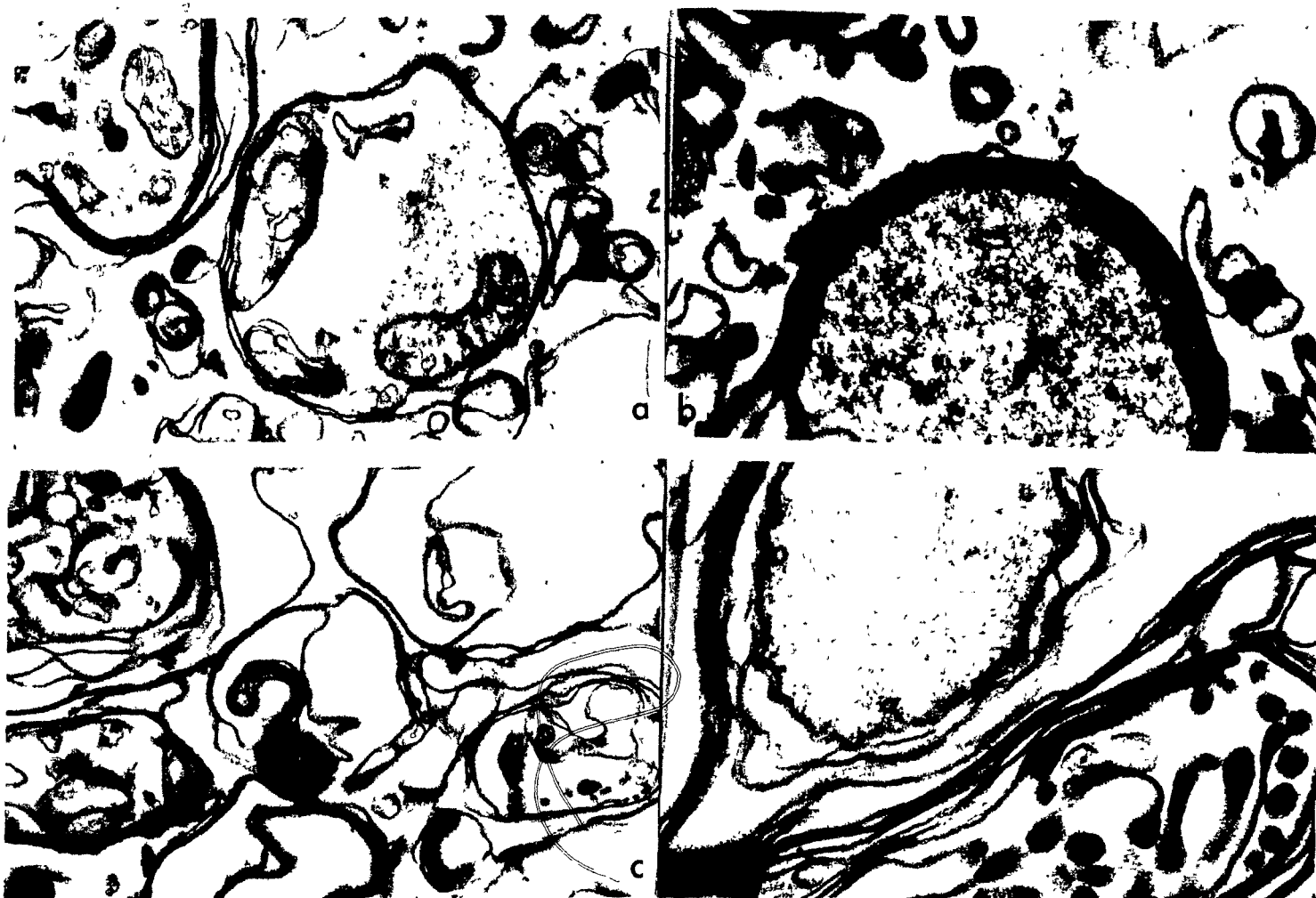


Figure 4.3.2. Electron micrographs of four myelin-containing subfractions of mouse brain (15 d).  
 a) P1A a; b) P2A a; c) P1B a; d) P2B a. Magnification: 49000 X.

The microsomal fraction  $P3\alpha'$  contains all the typical myelin proteins but its density (1.043) is lower than that of myelin-containing fractions. It appears transiently during early stages of myelinogenesis and has a characteristic, vesiculated EM morphology (Fig. 4.3.3a).

Another interesting microsomal fraction,  $P3\alpha$ , also contains typical myelin proteins, but the SDS-PAGE profiles are nevertheless quantitatively and qualitatively different from those of  $P3\alpha'$  (as presented and discussed below). Electron micrographs of  $P3\alpha$  (Fig. 4.3.3b) reveal a mixture of dense bodies, smooth vesicles and aggregated particles having the appearance of ribonucleoprotein aggregates.

Two other fractions of interest to us are  $P2B\gamma$  and  $P2B\delta$ , (see Table 4.3.1), which contain morphological structures of the Golgi apparatus (Fig. 4.3.3c and 4.3.3d). Although not previously recognized, these fractions are present in the so-called "heavy" myelin described by many investigators using a variety of standard myelin isolation techniques.

#### 4.3.3 Recovery of Subfractions Determined by Protein Content

The total protein recovered from a complete fractionation of mouse brain was 90 - 95% of starting material. The recovery of protein in each particulate subfraction is shown in Table 4.3.2, as an average of 8 separate subfractionation experiments. The % variations shown reflect the large experimental deviation in the protein content of the unpelleted subfractions (column 2, Table 4.3.2) as compared to the smaller variations in the % of protein pelleted (column 3, Table 4.3.2) in each subfraction. The difference in variation between these two determinations seems to indicate that variations among experiments are due mainly to differences in the amount of cells (soluble proteins) disrupted in the initial homogenization rather than to variations in the disruption patterns that give rise to each subfraction.

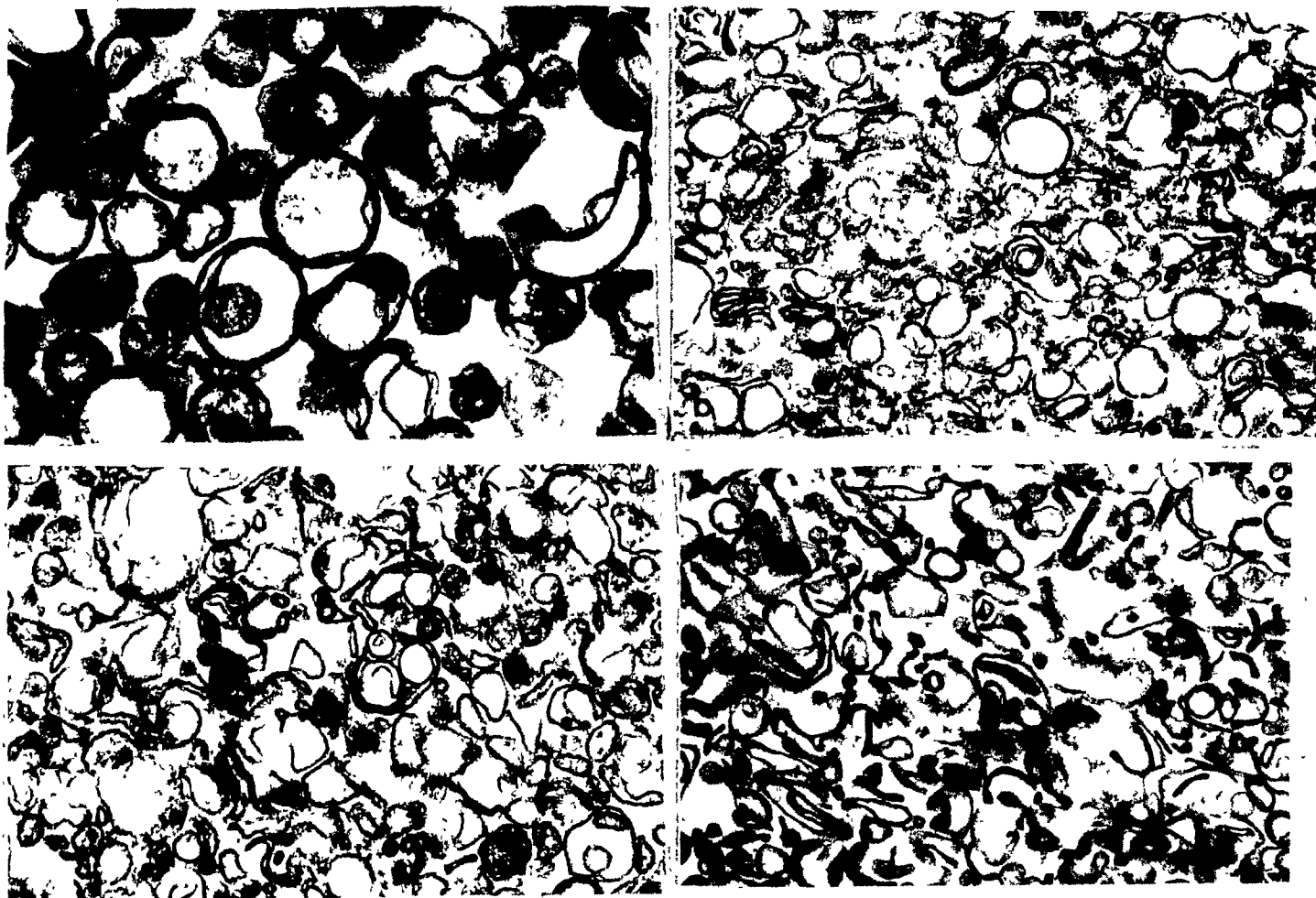


Figure 4.3.3. Electron micrographs of four microsomeal subfractions of mouse brain (15 d). a) P3 a'; b) P3 a; c) P2B<sub>g</sub>; d) P2D<sub>g</sub>. Magnification: 49000 X.



The small % variations in the sucrose concentration of each sub-fraction (column 3, Table 4.3.2) suggests that it is possible to achieve considerable uniformity and reproducibility in deciding boundaries of bands and in collecting them.

#### 4.3.4 Enzyme Markers and the Distribution of RNA

Our choice of enzyme markers was based not only on the need to identify subfractions but also included the objective of establishing some of their metabolic inter-relationships. The distribution of enzyme activities are summarized in Table 4.3.3.

##### a) Mitochondrial Markers

Electron micrographs of some of our subfractions which contain myelinated axons (P1A $\alpha$ , P2A $\alpha$ , P1B $\alpha$ , P2B $\alpha$ ) reveal the presence of a few axoplasmic mitochondria. In addition, small vesiculated inner and outer mitochondrial membrane fragments can be expected to co-isolate with microsomal subfractions. We assessed this by measuring the activity of two enzymes:

##### i) NADH-Cytochrome c Reductase

The antimycin A-sensitive form of this enzyme from brain has been reported to be localized in the outer mitochondrial membrane, and the insensitive form appears to be distributed among membranes of the endoplasmic reticulum, Golgi apparatus, and the cell surface (Mahler, 1955; Huang et al., 1979).

Only a small amount of total antimycin A-sensitive NADH-cytochrome c reductase activity was found in our subfractions (2.3% of brain homogenate), indicating very little contamination by intact or disrupted mitochondria (Table 4.3.3).

TABLE 4.3.2.

Sucrose Concentrations and Recovery of Total  
Protein in Mouse Brain (15 d) Subfractions #

SUBFRACTION OF TH*	PROTEIN % OF TH	PROTEIN % of subfraction obtained as pellet	% SUCROSE g/100 g soln.
	<u>% var.</u>	<u>% var.</u>	<u>% var.</u>
P1A $\alpha$	1.4	5.4	11.0
P2A $\alpha$	1.2	37.1	14.2
P2A $\beta$	.5	42.1	24.9
P2A $\gamma$	.4	20.9	32.1
P1B $\alpha$	.6	19.4	54.1
P1B $\beta$	.6	27.0	64.4
P1B $\gamma$	1.2	27.0	73.7
P2B $\alpha$	.2	30.0	79.2
P2B $\beta$	.6	38.2	51.2
P2B $\gamma$	1.8	35.5	95.0
P2B $\delta$	2.3	20.4	95.0
P3 $\alpha'$	1.0	15.3	6.0
P3 $\alpha$	.8	5.7	18.4
P3 $\beta$	1.7	31.9	26.4
P3 $\gamma$	1.2	22.6	50.1

\* TH is total homogenate.

# Values represent the average of 22 experiments

The inhibition of total NADH-cytochrome c reductase by antimycin A ranged from 30 - 90% and only 3 subfractions ( $P3\beta$ ,  $P3\alpha$  and  $P2A\beta$ ) showed no sensitivity toward this compound.

ii) INT-Succinate Dehydrogenase

This enzyme is present in the inner mitochondrial membrane and serves to corroborate the distribution of cytochrome c reductase. Again, we found a very low recovery of enzyme activity in our subfractions confirming the low level of mitochondrial contamination. The bulk of both of these mitochondrial marker activities occurred in  $P1C$  and  $P2C$  (data not shown).

Comparison of relative specific activities of these two enzymes (Table 4.3.3) suggests that any contamination of mitochondrial origin in the microsomal upper subfractions  $P3\alpha'$  and  $P3\alpha$  is derived primarily from the outer mitochondrial membrane.

b) Markers for Golgi Membranes

i) Galactosyl Transferases Utilizing Endogenous Microsomal Protein Acceptors

These activities are known to be involved in the post-translational modification of proteins in membranes of the Golgi apparatus, and can be used to assess the presence of Golgi membranes in all fractions (Lennarz, 1980).

We found only about 16% of the total homogenate activity in our subfractions (Table 4.3.3), with 12% appearing in only 2 subfractions,  $P2B\gamma$  and  $P2B\delta$ . This accords with our finding of numerous Golgi elements in electron micrographs of these subfractions (Fig. 4.3.3c and 4.3.3d).

ii) Galactosyl Ceramide Sulfotransferase

This enzyme has been attributed to the Golgi membranes of brain by

TABLE 4.3.3.

Characterization of Mouse Brain (15 d) Subfractions by  
Their Content of Marker Enzyme Activity and of RNA \*

SUBFRACTION	MITOCHONDRIAL + NADH Cyt. c Red		SUCCINATE-INT REDUCTASE		UDP-NAG1uA TRANSFERASE		UDP-Gal. TRANSFERASE		PAP <sup>35</sup> <sub>S</sub> TRANSFERASE		ACETYL-THIO CHOLINESTERASE		CNP		RNA	
	RSA	% T.U.	RSA	% T.U.	RSA	% T.U.	RSA	% T.U.	RSA	% T.U.	RSA	% T.U.	RSA	% T.U.	ug	% of Total
P1Aα			.8	.01	1.3	1.0	.2	.1	.1	.1	3.5	.6	15.9	2.5	4.9	.2
P2Aα	1.4	.1	.3	.04	2.4	.4	.2	.1	.7	.1	8.5	.2	17.4	3.1	7.4	.2
P2AB	0.0	0.0	.04	.01	.5	.1	.5	.1	.03	0.0	9.6	.3	9.3	2.8	1.4	.04
P2AY	.3	.2	0.0	0.0	1.2	.2	.8	.1	.8	.1	6.9	1.5	3.3	2.0	4.0	.1
P1Bα			.1	.02	5.4	1.9	.9	.3	.7	.2			14.6	5.1	6.1	.2
P1BB			.3	.2	2.6	.8	1.1	.3	1.3	.4	2.3	2.6	13.8	1.8	4.1	.1
P1BY			0.0	0.0	2.4	1.2	1.1	.5	1.5	.7			4.7	2.3	2.1	.06
P2Bα	.2	.1	0.0	0.0	4.0	.5	1.9	.2	2.4	.3	1.9	.4	18.7	2.2	3.8	.1
P2BB	.3	.2	.1	.04	2.3	.6	2.7	.7	4.6	1.2	6.8	1.7	8.5	2.2	5.4	.2
P2BY	.1	1.3	.1	.1	27.8	15.6	5.0	2.8	11.8	6.6	2.8	10.8	2.8	1.6	20.1	.6
P2Bδ			.2	.4	21.7	35.3	5.8	9.5	9.0	14.6			1.2	2.0		
P3 α'	3.0	.2	.1	0.0	2.0	.1	.8	.1	.3	.02	21.1	.7	14.3	1.0	9.0	.3
P3 α	.7	.2	.2	.1	0.0	0.0	.8	.04	.3	.01	2.8	.3	1.3	.1	64.4	2.0
P3 β	0.0	0.0	.2	.2	2.6	.9	.8	.3	1.2	.4	10.2	4.9	4.6	1.6	226.8	7.0
P3 γ	0.0	0.0	.03	0.0	.5	.3	1.2	.7	2.4	1.5	3.9	4.3	1.2	.8	146.5	4.5
	Σ = 2.3		Σ = 1.2		Σ = 58.7		Σ = 15.9		Σ = 26.3		Σ = 28.3		Σ = 31.2		Ribosomal total pellets	
															635.3	19.5

RSA is relative specific activity (with respect to homogenate).

% T.U. is % total units of enzyme activity.

\* Not all enzyme determinations were performed on the same preparation of subcellular fractions. They do not  
They do not have the same statistical validity as the values of protein in Table 4.3.2.

Siegrist et al. (1977). In our fractionation scheme its distribution correlates well (correlation coefficient (0.01) = 0.96) with the distribution of galactosyl transferase activity, well in agreement with their observations.

iii) UDP-N-Acetylglucosaminyl Transferase (Endogenous Microsomal Acceptor)

This activity represents a combination of all the various N-Acetylglucosaminyl transferases present in the Golgi apparatus. The specific activity of this enzyme was much lower than that of the other transferases, but a larger amount of the total activity (about 59%) was recovered in our subfractions (Table 4.3.3). This enzyme is distributed basically in the same way as the other two transferases, with the bulk of the activity found in only two subfractions, P2B $\gamma$  and P2B $\delta$ , which we believe to be major Golgi-enriched fractions. As is also the case for the other transferases, only 1 - 2% of the total activities occur in rough endoplasmic reticulum containing fractions (P3 $\beta$  and P3 $\gamma$ ), suggesting that these fractions contain only a small amount of Golgi contamination.

Despite these apparent similarities in distribution amongst transferase activities, two myelin-containing subfractions, P1A $\alpha$  and P1B $\alpha$ , are enriched by a factor of 10 in UDP-NAGluA transferase activity, compared to UDP-Gal transferase (comparison of % total units).

The absence of this large difference in recovery from other myelin-containing fractions (P2A $\alpha$  and P2B $\alpha$ ), as well as the very low levels of other transferase activities rules out a generalized, non-specific contamination by Golgi membranes. Thus, the possibility exists that a specific N-acetylglucosaminyl transferase for glycolipid synthesis is

actually a constituent of plasma membrane-derived structure in P1A $\alpha$  and P1B $\alpha$ . In fact, the methodology of the assay does not preclude the possibility that we are observing the incorporation of isotope into oligosaccharides and gangliosides. In this regard, some gangliosides are known to contain N-acetylglucosamine instead of N-acetylgalactosamine (Lennarz, 1980). Furthermore, we also cannot exclude the possibility of artifact due to non-specific binding to proteins and lipids of isotopic contaminants which can be present in the commercially labeled substrate.

#### iv) Acetylthiocholinesterase

This activity actually represents two enzymes: acetylcholinesterase, found mainly in neuronal surface membranes, and pseudocholinesterase which appears to be localized mainly in glial membranes and microsomal membranes in general. We were able to recover a maximum of 28% of total acetylthiocholinesterase activity in our subfractions (Table 4.3.3); the remainder of the activity appeared in fractions not shown here. The highest relative specific activities were located in the  $\beta$  or  $\gamma$  subfractions, with the exception of P2A $\alpha$  and P3 $\alpha'$ . This is what we expected given the possible appearance of dense, synaptosome-derived contaminants in the  $\beta$  and  $\gamma$  regions of the gradient. In fact, these specific activities do parallel the density distribution one expects of synaptosomally-derived elements containing acetylcholinesterase activity. The high RSA values for the light fraction P2A $\alpha$  is puzzling, and we offer no immediate explanation, except to indicate that the total units of this activity are very low. In P3 $\alpha'$  we cannot rule out some contamination by synaptic vesicles.

#### 4.3.5 RNA Determination

In the absence of salt buffers we anticipated a substantial quantity

TABLE 4.3.4

Comparison of RNA Content Among Microsomal Fractions of Mouse Brain (15 d) Obtained by Discontinuous Gradient Velocity Sedimentation (A) and Equilibrium Density Sedimentation (B)

A		B	
SUBFRACTION		SUBFRACTION	
3 hr/25K rpm/SW27	$\mu\text{g RNA}$	24 hr/25K rpm/SW27	$\mu\text{g RNA}$
P3 top	32.40	P3 $\alpha'$	8.90
P3A	406.60	P3 $\alpha$	64.40
P3B	365.60	P3 $\beta$	226.80
P3B/C	15.60	P3 $\gamma$	146.50
P3C	25.40	P3 pell.	430.00
P3C/D	1.20		
P3D	34.00		
$\Sigma = 880.$		$\Sigma = 876.$	

of free polysomes, ribosomes and RNA in some of our subfractions, especially since glial cells and their processes of the developing brain are filled with these structures. P1A was found to have up to 2% of the total RNA, consistent with the visual aggregates of free ribosomes interspersed with the large myelin fragments which were seen in electron micrographs. Centrifugational pelleting of these membranes by velocity sedimentation or separation by equilibrium density centrifugation removed about 90% of the RNA, concordant with the visual disappearance of ribosomal particles.

Fractionation of microsomal material by the procedure of Barbarese et al. (1979) resulted in the appearance of most of the RNA as ribonucleoprotein aggregates and ribosomes in the uppermost layers (P3A and P3B) of the step gradient (Table 4.3.4, panel A), fractions which contain MBP's and other myelin constituents during development. Centrifugation of particles in P3 to their equilibrium density produced four distinct bands of membranous material and a pellet containing ribosomes (Table 4.3.4, panel B). The small amount of RNA in the uppermost myelin related subfraction (P3 $\alpha'$ ) represents free RNA ( $S_{w,20} = 50$ ) rather than ribosomes. Note that there has been a redistribution of free and membrane associated RNA from the "light" myelin related subfractions P3A and P3B into the rough endoplasmic reticulum enriched subfractions P3 $\beta$  and P3 $\gamma$  by subjecting the same initial discontinuous gradient to isopycnic conditions. Table 4.3.3 lists the content of RNA in subfractions obtained by our current procedure (Fig. 4.2.1). Hence, we can identify P3 $\beta$  and P3 $\gamma$  as subfractions which contain rough endoplasmic reticulum, and show that only small amounts of RNA are associated with other lighter subfractions.



#### 4.3.6 Myelin Markers

Our objective was not only to show the distribution of typical myelin components amongst the various subfractions, but also to determine the way in which these fractions could be grouped according to common characteristics. In this way we hope to achieve a more comprehensive understanding of metabolically inter-related parameters in myelin assembly.

##### 1) 2',3'-Cyclic Nucleotide 3'-Phosphohydrolase

Although the function of this enzyme remains an enigma its structural association with the myelin sheath and oligodendroglial plasma membrane is firmly established (Braun and Brostoff, 1977). However, its presence in endomembranes of myelinating cells, as well as in membranes of non-neural tissues has also been reported (Dreiling et al., 1981; Weissbarth et al., 1981) and suggests a broader function than heretofore recognized.

Table 4.3.3 shows that only 31% of total units are recovered in our subfractions; the remainder of the activity was found in the post-microsomal supernatant and in P1C and P2C. The enzymatic activity is distributed very similarly amongst most of the subfractions (average of  $2.1\% \pm 0.3$ ) except in P2A $\alpha$ , P2A $\alpha$  and P1B $\alpha$  in which it varies from 2.8 to 5.1%, or in some microsomal subfractions in which activity accounts for 0.6 to 1% of total units.

Distribution of CNP on the basis of relative specific activity, however, is quite different. Subfractions which contain typical morphological characteristics of myelin (P1A $\alpha$ , P1B $\beta$ , P2A $\alpha$ , P1B $\alpha$ , P2B $\alpha$ ) are enriched 13- to 18.7-fold over total homogenate. Subfractions P2A $\beta$  and P2B $\beta$ , have RSA's around 9, and a third category (P1B $\gamma$ , P2A $\gamma$ , P2B $\gamma$ , P2B $\delta$ )

Group No.	Subfractions	Identification by immuno-electro blot			Gel Scan	CNP	
		MBP	MAG	PLP		RSA (range)	Σ% T.U.
I	PIAα, PIBα, P2Aα P2Bα, P3α' PIBβ	+++	+++	+++		13.2 - 18.7	16.3%
II	P2Aβ, P2Bβ	+	++	+		8.5 - 9.3	5.1%
III	PIBγ, P2Bγ, P2Bδ	+	++	-		1.22 - 4.72	5.9%
IV	P2Aγ, P3β, P3γ	-	++	-		1.6 - 4.4	4.4%
V	Ribosomal pellet	-	++	-		-	-

Table 4.3.5. Grouping of mouse brain (15 d) subfractions according to the presence or absence of specific myelin proteins, and comparison with protein profiles and CNP activity.

is enriched 1.2- to 5-fold over the homogenate. The microsomally-derived subfractions ( $P3\alpha'$ ,  $P3\alpha$ ,  $P3\beta$ ,  $P3\gamma$ ) also fall into the above three categories, according to their RSA of CNP.

Comparison of CNP activity (% total units) distribution to the distribution of other enzymes in Table 4.3.3 suggests that this enzyme is distributed widely among plasma membrane subfractions and endomembranes. It is worth noting that CNP activity was determined under conditions of maximal activation using media of high ionic strength and containing 2% Triton X-100, as recommended by Sims et al. (1979) and Clapshaw and Seifert (1980) and RSA values are therefore higher than under enzyme assay conditions which provide only incomplete activation of CNP, using deoxycholate, but the same assay procedure. Our distribution of activities (RSA) amongst vesiculated membrane subfractions could be ranked according to their apparent densities, i.e. activity of heavy medium light fractions with a correlation coefficient of 0.9. However, in the case of myelinated axon-enriched subfractions no such correlation was observed.

#### ii) Myelin-Specific Proteins

Membrane proteins were clearly separated by SDS-PAGE on pore-gradient slab gels. Representative spectrophotometric scans are shown in Table 4.3.5. Positive identification in each gel of proteolipid protein (lipophilin; 25K), the four myelin basic proteins (14K, 17K, 18.5K, 21.5K) and myelin-associated glycoprotein (105K) was achieved by the immuno-electroblot technique as we have described elsewhere (Macklin et al., 1982; Braun et al., 1982). On the basis of the immunochemical verification of these characteristic myelin proteins we have assigned each subfraction to one of the five groups shown in Table 4.3.5.

Table 4.3.6.

Ranking of Groups I and II Subfractions According to Their Enrichment in  
14K MBP and 18.5K MBP and Comparison with Their Particle Index ( $\phi$ )

Subfraction	14K MBP		17K MBP		18.5K MBP		21.5K MBP		PLP	$\phi$
P1A $\alpha$ '	6	:	2	:	3	:	1	:	3	5.28
P1B $\alpha$	4	:	1	:	3	:	1	:	2.5	5.28
P2A $\alpha$	3	:	1	:	2	:	1	:	1	3.94
P2B $\alpha$	3	:	1	:	2	:	1	:	1	3.94
P1B $\beta$	3	:	1	:	2	:	1	:	2	3.43
P2B $\beta$	1	:	2	:	1	:	1	:	3.5	3.25
<hr/>										
P3 $\alpha$ '	2	:	1	:	2	:	1	:	2	2.75

Protein profiles within each group were remarkably similar, differing only in the quantitative proportions of each component.

Groups I and II differ quantitatively in their protein profiles, but contain all three categories of myelin-specific proteins. Subfractions on Group I and II could be distinguished by the ratios of peak areas of blue-stained proteins, determined by triangulation (Table 4.3.6). We have found that these dye-binding ratios for adult mouse myelin (Norton and Poduslo, 1973) proteins are 10:1:3:1:4 for 14K/17K/18.5K/21.5K/25K. By comparison, the average ratios of 15-17 day myelin (prepared by the same procedure) are 3:1:2:1:2. Although the subfractions in Table 4.3.6 show a great deal of variation in these ratios, we have tentatively ranked them on the basis of a relative "maturity" profile of the MBP's, assuming as a first approximation that the most "mature" myelin will approach the adult ratios, and that this should agree generally with a ranking of a relative sedimentation index (column 7). Thus, in Groups I and II P1A $\alpha$  and P1B $\alpha$  contain the most mature and P2B $\beta$  the least mature myelin structures. We note that if we take into consideration the PLP component in ratio ranking we do not establish the same "maturity" sequence. Although this might be explained by variable aggregation of the PLP during experimental manipulations, our metabolic studies (Pereyra et al., 1983; this issue) suggest that the more likely reason resides in the relative proportions of PLP to MBP's message expressed at different stages of development.

Group III is characterized by the absence of detectable proteolipid protein, the presence of relatively very small amounts of basic proteins, and a moderate amount of myelin-associated glycoprotein. Group IV subfractions have no detectable proteolipid protein or basic proteins but

have an amount of myelin-associated glycoprotein comparable to that in authentic myelin-containing subfractions. Group V is the ribosomal pellet which has no detectable myelin proteins except several components of about 50K and 70K which react with the antiserum to myelin-associated glycoprotein. At this point we cannot be certain if these proteins are degradative fragments of MAG, incompletely synthesized precursors of MAG, or artifacts.

At this point such a ranking scheme is valid only to the degree that a specific component can be clearly identified. Comparisons of the content of any specific component must be analogous to comparisons of relative specific activities in the case of enzymes.

#### 4.4 Discussion

An integral aspect of our approach to the cellular mechanisms of myelinogenesis was to develop a methodology which would allow us to distinguish the various endo- and exomembrane fractions which are involved in this process. The methodology we describe here is not necessarily the best to achieve purity of any given fraction but rather is a compromise which permits the acquisition of the greatest number of identifiable myelin-related fractions without regard for purity. Thus, we sought to achieve a gentle, reproducible homogenization and fractionation protocol for developing mouse brain which would result in fractions that retain as many internodal axonal segments, organelles and endomembranes as possible in a simple procedure. For this reason we avoided the more extreme conditions of hyposmotic shock which are usually used to acquire the more heavily lamellated myelin elements from adult brain, free of other endomembrane and axoplasmic components.

We have paid careful attention to the physical principles which govern separation of particles by velocity and buoyant density sedimentation in order to assign to each of our subfractions operational parameters which we use as independent variables in the correlation of quantitative and qualitative differences among subfractions. These parameters are: 1) the average buoyant density determined by refractive index measurement of the sucrose gradient; 2) the calculated range of sedimentation rates, expressed as the logarithm of the Svedberg unit ( $\log S_{w,20}$ ; see Methods); and 3) the vector sum of these parameters, which we express as a "Particle Index". In general, our experience shows that although the buoyant density is a good parameter to distinguish various membrane types such as plasma membrane, Golgi membranes, and endoplasmic reticulum, the sedimentation index or the "Particle Index" is better suited to describe more complex elements such as myelinated axons.

Having taken into consideration the limitations and pitfalls of this approach with respect to marker distribution, we have arrived at a subfractionation scheme which yields physically and biochemically defined membrane fractions from myelinating brain. These can be grouped on the basis of their specific myelin protein content (Table 4.3.5) as determined by the immuno-electroblot technique.

We found that the four groups of membrane-containing subfractions (Table 5) fell into the following general categories: Group I, myelinated axons and associated elements; Group II, amorphous plasma membranes; Group III, Golgi membranes; Group IV, endoplasmic reticulum (rough and smooth). In making these assignments, we were careful not to over-interpret data from marker enzyme determinations; thus, some overlap exists.

Subfractions in Group I and II can be ranked according to their enrichment in the 14K and 18.5K MBPs (Table 4.3.6); this ranking correlates closely with the "Particle Index" ( $\emptyset$ ). We currently interpret this correlation as showing that the developmental characteristics of the myelin-axon unit are related more closely to the observed size distribution of myelinated axon fragments than to their bouyant densities.

Under specific conditions of homogenization, the separation of cellular organelles and nuclei by sedimentation techniques has been well documented. The literature in the area of myelin research shows that it is widely assumed that the relationship of myelin to the axon is completely disrupted by homogenization, and that a continuous range of particle size is generated, rather than several populations of discrete size ranges. However, even in mature brain, the disruption of myelinated axons will depend on the stability of the myelin-myelin and myelin-axon interactions, given a constant shear force. From this argument it follows that one can expect to obtain at least two discrete size populations, given an appropriate sedimentation protocol. One of these will be composed of a mixture of 'small' particles which arise from large, structurally unstable myelinated segments, or from small structurally stable or unstable myelinated internodes. The other population of particles will contain 'large' particles whose initial structural stability allows them to survive as relatively large myelin membrane aggregates or even as myelinated axon segments. Furthermore, in the case of water-shocked myelin subfractions the bouyancy of the myelin membranes will depend on the degree of integrity of association among the disrupted myelin lamellae. On the other hand, in the case of non-water-shocked myelinated axon fragments their structural integrity and size will determine their overall entrapped axoplasmic volume, and the extent of



TABLE 4.4.1

## Correlation Matrix\* of Marker Enzyme Distribution Among Subfractions

	UDP-NAG Trans (RSA)	UDP-NAG Trans (TU)	UDP-GAL Trans (RSA)	SULFO Trans (RSA)	SULFO Trans (TU)	AcTChE (RSA)	AcTChE (TU)	CNP (RSA)	CNP (TU)	RNA (µg/mg)	RNA (%)	UDP-GAL Trans (TU)
UDP-NAG Trans (RSA)	1.00	.85	.90	.94	.84	-.22	.85	-.32	.01	-.24	-.11	.76
UDP-NAG Trans (TU)		1.00	.88	.79	.99	-.25	.87	-.40	-.03	-.21	-.07	.98
UDP-GAL Trans (RSA)			1.00	.96	.91	-.30	.78	-.42	-.12	-.22	-.09	.85
SULFO Trans (RSA)				1.00	.82	-.31	.85	-.42	-.13	-.21	-.03	.73
SULFO Trans (TU)					1.00	-.28	.91	-.45	-.08	-.16	.02	.99
AcTChE (RSA)						1.00	-.22	.16	-.02	.13	.04	-.27
AcTChE (TU)							1.00	-.51	-.22	.06	.34	.91
CNP (RSA)								1.00	.51	.47	.49	-.41
CNP (TU)									1.00	-.57	.40	-.05
RNA (µg/mg)										1.00	.85	-.18
RNA (%)											1.00	.02
UDP-GAL Trans (TU)												1.00

\*Stepwise regression analysis with the Regression Analysis Pac of the HP-85 computer. (Tolerance = 0.01)

myelin lamellation will determine their impermeability to the surrounding sucrose medium, conditions which in turn will determine the bouyancy of the particle (Sarma and Sitaraman, 1982). Our own electron microscopic analysis of myelin-containing fractions supports this interpretation. For the moment, we are led to suggest that the size contribution to sedimentation behaviour of myelinated axonal segments is more related to the extent of myelin maturity than is the buoyant density contribution. Further investigation should clear this important interpretative proposal.

The microsomal subfraction  $P3\alpha'$ , which we have also assigned to Group I because of its shared properties with other subfractions in this category, actually consists of two vesicle populations: one consisting of large, trilamellar structures that contain myelin proteins in the same relative proportions as  $P2A\alpha$  and  $P2B\alpha$ ; and the other consisting of smaller, unilamellar vesicles which may or may not contain electron-dense material, and which have a myelin protein proportions intermediate between that of  $P2B\beta$  and  $P1B\beta$ . These vesicular subfractions appear only during the most active phase of myelination.

The subfractions in Group III represent only about a third of all the Golgi-associated membrane elements; most of these are found in  $P1C$  and  $P2C$ . However, they are characterized by a relatively high enrichment in three transferases which are known to be Golgi markers. All three enzymes show a high degree of correlation among these subfractions in both their total unit and specific activity distribution (Table 4.4.1). We believe that this argues for a common subcellular origin of these membrane elements even though they originate from several cell types. From the high correlation between acetylcholinesterase activity and the

transferase activities, in terms of their total activity distribution, we further conclude that Group III subfractions contain a significant amount of neuronal or synaptosomal membrane. The presence of MAG in these subfractions can be explained on the basis of the Golgi apparatus constituting the logical processing site for this glycoprotein en route to myelin, but we cannot exclude the possibility of its presence in small amounts of oligodendroglial plasma membrane which remains associated with the neuronal membrane. Discrimination between these possibilities must await more quantitative measurements of MAG.

Group IV subfractions represent only a very small fraction of the endoplasmic reticulum, most of which is found as large elements in the fractions P1C and P2C. The RNA in this group is mainly of the "free" type, with good correlation of specific enrichment and total unit distribution.

These subfractions also contain two antigenic components, of approximately 50K and 70K daltons, which react with our antiserum to MAG. We do not yet know if these represent MAG precursors or degradation fragments.

Since CNP is widely used as a marker for myelin we did an extensive survey of this enzyme and found activity in all of our membranous subfractions, with variable behaviour toward activating conditions and variable ratios of soluble to membrane bound forms of this enzyme. Other investigators in the myelin field have also noted this but have not dealt with the broad implications of the general distribution of CNP; instead the tendency has been to assume that this means subcellular fractions are contaminated by myelin. More recently, several reports have appeared showing the presence of CNP activity in tissues other than brain,

In the context of the above considerations, we presently view CNP to be distributed in a multifocal fashion, and are further investigating this problem, as well as the role that this enzyme might play in the regulatory machinery of oligodendroglia.

The following observations should be underscored:

- 1) Proteolipid protein is localized to only a restricted group of membranes or structures which possess a typical spectrum of myelin proteins; these membranes range in density from 1.04 to 1.08 g/ml. Absence of detectable amounts of this protein from Golgi-enriched fractions is potentially an important observation, given that the MAG is clearly present, as well as low levels of myelin basic proteins. We are attempting to provide independent corroboration of these immunochemical data, which are reproducible and apparently reliable.

- 2) Myelin basic proteins are present in three membrane categories, but appear most prominently in only the myelin-containing compartments. Even though immunochemical staining for these antigens on nitrocellulose electroblots of the gels is not a strictly quantitative procedure, a relative assessment of amount of protein is nevertheless possible. Indeed, examination of the relevant gel scans in Table 4.3.5, offers a visual confirmation of diminished MBP bands in the protein profile.

- 3) The distribution of MAG is a more general phenomenon, encompassing all membrane fractions as well as the ribosome-containing pellet.

- 4) Quantitative differences in protein profiles (gel scans) are observed within each major group of subfractions, and qualitative differences are evident when comparing the major groups to each other.

- 5) CNP, when maximally activated is widely distributed among brain subfractions. We interpret this as multifocal distribution and not as

myelin contamination.

Although more definitive structural and functional descriptions of myelin-related membranes will only be derived from purified subfractions, the approach we describe here, based on size and buoyant density considerations provides a complex overview of protein and enzyme distribution and their interrelationships, with respect to an early stage of myelination. We wish to emphasize that our present, as well as future experimental designs are not and will not be constrained by the details of the subfractionation protocol presented here, but rather will employ the strategy embodied in it. A combination of fractionation refinement techniques, protein isolation, immunochemical procedures and studies of metabolic dynamics by isotope methodologies should provide us with deeper insights into the biogenic sequence of events in which these membranes are involved. The companion paper (Pereyra and Braun, 1983) addresses the kinetic isotope approach.

#### 4.5 References

- Adelman, M.R., Blobel, G. and Sabatini, D.D. (1974) Nondestructive Separation of Rat Liver Rough Microsomes into Ribosomal and Membranous Compartments. in Methods in Enzymology, Vol. 31 (Edited by Fleisher, S. and Packer, L.) pp. 201-225 Academic Press, New York.
- Barbarese, E. and Pfeiffer, S.E. (1981) Developmental regulation of basic protein in dispersed cultures. Proc. Natl. Acad. Sci. USA 78, 1953-1957.
- Barbarese, E., Carson, J.H. and Braun, P.E. (1979) Subcellular Distribution and Structural Polymorphism of Myelin Basic Protein in Normal and Jimmy Mouse Brain. J. Neurochem. 32, 1437-1446.

- Benjamins, J.A. and Morell, P. (1978) Proteins of myelin and their metabolism. Neurochem. Res. 3, 137-174.
- Borgese, N. and Meldolesi, J. (1980) Localization and biosynthesis of NADH-cytochrome  $b_5$  reductase, an integral membrane protein, in rat liver cells. I. Distribution of the enzyme activity in microsomes, mitochondria and Golgi complex. J. Cell Biol. 85, 501-515.
- Borgese, N., Pietrini, G. and Meldolesi, J. (1980) Localization and biosynthesis of NADH-cytochrome  $b_5$  reductase, an integral membrane protein, in rat liver cells. III. Evidence for the independent insertion and turnover of the enzyme in various subcellular compartments. J. Cell Biol. 86, 38-45.
- Bradford, M. (1976) A rapid sensitive method for the quantitation of micro-gram quantities of protein utilizing the principle of protein-dye binding. Anal. Biochem. 72, 248.
- Braun, P.E., Frail, D.E. and Latov, N. (1982) Myelin-associated glycoprotein is the antigen for a monoclonal IgM in polyneuropathy. J. Neurochem. 39, 1261-1265.
- Braun, P.E., Pereyra, P.M. and Greenfield, S. (1980) Mechanisms of assembly of myelin in mice: a new approach to the problem. in INSERM Symposium No. 14 (edited by Braumann, N.) pp. 413-421. Elsevier, North Holland.
- Braun, P.E., Pereyra, P.M. and Greenfield, S. (1980) Myelin organization and development: a biochemical perspective in Myelin: Chemistry and Biology, pp. 1-17, Alan R. Liss, New York.
- Braun, P.E. and Brostoff, S. (1977) Proteins of Myelin in Myelin, Morell, P. ed., pp. 201-231, Plenum Press, New York.

- Braun, P.E. and Pereyra, P.M. (1979) Characteristics of myelin precursor vesicles. Trans. Amer. Soc. Neurochem. 10, 215.
- Bretz, R., Bretz, H., and Palade, G.E. (1980) Distribution of terminal glycosyltransferase in hepatic golgi fractions. J. Cell Biol. 84, 87-101.
- Clapshaw, P.A. and Seifert, W. (1980) Effects of detergents, proteins and lipids on 2',3'-cyclic nucleotide 3'-phosphodiesterase activity. J. Neurochem. 35, 164-169.
- deDuve, C. (1964) Principles of tissue fractionation. J. Theoret. Biol. 6, 33.
- DePierre, J. and Dallner, G. (1976) Isolation, subfractionation and characterization of the endoplasmic reticulum. in Biochemical Analysis of Membranes (edited by Maddy, A.H.) pp. 79-131. John Wiley, New York.
- Dreiling, C.E., Schilling, R.J. and Reitz, R.C. (1981) 2',3'-cyclic nucleotide 3'-phosphohydrolase in rat liver mitochondrial membranes. Biochim. Biophys. Acta 640, 114-120.
- Farrell, D.F. and McKhann, G.M. (1971) Characterization of cerebroside sulfotransferase from rat brain. J. Biol. Chem. 246, 4694-4702.
- Fleck, A., and Munro, H.N. (1962) The precision of UV absorption measurements in the Schmidt-Thannhauser procedure for nucleic acid estimation. Biochim. Biophys. Acta 55, 571-583.
- Folch, J., Lees, M. and Stanley, G.H.S. (1957) A simple method for the isolation and purification of total lipids from animal tissues. J. Biol. Chem. 226, 497-509.
- Friede, R.L. and Bischhausen, R. (1982) How are sheath dimensions affected by axon calibre and internode length? Brain Res. 235, 335-350.

- Greenfield, S., Braun, P.E., Gantt, G. and Hogan, E.L. (1981) Routes of assembly of myelin proteins. In Comparative Pathobiology, Chang, T. ed. Plenum Press, in press.
- Greenfield, S., Williams, N.I., White, M., Brostoff, S.W. and Hogan, E.L. (1979) Proteolipid protein: synthesis and assembly into Quaking mouse myelin. J. Neurochem. 32, 1647-1651.
- Howell, K.E., Ito, A. and Palade, G.E. (1978) Endoplasmic reticulum marker enzymes in Golgi fractions - What does it mean? J. Cell Biol. 79, 581-589.
- Huang, C.M., Goldenberg, H., Frantz, C., Morré, D.J., Keenan, T.W. and Crane, F.L. (1979) Comparison of NADH-linked cytochrome c reductases of endoplasmic reticulum, golgi apparatus and plasma membrane. Int. J. Biochem. 10, 723-731.
- Klingman, G.J., Klingman, J.D. and Poliszczuk, A. (1968) Acetyl- and pseudo-cholinesterase activities in sympathetic ganglia of rats. J. Neurochem. 15, 1121-1130.
- Ko, G.K.W. and Raghupathy, E. (1972) Microsomal galactosyltransferase utilizing endogenous and exogenous protein acceptors. Biochim. Biophys. Acta 244, 396-409.
- Ko, G.K.W. and Raghupathy, E. (1972) Microsomal galactosaminyltransferase utilizing endogenous and exogenous protein acceptors. Biochim. Biophys. Acta 264, 129-143.
- Laemmli, U.K. (1970) Cleavage of structural proteins during the assembly of the head of bacteriophage T4. Nature 227, 680-685.
- Lennarz, W.J. (1980) The Biochemistry of Glycoproteins and Proteoglycans, pp. 1-373, Plenum Press, New York.
- Macklin, W.B., Braun, P.E. and Lees, M.B. (1982) Electrophoretic analysis of the myelin proteolipid protein. J. Neurosci. Res. 7, 1-10.



- Mahler, H.R. (1955) DPNH cytochrome c reductase in Methods in Enzymology (Edited by Colowick, S.P. and Kaplan, N.O.) Vol. 2, 688-693. Academic Press, New York.
- McEwen, C.R. (1967) Tables for estimating sedimentation through linear concentration gradients of sucrose solutions. Anal. Biochem. 20, 114-149.
- Meier, P.J., Spycher, M.A. and Meyer, U.A. (1981) Isolation and characterization of rough endoplasmic reticulum associated with mitochondria from normal rat liver. Biochim. Biophys. Acta 646, 283-297.
- Meldolesi, J., Corte, G., Pietrini, G. and Borgese, N. (1980) Localization and biosynthesis of NADH-cytochrome  $b_5$  reductase, an integral membrane protein, in rat liver cells. II. Evidence that a single enzyme accounts for the activity in its various subcellular locations. J. Cell Biol. 85, 516-526.
- Morré, D.J., Kartenbeck, J. and Franke, W.W. (1979) Membrane flow and interconversions among endomembranes. Biochim. Biophys. Acta 559, 71-152.
- Müller, H.W., Clapshaw, P.A. and Seifert, W. (1981) Intracellular localization of 2',3'-cyclic nucleotide 3'-phosphodiesterase in a neuronal cell line as examined by immunofluorescence and cell fractionation. J. Neurochem. 37, 947-955.
- Norton, W.T. (1976) Formation, structure and biochemistry of myelin. in Basic Neurochemistry, Second Edition, pp. 74-99, Little, Brown and Co., Boston.
- Peters, A., Palay, S.L. and Webster, H. de F. (1976) The fine structure of the nervous system: Neurons and supporting cells. pp. 1-406, Saunders, Philadelphia.

- Pereyra, P.M., Braun, P.E., Greenfield, S. and Hogan, E. (1983) Studies on subcellular fractions which are involved in myelin assembly: labeling of myelin proteins by a double radioisotope approach indicates developmental relationships. J. Neurochem. this issue.
- Rasmussen, H.N. (1973) Nomogram for calculation of centrifugal data. Eur. J. Biochem. 34, 502-505.
- Rothman, J.E. and Fine, R.E. (1980) Coated vesicles transport newly synthesized membrane glycoproteins from the endoplasmic reticulum to plasma membrane in two successive stages. Proc. Natl. Acad. Sci. USA 77, 780-784.
- Rothman, J.E. and Lenard, J. (1977) Membrane asymmetry. Science 195, 743-753.
- Sabatini, D.D., Kreibich, G., Morimoto, T. and Adesnik, M. (1982) Mechanisms for the incorporation of proteins in membranes and organelles. J. Cell Biol. 92, 1-22.
- Sarma, M.K.J. and Sitararamam, V. (1982) Myelosomes: the osmotically sensitive myelin particles. Biochem. Biophys. Res. Comm. 105, 362-369.
- Siegrist, H.P., Jutzi, H., Steck, A.J., Burkart, T., Wiesmann, U. and Herschkowitz, N. (1977) Age-dependent modulation of 3'-phospho-adenosine 5'-phosphosulfate-galactosylceramide sulfotransferase by lipids extracted from the microsomal membranes. Biochim. Biophys. Acta 489, 58-63.
- Sims, N.R., Horvath, L.B. and Carnegie, P.R. (1979) Detergent activation and solubilization of 2',3'-cyclic nucleotide 3'-phosphodiesterase from isolated myelin and C<sub>6</sub> cells. Biochem. J. 181, 367-375.

- Sogin, D.D. (1976) 2',3'-cyclic NADP as a substrate for 2',3'-cyclic nucleotide 3'-phosphohydrolase. J. Neurochem. 27, 1333-1337.
- Towbin, H., Staehlin, T. and Gordon, J. (1979) Electrophoretic transfer of proteins from polyacrylamide gels to nitrocellulose sheets: procedure and some applications. Proc. Natl. Acad. Sci. USA 76, 4350-4354.
- Waksman, A., Hubert, P., Cremel, G., Rendon, A. and Burrin, C. (1980) Translocation of proteins through biological membranes. A critical review. Biochim. Biophys. Acta 604, 249-296.
- Weissbarth, S., Maker, H.S., Raes, I., Brannan, T.S., Lapin, E.P. and Lehrer, G.M. (1981) The activity of 2',3'-cyclic nucleotide 3-phosphodiesterase in rat tissues. J. Neurochem. 37, 667-680.
- Whittaker, V.P. (1969) The synaptosome in Handbook of Neurochemistry (edited by Lajtha, A.) Vol. 2, pp. 327-364, Plenum Press, New York.
- Wickner, W. (1979) The assembly of proteins into biological membranes: the membrane trigger hypothesis. Ann. Rev. Biochem. 48, 23-45.

## 5. STUDIES ON SUBCELLULAR FRACTIONS WHICH ARE INVOLVED IN MYELIN ASSEMBLY: LABELING OF MYELIN PROTEINS BY A DOUBLE RADIOISOTOPE APPROACH INDICATES DEVELOPMENTAL RELATIONSHIPS

### 5.1 Introduction

Our objective is to define the early events of oligodendroglial membrane assembly as part of the myelinogenesis process from the site of protein synthesis to the ultimate appearance of specific proteins in lamellar myelin (Braun et al., 1980). We have developed a fractionation scheme to isolate a number of membrane fractions from mouse brain which are related to this process, including several microsomal fractions which have properties of special interest (Pereyra and Braun, 1983; this issue). Briefly, we have shown that 5 major myelin proteins of mouse brain (14K MBP; 17K MBP; 18.5K MBP; 21.5K MBP; PLP) are all present in two of five categories of subfractions identified and grouped according to their immuno-reactivity toward specific antisera (Pereyra and Braun, 1983; this issue). Six subfractions (P1A $\alpha$ , P2A $\alpha$ , P1B $\alpha$ , P2B $\alpha$ , P3 $\alpha$ ' and P1B $\beta$ ) had electrophoretic protein profiles typical of myelin, and two subfractions (P2A $\beta$ , P2B $\beta$ ) had profiles which were enriched in proteins having molecular weights greater than 30K.

In order to study the possibility that these subfractions are related to a temporal sequence of events in the assembly process we decided to approach this problem by observing the incorporation of radioactive amino acids into specific proteins which are common to these fractions, using a time-staggered double isotope (TSDI) methodology similar to that described by Benjamins and Morell (1978). The initial idea was to inject a pulse of label (eg.  $^{14}\text{C}$ -leucine) followed after an

appropriate interval by a pulse of a second label (eg.  $^3\text{H}$ -leucine) and to terminate labeling by homogenizing the brain after a second appropriate interval. The notion is that the first isotope journeys from the point of protein synthesis through various intracellular compartments to the site of myelin assembly. The second isotope traverses the same route but since its duration is shorter it cannot label all compartments to the same extent. Progressions of isotopic ratios among different subfractions for a given protein have been interpreted to indicate precursor-product relationships among the membranes containing the protein under study. Assuming this to be a valid assumption, we presented some preliminary data on this system (Braun et al., 1980; Greenfield et al., 1981). However, this interpretation requires not only that the specified proteins in any given compartment are not being degraded during the selected time interval, but also that a net transfer of labeled material can be demonstrated to occur from the precursor membranes to the product. Since this latter condition is hard to meet in broken cell systems, independent characterization data from morphological and enzyme marker studies are necessary for any conclusions to be reached on precursor-product relationships. These data have led us to suggest that those subfractions from developing mouse brain, which have characteristics of myelin, represent mainly, but not only, developmental stages of myelination, whereas in mature brain they represent myelinated segments of various sizes and degree of disruption (Pereyra and Braun, 1983; this issue). The metabolic relationships of five myelin-specific proteins (derived from TSDI ratios) among these subfractions are complex and are presented here in the light of a mathematical conceptualization of label compartmentation and net protein turnover as developed by one of

0  
us (P.M.P.) and is given in an expanded formal treatment elsewhere (Chapter 3).

## 5.2 Experimental Procedures

### 5.2.1 Materials

All radioisotopes and chemicals for scintillation counting were purchased from New England Nuclear, Corp., Boston. All other biochemicals were products of Sigma Chemical Co., St. Louis.

### 5.2.2 Subfractionation Protocol

Subfractionation and recovery of myelin and myelin related subfractions was done according to Chapter 4. The microsomal subfraction P3 $\alpha$ ' was further processed into two subfractions. Briefly, P3 $\alpha$ ' was isolated and diluted 1:1 with cold water and pelleted for 30 min at 37 Krpm in a Ti 75 rotor. The pellet was designated P3 $\alpha$ '1 (large) and resuspended in 1 ml of water. The turbid supernatant was then centrifuged again for 60 min at 37 Krpm in the same rotor. The pellet, designated P3 $\alpha$ 's (small), was then resuspended in 1 ml water. The clear supernatant was discarded. Enzyme analysis of these two fractions did not differ significantly. However, electron microscopy showed enrichment of multilamellar vesicles in the P3 $\alpha$ '1 and of smooth, unilamellar vesicles in P3 $\alpha$ 's.

### 5.2.3. Isotope Administration

#### (1) Time-staggered double isotope method (TSDI).

Twelve C57 Black mice (15 days old) received an intracranial injection, in the left ventral parieto-temporal region, of 30  $\mu$ Ci  $^{14}$ C(U)-leucine in 10  $\mu$ l potassium phosphate buffered saline, pH 7.5, using a 25  $\mu$ l Hamilton syringe fitted with a 6 mm needle. Sixty minutes later the same animals received, in the same sequential order, a similar injection

of 110  $\mu\text{Ci}$   $^3\text{H}(3,4,5)$ -leucine in the contralateral region. After an additional 15 min each animal was decapitated in the same sequence, the brain rapidly removed and immediately homogenized in 1.2 ml of ice-cold 0.25 M sucrose containing 11 mM unlabeled leucine. This homogenization was accomplished by 2 up-and-down passes at 300 rpm in a motor-driven Teflon-glass homogenizer. We found that spacing the injection at 60 sec intervals allowed adequate time for all subsequent steps to be adequately performed. Immediately following the last labeled animal, 24 unlabeled brains (from size-matched litter-mates of the above) were homogenized under identical conditions in 30 ml of 0.25 M sucrose containing 11 mM leucine and homogenates of the 32 brains were pooled and further homogenized by 8 up-and-down passes at 800 rpm. Fractionation by velocity and buoyant density centrifugation, and recovery of subfractions is described in detail in the first paper of this series (Pereyra and Braun, 1983; this issue). Aliquots were removed at each step for determination of radioactivity and protein. All membrane subfractions were obtained ultimately as pellets, resuspended in a specific volume of water, and were analyzed for protein content, as described. Measured aliquots of these suspensions were transferred to 15 ml Corex tubes, lyophilized, and delipidated in cold ( $-20^\circ$ ) ether-ethanol (3:2; 2 ml per tube) and collected as pellets after centrifuging for 35 min at 10K rpm in a Sorval rotor at  $-10^\circ$ . Supernatants were transferred to scintillation vials, and the pellets were treated once more in the same way. Supernatants were combined and evaporated to dryness. Pellets were dried under vacuum.

In a slight variation of this approach one experiment was conducted in which the time interval of the second injection was varied; this provided a kinetic assessment of the TSDI protocol. The first isotope

( $^{14}\text{C}$ -leu) was followed 60 min later ( $\Delta t_1$ ) by the second isotope ( $^3\text{H}$ -leu). Animals were sacrificed at various time intervals ( $\Delta t_2$ ) from 3 to 90 min. Eight mice were injected for each time point, and the same general procedure as for the SDI experiment was followed.

(ii) Synchronous double isotope incorporation (SDI).

Pairs of C57 Black mice were injected intracranially with a mixture of leucine radioisotopes which were prepared as follows:

1 mCi  $^3\text{H}(3,4,5)\text{leu}$  (110 Ci/mmol) in 1.0 ml 0.01 N HCl

250  $\mu\text{Ci}$   $^{14}\text{C}(1)\text{leu}$  (53.7 mCi/mmol) in 2.5 ml 0.1 N HCl

93 mM  $\text{K}_2\text{HPO}_4$ , 8.4% NaCl (pH 8) in 0.430 ml

This mixture was brought to pH 7.4 with 5N NaOH and the final volume adjusted to 4.0 ml with  $\text{H}_2\text{O}$ . Each animal received 15  $\mu\text{l}$  of this 1:4 ( $^{14}\text{C}/^3\text{H}$ ) mixture. At specific intervals each pair of animals was sacrificed and each brain homogenized separately in 4 ml of 0.4N perchloric acid (PCA). Homogenates were centrifuged for 35 min at 10 Krpm in the Sorval SS-34 rotor. The supernatant fluids were measured and counted for radioactivity. Pellets were washed twice with 0.2 N PCA and delipidated twice with ether:ethanol (3:2). Solvent washes were collected for radioactivity counting. The dry pellets were resuspended in 2 ml of 0.3 N KOH.

#### 5.2.4 Determination of Radiolabel Purity

The commercial preparations of radiolabeled leucine were routinely checked for purity. A mixture was made of  $^{14}\text{C}$ -leu (1  $\mu\text{Ci}$ ) and  $^3\text{H}$ -leu (2.5  $\mu\text{Ci}$ ) in 500  $\mu\text{l}$  of aqueous 3.4 mM unlabeled leu. Ten  $\mu\text{l}$  of this was reserved for counting and the rest was passed over a 2.5 cm AG 50W X 4 cation exchange column, prepared in a Pasteur pipet. This column was then washed four times with 1 ml  $\text{H}_2\text{O}$  and eluted with 8 X 1 ml portions of



1 N  $\text{NH}_4\text{OH}$ . All eluants were collected as 0.5 ml fractions and counted directly in 10 ml of Aquasure R. Leucine appeared between one and two ml of eluate; degradation products appeared in later fractions. The degree of purity was calculated from the elution profile of each isotope. As much as 20% of the original starting material can be degradation products after one month from the time the sealed ampoule has been opened.

#### 5.2.5 Separation of Proteins

Delipidated subfractions were resuspended in appropriate volumes of SDS-containing buffer to obtain a protein concentration of 2 mg/ml. Pore gradient (5 - 25%) SDS-polyacrylamide slab gel electrophoresis was performed as described (Pereyra and Braun, 1983; this issue) on samples run in duplicate. After staining and destaining, Coomassie blue-stained gels were scanned spectrophotometrically and photographed to obtain a record. Peak areas were integrated by triangulation and computed with a Hewlett-Packard 41C programmable system.

#### 5.2.6 Determination of Radioactivity

Protein bands were excised from the gel and finely chopped with a scalpel. Following transfer to glass vials, 50  $\mu\text{l}$  of water was added, followed 1 hr later by 450  $\mu\text{l}$  of solubilizer (Protosol). Vials were tightly capped and held at 56° for 15 hr. After cooling to 20°, 10 ml of scintillation mixture (Econofluor) was added. Dried lipid extracts were similarly solubilized and prepared for counting.

Counting efficiencies were determined by use of internal standards ( $^3\text{H}$  and  $^{14}\text{C}$ -Toluene), and quenching assessed by the channels ratio method. Optimum window settings of the Intertechnique counter, counting efficiency and spillover for the two isotopes were calculated by the method of Engberg as described by Kobayashi and Maudsley (1972).

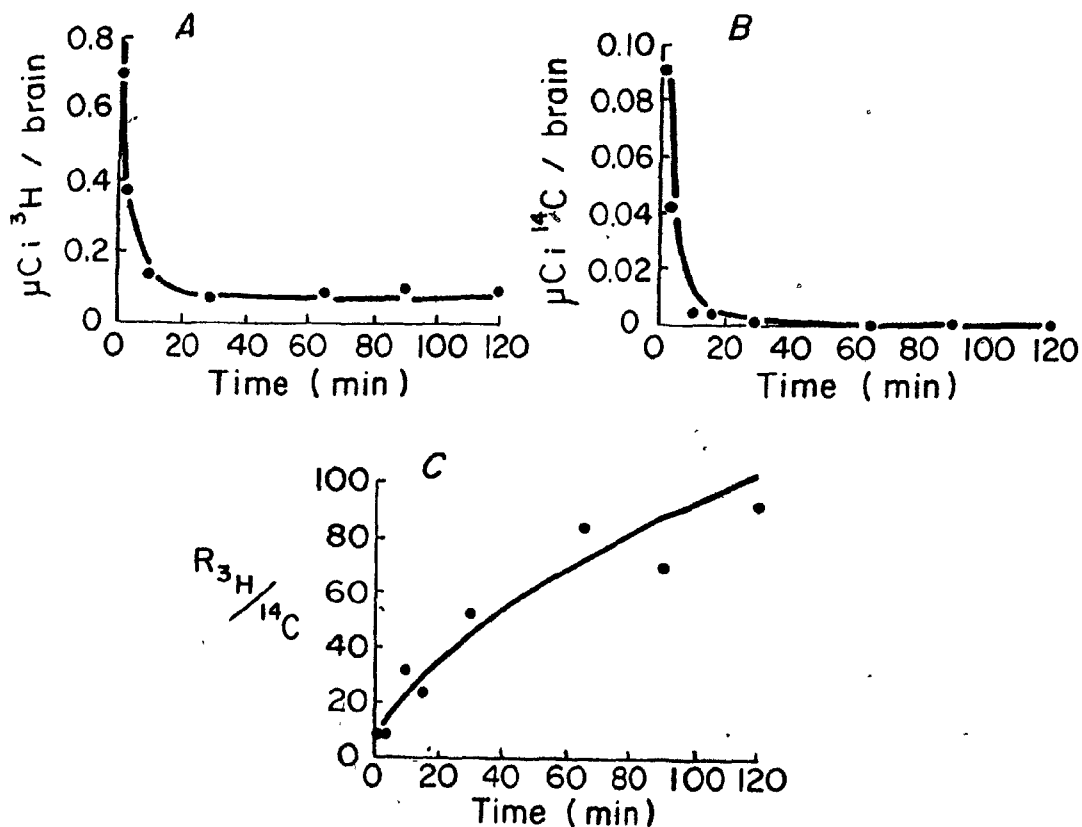


Figure 5.3.1. Behavior of the PCA-soluble pool of 15.d mouse brain following intracranial SDI administration of H [3,4,5- $^3\text{H}$ (N)] and C [1- $^{14}\text{C}$ ]-labeled leucine. Two brains were used for each determination (see Methods).

Regression analysis of both isotopes showed a best fit ( $r^2 > 0.9$ ) with a power regression of the type:

$\text{Ci per brain} = A t^k$

A) For H;  $A_1 = 0.51$  and  $K = -0.43$ .

B) For C;  $A_1 = 0.07$  and  $K = -0.99$ .

C) Regression analysis of  $^3\text{H}/^{14}\text{C}$  ratios ( $r^2 = 0.97$ ) for the power regression  $R = R_1 t^{K_r}$  ( $R_1 = 6.03$  and  $K_r = 0.59$ ).

### 5.2.7 Data Handling and Standardization

Experimental parameters were standardized as much as possible to permit maximum comparisons among data from a variety of experiments. Animals were individually weighed and only those were used whose weight did not differ by more than 5% of the average weight previously established for 15- to 17-day old mice. Injected isotope ratios were corrected for substrate purity, as described above. TSDI ratios represent the average of four experiments. Peak areas in the gel scans, Q and  $\Delta Q$  values, are the average of only two determinations.

## 5.3 Results and Discussion

### 3.1 Characteristics of the System and the TSDI Protocol

TSDI protocols require that the labeled leucine free amino acid pool for protein synthesis becomes rapidly saturated given that the resolution of the method will be a function of the pulse sharpness. Furthermore, the administered label has to be metabolized only to a minimal extent during the duration of the experiment in order to avoid label incorporation into other amino acids.

Analysis of the PCA soluble pool, using an SDI protocol and intracranial injections (10-15  $\mu$ l in 30 sec), shows an inverse power relationship<sup>5</sup> for the removal of label from the brain (see Fig. 5.3.1A and B). The results indicate that by 5 min after label administration 95% of the radioactive amino acid has been removed from the combined intracellular and brain blood bed free amino acid pools.

The values that have been found to describe the behavior of leucine only, are given by the label saturation curve of the [1-C]  $^{14}$ C leu (Fig. 5.3.1B). Any degradation of this labeled leucine, by general catabolism

or simply by enzymatic decarboxylation, will produce an unlabeled molecule and therefore remain invisible. However, the  $^3\text{H}$  labeled leucine [3,4,5- $\text{H}(\text{N})$ ] will produce a shift in the injected ratio ( $R > R_0 = 5.24$ ) if degradation occurs. The rapid metabolic decarboxylation of leucine is reflected in the rapid increase of the isotope ratios (Fig. 5.3.1C). Rapid metabolic activity can also be shown by the difference in the exponent  $K$  (see Footnote Fig. 5.3.1) of the power fit VIZ  $K_{14\text{C}} = -0.99$ , compared to  $K_{3\text{H}} = -0.43$  (See Figures 5.3.1A and B). The higher  $K$  value for the  $^3\text{H}$ -leu results from the accumulation in the brain of decarboxylated leucine metabolites. (Note that  $\Delta K \approx K_R \approx 0.6$ ). These metabolic events could affect the intracellular amino acid pool through the formation of labeled glutamate and aspartate, with a subsequent alteration of label incorporation into protein. However, analysis of the total protein, obtained by delipidation of the cold PCA pellet, shows that even after two hours there is no change in the isotope ratio ( $R_{\text{PCA}} = 5.33 \pm 0.11$ ). This observation indicates that the decarboxylation product of leucine is not primarily isovaleryl-CoA, but possibly isoamylamine. This is further supported indirectly by the observation (data not shown) that variations in the site of injection in relationship to localization of venous or arterial blood produce variations in the  $K$  value for  $^3\text{H}$ , ranging from  $-0.5$  to  $-0.9$ , which suggests a blood-related decarboxylation. Ames et al. (1980) have reported 30% reutilization of leucine in one hour in retinas in vitro. If we assume that this event also occurs in mouse brain, without decarboxylation, then our methodology will not detect reutilization. In summary, the use of intracranial administration leucine isotopes allows for relatively sharp label pulses with an average duration of less than 5 min and a minimal diversion of

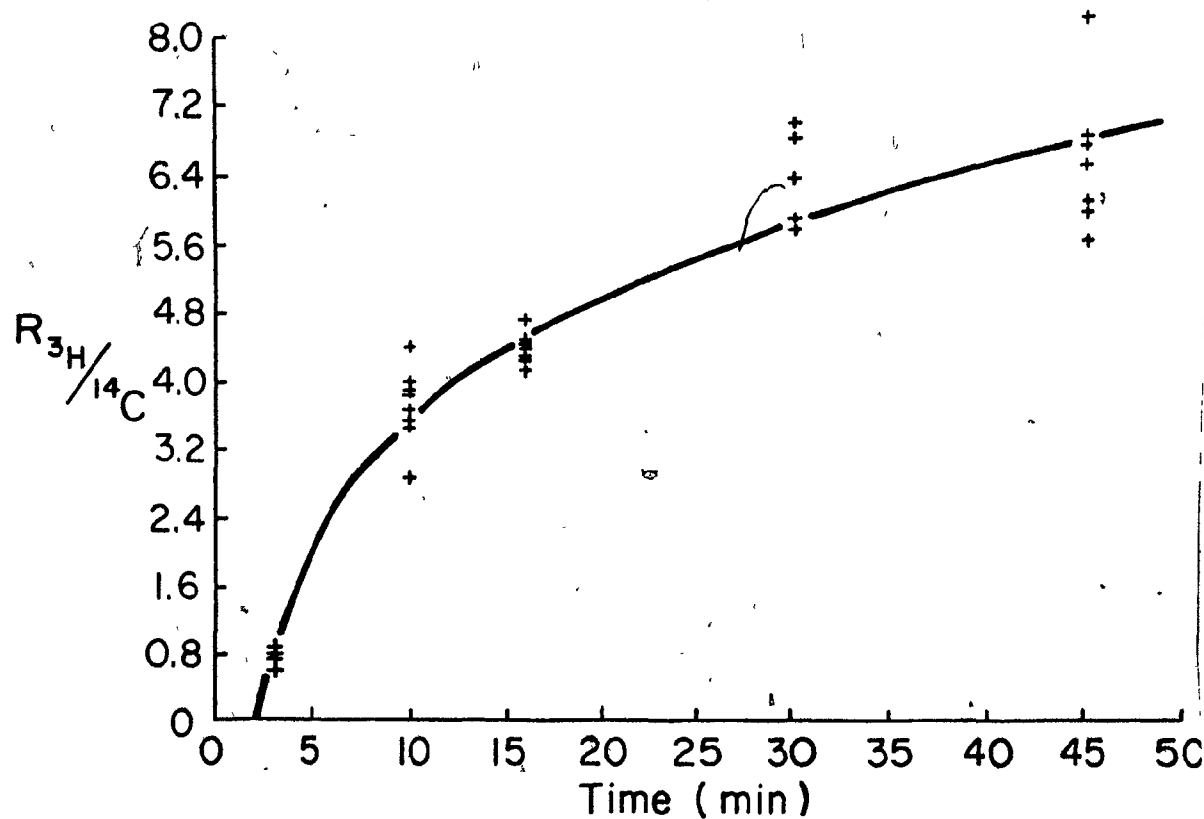


Figure 5.3.2. Change with time ( $\Delta t_2$ ) in the isotope ratio ( $R$ ) of the protein pool in 15 d whole mouse brain (delipidated, PCA insoluble pool), following intracranial TSDI administration of  $3H$  and  $14C$ -labeled leucine ( $R_0 = 4$ ) ( $\Delta t_1 = 60$  min). Each experimental point represents one brain. Regression analysis showed a best fit for the expression  $R = -1.5 + 2.16 \ln \Delta t_2$  ( $r^2 = 0.95$ ;  $F = 684$ ; and 38 degrees of freedom). This analysis was used to determine the comparability of results among different TSDI experiments by determining the expected isotope ratio for total brain protein when  $t_2 = 15$  min and  $R_0$  is known.

labelled molecules into other metabolites.

The selection of time intervals for the TSDI protocol depends on the type of system to be studied. In general, the first time interval ( $\Delta t_1$ ) has to be larger than the average transit time of the proteins being investigated, and shorter by a factor of 5, if possible, than the average half-life of degradation of these proteins. The second time interval ( $\Delta t_2$ ) can then be chosen to be shorter or longer than the average transit time, depending on the experimental objectives. Figure 5.3.2 shows the change in isotope ratio for a TSDI protocol where  $\Delta t_1 = 60$  min, and  $\Delta t_2$  varies from 3 to 45 min. It should be noted that in a system where there is no degradation the maximum attainable ratio is the same as the proportion of labels injected. The larger values of R after 13 min are due to protein degradation.

From the regression analysis of Figure 5.3.2 and the selected time intervals ( $\Delta t_1 = 60$  min;  $\Delta t_2 = 15$  min) the ratio for total brain protein was calculated to be  $R = 4.36 \pm 0.2$ . The actual value obtained from four independent TSDI experiments on myelin proteins (normalized for comparison) was found to be  $R = 4.34$ . This close agreement between the predicted and experimental value was obtained despite anticipated variations due to: 1) non-stereotaxic, intracranial administration of label; 2) isotope purity, affecting  $R_0$ ; and 3) the general state of shock produced in the young animals due to injection, a factor which has a considerable influence on the cerebral blood flow.

### 5.3.2 Application of the TSDI Protocol

On the basis of our previously isolated and characterized sub-fractions from developing mouse brain we were able to select subfractions (designated Groups I and II, in Chapter 4) for which we

TABLE 5.3.1

<sup>3</sup>H-Leucine to <sup>14</sup>C-Leucine Ratios in Specific Myelin Proteins of Mouse Brain (15 d) Subfractions\*

Subfraction	14K MBP		17K MBP		18.5K MBP		21.5K MBP		PLP	
	R <sub>3H/14C</sub>	± S.D.	R <sub>3H/14C</sub>	± S.D.	R <sub>3H/14C</sub>	± S.D.	R <sub>3H/14C</sub>	± S.D.	R <sub>3H/14C</sub>	± S.D.
P1A $\alpha$	3.86	.37	4.65	1.27	4.33	.61	1.99	.33	.87	.06
P1B $\alpha$	4.16	.53	4.43	.77	4.22	.84	1.80	.23	1.01	.05
P2A $\alpha$	4.71	.46	4.50	.39	4.40	.42	2.18	.28	1.23	.24
P2B $\alpha$	4.21	.24	4.24	.91	4.27	.31	2.49	.23	1.78	.12
P1B $\beta$	5.22	1.11	4.90	.37	5.16	1.70	3.05	.42	2.51	.20
P2B $\beta$	6.20	.51	6.22	.42	6.27	.44	6.31	1.27	5.84	.49
P3 $\alpha$ 's	5.24	.31	5.85	.47	5.87	.20	3.10	.20	1.92	.17
P3 $\alpha$ '1	6.06	.61	5.14	.78	4.97	.79	2.89	.32	1.82	.13

\*  $\Delta t_1 = 60$  min;  $\Delta t_2 = 15$  min.

could confidently analyze isotope ratios in specific myelin proteins.  $^3\text{H}$  to  $^{14}\text{C}$ -leucine ratios in such specific proteins are presented in Table 5.3.1, and specific radioactivities (SR) for  $^{14}\text{C}$  and  $^3\text{H}$  are given in Table 5.3.2, for a TSDI protocol with  $\Delta t_1 = 60$  min and  $\Delta t_2 = 15$  min. In general, clear and unambiguous separation of proteins was achieved by a pore-gradient PAGE system (Fig. 5.3.3). However, the bands corresponding to the 17K and 18.5K MBP's migrated quite close together, and examination of the data show similarity of ratios between these two proteins in most subfractions which suggests a possible overlap. We intend to clarify this in the future by modifying the pore-gradient and using longer gels. The minor band which migrated to a final position between the 18.5K and 21.5K MBP's is, presumably, the DM-20 protein (Agrawal et al., 1972; Cammer and Norton, 1976), since it reacts with antiserum raised against proteolipid protein but not against myelin basic protein, and since it is the only radioactive protein in this region when mouse myelin is labeled with  $^{35}\text{S}$ -cysteine (unpublished data from our laboratory). We did not include this protein in our present study because it is quantitatively a very minor component at 15 days.

Other proteins we examined were those in the  $M_r$  regions of 50K and 100K, which include the enzyme CNP and the MAG. However, no detailed analysis was undertaken because other proteins of neuronal and axoplasmic origin overlap these regions. Rapidly turning over components in heterogeneous mixtures, such as this class comprises, seriously mask isotopic relationships of myelin elements having slower turnover rates (for a detailed analysis, see Ames et al., 1980).

The results we have obtained from the TSDI experiments are evaluated and interpreted according to the conceptual framework outlined in Section 3.3. Briefly, three isotopic proportions have been defined:



TABLE 5.3.2

Specific Radioactivities of Leucine-Labeled Myelin Proteins in Mouse Brain (15 d) Subfractions\*

Subfraction	14K MBP		17K MBP		18.5K MBP		21.5K MBP		PLP	
	<sup>14</sup> C	<sup>3</sup> H	<sup>14</sup> C	<sup>3</sup> H	<sup>14</sup> C	<sup>3</sup> H	<sup>14</sup> C	<sup>3</sup> H	<sup>14</sup> C	<sup>3</sup> H
P1A $\alpha$	15.5	12.7	13.5	12.3	11.0	9.2	32.7	12.7	30.4	4.4
P1B $\alpha$	22.3	20.0	21.4	18.9	9.6	7.4	34.1	11.8	31.7	5.6
P2A $\alpha$	44.5	39.0	26.5	22.7	35.5	27.5	42.8	18.8	66.2	16.7
P2B $\alpha$	35.8	32.5	37.2	30.8	25.6	20.0	44.5	19.5	74.6	23.0
P1B $\beta$	18.6	16.9	12.3	12.0	14.1	17.8	32.1	16.4	53.8	17.6
P2B $\beta$	49.0	60.0	48.7	59.7	25.6	87.1	111.5	118.5	50.7	11.6
P3 $\alpha$ 's	81.7	89.9	121.4	109.2	63.4	61.9	119.4	68.4	88.4	38.0
P3 $\alpha$ 'l	48.2	52.9	52.7	54.8	41.1	36.1	56.6	37.3	46.8	10.6

\* dpm per equivalent area under the curve.

Isotope Ratios (R): these show the proportion of the second isotope with respect to the first isotope for any given protein in any given compartment (or subfraction).

Q Ratios: these show the proportion of a given isotope of the specific radioactivity of a given protein in a given compartment with respect to the specific radioactivity for the same isotope and protein in the reference compartment (M). The reference subfraction P1A $\alpha$  was selected to represent an M-type compartment because 1) it has the characteristic morphological features of myelin; 2) it has a well-defined protein profile that is characteristic of myelin; 3) the leucine incorporation data shows that this subfraction contains the lowest isotope ratios and the lowest SR's in the four MBP's and in PLP. This indicates that these membrane elements are metabolically the least active of all subfractions and contain a large pool of unlabeled proteins with minimal turnover or degradation, in agreement with the well-established data showing a very low rate of protein turnover or degradation in myelin (Benjamins and Morell, 1978). The difference between the  $^{14}\text{C}$  Q value and the  $^3\text{H}$  Q value for a given protein in a given compartment is designated  $\Delta Q$ . This parameter serves as an indication of the dynamic similarities between the protein pools in the given compartment and the reference compartment, M (P1A $\alpha$ ).

P Ratios: these show a comparison of the specific radioactivities of a given protein, labeled by the first isotope ( $^{14}\text{C}$ ) with the  $^{14}\text{C}$  specific radioactivity of the 14K MBP in the reference compartment, M (P1A $\alpha$ ). Under appropriate conditions this ratio contains information about the relative dynamics of saturation of the protein bound leucine

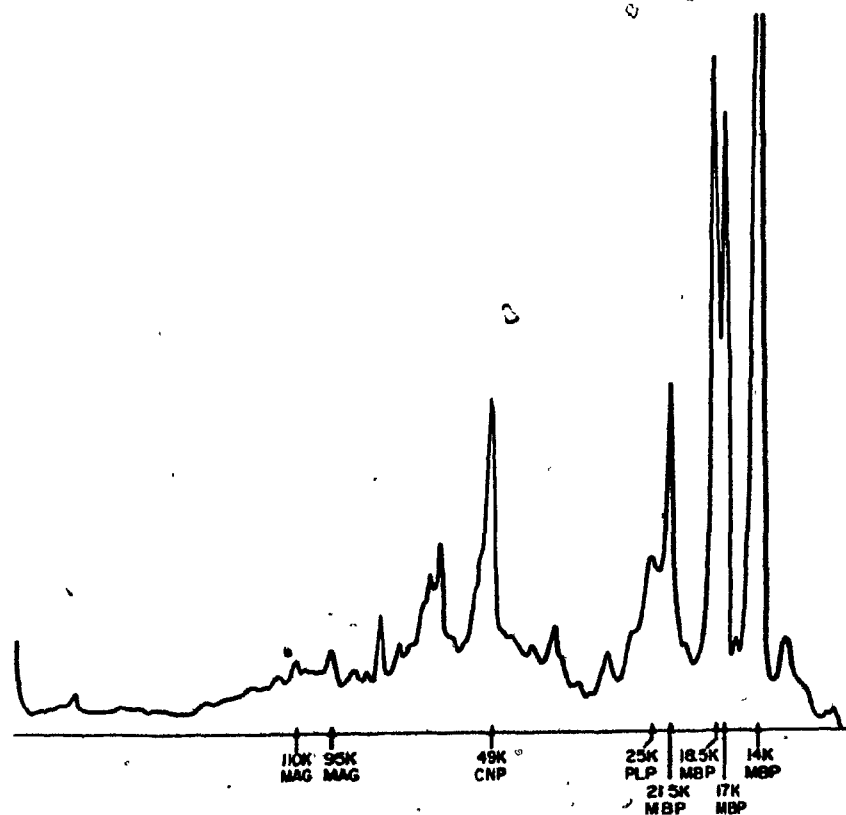


**Figure 5.3.3** Spectrophotometric profile of Coomassie blue stained protein of P2Aa, a representative myelin-containing subfraction of 15 d mouse brain. Characteristic proteins were identified by immunochemical criteria.

pool, and can be used to assess differences in the synthesis pools of several proteins due to differential regulation at the translational level, mRNA stability, or the size of the free pool of leucine available for protein synthesis.

Table 5.3.3 contains the calculated Q ratios for the five myelin proteins in the subfractions previously designated Groups I and II. Table 5.3.4 shows the  $\Delta Q$  values for these proteins in subfractions P2B $\beta$  and P3 $\alpha'$ . The  $\Delta Q$  values for the 21.5K MBP and proteolipid protein are presented in Table 5.3.5.

### 5.3.3 Determination of Accumulative Product Compartments Through the Interpretation of Q Values

Interpretation of Q values will depend on the relative interpretation of the  $\Delta Q$  and R for the proteins in a given compartment. The interpretation of  $\Delta Q$  ( $\Delta Q = 0$ ;  $\Delta Q > 0$ ;  $\Delta Q < 0$ ) is dependent on the overall dynamics of the protein translocation process and the presence or absence of degradation in each step of the pathway. Tables 3.3.2 and 3.3.3 summarize the interpretations derived from the premise of a transport function  $\alpha(r,t)$  and a degradation function  $\beta(t)$ ; where r designates metabolic distance or index of biochemical transformation (see Section 3.3.1) and t designates time. Two reference systems have been defined. The first one is for proteins that arrive at the reference compartment M in less than the second time interval ( $t_{\alpha_M} < \Delta t_2$ ) (Table 3.3.2).

Alternatively, the other system is defined for the condition  $t_{\alpha} > \Delta t_2$  (Table 3.3.3). Hence, given a pair of nominal  $\Delta Q$  and R (Tables 3.3.2 and 3.3.3, columns 1 and 2) it is possible to infer the characteristics of the compartment with respect to a given protein (column 3). The other

**TABLE 5.3.3**

**Q Values for Myelin Proteins in Developing  
Mouse Brain (15 d) Subfractions**

Subfraction	Group	14K MBP*	17K MBP*	18.5K MBP*	21.5K MBP**	25K (PLP)**
P1A $\alpha$	A	1.0	1.0	1.0	1.0	1.0
P1B $\alpha$		1.5	1.6	.9	1.0	1.0
P1B $\beta$		1.3	1.0	1.4	1.2	1.8
P2B $\alpha$	B	2.5	2.7	2.3	1.5	2.5
P2A $\alpha$		3.0	1.9	3.1	1.4	2.2
P2B $\beta$		3.2	3.6	6.4	3.4	1.7
P3 $\alpha$ '1	C	1.3	3.9	3.7	1.7	1.5
P3 $\alpha$ 's		5.3	9.0	6.2	3.7	2.9

\*Values represent the average of  $Q^{14C}$  and  $Q^{3H}$ . For these cases  $Q^{14C} \approx Q^{3H}$ .  
A difference of  $\pm 0.3$  was found to be not significantly different from zero using the student-t test.

\*\*Values represent  $Q^{14C}$  only;  $Q^{14C} < Q^{3H}$ .

columns summarize the degradation state and the temporal conditions of deposition and residence that can be expected from the given  $\Delta Q$  and R values.

The Q values for  $^{14}\text{C}$  and  $^3\text{H}$  proved to be equivalent for the 14K, 17K and 18.5K MBP's in most subfractions except P2B $\beta$  and the microsomal P3 $\alpha'$  (both small and large vesicles). As described in Table 3.3.2, this situation, where  $\Delta Q \approx 0$ , shows that the average time of deposition  $t_{aj} < \Delta t_2$ . Under these conditions Q values are proportional to the ratio of the function  $F(r)$  which encompasses information about the relative pool proportions in the respective compartments and at the site of synthesis.

Arrangement of the subfractions on the basis of their Q values (Table 5.3.3) for the 14K MBP leads to the automatic formation of subfraction clusters which we interpret to represent isotopically equivalent compartments. The first such group (A) is composed of P1A $\alpha$  and P1B $\alpha$ . These subfractions have  $\Delta Q \approx 0$  for all proteins and Q values close to unity. Isotope ratios have values below  $R_0$ . Morphologically, both subfractions are made of compact multilamellar myelin, arranged around well preserved axons. From the point of view of sedimentation properties, both have the same particle index ( $\theta = 5.28$ ; Pereyra and Braun, 1983; Chapter 4) although P1B $\alpha$  is found at a slightly higher sucrose density. The second group of subfractions (B) is composed of P2A $\alpha$  and P2B $\alpha$ . These subfractions have  $\Delta Q \approx 0$  only for the four MBP's and Q values in all cases are an average of 2.5 times larger than those in group A, which indicates that the SR in these subfractions are higher as the result of a smaller, unlabeled protein pool. Morphological examination of these subfractions shows compact multilamellar myelinated axons

TABLE 5.3.4

$\Delta Q$  Values in Three Subfractions\*

Subfraction	14K MBP	17K MBP	18.5K MBP	21.5K MBP	PLP (25K)
P2B $\beta$	-1.6	-0.7	-3.1	-5.9	-0.9
P3 $\alpha$ 's	-1.8	-0.2	-0.9	-1.8	-5.7
P3 $\alpha$ '1	-2.9	0.6	-0.2	-1.2	-0.9

\* Q values for the 14K, 17K, and 18.5K MBPs in other subfractions are zero.

TABLE 5.3.5

$\Delta Q$  Values for 21.5K MBP and 25K PLP

Subfraction	21.5K MBP		25K PLP	
P1A $\alpha$	0	} $\approx 0$	0	} $\approx 0$
P1B $\alpha$	0.1		-0.3	
P1B $\beta$	-0.3		-2.2	
P2A $\alpha$	-0.2		-1.6	
P2B $\alpha$	-0.1	} $\approx 0$	-2.7	} $-21 \pm 0.5$
P2B $\beta$	-5.9		-0.9	
P3 $\alpha$ '1	-1.2		-0.9	
P3 $\alpha$ 's	-1.8		-5.7	

with a well preserved axoplasm. The particle index ( $\emptyset$ ) is 3.95 for these subfractions, and the density ranges from 1.08 for P2B $\alpha$  to 1.06 for P2A $\alpha$ . Isotope ratios are below  $R_0$  for all five proteins in this category. Both groups (A and B) can be confidently described as A-type compartments with no significant turnover ( $\beta = 0$ ).

P1B $\beta$  has not been included in any of the above groups. From its  $\Delta Q$  values ( $\Delta Q \approx 0$ ) and its  $Q$  values for all four MBP's it can be classified as an A-type compartment. However, isotope ratios for the 14K, 17K and 18.5K MBP's are slightly higher than  $R_0$  ( $R = 5.1 \pm .2$ ), most probably because of degradation, or contamination by nonmyelin proteins (axonal). Morphologically, P1B $\beta$  is made of large membrane fragments and very loosely ensheathed axons. It has  $\emptyset = 3.4$  and a bouyant density of 1.09.

A third group (C) can be identified on the basis of the  $Q$  values for 14K MBP. This group is represented by P2B $\beta$  and the microsomal sub-fraction P3 $\alpha'$ , both large and small vesicles.  $\Delta Q$  values are in all cases less than zero and therefore  $Q^{14C}$  can not be interpreted as differences in protein pools to differences in the metabolic distance. The  $Q^{14C}$  values presented in Table 5.3.3 indicate that the overall unlabeled protein pool in these subfractions is small (large  $Q$  values), either because of degradation or turnover, or perhaps because of the relative state of differentiation (architectural modification) of the compartment ( $R > R_0$ ).

Table 5.3.5 shows  $\Delta Q$  values for the 21.5K MBP and PLP (25K) among all subfractions. A difference of zero indicates, as for the other MBP's discussed above that  $Q^{14C} = Q^{3H}$ . Note, however, that both proteins are present in a number of subfractions for which the  $\Delta Q$  is negative. On the other hand, both proteins have isotope ratios that are smaller than  $R_0$ .



TABLE 5.3.6.

Delay Times for Appearance of Myelin Proteins in Subfractions

Group	Subfraction	DELAY TIMES		
		14K, 17K and 18.5K MBP	21.5K MBP	PLP (25K)
A	P1A $\alpha$		13 min	> 15 min
	P1B $\alpha$	4 $\pm$ 1 min		
B	P2A $\alpha$		11 min	14 min
	P2B $\alpha$			
	P1B $\beta$ *	< 4 min	9 min	12 min
	P3 $\alpha$ 's**	-	10 min	13 min
	P3 $\alpha$ '1	-		
	P2B $\beta$ ***	-	-	-

\*For the 14K, 17K and 18.5K MBP's,  $R = 5.1 \pm .2$ ;  $\Delta Q \approx 0$  which we interpret as  $t_{\alpha_i} < t_{\alpha_M}$  with degradation.

\*\*For the 14K, 17K and 18.5K MBP's,  $R = 5.5 \pm .5$ ;  $\Delta Q < 0$  (degradation of these proteins is suspected).

\*\*\*For all proteins,  $R = 6.2 \pm .2$  and  $\Delta Q < 0$  (indicates turnover or degradation).

and as outlined in Table 3.3.2, this indicates the average deposition time of the reference compartment  $t_{\alpha_M} > \Delta t_2$ . Although we cannot extract any direct data concerning the relative residence time ( $t_r$ ) of a protein in a compartment we can be sure that for the observed isotopic conditions  $t_r > \Delta t_1 + \Delta t_2$ . When this is taken together with our conclusions on the MBP's in the subfractions of groups A and B, we anticipate that  $t_r$  for the 21.5K MBP and for PLP in the same subfractions will be large, and that the degradation function will be close to zero.

In summary, the fractions P1A $\alpha$ , P1B $\alpha$ , P2A $\alpha$ , and P2B $\alpha$  can be considered to behave as accumulative compartments (product compartments) with a minimal degradation rate ( $\beta = 0$ ) and a residence time  $t_R > (\Delta t_1 + \Delta t_2)$ . Under these conditions it is possible to calculate the minimal delay time of deposition as defined by the linear relationship:

$$\text{Delay time} = \Delta t_2 - \Delta t_2 \frac{R}{R_0} + \gamma$$

where  $\gamma$  indicates the minimal time of synthesis of the given protein (see Table 5.3.5 and Section 3.3.5 for further details).

It was of interest to us to assess the possibility that the delay times for the deposition of PLP could be consistent with an endomembrane pathway involving the Golgi apparatus. Recent studies on Golgi turnover in a variety of systems (Morré et al., 1979) suggest that on average two to three minutes are required for the complete turnover of one Golgi stack. Since 5 to 8 min are regarded as an acceptable time frame for the synthesis, insertion into and transport of a protein out of the endoplasmic reticulum, and 2 min for its transfer from the Golgi to the cell surface, then the delay time of 14 min for PLP deposition in myelin

suggests a residence time in the Golgi of 4 to 7 min, if in fact it passes through this organelle. If so, it would also suggest a very small Golgi of 3 to 5 stacks. These are, of course, only rough estimates, subject to many assumptions and limitations. Nevertheless, estimations of this sort have been helpful in assessing the possible routes for processing of myelin proteins, particularly the PLP. On the basis of our results to date, and in the light of the above considerations, we are led to suggest that PLP might be translocated from its site of synthesis to its ultimate destination in myelin by a mechanism which bypasses the Golgi apparatus. This notion of a non-conventional route for the insertion of integral myelin proteins has also been suggested by Friedrich et al. (1980) from a morphological point of view.

The delay (10 to 14 min) in the insertion of 21.5K MBP, compared to the much shorter times for the other MBP's, was a surprise to us. So far our efforts to account for this suggest that it is not a result of methodological inadequacy (overlap with PLP and DM20); nevertheless, corroboration by other means will be necessary.

#### 5.3.4 Determination of Degrading or Precursor Compartments Through the Interpretation of Q Values

Situations where  $\Delta Q = 0$  and  $R = R_0$  can be interpreted in two ways: 1) when dealing with an M-type compartment the resultant increased isotope ratio will be due to protein degradation  $\{A\beta\}$ ; and 2) when dealing with an intermediate (precursor) compartment  $\{P\}$  the elevated ratios are due mainly to protein transit (turnover). Three subfractions meet these conditions for some or all of their proteins (Table 5.3.4). P2B $\beta$  has these characteristics for all five proteins (see Table 5.3.1 for isotope ratios;  $R = 6.2 \pm 0.2$ ). This subfraction, which has a sucrose-

equivalent density of 1.09 and  $\rho = 3.2$ , contains well-preserved axons which are enveloped by only a few lamellae and some cytoplasmic pockets. It also contains vesiculated structure containing electron-dense material.

Our data at this point do not yet allow us to state with certainty that the proteins of P2B $\beta$  are being degraded or are turning over. However, if this subfraction represents an intermediate compartment for all myelin proteins we have to account for the fact that even for the deposition (delay) time of PLP (Table 5.3.6) the average residence time in a myelin "precursor" compartment would be relatively short and isotope ratios would be expected to be at least two orders of magnitude higher than we observe. This does not preclude the possibility that proteins in this compartment are turning over.

However, this turnover means that there must be a relatively longer residence time (on the order of 12 hours, calculated by assuming a normal distribution of transit times). Such a scenario would likely represent more a process of membrane (myelin) modification (differentiation) rather than the initial process of membrane assembly. If one wants to argue that significant degradation is occurring, then half-lives of this process on the order of 3 to 4 hours are required in order to obtain the observed ratios (eg.  $R = 5.5$ ), calculated by assuming exponential decay kinetics. These possibilities can only be distinguished by additional experimentation. (For further comments on developmental precursor compartments see Appendix).

The other subfraction which is characterized by  $\Delta Q < 0$  and  $R > R_0$  (for 3 MBP's) is P3 $\alpha'$  (see Table 5.3.1 and Table 5.3.4). The membranes in this subfraction can be separated into two categories, based on their

relative size, by velocity sedimentation; we refer to these as the "large" and "small" vesicles. According to their average sedimentation characteristics ( $\bar{S} = 2.75$ ) these fall into the category of "microsomes".  $P3\alpha'$  (large) has a sedimentation constant greater than 162 S, is enriched in large, trilamellar elements of various sizes and contains a minor contamination by ribonucleoprotein.  $P3\alpha'$  (small) is characterized by a sedimentation constant of less than 162 S, is a collection of vesicles of relatively homogeneous size, enclosing a lightly electron-dense material. Both have a fairly typical myelin protein profile by SDS-PAGE, showing slightly less 14K MBP and PLP than the myelin subfractions in groups A and B. These microsomes are also characterized by their very low buoyant density ( $\delta = 1.04$ ) and by the fact that they accumulate only during the peak of myelination (between day 13 and 20). In preliminary reports, we suggested that these microsomes could represent intracellular transport vesicles. However, our current analysis of the TSDI experiments, as we present here, shows that this interpretation is no longer valid. The fact that the isotope ratios for the 21.5K MBP and for PLP are lower than  $R_0$  means that, irrespective of degradative events, deposition times of these two proteins into the membranes contained in  $P3\alpha'$  (small and large) are similar to those calculated for the myelin fractions in groups A and B (Table 5.3.6). Likewise the delay times observed for the 14K, 17K and 18.5K MBP's in groups A and B (less than 5 min) are consistent with a free ribosomal synthesis of these proteins occurring very close to the insertion site, rather than with a mechanism involving intracellular transport. Since the 21.5K MBP and the PLP have relatively longer delay times for deposition in myelin, one might conclude that they reach their desti-

TABLE 5.3.7.

P Values for Myelin Proteins and their Adjustment for Leucine Content

	14K MBP	17K MBP	18.5K MBP	21.5K MBP	25K PLP
$P^{14}C$ ratios <sup>†</sup>	1.0	1.0 ± .2	0.8 ± .3	1.6 ± .4	1.8 ± .9
Leucine proportions*	1.0	1.5	1.5	1.7	3.0
$P^{14}C$ ratios (adjusted)	1.0	0.5	0.5	1.0	0.6

<sup>†</sup>P values for 18.5K and 21.5K MBP's and for PLP are significantly different from unity ( $p > 0.95$ ) as determined by student t statistics.

\*Obtained by averaging values obtained in our laboratory and from the literature for bovine and rat myelin proteins (Braun and Brostoff, 1977; Barbarese, 1979; Agrawal *et al.*, 1982).

nation by more complex, intracellular transport mechanisms; no further data, however, exist to support this notion. We are left, therefore, with the possibility that the microsomes of P3 $\alpha$ ' are membranes of the A-type, undergoing degradation with half-lives of about 6 to 7 hours. At this point we can only speculate as to the functional nature of these apparently unstable vesicles which can be obtained only during the most active stage of myelination.

#### 5.3.5 Interpretation of P Values

Analysis of P ratios for the four MBP's is possible, given that the dye-binding affinity for these proteins in gel electrophoresis, is the same. As stated in Section 3.3, P ratios among this set of proteins would have to be unity if the only difference among them is the proportion of available message (transcriptional control; Darnell, 1982). As seen in Table 5.3.7, P values for the 18.5K, 21.5K MBP's and PLP are significantly different from unity. In order to take into account the different leucine content of these proteins, we have adjusted them for their relative proportion of leucine. As illustrated in Table 5.3.7, adjusted values of P indicate that the 14K and 21.5K MBP's appear to have a common radioactive leucine pool; their proportions in myelin might be regulated by transcriptional control. From our isotope data we can suggest that the 17K and 18.5K MBP's are transported from the site of synthesis to the point of insertion by a process that is not very different from that for the 14K MBP. From this it follows that the comparatively lower adjusted P value for 17K and 18.5K MBP's may indicate that these proteins are handled differently from the other two MBP's at their site of synthesis (perhaps by differences in mRNA processing, and in the stability of the message or differences in their relative radioactive leucine pools).

Benjamins et al. (1975; 1976b) have reported that, in general, the specific radioactivities for PLP are higher than for MBP. From the P value for PLP it can be seen that, in our experiments after 75 min of labeling, the P ratio of PLP is 1.8. From Benjamins et al. (1975) we have calculated that the same proportion is obtained after one hour labeling with  $^3\text{H}$ -leu. After 24 hr their incorporation values indicate that the ratio of PLP to MBP (14K plus 18.5K) is 2.88, very close to the expected value for the ratio of leucine between the two proteins and PLP (Table 5.3.7). The difference in our adjusted P value for PLP is, therefore, consistent with a mechanism of delayed incorporation, and the proportion of this protein in myelin might also be expected to be controlled at the transcriptional level.

#### 5.4 Concluding Remarks

Our long-term objective is to relate the characteristics of our sub-fractions from developing brain to specific morphological and biochemical properties of membrane compartments which are involved in myelin biogenesis. Once we have established this relationship we will be able to design experiments to examine current views on the molecular events in myelin assembly.

We would like to recommend that the use of the term "precursor-product relationship", in the context of myelinogenesis, be only used to define the events which occur in the de novo processing of myelin components, from site of synthesis to the site of incorporation into the end-product, the oligodendroglial plasma membrane, especially at the mesaxonal site and beyond. Furthermore, a clear distinction should be made between this assembly process and the structural modifications which



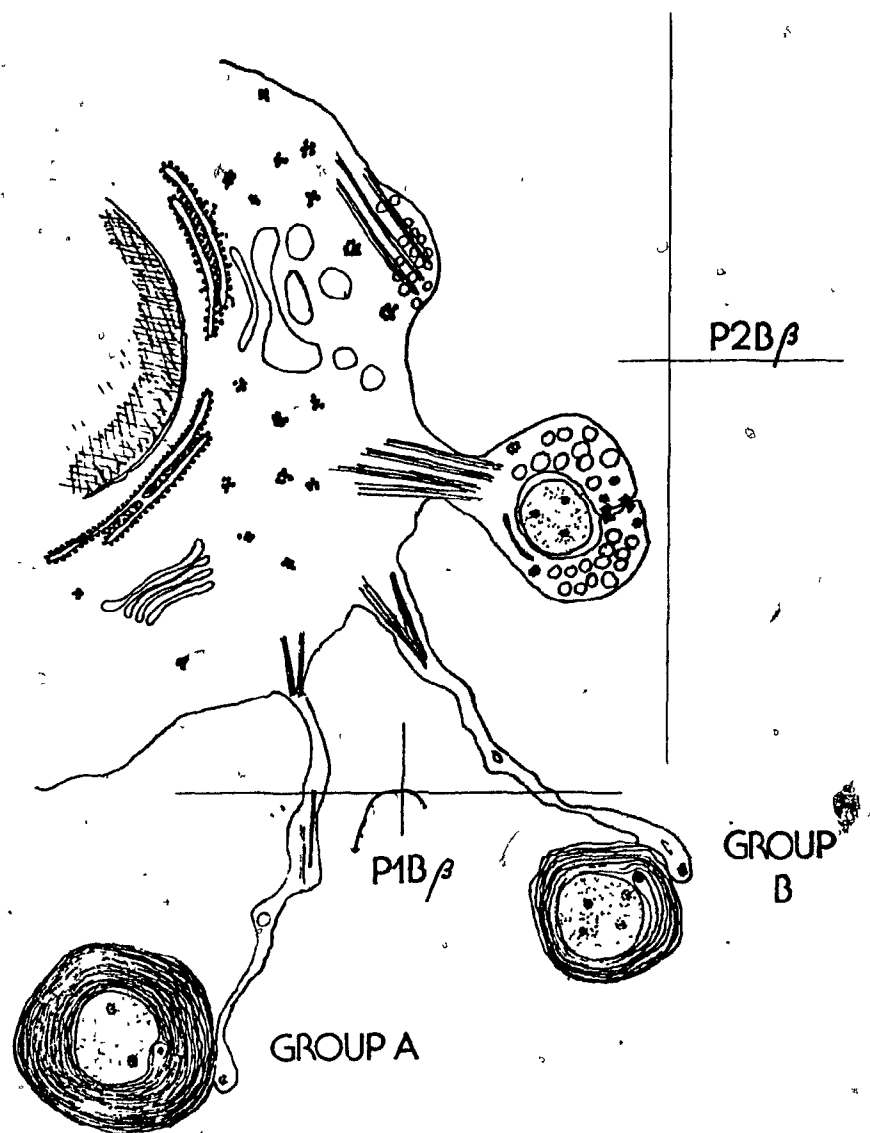


Figure 5.4.1 .

A) Diagrammatic representation of an oligodendroglial cell showing different stages of myelin development (architectural differentiation). Isolated subfractions have been assigned to different regions of the cell surface and to different stages of development on the basis of morphological, enzymatic and label incorporation data. Subfraction P2B $\beta$  has been tentatively assigned to the early stages of myelin formation where significant amounts of cytoplasm are still contained in the mesaxonal space and in between the myelin lamellae. P1B $\beta$  has been interpreted as myelin membranes at a more mature stage. This subfraction contains loose membranes, probably originating from the oligodendroglial processes, plasma membrane or outer lamellae of myelinated axons. Cross contamination between these two B subfractions is evident from their sedimentation rates and densities. Group B subfractions (P2Aa and P2Ba) seem to be representative of a small myelin protein pool with labeling dynamics characteristic of mature myelin. These subfractions have been assigned to the early compaction stages of myelin formation. Group A (P1Aa and P1Ba) is consistent with a large myelin protein pool with label deposition kinetics, protein profiles and morphological features typical of well developed myelinated axons.

take place during the architectural differentiation of the developing myelin sheath. The ability to discriminate between these two temporal sequence of events is, in our view, a fundamental requirement for the interpretation of data relating to mechanisms of myelination. Previous investigators, including ourselves, have not always appreciated this distinction and have ascribed a biogenic interpretation to data pertaining more to post-assembly modification of myelin.

From the results presented in this paper and our preceding work (Pereyra and Braun, 1983; Chapter 4) we have been able to construct a preliminary working scheme (Figure 5.4.1) which permits us to frame questions concerning the mechanisms of myelin assembly and the morphological modifications of the myelin sheath during development. In part "a" of Figure 5.4.1 we have tentatively assigned group A subfractions to well-developed myelin sheaths, and group B subfractions to the incompletely myelinated axons. However, the biochemical and metabolic (isotope incorporation) characteristics of both groups are also consistent with two myelin pools that may result from regional morphological and developmental differences. We have assigned P2B $\beta$ , on the basis of morphology and biochemical features, to the initial stages of myelin formation, while P1B $\beta$  appears to fit best with the first myelin wrappings or perhaps oligodendroglial plasma membrane. We also propose that the microsomal subfraction, P3 $\alpha$ ', represents an unfinished and "unstable" myelin compartment, subject to limited degradation.

Deposition of "recently" synthesized proteins occurs by a series of short-time events (i.e. short-term turnover characteristics). These events are represented schematically in Figure 5.4.1b. PLP is shown to be transported from the endoplasmic reticulum of the perikaryon to the

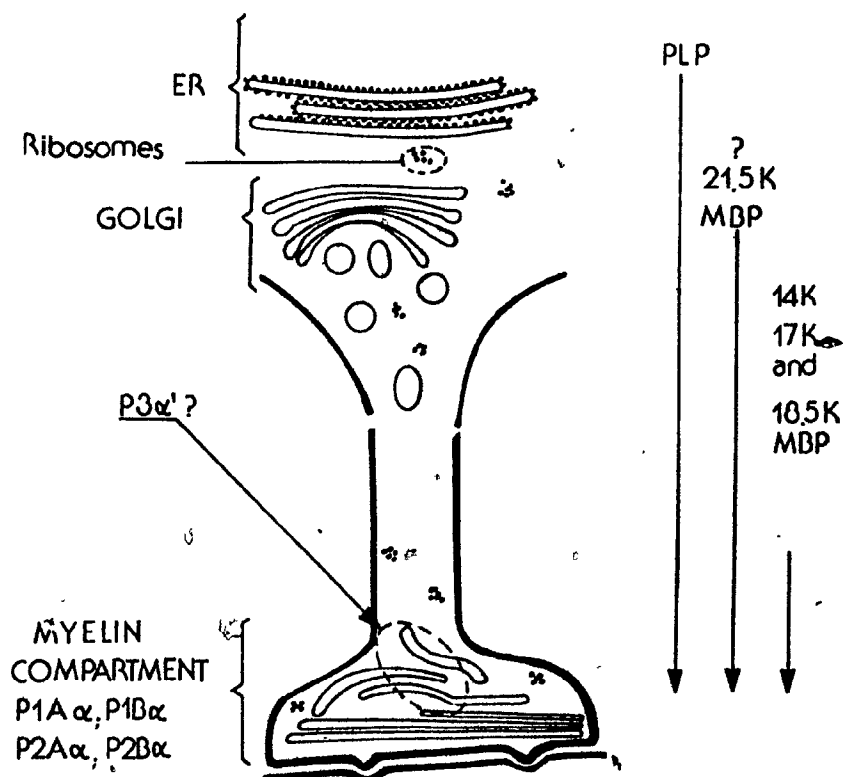


Figure 5.4.1.

B) Diagrammatic representation of intracellular membrane differentiation in an oligodendroglial process in accordance with morphological observations (Friedrich et al., 1980), and an illustration of relative delay times in the incorporation of major myelin proteins. In better agreement with our experimental results, P3a' has been assigned to para-myelin membrane elements adjacent to the growing myelin sheath.

myelin compartment, whether or not it passes through intermediate compartments such as the Golgi apparatus. We observed delayed incorporation of this protein, as had been previously reported by Benjamins et al. (1975; 1976b). Our data, however, showed a delay time of only 14 to 20 min, instead of the 30 or more min reported by these workers. We interpret this time range for PLP to be due to differences in the average deposition times or the "metabolic distances" among the various myelin compartments (see Section 3.3.1). The 14K, 17K and 18.5K MBP's, on the other hand, are inserted directly into the myelin with only a very short delay. The 21.5K MBP showed an unexpected delay in its incorporation into all myelin subfractions and further research on this is now in progress in order to corroborate this observation.

The similar experimental approach by Benjamins et al. (1976a and b) led to suggestions that subfractions of myelin are metabolically different from each other. Unfortunately, an oversimplified interpretation of isotope ratios, in the absence of true  $R_0$  values (the results from several leucine and glycine isotopes were mixed) resulted in a premature conclusion about a precursor-product relationship among their myelin subfractions. Other investigators who have also sought to establish "precursor-product" events by studying myelin subfractions have not taken into account that these are the end-product of myelin assembly, representing instead a variety of developmental stages of the myelin sheath (maturation stages).

Studies on murine mutants such as Quaking have so far yielded only qualitative rather than mechanistic differences in the myelination process (Brostoff et al., 1977; Greenfield et al., 1977). However, this type of approach to mutants as well as TSDI approaches to Wallerian

degeneration (Patsalos et al., 1982) has considerable potential and should yield new and useful information upon the application of conceptual approaches to data interpretation, such as the one we present here, and when adequate characterization of subfractions is pursued.

We are currently developing our subfraction scheme for a wider recovery of size and density ranges in order to obtain large fragments of the endoplasmic reticulum and dense Golgi membranes. These developments and the use of 5 to 10 day old mice in new TSDI strategies will allow us to address various questions which have been prompted by the results we report here, and to study true precursor-product relationships among endomembranes of the initial stage of myelination, as well as their developmental interrelationships.

This work has called into question several commonly accepted assumptions and procedures used in the biochemical studies of myelin. On the one hand, we believe that a distinction must be made between the dynamics of intracellular events involved in the assembly of myelin and the dynamics of myelin maturation in order to design and interpret isotope incorporation experiments. In the first case precursor-product relationships are being considered, while in the second case consideration is given to changes occurring in the product (myelin) because of variations in the phenotypic expression of the maturing myelinating cell, or because of intrinsic metabolic transformations.

On the other hand, the interpretation and understanding of brain subfractions is an essential requirement in order to extrapolate the experimental work to the in vivo situation. The rationale for applying subfractionation protocols to developmental studies rests on the assumption that under adequate conditions it is possible to isolate

different intracellular components and various intercellular associations. The isolation of myelin subfractions after extensive homogenization and osmotic shock is a procedure that defeats this objective. Incomplete characterization of subfractions, even if care is taken in the homogenization step and osmotic shocks are avoided, leads, on the other hand, to meaningless interpretations. If the size heterogeneity of myelinated internodes, and the variation in the maturation stage of myelin and its association with the axon is taken into consideration, then the only valid a priori conclusion possible is that upon homogenization and subfractionation of developing CNS tissue, one should expect several populations of particles within a discrete range of rate and bouyant sedimentation properties.

Our experimental results confirm this expectation rather than the more common view among myelin investigators that myelin differences are only reflected in particle density changes. Furthermore, the above statements and our empirical observations have lead us to consider that:

- 1) Homogenization of developing brain tissue can give rise to operationally discrete myelin and myelinated axon fragments with different metabolic characteristics that are interpreted as different maturational stages of myelin.

- 2) Important endomembrane components are commonly contained in fractions derived from procedures that use only discontinuous gradient rate-sedimentation conditions.

- 3) The range of observed isotope ratios in our work as well as that of Benjamins (Benjamins and Morell, 1978) are insufficient on kinetic grounds to justify a "precursor-product" relationship even in a maturational sense among the various myelin-containing subfractions.

0 Rather the differences are interpreted as an indication of either differences in the metabolic distance of myelin proteins or in their rates of deposition and assembly.

4) Making use of sedimentation protocols that separate myelin and myelinated axon fragments as a function of their size and density it is possible to show that the metabolic differences observed in these myelin compartments are related to the size of the particle rather than to their bouyancy. Previous reports which assigned metabolic differences to "light, medium and heavy" myelin subfractions are thus interpreted to be erroneous due to contamination of the "heavy myelin" subfractions by endomembrane components, and the presence in the "medium and light" subfractions of dense vesicular elements which are too small to have been removed in the relatively short sedimentation times which were employed. In addition, these latter two subfractions also contain varying proportions of the large and small myelin compartments, thereby greatly affecting the distribution of metabolic markers.

#### 5.5 References

- Agrawal, H.C., Burton, R.M., Fishman, M.A., Mitchell, R.F. and Premsky, A.L. (1972). Partial characterization of a new myelin protein component. J. Neurochem. 19, 2083-2089.
- Agrawal, H.C., O'Connell, K., Randle, C.L. and Agrawal, D. (1982). Phosphorylation in vivo of four basic proteins of rat brain myelin. Biochem. J. 201, 39-47.
- Ames, A., Parks, J.M. and Nesbett, F.B. (1980). Protein turnover in retina. J. Neurochem. 35, 131-142.
- Apple, M.S. and Korostyshevskiy. (1980). Why many biological parameters are connected by power dependence. J. Theor. Biol. 85, 569-573.

- Arias, I.M., Doyle, D. and Schimke, R.T. (1969). Studies on the synthesis and degradation of proteins of the ER of rat liver. J. Biol. Chem. 244, 3303-3315.
- Barbarese, E. (1978). Studies on myelin basic proteins, Ph.D. Thesis, McGill University.
- Benjamins, J.A., Jones, M. and Morell, P. (1975). Appearance of newly synthesized protein in myelin of young rats. J. Neurochem. 24, 1117-1122.
- Benjamins, J.A., Miller, S.L. and Morell, P. (1976a). Metabolic relationships between myelin subfractions: entry of galactolipids and phospholipids. J. Neurochem. 27, 565-570.
- Benjamins, J.A., Gray, M. and Morell, P. (1976b). Metabolic relationships between myelin subfractions: entry of proteins. J. Neurochem. 27, 571-575.
- Benjamins, J.A. and Morell, P. (1978). Proteins of myelin and their metabolism. Neurochem. Res. 3, 137-174.
- Bock, K.W., Siekevitz, P. and Palade, G.E. (1971). Localization and turnover studies of membrane NAD glycohydrolase in rat liver. J. Biol. Chem. 246, 188-195.
- Braun, P.E. and Brostoff, S. (1977). Proteins of myelin, in Myelin, Morell, P., ed., pp. 201-231, Plenum Press, N.Y.
- Braun, P.E., Pereyra, P.M. and Greenfield, S. (1980). Mechanisms of assembly of myelin in mice: a new approach to the problem. In INSERM Symposium No. 14 (edited by Braumann, N.) pp. 413-421, Elsevier, North Holland.
- Brostoff, S.W., Greenfield, S. and Hogan, E.L. (1977). The differentiation of synthesis from incorporation of basic protein in Quaking mutant mouse myelin. Brain Res. 120, 517-520.



- Cammer, W. and Norton, W.T. (1976). Disc gel electrophoresis of myelin proteins: new observations on development of the intermediate proteins (DM-20). Brain Res. 109, 643-648.
- Darnell, J.E. (1982). Variety in the level of gene control in eukaryotic cells. Nature 297, 365-371.
- Friedrich, V.L., Massa, P. and Mugnaini, E. (1980). Fine structure of oligodendrocytes and central myelin sheaths, in Proceed. First Inter. Symp. of the search for the cause of Multiple Sclerosis and other chronic diseases of the nervous system, Boese, A., ed., pp. 27-46, Verlag Chemie, Weinheim.
- Greenfield, S., Brostoff, S.W. and Hogan, E.L. (1977). Evidence for defective incorporation of proteins in myelin of the Quaking mutant mouse. Brain Res. 120, 507-515.
- Greenfield, S., Braun, P.E., Gantt, G. and Hogan, E.L. (1981). Routes of assembly of myelin proteins. In Comparative Pathobiology, Chang, T., ed., Plenum Press, in press.
- Kobayashi, Y. and Maudsley, D.V. (1972). Practical aspects of double isotope counting. In The Current Status of Liquid Scintillation Counting, Bransome, E.D., ed., pp. 76-85, Grune and Stratton, New York.
- Morré, D.J., Kartenbeck, J. and Franke, W.W. (1979). Membrane flow and interconversions among endomembranes. Biochim. Biophys. Acta 559, 71-152.
- Patsalos, P.N., Bell, M.E. and Wiggins, R.C. (1980). Pattern of myelin breakdown during sciatic nerve Wallerian degeneration: reversal of the order of assembly. J. Cell Biol. 87, 1-5.
- Pereyra, P.M. (1983). Doctoral dissertation, McGill University.

Pereyra, P.M. and Braun, P.E. (1983). Studies on subcellular fractions which are involved in myelin assembly: isolation from mouse brain and characterization by enzyme markers, electron microscopy and electrophoresis. J. Neurochem., this issue.

Sage, J.I., Van Uiter, R.L. and Duffy, T.E. (1981). Simultaneous measurement of cerebral blood flow and unidirectional movement of substances across the blood-brain barrier: Theory, method and application to leucine. J. Neurochem. 36(5), 1731-1738.

Schimke, R.T., Sweeney, E.W. and Berlin, C.M. (1964). An analysis of the kinetics of rat liver tryptophan pyrrolase induction: the significance of both enzyme synthesis and degradation. Biochem. Biophys. Res. Comm. 15, 214-219.

Zierler, K.L. (1965). Equations for measuring blood flow by external monitoring of radioisotopes. Circulation Res. 16, 309-321.

## 6. EPILOGUE

### 6.1. Commentary on Theoretical Contributions

The first three chapters of this thesis contain a series of theoretical considerations with implications on current views of myelin function, phylogenesis and ontogenesis. It was emphasized that the association of glia with neuron is not only determined by ontological factors but also by phylogenetic ones. It is these latter factors which, as suggested, have given rise to the present ontological relationship between these various cell types. Viewed from this perspective, these cells must be considered as cooperative working units or ERGONs. This concept merges other important theoretical considerations previously described in the literature; such as the "multiplex neuron" concept of Waxman (1972), the concept of "cooperating cell sets" of Boyse and Cantor (1978) and the important morphological observations of the intricate intercellular junctions among CNS cells (Mugnaini, 1978; Dermietzel and Kroczeck, 1980; Dermietzel et al. 1980; Massa and Mugnaini, 1982).

Similar approaches to myelination have been attempted by other authors. Of these, the work of Johnston and Roots (1972) deserves especial mention, where many similar ideas to the ones I have exposed have been extensively explored.

This holistic perspective leads to the distinction of stages in the process of myelination. Furthermore, these stages, as proposed in this thesis, involve not only changes in the morphogenesis of myelin, but also discrete phenotypic alterations which are indicative of continuous cellular

differentiation. These cellular phases have been described tentatively on the basis of combined morphological and biochemical observations. Developmental studies of myelination, however, have not yet been designed in the context of this proposal and many large gaps have yet to be covered.

The morphogenic model in Chapter 2. is one step further in the theoretical analysis of myelination which takes into consideration the available morphological descriptions. This model focuses on the events of phase II, when myelin membranes are assembled into a continuous spiral. How this process occurs is not yet clear. Data to delineate these events are simply not available. All indirect evidence suggests a fairly complex involvement of cytoplasmic structures in this event. The model presented here was developed as a formal alternative to the general "Spiral-Wrapping" hypothesis (Peters et al. 1976) which has by now become a dogma. The theoretical consequence of this new model - and one of its main intentions - is the generation of new experimental approaches to the myelination process. This model also points toward a classification of demyelinating neuropathies based on molecular considerations rather than on the more ambiguous immunomorphological descriptions.

#### 6.2. Commentary on Empirical Results

On my arrival in this laboratory I was presented with the interesting problem of purifying a microsomal fraction from the mouse brain, originally described by Barbarese et al (1978) as P3A. This fraction showed characteristics of

developmental kinetics, that were prematurely interpreted to indicate that these vesicles were transport structures involved in the assembly of myelin (Braun et al. 1980). However, a closer examination of this fraction showed very light smooth vesicles with a typical myelin protein profile (P3A<sup>1</sup>; Chapters 4. and 5.). Moreover, their appearance with development was best described by assuming the presence of a type of myelin that vesiculates easily during homogenization of myelinating brain, rather than being transport vesicles as initially proposed.

During the isolation and characterization of these vesicles, it became apparent that the subfractionation of developing brain gave rise to a series of myelin related subfractions with consistent and specific morphological, biochemical and kinetic characteristics which were related to the developmental stages of the brain. On kinetic grounds alone, it was possible to differentiate among three major groups of subfractions (see Table 5.3.3). On the basis of the kinetic analysis presented in Chapter 3, these results were interpreted to indicate either differences among the groups in the rate of deposition of their myelin constituents or their metabolic distance. Moreover, taking into consideration the morphology, marker enzymes and protein characteristics of these subfractions, it was concluded that all of them represented myelinated axon and myelin membrane fragments with different metabolic properties. The correlation of the groups in Table 5.3.3 with that of the arrangement of subfractions on the basis of their relative size and density

index (Table 4.3.6.) suggested to us that under certain "mild" conditions of homogenization, myelinated axons and myelin membranes subfractionate as particles of a size that is proportional to the original size of the myelinated internode. For CNS tissue, this assumption implies that small and dense particles represent predominantly axons at an early stage of myelination (phase I and beginning of II; Section 1.3), while light, small and large, particles would be enriched, predominantly, with myelinated axons or myelin membranes at different stages of maturity.

Future research using the methodology proposed in this work will attempt to achieve two main goals. One is the extensive characterization of myelin subfractions during mouse brain development, trying to correlate myelination activities, myelin protein and lipid deposition kinetics with the morphological maturation of myelin in order to identify, on molecular terms, the proposed stepwise differentiation of the myelinating cell. The other direction is the application of these procedures to specific pathogenic and pathological experimental systems. This approach should permit the identification of specific molecules in the morphogenesis of myelin as suggested by the myelination model.

## REFERENCES CHAPTER 6

- Braun, P.E., Pereyra, P.M. and Greenfield, S. (1980). 'Mechanisms of assembly of myelin: a new approach to the problem'. In 'Neurological Mutations Affecting Myelination'. (Ed. Baumann, N.). Elsevier/North Holland Biomedical Press. pp: 413
- Boyse, E.A. and Cantor, H. (1978). 'Immunogenetic Aspects of Biological Communication: A hypothesis of evolution by Programme Duplication'. In 'Birth Defects: Original Article Series'. VolXIV(2). Liss, N.Y. pp:249
- Dermietzel, R. and Kroczeck, H. (1980). Interlamellar tight junctions of cerebral myelin I. Developmental mechanisms during myelination.. Cell Tiss. Res., 213: 81
- Dermietzel, R., Leibstein, A.G. and Schunke, D. (1980). Interlamellar tight junctions of central myelin II.. Cell Tiss. Res., 213: 95
- Johnston, P.V. and Roots, B.I. (1972).. 'Nerve Membranes: A study of the biological and chemical aspects of the neuro-glia relationships'. Pergamon Press. Toronto
- Massa, P.T. and Mugnaini, E. (1982). Cell junctions and intramembrane particles of astrocytes and oligodendrocytes: a freeze-fracture study.. Neuroscience, 7: 523
- Mugnaini, E. (1978). 'Fine structure of myelin sheaths'. In Proc. of the European Soc. for Neurochem. (Ed. Neuhoff, V.) Vol1 pp:3
- Peters, A., Palay, S.L. and Webster, H. deF. (1976). 'The Structure of the Nervous System: the neurons and supporting cells
- Waxman, S.G. (1972). Regional differentiation of the axon: a review with special reference to the concept of the multiplex neuron. Brain Res., 47: 269

### CONTRIBUTIONS TO ORIGINAL KNOWLEDGE

A) This work presents a new model of myelination based on the intracytoplasmic and semi-concentric deposition of endomembrane figures or plates. This model represents a formal alternative to existing hypotheses on the mechanisms of myelination. It suggests a common principle of ensheathment that can explain both normal and aberrant myelin formations.

B) I have proposed a mathematical conceptualization of protein translocation based on current concepts of membrane biogenesis and membrane flow. This approach presents the initial results of a kinetic description of protein translocation as a function of the metabolic distance, a variable that incorporates the chemical interconversions (post-translational modifications) of proteins along the endomembrane pathway within a thermodynamic framework.

This outline was applied to the interpretation of time-staggered double isotope (TSDI) studies of protein incorporation during myelin membrane assembly. As a result it was possible to define precursor-product relationships involved in the interconversion of endomembranes, as a function of three experimental parameters. A simple method to calculate the delay of protein incorporation into a given compartment that fulfills the biological characteristics of "mature" myelin, is also presented.

C) In order to perform a complete developmental study of the biochemistry of myelination using normal and neurological mutant mice, it was necessary to develop an extensive subfractionation protocol. This thesis presents the description of this endeavour



and its results, of which the following must be underscored :

- 1) The proteolipid protein is localized to only a restricted group of membranes or structures which possess a typical spectrum of myelin proteins and sedimentation properties. Absence of detectable amounts of this protein from Golgi-enriched fractions is potentially an important observation, given that the myelin glycoprotein (MAG) is clearly present.
- 2) The distribution of MAG is a more general phenomenon, encompassing all membrane fractions.
- 3) Myelin basic proteins (MBPs) are present mainly in myelin-containing compartments. Its presence in other well defined membrane fractions can be explained by contamination of these fractions with myelin.
- 4) 2'3'-cyclic nucleotide 3'-phosphodiesterase (CNP), when maximally activated is widely distributed among brain subfractions. The specific activity in myelin fractions, although very high, represents less than 30 % of the total units.
- 5) Synchronous double isotope incorporation studies indicated that the total brain pool of labelled leucine rapidly exchanges with the blood following power decay kinetics rather than exponential decay kinetics as normally assumed.
- 6) The range of observed isotope ratios, using TSDI protocols, are insufficient on kinetic grounds to justify a "precursor-product" relationship among

subfractions, even in a maturational sense. Rather the differences are interpreted to represent either differences in the metabolic distance of myelin proteins or in their rates of deposition and assembly.

7) Three of the four MBPs (14K, 17K and 18.5K) could be characterized as isokinetic with respect to their rates of deposition onto myelin membranes. For these proteins very short delay times - in the order of two to five minutes - were calculated. This is in agreement with their syntheses, by free ribosomes, occurring very close to their site of incorporation.

8) Proteolipid protein (PLP) was characterized by a delayed incorporation into myelin membranes (ten to twenty minutes), although these values are considerably lower than previously reported. The delay is in agreement with the synthesis of this protein by membrane bound ribosomes and its transport by endomembranes to the myelination site; the Golgi apparatus could or could not be involved.

#### FOOTNOTES

1. The use of the terms 'myelination' and 'myelogenesis' is not interchangeable. Myelinogenesis is used here with developmental and biological implications. Myelination on the other hand denotes the morphogenic and molecular aspects of myelin formation.
2. All these structures are commonly considered the end-products of the endomembrane network.
3. It has been common practice to equate turnover of proteins in a given compartment with protein degradation. In the strictest sense of membrane biogenesis this equation does not hold. The term "turnover", where in quotation, will be taken in this thesis to imply only the transient residence of a macromolecule in a given endomembrane component (RER, GA, PM, etc.). Degradation, or further flow of any macromolecule to other components of the endomembrane network are taken as reasons for the "turnover". "Turnover" is thus defined as a descriptive term and not an explanatory one. Should the discussion require the definition given to it by researchers in the field of macromolecular synthesis and degradation, the word turnover will be left without quotation marks.
4. Using immunocytochemical techniques, Sternberger et al., (1980) were able to demonstrate that the immunolocalization of MPB and

PLP shifted from a somatic to an exclusive myelin localization with development. Similar results have been reported recently by Hartman et al. (1982).

5. Power relationships among biological parameters have been widely described. These relationships can be explained by the dependence of the parameters under study (in our case the influx and efflux of leucine) on a common governing cause (the cerebral blood flow CBF) (Apple and Korostyshevskiy, 1980). According to Zieler (1965) the amount of label in the brain blood bed can be described by the fraction of material left in the blood bed at any time (desaturation of label). This fraction of material is, itself, a function of a distribution function which describes the behaviour of the label across the blood-brain barrier. In the case of leucine, this relationship involves both the label in the brain blood bed and the fraction of it that has exchanged with the intracellular pool (Sage et al., 1981).

6. The length of this unidimensional path ( $\delta$ ) has been termed "Metabolic Distance" to indicate its nature as the effective physical distance that a protein has to transit from its site of synthesis to that of its functional or structural deposition, as a result of specific biophysical or biochemical forces.
7. This type of representation makes it easier to identify the possible codistributions of enzymes among subfractions. This information can be used to assess the

effects that a given subfractionation protocol has on the discrimination of endomembranes, based on specific enzyme markers. Its use is intended as an interpretative aide only. Hence, for example, the agreement between the distribution of total units (T.U.) and relative specific activities (R.S.A.) among the transferases is a strong indication of their common subcellular origin. These results are in contrast with the lack of codistribution of T.U.s and R.S.A.s in the cases of CNP and AcTChE, a result that favors the interpretation of their presence in membranes or cellular structures with different sedimentation properties.